

**Alma Mater Studiorum – Università di Bologna**

RESEARCH DOCTORATE

***Environmental Science: Protection and management  
of natural resources***

*Course XXIII*

Scientific-disciplinary sector: CHIM/01

*TITLE*

**Chemical analysis and reactivity of biomass pyrolysis products.  
Application to the development of carbon-neutral biofuels and  
chemicals.**

**Presented by: CRISTIAN TORRI**

***Doctorate school coordinator***

**PROF. ENRICO DINELLI**

***Supervisor***

**PROF. DANIELE FABBRI**

***Esame finale anno 2011***

# Summary

pg

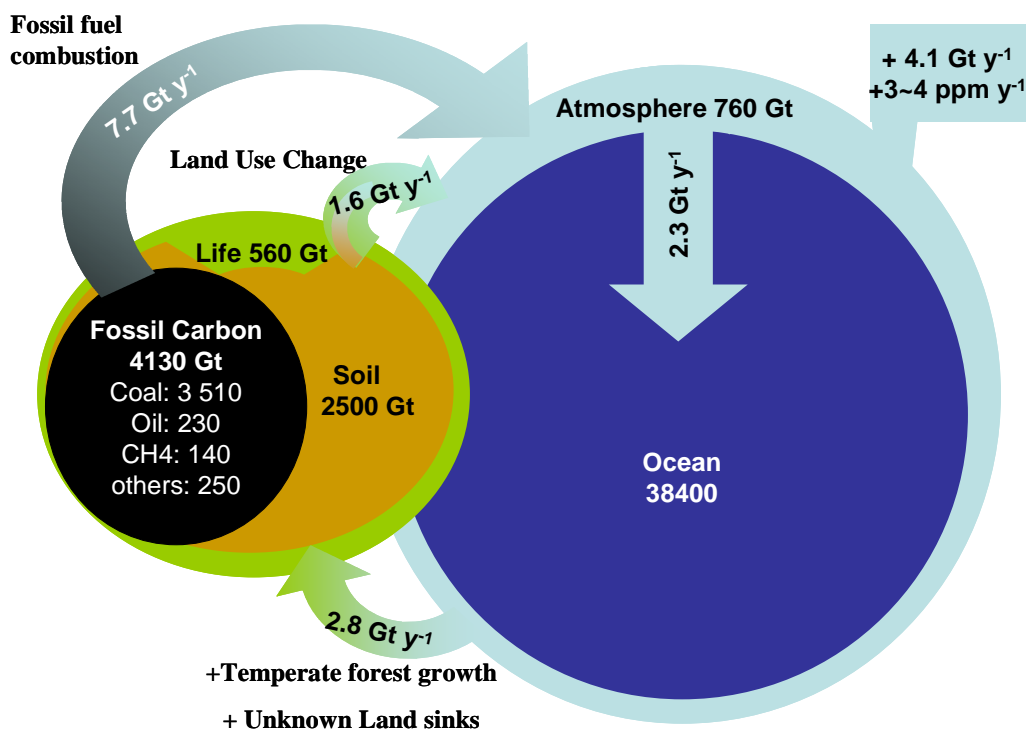
<b>1.</b>	<b>Introduction</b>	
1.1	Biomass and global warming	3
1.2	Pyrolysis of Biomass	7
1.3	Biochar for environmental management	17
<b>2.</b>	<b>Aim of the Thesis</b>	21
<b>3.</b>	<b>Development of analytical methods for the study of biomass pyrolysis</b>	
3.1	Comparative Analysis of Pyrolysate from Herbaceous and Woody Energy Crops by micro-scale analytical pyrolysis techniques.	24
3.2	Application of off-line pyrolysis with dynamic solid-phase microextraction to the GC-MS analysis of volatile biomass pyrolysis products.	38
3.3	Micro-scale GC-MS determination of polycyclic aromatic hydrocarbons (PAHs) evolved from pyrolysis of biomass.	52
3.4	Structural analysis of bio-chars by Py-GC-MS.	61
3.5	Direct in-situ catalytic pyrolysis of biomass: catalyst screening by Py-GC-AED.	76
<b>4.</b>	<b>Applied pyrolysis for carbon-neutral fuels and chemicals</b>	
4.1	Upgrading of Bio-oil by hydrogenation and catalytic cracking over H-ZSM-5	92
4.2	Production of chiral chemicals from cellulosic biomass pyrolysis: influence of pre-treatment and catalysis	105
4.3	Carbon-negative bio-hydrogen and bio-fuels production through pyrolysis of <i>Chlamydomonas reinhardtii</i> by-product.	117
4.4	Evaluation of Pyrolysis coupled to soil carbon sequestration as GHGs saving strategy in the Ravenna province (Italy):	131
<b>5.</b>	<b>Conclusions</b>	153
	<b>Aknowlegments</b>	156

# 1. Introduction

## 1.1 Biomass and Global Warming

Human activities, in particular the use of fossil fuels, are changing the composition of the atmosphere and its properties; one of the major and important effects is the increasing of Greenhouse Gases (GHGs) from 280 ppm of pre-industrial level to the current CO<sub>2</sub>eq concentration of 430 ppm (CO<sub>2</sub> and other GHGs).<sup>1</sup> The total emission of GHGs deriving from human activities in 2004 was 49 GtCO<sub>2</sub>eq of which 77% was CO<sub>2</sub>, 14% methane, 8% nitrous oxide and 1% other GHGs (e.g. perfluorocarbon and sulphur hexafluoride).<sup>2</sup>

**Figure 1.1.1:** scheme of major net carbon fluxes and sinks (the data on Carbon pool are adapted from Lal, 2007<sup>3</sup> and the data on fluxes are from IPCC, 2001.<sup>2</sup>



Focusing on carbon cycle (Figure 1.1.1), out of the 9.3 Gt y<sup>-1</sup> of carbon that human activity converts into CO<sub>2</sub> each year (30 Gt), 7.7 Gt y<sup>-1</sup> come from fossil-fuel emissions and 1.6 Gt y<sup>-1</sup> from land use change, mainly in the tropical regions. On average, 2.3 Gt y<sup>-1</sup> are stored in the oceans and 2.8 Gt y<sup>-1</sup> are sucked up by land-based carbon sinks (mainly growing temperate forests and other unknown

<sup>1</sup> [http://www.esrl.noaa.gov/gmd/obop/mlo/programs/search\\_pages/search\\_ccgg.html](http://www.esrl.noaa.gov/gmd/obop/mlo/programs/search_pages/search_ccgg.html)

<sup>2</sup> IPCC 2007: 4th Assessment Report: Climate Change 2007: Synthesis Report.

[http://www.ipcc.ch/publications\\_and\\_data/publications\\_ipcc\\_fourth\\_assessment\\_report\\_synthesis\\_report.htm](http://www.ipcc.ch/publications_and_data/publications_ipcc_fourth_assessment_report_synthesis_report.htm)

<sup>3</sup> R. Lal. Carbon Sequestration. Phil. Trans. R. Soc. B 363 (2008) 815–830.

sinks), and 4.1 Gt  $y^{-1}$  remain in the atmosphere causing an increase of the GHGs concentration with an annual rate of 3-4 ppm  $y^{-1}$ , as CO<sub>2</sub>eq.<sup>4</sup>

There are compelling evidences that the increasing in Green House Gases (GHGs) emissions could have an effect on climate and determine an increase of global temperatures.

The latest predictions indicate that if GHGs emissions will remain at the current level, their concentration would triplicate the pre-industrial level within 2100, causing a warming of 1.1-6.4°C. In fact, a warming of 5°C on a global scale would be far outside the experience of human civilization and comparable to the temperature difference between last ice age and today.

Although different previsions have been claimed and there is a large uncertainty of the expected warming, there are evidences that the temperature increasing and the consequential climate change effects (e.g. change in surface runoff or increase of coastal areas vulnerability) will have an adverse effect on human economy and on biodiversity.

In order to reduce the risk of global warming, at least 3.2 Gt of CO<sub>2</sub>eq  $y^{-1}$  have to be removed from the atmosphere, and this could be done following different approaches, such as the reduction of CO<sub>2</sub> emissions, obtainable by reducing energy consumption and raising of energetic efficiency, the decreasing of the emissions due to concrete building<sup>5</sup>, and the substitution of fossil fuel energy with renewable GHGs neutral energy.

Among the available options for GHGs saving, a possibility is to exploit the chemical energy captured into biomass, to substitute fossil carbon, energy and fuels by combustion or other conversion techniques.

Biomass fixation represents a huge carbon flow (net primary production, NPP) which consists in about 57 Gt  $y^{-1}$  and 50 Gt  $y^{-1}$  in terrestrial and oceanic ecosystems, respectively.<sup>6</sup>

A portion of the global NPP can be diverted from its natural fate (e.g. decomposition and feeding of natural trophic webs), to produce renewable energy or, more in general, to obtain some GHGs offsets.

Before the beginning of the industrial revolution, biomass energy was the dominant energy source worldwide.<sup>7</sup> Nowadays, it is still important, accounting for 14% of world primary energy consumption, or roughly one-third of the energy from renewable resources.<sup>8</sup>

---

<sup>4</sup> IPCC 2001 Climate change 2001: the scientific basis. Intergovernment panel on climate change. Cambridge, UK: Cambridge University Press.

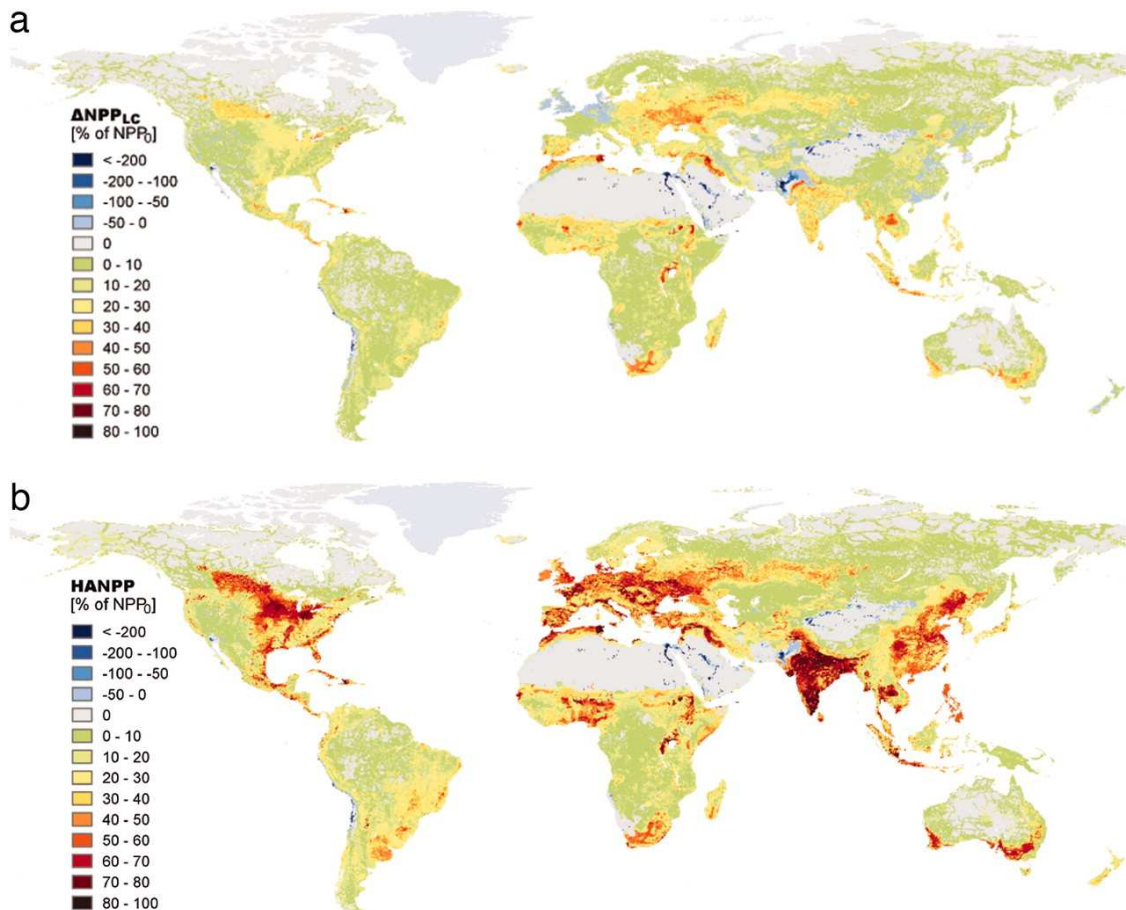
<sup>5</sup> L. Gustavsson, K. Pinguod, R. Sathre. Carbon Dioxide Balance of Wood Substitution: Comparing Concrete- and Wood-Framed Buildings. *Mitigation and Adaptation Strategies for Global Change* 11(2006) 667-691.

<sup>6</sup> M. J. Behrenfeld, J.T. Randerson, C.R. McClain, G.C. Feldman, S.O. Los, C.J. Tucker, P.G. Falkowski, C.B. Field, R. Frouin, W.E. Esaias, D.D. Kolber, N. H. Pollack. Biospheric primary production during an ENSO transition. *Science* 291 (2001) 2594–2597.

<sup>7</sup> S. D. Fernandes, N.M. Trautmann, D. G. Streets, C.A. Roden, T.C. Bond. Global biofuel use, *Global Biogeochem. Cycles* 21 (2007) 1850-2000.

Beyond the actual biomass use, a larger and more effective biomass use is currently proposed as one of the solutions for substantial cutting the excess CO<sub>2</sub> released. These solutions comprised the use of biodiesel from oleaginous crops (e.g. rapeseed or oil palm) and ethanol based fuels produced from corn or sugarcane.

**Figure 1.1.2:** percentage of human appropriated NPP ( $C_h/C_{NPP}$ ) from (a) land use change and (b) biomass withdrawal (HANPP), with permission from Haberl et al.<sup>10</sup>



Nevertheless, it should be noticed that human appropriation of terrestrial NPP is estimated to be already in the range of 23–40% of the total, due to the harvest (12% of terrestrial NPP), the decrease in NPP resulting from replacement of natural ecosystems by human-modified ecosystems, and the shift of NPP from natural pathways to human-mediated loss pathways, including deforestation and wildfire.<sup>9,10,11</sup> Moreover, as shown in figure 1.1.2, this NPP appropriation rate is geographically heterogenous and approaches 80% in most densely populated areas (e.g. Po valley in Italy).

<sup>8</sup> M. Parikka. Global biomass fuel resources. *Biomass and Bioenergy* 27 (2004) 613-620.

<sup>9</sup> C. B. Field, J. E. Campbell, D.B. Lobell. Biomass energy: the scale of the potential resource *Trends in Ecology and Evolution* 23 (2007) 65-72.

These numbers and facts, especially for terrestrial resources, highlight how a further potential sustainable exploiting of biomass could be seriously limited.

A key point for sustainable biomass utilization could be an increase of crops yields or oceanic NPP. This approach (e.g. farming improvement, genetic engineering, production of microalgal biomass) acts in the direction of “artificially” raising up the overall NPP. By this way it is possible to grow and harvest more biomass for energetic use without reducing the nature owned NPP, and therefore without damaging bio-diversity and ecosystem functionalities. Another option is to produce renewable energy from agricultural residues (ARs) already owned by human activities and consisting in about 2-3 Gt of carbon,<sup>12</sup> that under the current situation are mainly buried in soil and open burnt. ARs represent an enormous carbon flow relatively easy to manage<sup>12</sup> avoiding any further NPP withdrawal or competition with food. The current management does not guarantee any significative carbon offset under warm and wet climates (due to a too fast decomposition of humic carbon formed from ARs degradation) and allows only a little carbon offset in temperate and cold climates (10-20%  $C_{HUM}/C_{AR}$  effectiveness due to accumulation of humus into soil as relative stable sink ).<sup>13</sup>

Despite ARs are often characterized by high ash, water and nitrogen content in comparison to standard fuel wood, by using a large array of thermochemical or biological conversions it is technically possible to convert a large range of materials into renewable energy, and then it is possible to gain a significant fossil fuel substitution.

For these reasons, ARs are one of most interesting photosynthesis by-products for carbon neutral bio-energy production and alternative geo-engineering options.<sup>14</sup> Nevertheless, the removal of ARs from soil is a debated option from an environmental point of view, mainly due to the risk of soil carbon decrease and consequential fertility loss.<sup>15</sup>

These facts lead to the so-called climate, food and soil “trilemma”,<sup>16</sup> that stresses the importance of a fine tuning of the quantities and the qualities of biomass withdrawal together with the

---

<sup>10</sup>H. Haberl, K.H. Erb, F. Krausmann, V. Gaube, A. Bondeau, C. Plutzer, S. Gingrich, W. Lucht, M. Fischer-Kowalski. Quantifying and mapping the human appropriation of net primary production in earth’s terrestrial ecosystems. *Proc. Natl. Acad. Sci. U. S. A.* 104 (2007) 12942–12947.

<sup>11</sup>P.M. Vitousek, P.R. Ehrlich, A.H. Ehrlich, P.A. Manson, Human appropriation of the products of photosynthesis. *Bioscience* 36 (1986) 368–373.

<sup>12</sup>J.S. Gregg, S.J. Smith. Global and regional potential for bioenergy from agricultural and forestry residue biomass. *Mitig. Adapt. Strateg Glob Change* 15 (2010) 241-262.

<sup>13</sup>J.S. Jenkinson. The turnover of organic carbon and nitrogen in soil: Quantitative Theory in Soil Productivity and Environmental Pollution, *Philosophical Transactions: Biological Sciences* 329 (1990) 361-368.

<sup>14</sup>S.E. Strand, G.B. Benford. Ocean sequestration of crop residue carbon: recycling fossil fuel carbon back to deep sediments. *Environ. Sci. Technol.* 43 (2009) 1000-1007.

<sup>15</sup>D.L. Karlen, R. Lal, R.F. Follett, J.M. Kimble, J.L. Hatfield, J.M. Miranowski, C.A. Cambardella, A. Manale, R.P. Anex, C.W. Rice. Crops Residues: the rest of the story. *Environ. Sci. Technol.* 43 (2009) 8011-8015.

<sup>16</sup>D. Tilman, R. Socolow, J.A. Foley, J. Hill, E. Larson, L. Lynd, S. Pacala, J. Reilly, T. Searchinger, C. Somerville, R. Williams. Beneficial Biofuels—The Food, Energy, and Environment Trilemma. *Science* 325 (2009) 270-271

improvement of environmentally friendly solutions (e.g. bio-char systems)<sup>17</sup> and the increasing in efficiency of conversion technologies.

## 1.2 Pyrolysis of Biomass

### 1.2.1 Liquid energy carrier from pyrolysis of biomass

In order to obtain renewable energy from relatively dry biomass, one of the simplest ways is to subject the feedstock to thermochemical treatments: basically they consist in the application of heat under controlled conditions, with the final result of converting the biomass into desired materials and energy. This can be done by following different strategies, each one able to provide different conversion effectiveness to energy (heat or electricity), energetic products (fuels) and materials (char or chemicals).

- by direct combustion to provide heat for use in domestic heating, for steam production and hence electricity generation.
- by gasification to provide a fuel gas that can be burnt for energy or converted to syngas by steam reforming (in turn convertible into a large array of fuels and chemical products).
- by fast pyrolysis to provide a liquid fuel (bio-oil), a substitute for heavy fuel oil in static heating or electricity generation.

Among all the different thermochemical conversion processes, pyrolysis of biomass consists in heating under a stream of inert gas. This process degrades biomass polymers in partially volatile fragments, rapidly swept off to cold collectors and separated into a condensed phase and a gas phase. During this process, a variable amount of char (consisting of carbonaceous matter) is formed. The basic aim of pyrolysis is to transform a solid ash-rich feedstock into an ash-poor liquid product, called bio-oil.

Nowadays the biomass-to-bio-oil route is the biomass-to-liquid process with the highest processing efficiency (mainly thanks to relatively low operating temperature), and bio-oil is widely considered the cheapest liquid fuel obtainable from waste ligno-cellulosic biomass.<sup>18</sup> The liquid form of fuels

---

<sup>17</sup>J. Lehmann. A Handful of Carbon. *Nature* 447 (12007) 43-144.

<sup>18</sup>R. P. Anex, A. Aden, F. K. Kazi, J. Fortman, R. M. Swanson, M. M. Wright, J. A. Satrio, R.C. Brown, D.E. Daugaard, A. Platon, G. Kothandaraman, D. D. Hsu, A. Dutta. Techno-economic comparison of biomass-to-transportation fuels via pyrolysis, gasification, and biochemical pathways. *Fuel* 89 (2010) S29-S35.

offers some advantages with respect to solid feedstock, because it can be readily stored and transported and (when economically viable) possibly used for production of chemicals. Bio-oil, also known as pyrolysis oil, pyrolysis liquid and others, is usually a dark brown, free-flowing liquid with a distinctive smoky smell. The physical properties of bio-oils have been described in several publications.<sup>19,20,21,22</sup> These properties derive from the chemical composition of the oils themselves which are significantly different from petroleum-based oils. Bio-oils are multicomponent mixtures of different size molecules primarily deriving from thermal induced depolymerization and fragmentation reactions of key biomass building blocks: cellulose, hemicellulose, lignin and, in some case, lipids, extractives and proteins.<sup>23</sup> A large range of pyrolysis process (e.g. Figure 1.2.1 shows the well known dynamotive™ pyrolysis process) based on different feedstocks have been patented. Different equipments are characterized by different heat and mass transfer rates as well as different actual reaction temperatures. Several reactor configurations have been studied to ensure acceptable quality of liquid and to achieve yields of liquid product as high as 70–80% based on the starting dry biomass weight.<sup>24</sup> They include bubbling fluid beds,<sup>25,26,2,3</sup> circulating and transported beds,<sup>27,28</sup> cyclonic reactors,<sup>29,30</sup> and ablative reactors<sup>31</sup>. In the 1990s, several fast pyrolysis technologies have reached near-commercial status.

---

<sup>19</sup>D.C. Elliott, Analysis and Comparison of Biomass Pyrolysis/Gasification Condensates – Final Report. PNL-5943, Contract DE-AC06-76RLO 1830, 1986.

<sup>20</sup>G.V.C. Peacocke, P. A. Russel, J. D. Jenkins, A.V. Bridgwater. Physical Properties of Flash Pyrolysis Liquids, Biomass Bioenergy 7 (1994)169-178.

<sup>21</sup>L. Fagernäs. Chemical and Physical Characterisation of Biomass-based Pyrolysis Oils. Literature Review. Espoo 1995, Technical Research Centre of Finland.

<sup>22</sup>A. Oasmaa, Y. Solantausta, V. Arpiainen, E. Kuoppala, K. Sipila. Fast Pyrolysis Bio-Oils from Wood and Agricultural Residues, Energy Fuels, 24 (2010) 1380-1388.

<sup>23</sup>S. Czernik, A.V. Bridgwater. Overview of Applications of Biomass Fast Pyrolysis Oil. Energy Fuels 18 (2004) 590-598.

<sup>24</sup>A.V. Bridgwater, G.V.C. Peacocke. Fast pyrolysis processes for biomass. Sustainable and Renewable Energy Reviews, 4 (1999) 1-73.

<sup>25</sup>D. S. Scott, J. Piskorz, D. Radlein. Liquid Products from the Continuous Flash Pyrolysis of Biomass. Ind. Eng. Chem. Process Des. Dev., 24 (1985) 581-586.

<sup>26</sup>A. Robson. 25 tpd Border Biofuels/Dynamotive Plant in the UK. PyNe Newsletter 11, May 2001, Aston University, UK, 1-2.

<sup>27</sup>R.G. Graham, B.A. Freel, M.A Bergougnou. The Production of Pyrolysis Liquids, Gas, and Char from Wood and Cellulose by Fast Pyrolysis. In Research in Thermochemical Biomass Conversion; Bridgwater, A. V., Kuester, J. L., Eds.; Elsevier Applied Science: London 1988; pp 629-641.

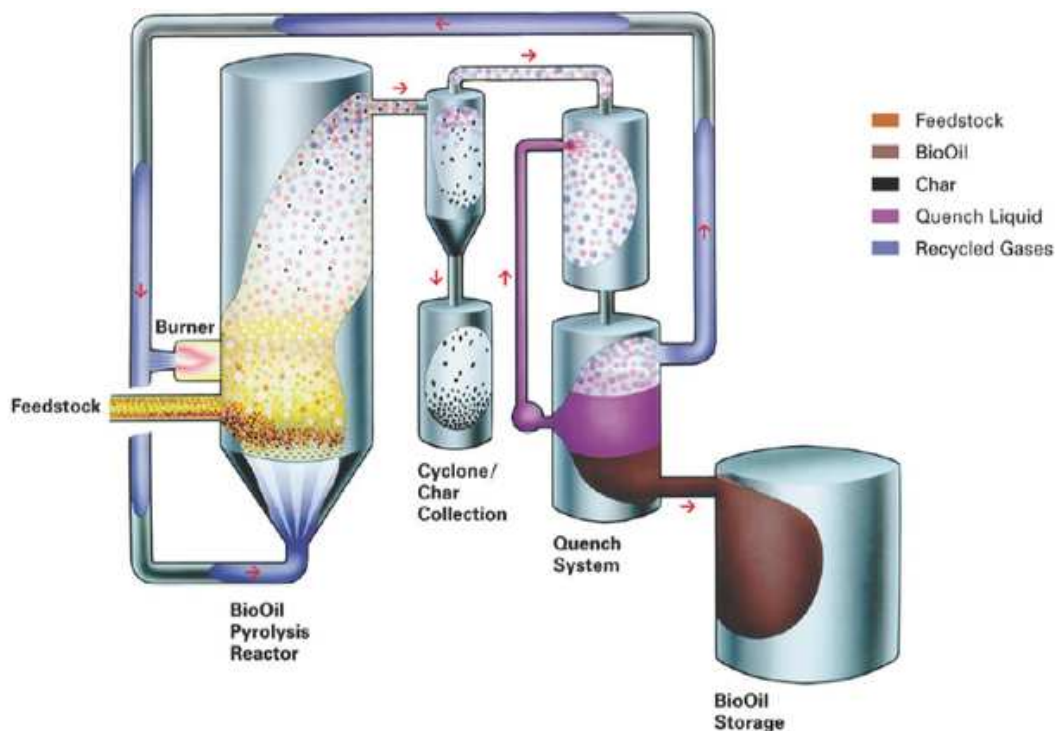
<sup>28</sup>B. M. Wagenaar, R. H. Vanderbosch, J. Carrasco, R. Strenziok, Scaling-up of the Rotating Cone Technology for Biomass Fast Pyrolysis. In 1st World Conference and Exhibition on Biomass for Energy and Industry, Seville, Spain, June 2000.

<sup>29</sup>S. Czernik, J. Scahill, J. Diebold, The Production of Liquid Fuel by Fast Pyrolysis of Biomass. J. Sol. Energy. Eng. 117 (1995) 2-6.

<sup>30</sup>G.V.C. Peacocke, A. V. Bridgwater. Ablative fast pyrolysis of biomass for liquids: results and analyses. In Bio-oil production and utilisation; Bridgwater, A. V., Hogan, E. H., Eds. CPL Press: Newbury, UK, 1996; pp 35–48.

<sup>31</sup>J. Diebold, J. Scahill, Production of Primary Pyrolysis Oils in a Vortex Reactor. In Pyrolysis Oils from Biomass: Producing, Analyzing, and Upgrading; Soltes, E. J., Milne, T. A., Eds.; ACS Symposium Series 376, ACS, Washington, DC (1988) 31-40.

**Figure 1.2.1:** example of fast pyrolysis process from Dynamotive™.<sup>32</sup>



In all the reactor configuration, from a chemical point of view, flash pyrolysis could be conceptually considered as a rapid auto-catalyzed reaction.<sup>33</sup> Biomass constituents, subjected to heating, start to break and produce a significant amount of polar compounds, which impregnate the feedstock and catalyze a prompt increase of reaction rate. At this time, biomass foams out pyrolysis products, that carry on (as aerosol droplets) polymers, melted lignin and some ash.

### 1.2.2 Bio-oil as energy carrier

The liquid fraction resulting from fast pyrolysis is a complex matrix, usually biphasic, that consists of many including (as major categories): hydroxyaldehydes, hydroxyketones, sugars, anhydrosugars, sugar oligomers and polymers, carboxylic acids, monomeric phenolic compounds and pyrolytic lignin.

Bio-oil can be considered a microemulsion in which the continuous phase is an aqueous solution of holocellulose decomposition products and small molecules from lignin decomposition. The continuous liquid phase stabilizes a discontinuous phase that is largely composed of pyrolytic lignin

<sup>32</sup> [http://www.dynamotive.com/technology/fast\\_pyrolysis/](http://www.dynamotive.com/technology/fast_pyrolysis/)

<sup>33</sup> V. Mamleev, S.Bourbigot, M. Le Bras, J. Yvon. The facts and hypotheses relating to the phenomenological model of cellulose pyrolysis Interdependence of the steps. *Journal of Analytical and Applied Pyrolysis*. 84 (2009) 1-17.

macromolecules (consisting in large lignin fragments of 650-1300 dalton).<sup>34,35</sup> Microemulsion stabilization is achieved by hydrogen bonding and nanomicelle and micromicelle formation. Bio-oil, from some points of view, could be considered as a renewable substitute to heavy fuel oil (HFO), usually used for electricity generation and as source of heat in cement kilns.

**Table 1.2.1:** properties of wood derived bio-oil and heavy fuel oil.<sup>23</sup>

<i>physical property</i>	<i>Wood Bio-oil</i>	<i>Heavy fuel oil</i>
moisture content %	15–30	
pH	2.5	-
specific gravity	1.2	0.94
elemental composition ~	~CH <sub>1.2</sub> O <sub>0.6</sub> N <sub>0.001</sub>	~CH <sub>1.6</sub> O <sub>0.15</sub> N <sub>0.05</sub>
ash	0-0.2	0.1
HHV, MJ/kg	16-19	40
viscosity (at 50 °C), cP	40-100	180
solids, wt %	0.2-1	1
distillation residue, wt %	<50	1

Nevertheless two fuels exhibit marked chemico-physical differences, that are examined in table 1.2.1. In fact bio-oil is a relatively corrosive liquid characterized by a pH around 2.5. Acidity becomes really problematic in high temperature zones of engines or turbines, with fast deterioration of materials commonly used in energy generation systems.<sup>36,37</sup> Moreover elemental composition (bio-oil is enriched in oxygen and sometimes in nitrogen) of bio-oil determines a lower (16-19 MJ/kg) higher heating value (HHV), when compared to HFO. Last but not the least, bio-oil is a reactive liquid (mainly due to co-presence of aldehydes and phenols) that polymerize and carbonize when heated, with the consequence that pyrolysis oil is not distillable (distillation residue is up to 50% by weight) and then not easily vaporizable.

These properties have important impacts on the behavior of bio-oil during combustion and consequently on the applications for energy production in standard equipments. Bio-oil is combustible but not flammable (because of the low content of volatile components), this implies

<sup>34</sup>B. Scholze, C. Hanser, D. Meier. Characterization of the water-insoluble fraction from fast pyrolysis liquids (pyrolytic lignin) Part II. GPC, carbonyl groups, and 13C-NMR. *Journal of Analytical and Applied Pyrolysis* 58-59 (2001) 387-400.

<sup>35</sup>J. Piskorz, D. S. Scott, D. Radlien. Composition of oils obtained by fast pyrolysis of different woods. In *Pyrolysis Oils from Biomass: Producing Analyzing and Upgrading*; American Chemical Society: Washington, DC, 1988; pp 167–178.

<sup>36</sup>S. Gros. Pyrolysis oil as diesel fuel. In: *Power production from biomass II*. VTT Symposium 164, Espoo, 1996.

<sup>37</sup>J. Leech. Running a dual fuel engine on pyrolysis oil. In *Biomass gasification and pyrolysis: state of the art and future prospects*. M. Kaltschmitt, A.V. Bridgwater, Eds. CPL Press, Newbury, UK, (1996) 175–85.

that it requires significant energy for ignition, but once ignited, it burns with a stable self-sustaining flame.

Despite large differences in fuel properties and combustion mechanisms, the burning times of bio-oils were comparable to those of No. 2 fuel oil under the same conditions.<sup>38,39</sup>

Concerning real equipment tests, combustion behavior of bio-oil was evaluated using different scale boilers and internal combustion engines, gas-turbine injectors and systems and pyrolysis liquid could be burnt efficiently in standard or modified stationary equipments for electrical energy generation.<sup>40</sup>

Concerning the use of bio-oil as transportation fuel, the largest drawback came out from acidity of the bio-oil that determines the corrosion of engines alloys. Anyway, it was demonstrated that the problem can be partially solved by admixing bio-oil, by means of microemulsion technique, with hydrocarbon (or bio-diesel) fuels, minimizing the effective surface interaction between corrosive fuel and metallic components.<sup>41,42,43</sup>

### 1.2.3 Bio-oil as source of advanced transportation fuels and chemicals

Beyond the direct fuel application of pyrolysis oil, another option is to use bio-oil as feedstock for the synthesis of upgraded transportation fuels or as source of chemical intermediates.

Three routes that produce “chemicals commodities” or current transportation fuel could be envisaged:

- Steam reforming or gasification of bio-oil (or bio-oil and char slurry)<sup>44,45,46</sup> into syngas (as coal derived syngas substitute) and optional catalytic conversion of syngas to Fischer-

---

<sup>38</sup> M. Wornat, G. Bradley, N. Yang. Single Droplet Combustion of Biomass Pyrolysis Oils. *Energy Fuels* 8 (1994) 1131–1142.

<sup>39</sup> R. Shaddix, S. Huey. Combustion characteristics of fast pyrolysis oils derived from hybrid poplar. In *Developments in Thermochemical Biomass Conversion*. A. V. Bridgwater, D.G.B. Boocock, Eds.; Blackie Academic & Professional: London (1997) 465–480.

<sup>40</sup> D. Chiamonti, A. Oasmaa, Y. Solantausta. Power generation using fast pyrolysis liquids from biomass. *Renewable and Sustainable Energy Reviews*. 11 (2007) 1056–1086

<sup>41</sup> M. Ikura, M. Stanculescu, E. Hogan, Emulsification of pyrolysis derived bio-oil in diesel fuel. *Biomass and Bioenergy* 24 (2003) 221-232.

<sup>21</sup> Ikura et al. US patents

<sup>43</sup> R. Calabria, F. Chiariello, P. Massoli Combustion fundamentals of pyrolysis oil based fuels. *Experimental Thermal and Fluid. Science* 31 (2007) 413–420

<sup>44</sup> D. Wang, S. Czernik, D. Montane, M. Mann, E. Chornet. Biomass to Hydrogen via Fast Pyrolysis and Catalytic Steam Reforming of the Pyrolysis Oil or Its Fractions. *Ind. Eng. Chem. Res.* 36 (1997) 1507-1518

<sup>45</sup> G. van Rossum, S. R. A. Kersten, and W. P. M. van Swaij. Catalytic and Noncatalytic Gasification of Pyrolysis Oil. *Ind. Eng. Chem. Res.* 46 (2007) 3959-3967

<sup>46</sup> S. Czernik, R. Evans, R. French. Hydrogen from biomass-production by steam reforming of biomass pyrolysis oil. *Catalysis Today* 129 (2007) 265–268.

Tropsch diesel,<sup>47</sup> syn-methane,<sup>48,49</sup> ethanol<sup>50,51</sup> or methanol<sup>52,53</sup> (usable as automotive fuel after conversion to dimethyl-ether).<sup>54,55</sup>

- Hydrogenation of bio-oil and catalytic cracking of hydrogenated bio-oil over shape selective zeolites (e.g. H-ZSM-5) with the production of aromatic and alkyl aromatic compounds, usable in chemical synthesis or blended with standard gasoline.<sup>56,57,58</sup>
- Fermentation of bio-oil obtained from low ash biomass (e.g. pre-treated cellulosic biomass) for ethanol (or other biogenic alcohol) and chemical production, in thermochemical-biologic hybrid systems.<sup>59,60</sup>

Figure 1.1.2 (a) (b) (c) shows a simplified scheme of the three thermochemical Biomass-to-fuel routes and an integrated thermo-biochemical biomass-to-fuel scheme.

Gasification (figure 1.1.2a) route is a well established commercial process (mainly on coal and raw biomass) representing more than half century of strategical researches for the obtainement of automotive liquid fuels form coal.<sup>61</sup> On the contrary, other two routes feseabilities were tested only in pilot or in lab scale.

---

<sup>47</sup>R.W.R. Zwar, H. Boerringer, A. van der Drift. The impact of biomass pretreatment on the feasibility of overseas biomass conversion to Fisher-Tropsch products, *Energy and Fuels* 20 (2006) 2192-2197.

<sup>48</sup>M. Seemann, S. Biollaz, S. Stucki, M. Schaub, C. Aichernig, R. Rauch. Methanation of biosyngas and simultaneous low-temperature reforming: first results of long duration tests at the FICFB Gasifier in Güssing. In: 14th European biomass conference & exhibition. Biomass for Energy Industry and Climate Protection, 17–21 October 2005, Paris, France.

<sup>49</sup>S. Biollaz, S. Stucki. Synthetic natural gas/biogas (Bio-SNG) from wood as transportation fuel—a comparison with FT liquids. In: Second world conference on biomass for energy, industry and climate protection, 10–14 May 2004, Rome, Italy.

<sup>50</sup>J.J. Spivey, A. Egbeki. Heterogeneous catalytic synthesis of ethanol from biomass derived syngas, *Chemical Society Reviews*, 36 (2007)1514-1528.

<sup>51</sup>X. Pan, Z. Fan, W. Chen, Y. Ding, H. Luo, X. Bao. Enhanced ethanol production inside carbon-nanotube reactors containing catalytic particles. *Nature Materials* 6 (2007) 507-511.

<sup>52</sup>K.Kumabe, S. Fujimoto, T. Yanagida, M. Ogata, T. Fukuda, A. Yabe, T. Minowa. Environmental and economic analysis of methanol production process via biomass gasification. *Fuel* 87 (2008) 1422-1427.

<sup>53</sup>C.N. Hamelinck, A.P.C. Faaij. Future prospects for production of methanol and hydrogen from biomass. *Journal of Power Sources* 111 (2002) 1-22.

<sup>54</sup>M. Xu, J. H. Lunsford, D. W. Goodman, A. Bhattacharyya. Synthesis of dimethyl ether (DME) from methanol over solid-acid catalysts. *Applied Catalysis A: General* 149 (1997) 289-301

<sup>55</sup>T. A. Semelsberger, R. L. Borup, H. L. Greene. Dimethyl ether (DME) as an alternative fuel. *Journal of Power Sources* 156 (2006) 497-511.

<sup>56</sup>M. C. Samolada, W. Baldauf, I. A. Vasalos. Production of a bio-gasoline by upgrading biomass flash pyrolysis liquids via hydrogen processing and catalytic cracking. *Fuel* 77 (1998) 1667-1675.

<sup>57</sup>A. Corma, G.W. Huber, L. Sauvanaud, P. O. Connor. Processing biomass-derived oxygenates in the oil refinery: Catalytic cracking (FCC) reaction pathways and role of catalyst. *Journal of Catalysis* 247 (2007) 307–327.

<sup>58</sup>T. P. Vispute, H. Zhang, A. Sanna, R. Xiao, G.W. Huber. Renewable Chemical Commodity Feedstocks from Integrated Catalytic Processing of Pyrolysis Oils. *Science* 26 (2010) 1222-1227.

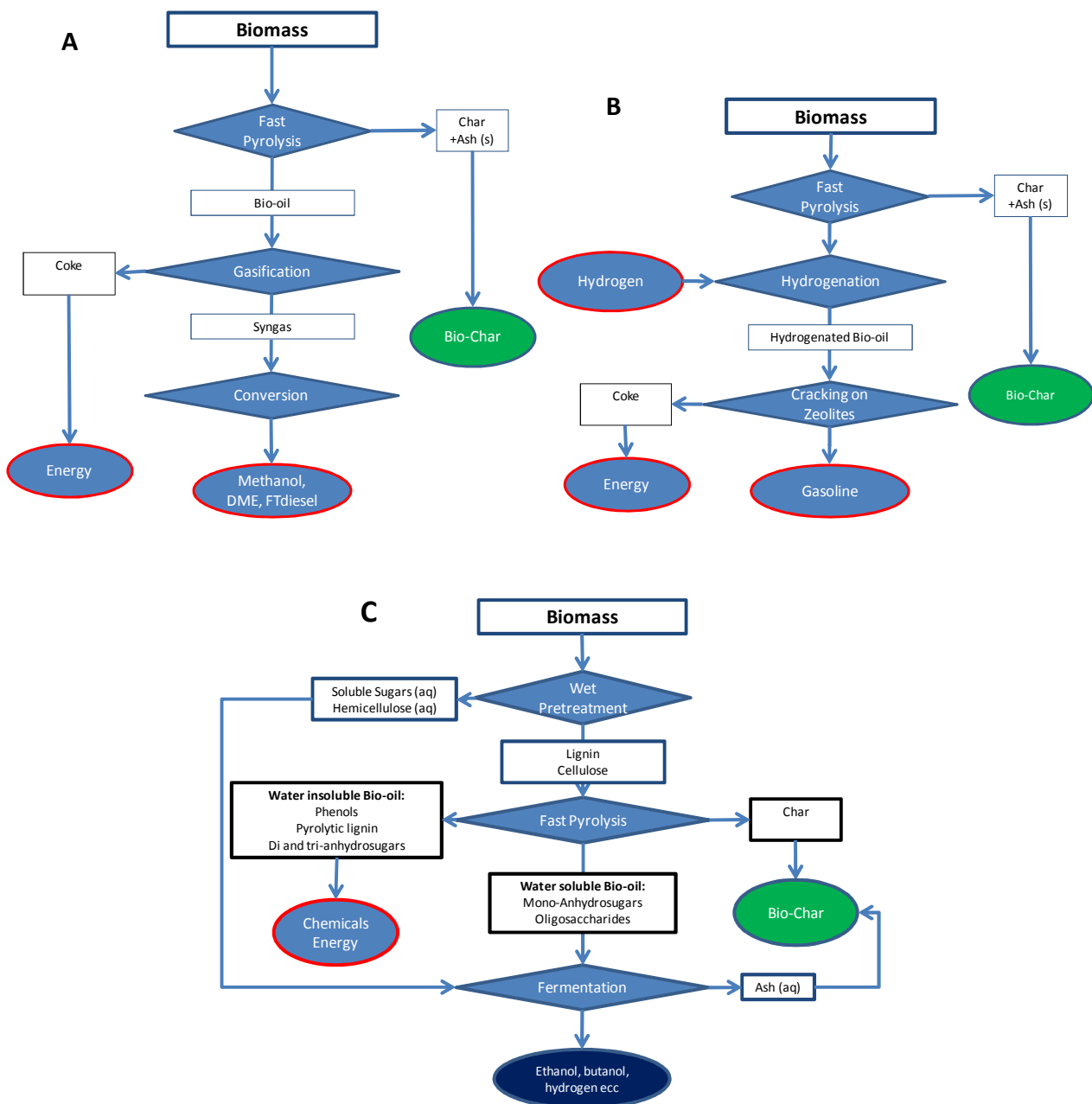
<sup>59</sup>R.C. Brown. Hybrid Thermochemical/Biological Processing Putting the Cart Before the Horse? *Applied Biochemistry and Biotechnology* 137-140 (2007) 947-956.

<sup>60</sup>J. Lian, S. Chen, S. Zhou, Z. Wang, J. O'Fallon, C-Z Li, M. Garcia-Perez. Separation, hydrolysis and fermentation of pyrolytic sugars to produce ethanol and lipids. *Bioresource Technology* 101 (2010) 9688–9699.

<sup>61</sup>M.E. Dry. The Fischer–Tropsch process: 1950–2000. *Catalysis Today* 71 (2002) 227-241.

In the first scheme steam reforming or gasification are performed, then the overall reaction comprises thermic decomposition of bio-oil (steam reforming can be considered  $\text{CH}_2\text{O} + \text{H}_2\text{O} \rightarrow \text{CO}_2 + 2\text{H}_2$ , where gasification can be conceptually considered as  $\text{CH}_2\text{O} \rightarrow \text{CO} + \text{H}_2$ ) and then eventual gas-water shift (if needed by subsequent process stoichiometry), followed by synthesis of methanol or Fischer-Tropsch process.

**Figure 1.2.2:** Pyrolysis based conversion processes for the obtainement of liquid fuels and materials through (a) pyrolysis-gasification (b) pyrolysis-catalytic de-oxygenation (c) hybrid thermo-bio-chemical route.



The main advantages of fast-pyrolysis/gasification systems on direct gasification of biomass are due to the liquid nature of feedstock (easier pressurized injection and easier feedstock storage)<sup>47</sup> and to the relative low amount of ash in the pyrolysis oil, both crucial factors in the case of ARs treatment (ARs have usually high content of “slagging ashes”).

Since the gasification plant has to be large in scale,<sup>62</sup> whereas pyrolysis is a relatively smaller process, the overall scheme allows the de-centralization of bio-oil production (small diffused pyrolysers), but it maintains the centralized gasification plant scale required for economics of process.

The second scheme (figure 1.1.2b) involves the pyrolysis oil processing in standard refineries equipment (e.g. fluid catalytic cracking units) equipped with shape selective catalysts (e.g. ZSM-5 zeolite), able to convert pyrolysis oil into small fragments addicatable to gasoline-like compounds (mainly benzenes alkylbenzenes and naphtalenes). During cracking, a large amount of coke is usually formed, and the amount of coke dramatically increases by using reactive bio-oils (bio-oils high in aldehydes and lignin derivatives) and raw bio-oil with a larger oxygen content with respect to stechiometric ratio. In order to overcome these phenomena, preliminary hydrogenation<sup>58</sup> of bio-oil together with methanol or hydrocarbons co-cracking has been proposed.<sup>63,64</sup>

An interesting recent proposal was that to couple a thermochemical treatment with a biological upgrading. The basic idea is to use fast pyrolysis as a de-polymerizing procedure for recalcitrant fibrous biomass (cellulose and lignin).

Since it has been proven that bio-oil obtained from de-ashed biomass (as well as hydrolyzed biomass) is substantially a mixture of water soluble carbohydrates (e.g. levoglucosan and oligosaccharides) and lignin pyrolysis products,<sup>65</sup> then these two fractions can be splitted by the addition of water to pyrolysis oil or by organic solvent extraction.<sup>66</sup> According to its composition, the water soluble fraction can be used for chemical synthesis<sup>67</sup> or (after detoxification) as feedstock for the fermentative production of ethanol or methane.<sup>68,69,70,71,72,73,74</sup>

---

<sup>62</sup> AV Bridgwater. The technical and economic feasibility of biomass gasification for power generation. *Fuel*. 74 (1995) 631-653.

<sup>63</sup> P.A. Horne, N.Nugranad, P.T. Williams. Catalytic coprocessing of biomass-derived pyrolysis vapours and methanol. *Journal of Analytical and Applied Pyrolysis* 34 (1995) 87-108

<sup>64</sup> G.W. Huber, A. Corma. Synergies between Bio- and Oil Refineries for the Production of Fuels from Biomass. *Angew. Chem. Int. Ed.* 46 (2007) 7184 – 7201

<sup>65</sup> D. S. Scott, L. Paterson, J. Piskorz, D. Radlein, Pretreatment of poplar wood for fast pyrolysis: rate of cation removal, *Journal of Analytical and Applied Pyrolysis* 57 (2000)169–176.

<sup>66</sup> A. Oasmaa, E. Kuoppala. Solvent fractionation method with brix for rapid characterization of wood fast pyrolysis liquids. *Energy Fuels* 22 (2008) 4245-8.

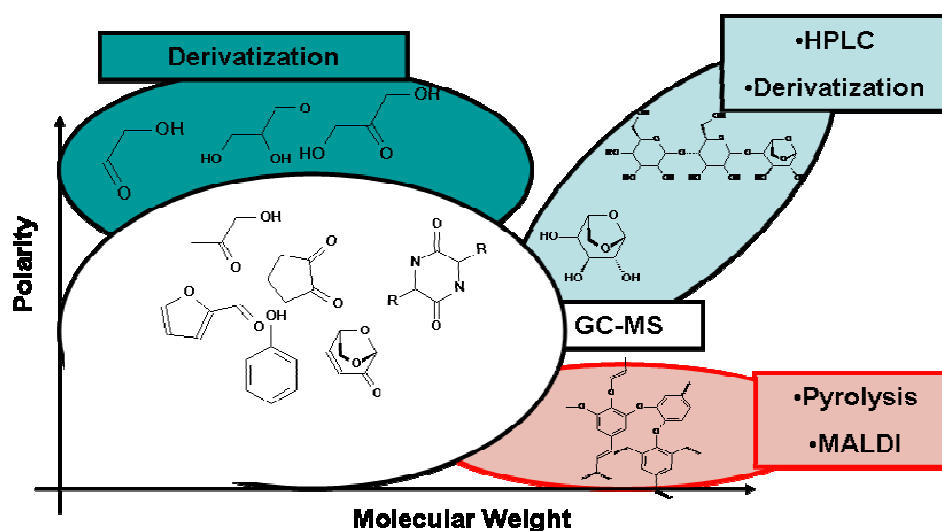
<sup>67</sup> F.W Lichtenthaler, S. Petersa. Carbohydrates as green raw materials for the chemical industry. *Comptes Rendus Chimie* 7 (2004) 65-90.

<sup>68</sup> F. Shafizadeh, T.T. Stevenson. Saccharification of douglas-fir wood by a combination of prehydrolysis and pyrolysis. *Journal of Applied Polymer Science* 27 (1982) 4577–4585.

The remaining non-sugar like fraction (or organic solvent extractable) is composed by in a variable amount of phenols or other special chemicals (like di and trianhydrosugars) that, if isolation of single compounds would be relatively cheap, could be considered as high added value by-products of the process.<sup>67,75,76</sup> The main drawback of this process is the need of energy costly wet pre-treatment, and then a subsequent need of biomass drying. Moreover, the process produces a significant amount of wastewater that has to be treated and eventually used as ferti-irrigating liquid.<sup>77</sup>

### 1.2.3 Bio-oil chemical characterization

**Figure 1.2.3:** Example of compound families (classes) analyzable by different analytical tools



<sup>69</sup> N.M. Bennett, S.S. Helle, S.J.B. Duff. Extraction and hydrolysis of levoglucosan from pyrolysis oil. *Bioresource Technology* 100 (2009) 6059–6063.

<sup>70</sup> E. M. Prosen, D. Radlein, J. Piskorz, D. S. Scott, R.L. Legge. Microbial utilization of levoglucosan in wood pyrolysate as a carbon and energy source. *Biotechnology and Bioengineering*. 42 (1993) 538–541.

<sup>71</sup> J.K.S. Chan, S.J.B. Duff. Methods for mitigation of bio-oil extract toxicity. *Bioresource Technology* 101 (2010) 3755–3759.

<sup>72</sup> M.A. Khiyami, A.L. Pometto III, R.C. Brown. Detoxification of Corn Stover and Corn Starch Pyrolysis Liquors by *Pseudomonas putida* and *Streptomyces setonii* Suspended Cells and Plastic Compost Support Biofilms. *J. Agric. Food Chem.* 53 (2005) 2978-2987

<sup>73</sup> V. Andreoni, P. Bonfanti, D. Daffonchio, C. Sorlini, M. Villa. Anaerobic digestion of wastes containing pyrolytic acids. *Biological Wastes* 34 (1990) 203-214.

<sup>74</sup> T. Willner, P. Scherer, D. Meier, W. Vanselow. Vergärung von Flash-Pyrolyseöl aus Holz zu Biogas. *Chemie Ingenieur Technik* 76 (2004) 838–842.

<sup>75</sup> A. Effendi, H. Gerhauser, A.V. Bridgwater. Production of renewable phenolic resins by thermochemical conversion of biomass: A review. *Renewable and Sustainable Energy Reviews* 12 (2008) 2092–2116

<sup>76</sup> C. Amen-Chen, H. Pakdel, C. Roy. Production of monomeric phenols by thermochemical conversion of biomass: a review. *Bioresource Technology* 79 (2001) 277-299.

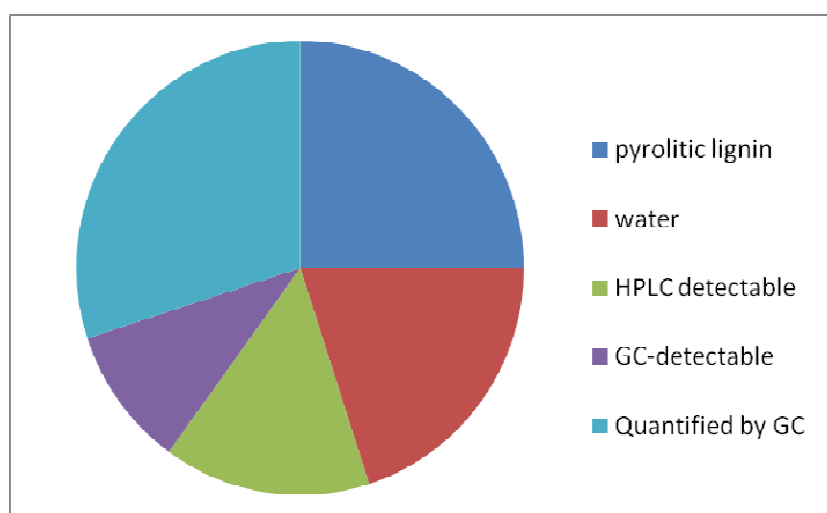
<sup>77</sup> G.J. Sheehan, P. F. Greenfield. Utilisation, treatment and disposal of distillery wastewater. *Water Research* 14 (1980) 257-277.

A complete molecular characterization of bio-oil is a difficult task. In fact, bio-oil contains higher-molecular-weight species, including degradation products of pentoses, hexoses, lignin and other biomass constituents.

Figure 1.2.3 depicts some typical constituents of bio-oil in a polarity vs. molecular weight plot. The main analytical problem of bio-oil, if compared with fossil fuels, is the co-presence of substances with molecular weight (and then with different volatility) and polarity largely different.

For this reason, the obtainment of a global picture of bio-oil chemical nature might be gathered by means of various analytical techniques. Figure 1.2.4 depicts a typical distribution of the analytical class amounts typically found in bio-oil, which indicate the analytical complexity of the chemical characterization. Therefore, fast and cheap methods for bio-oil chemical characterization is nowadays lacking.

**Figure 1.2.4:** abundance of different analytical classes in wood bio-oil<sup>78</sup>



Only a portion of the bio-oil can be detected via GC, even using robust columns and high-temperature programs. In the basic research field, information on the chemical nature of pyrolysis liquids can be analyzed by combining a large array of techniques: GC-MS (volatile compounds), HPLC and HPLC/electrospray MS (nonvolatile compounds),<sup>78</sup> Fourier transform infrared (FTIR) spectroscopy (functional groups), gel permeation chromatography (GPC) (molecular weight distributions),<sup>79</sup> size exclusion chromatography (SEC),<sup>80,81</sup> nuclear magnetic resonance (NMR)

<sup>78</sup> D. Mohan, C. U. Pittman, Jr. P.H. Steele, Pyrolysis of Wood/Biomass for Bio-oil: A Critical Review, Energy & Fuels 20 (2006) 848-889.

<sup>79</sup> C. Gerdes, M. Simon, T. Ollesch, D. Meier, W. Kaminsky. Design, Construction and Operation of Fast pyrolysis Plant for biomass. Eng. Life Sci. (2002) 167-174.

<sup>80</sup> R. Bayerbach, V. Dy Nguyen, U. Schurr, D. Meier. Characterization of the water-insoluble fraction from fast pyrolysis liquids (pyrolytic lignin): Part III. Molar mass characteristics by SEC, MALDI-TOF-MS, LDI-TOF-MS, and Py-FIMS. Journal of Analytical and Applied Pyrolysis 77 (2006) 95-101.

(types of hydrogens or carbons in specific structural groups, bonds, area integrations)<sup>34</sup> or by fragmentation to MS detectable compounds (with Py-GC or MALDI-TOF).<sup>82,80,83,84</sup>

Nonetheless, the understanding of a large number of bio-oils obtainable from different reactor configurations, different feedstock or from catalytical pyrolysis, requires fast and cheap methods for bio-oil molecular characterization. In this field, micro-scale systems, based on analytical pyrolysis, can be envisaged as powerful techniques, which will be dealt with in section 3.

#### 1.2.4 Bio-char for environmental management

As examined in the previous section, the destination of ARs as energy source (in place of ARs mulching), even though some advantages on the use of biomass from dedicated crops, can lead to soil carbon impoverishment. Therefore, management of agricultural wastes use should be carefully planned, to avoid the adverse consequence of soil carbon loss (erosion and reduction of fertility).

Soil carbon depletion is main concern in modern agricultural practice, and it is one of most relevant positive feedback of global warming. For this reason, no-till management or mulching are usually proposed for both climate mitigation and long term fertility enhancement.

Nonetheless, soil carbon incorporation is relatively ineffective (in term of GHGs offset) in tropical and temperate climates, due to the fast decomposition of humus (warm and wet climates) and an ineffective residue conversion to humus (sandy loamy soils). In most of the cases, even mulching of ARs or no till management is not satisfactory and some other solutions are needed, since food production can not be reduced,

An interesting idea came out from studies on archaeological soils in the tropical area of “terra preta” near Manaus (Brazil). Basically, amazon civilizations (around 200 B.C and 1500 A.D) successfully practiced sedentary agriculture (usually impossible in tropical amazonic climate) by changing the soil composition through charcoal addition.<sup>85</sup> This traditional practice allowed to increase the soil carbon to astonishing high levels,<sup>86</sup> with significant increase (in comparison to adjacent untreated

---

<sup>81</sup> E. Hoekstra, S.R.A. Kersten, A. Tudos, D. Meier, K.J.A. Hogendoorn. Possibilities and pitfalls in analyzing (upgraded) pyrolysis oil by Size Exclusion Chromatography (SEC). *J. Anal. Appl. Pyrolysis Article in press* (2011).

<sup>82</sup> B. Scholze, D. Meier. Characterization of the water-insoluble fraction from pyrolysis oil (pyrolytic lignin). Part I. PY-GC/MS, FTIR, and functional groups *Journal of Analytical and Applied Pyrolysis* 60 (2001) 41-54.

<sup>83</sup> R. Bayerbach, V. Dy Nguyen, U. Schurr, D. Meier. Characterization of the water-insoluble fraction from fast pyrolysis liquids (pyrolytic lignin): Part III. Molar mass characteristics by SEC, MALDI-TOF-MS, LDI-TOF-MS, and Py-FIMS. *Journal of Analytical and Applied Pyrolysis* 77 (2006) 95-101.

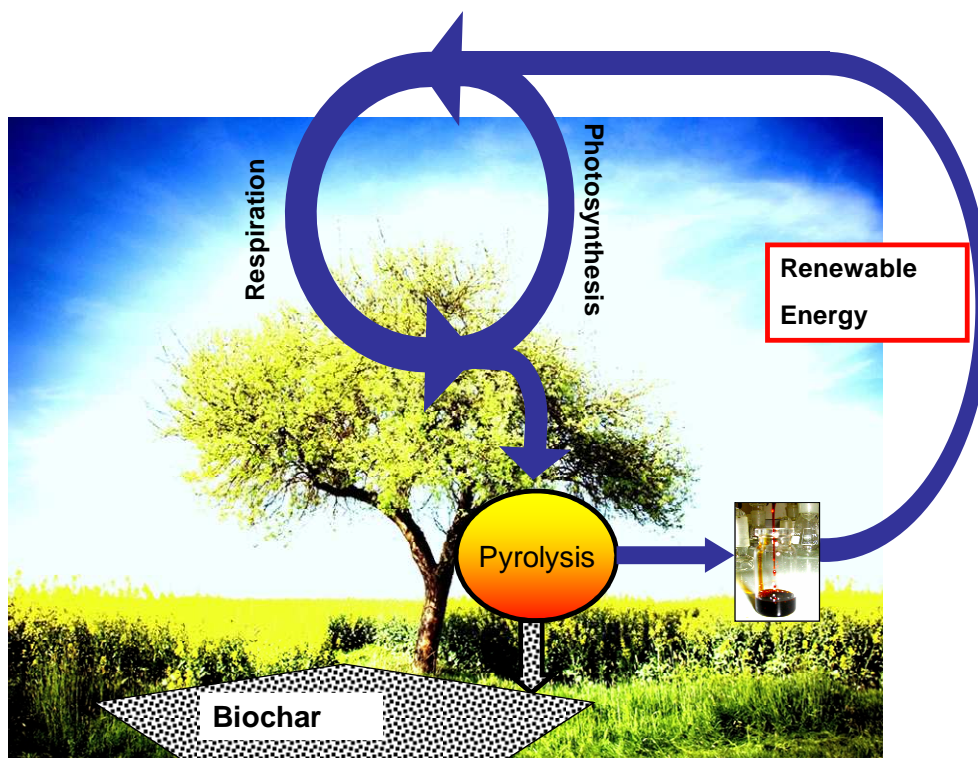
<sup>84</sup> R. Bayerbach, D. Meier. Characterization of the water-insoluble fraction from fast pyrolysis liquids (pyrolytic lignin). Part IV: Structure elucidation of oligomeric molecules). *J. Anal. Appl. Pyrolysis* 85 (2009) 98-107.

<sup>85</sup> H. N. Lima, C.E.R. Schaefer, J.W.V. Mello, R.J. Gilkes, J.C. Ker. Pedogenesis and pre-Colombian land use of “Terra Preta Anthrosols” (“Indian black earth”) of Western Amazonia. *Geoderma* 110 (2002) 1-17.

<sup>86</sup> B. Glaser, E. Balashov, L. Haumaier, G. Guggenberger, W. Zech. Black carbon in density fractions of anthropogenic soils of the Brazilian Amazon region. *Organic Geochemistry* 31 (2000) 669-678.

soils) of crop yields.<sup>87, 88</sup> In the case of terra preta, Amazon climate was extreme and organic carbon input relatively high (due to traditional agriculture practice),<sup>89</sup> but the same idea can be also applied to other tropical (e.g. desertification threatened) areas<sup>90</sup> and in temperate climates with low organic carbon input (as modern soils subjected to intensive farming).<sup>91</sup>

**Figure 1.1.4:** scheme of pyrolysis driven soil carbon sequestration.



The basic idea is to integrate fast pyrolysis with “biochar” soil management: pyrolysis converts forestry branches, grasses or crop residues into carbon rich bio-char and energy (or energy carrier like bio-oil)<sup>92</sup>. Biochar rapidly locks up decomposing carbon into plant biomass in a much more durable form, and then it “artificially” stabilizes organic matter into soil.<sup>93</sup>

<sup>87</sup> B. Glaser, L. Haumaier, G. Guggenberger, W. Zech. The ‘Terra Preta’ phenomenon: a model for sustainable agriculture in the humid tropics. *Naturwissenschaften* 88 (2001) 37-41.

<sup>88</sup> B. Glaser, J. Lehmann, W. Zech. Ameliorating physical and chemical properties of highly weathered soils in the tropics with charcoal – a review. *Biol Fertl Soils* 35 (2002) 219-230.

<sup>89</sup> C. Steiner, W.G. Teixeira, J. Lehmann, T. Nehls, J. Luis, V. de Macêdo, W.E.H. Blum, W. Zech. Long term effects of manure, charcoal and mineral fertilization on crop production and fertility on a highly weathered Central Amazonian upland soil. *Plant and Soil* 291 (2007) 275-290.

<sup>90</sup> T. Whitman, J. Lehmann. Biochar—One way forward for soil carbon in offset mechanisms in Africa?. *Environmental Science & policy* 12 ( 2009) 1024-1027.

<sup>91</sup> C. J. Atkinson, J. D. Fitzgerald, N. A. Hips. Potential mechanisms for achieving agricultural benefits from biochar application to temperate soils: a review. *Plant and Soil* 337 (2010) 1–18.

<sup>92</sup> J.A. Mathews. Carbon-negative biofuels. *Energy Policy* 36 (2008) 940–945.

<sup>93</sup> J. Lehmann, J.O. Skjemstad, S. Sohi, J. Carter, M. Barson, P. Falloon, K. Coleman, P. Woodbury, E. Krull. Australian climate-carbon cycle feedback reduced by soil black carbon. *Nature Geoscience* 1 (2008) 832-835.

As shown above, char represents the most important byproduct of fast pyrolysis. This byproduct is usually burnt to produce the heat required for the pyrolysis reaction (usually endothermic).<sup>34</sup> For high quality woody biomass characterized by low ash content, this option maximizes liquid yield and energy output of the pyrolysis plant, as no external fossil fuel or produced bio-oil are burnt for obtaining the heat required. Nonetheless, biochar represents a problematic fuel, especially for ash containing feedstock (ARs), since the combustion of a fuel rich in low melting point ash (as the major part of annual crops ARs) could determine slagging in the burner<sup>94</sup> and a large production of not easily disposable wastes.<sup>95</sup>

Given these considerations, for the major part of ARs biochar is rich in carbon but poor as fuel, thus it can be advantageous to lose a portion of energy and to store more carbon in the form of biochar applicable on soils. This operational change is similar to the substitution of coal with natural gas in electricity production<sup>96</sup> and, despite a decrease in pyrolysis process economics, can be justified by additional benefits obtainable from agronomic biochar application.<sup>97</sup>

A large number of studies propose the application of char on soil (bio-char strategy, figure 1.2.4) for increasing the soil organic carbon;<sup>98</sup> According to the major part of them, the use of char as bio-char could be an alternative fate for a large range of solid residue products, offering a lower-risk strategy than other sequestration options,<sup>17</sup> in which stored carbon can be released by forest fires, by converting no-tillage back to conventional tillage, or by leaks from geological carbon storage. On local or field scale, biochar can usefully enhance the existing sequestration approaches. It can be mixed with manures or fertilizers and included in no-tillage methods, without the need for additional equipment. Biochar enhances the retention<sup>99</sup> and therefore the efficiency of fertilizers and it decreases fertilizer run-off by the same mechanism.<sup>100</sup> Finally, especially for staple grain crops and acidic and highly weathered soils, a significant increase of crop yields could be obtained.<sup>101</sup>

---

<sup>94</sup> S.Xiong, J.Burvall, H. Örborg, G. Kalen, M. Thyrel, M. Ohman, D. Bostro. Slagging Characteristics during Combustion of Corn Stovers with and without Kaolin and Calcite. *Energy & Fuels* 22 (2008) 3465-3470.

<sup>95</sup> L. Reijnders. Disposal, uses and treatments of combustion ashes: a review. *Resources, Conservation and Recycling* 43 (2005) 313-336.

<sup>96</sup> K. Hayhoe, H. S. Khesghi, A. K. Jain and D. J. Wuebbles. Substitution of Natural Gas for Coal: Climatic Effects of Utility Sector Emissions. *Climatic Change* 54 (2002) 107-139.

<sup>97</sup> B.A. McCarl, C. Peacocke, R. Chrisman, C-C Kung, R.D. Sands. Economics of Biochar Production, Utilization and Greenhouse Gas Offsets. *Biochar for Environmental management*. Johannes Lehmann. Stephen Joseph ed. London 2009.

<sup>98</sup> J. Lehmann, J. Gaunt, M. Rondon. Bio-char sequestration in terrestrial Ecosystems-a Review. *Mitigation and Adaptation Strategies for Global Change* 11 (2006) 403-427

<sup>99</sup> B. Liang, J. Lehmann, D. Salomon, J. Kinyangi, J. Grossman, B. O'Neill, J. Skjemstad, J.O. Thies, F.J. Luzão, J. Petersen, E.G. Neves. Black carbon increases cation exchange capacity in soils. *Soil Sci. Soc. Am. J.* 70 (2006) 1719-1730.

<sup>100</sup> Y. Ding, Y-X Liu, W-X Wu, D-Z Shi, M. Yang, Z-K Zhong. Evaluation of Biochar Effects on Nitrogen Retention and Leaching in Multi-Layered Soil Columns. *Water Air Soil Pollut.* 213 (2010) 47-55.

<sup>101</sup> S.P.Sohi, E. Krull, E. Lopez-Capel, R. Bol. A Review of Biochar and Its Use and Function in Soil. *Advances in Agronomy* 105 (2010) 47-82.

According to recent studies, emission reductions can be 12–84% greater if biochar is put back into the soil instead of being burned to offset fossil-fuel use.<sup>102</sup>

Basically, biochar sequestration offers the chance to turn bioenergy into a real carbon-neutral (and in some cases carbon-negative) industry. Nonetheless, several doubts remain on the table as the pollutant content of modern synthetic biochars, the actual stability of bio-char and the environmental effects of bio-char application in non tropical climates.

Actually, the exact duration of biochar's storage time is under debate, with opinions ranging from millennial (as suggested by some dating of naturally occurring biochar) to centennial timescales (as indicated by some field and laboratory trials).<sup>103</sup> Whether biochar remains in soils for hundreds or thousands of years, it would be considered a long-term sink for the purposes of reducing carbon dioxide emissions.

---

<sup>102</sup> K.G. Roberts, B. A. Gloy, S. Joseph S., N.R. Scott, J. Lehmann. Life Cycle Assessment of Biochar Systems: Estimating the Energetic, Economic, and Climate Change Potential. *Environ. Sci. Technol.* 44 (2010) 827–833.

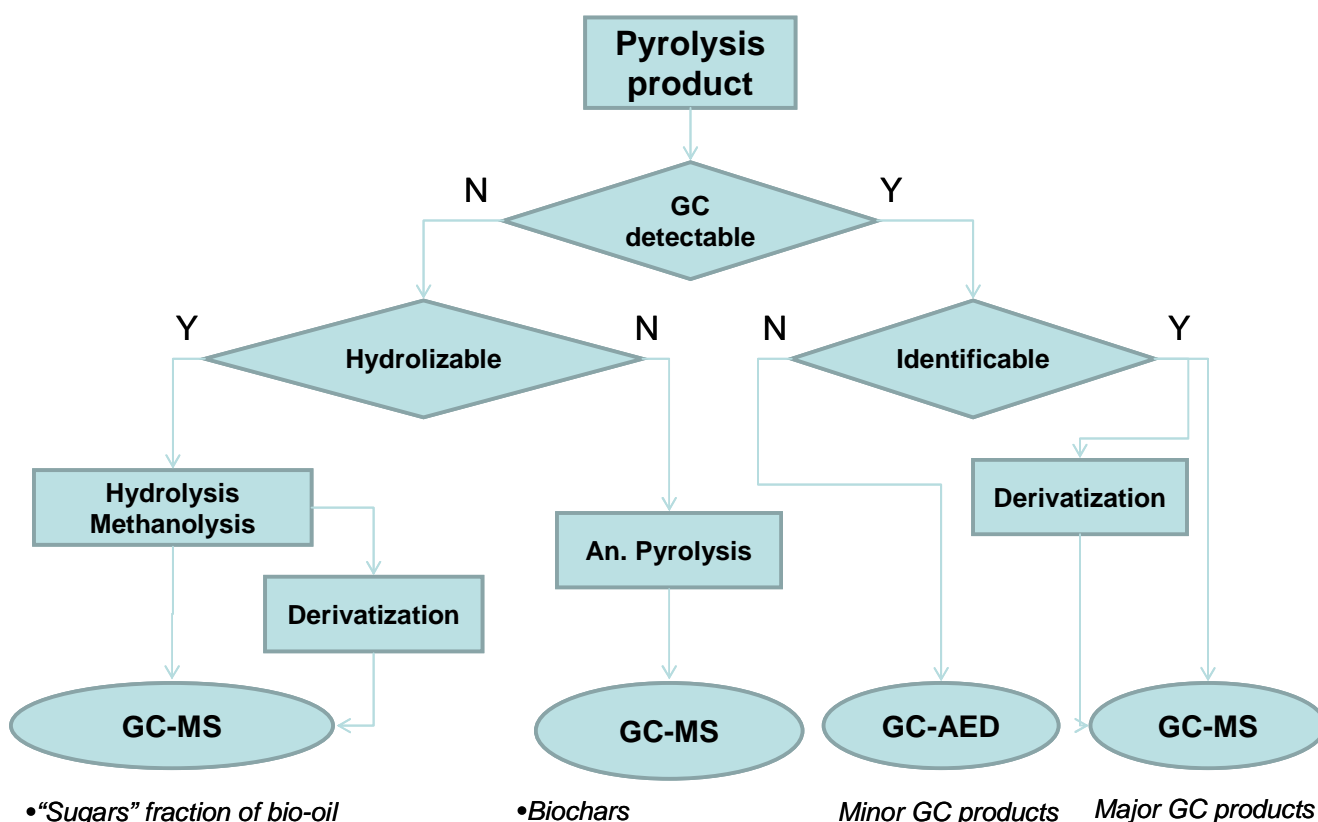
<sup>103</sup> J. Lehmann, C. Czimczik, D.A. Laird . Stability of biochar in soil. In *Biochar for environmental management Biochar for Environmental management*. Johannes lehmann. Stephen Joseph Eds. London 2009.

## 2. Aim of the Thesis

### 2.1 Development of improved analytical pyrolysis techniques.

As shown above, different biomass-to-liquid and biomass-to-chemicals routes need a deep knowledge of bio-oil and bio-char composition. This information is especially important for process optimization and environmental risk assessment.

**Figure 2.1.1:** overall characterization scheme used for pyrolysis products.



Since pyrolysis could be proposed as a method to distributed generation of liquid fuels, bio-oil from different feedstocks should be adequately characterized from an health safety point of view because the contacts with the end-users could be frequent. For this reason this thesis was focused on the development and application of fast and reliable analytical tools to the evaluation of bio-oil and biochar chemical nature.

In order to meet this target, analytical pyrolysis techniques (Py, on milligram scale) were selected, mainly thanks to the large diffusion and low cost/information obtainable through an advanced use of this instrument. In order to overcome the main limitations of this equipment (volatility and stability of analytes), the strategy was to interpose sample preparation steps (SPME or SPE with

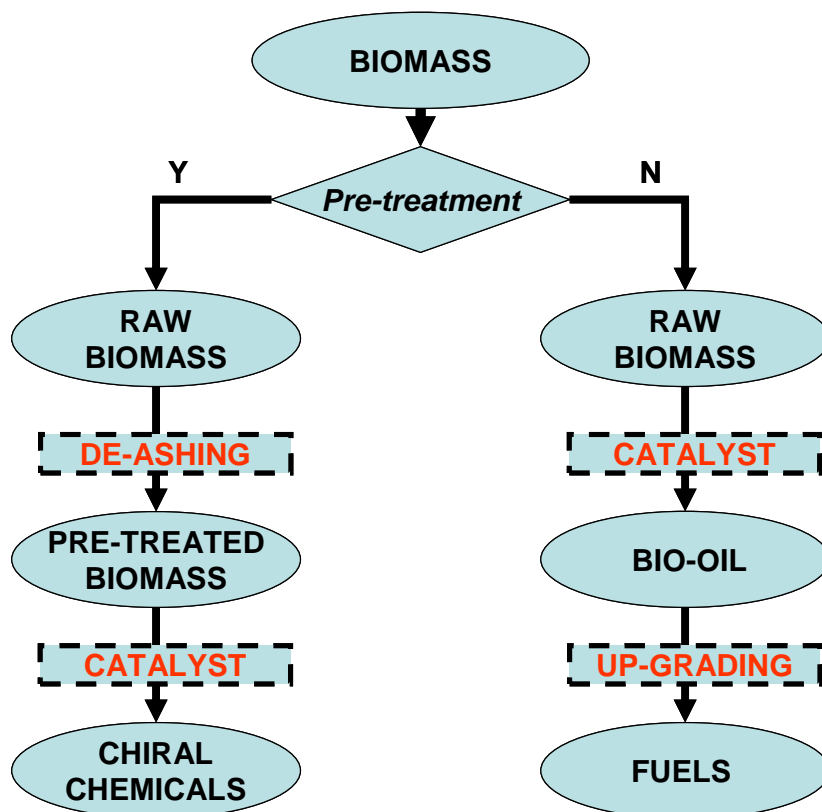
derivatization) and to combine different detectors (MIP-AED and EI-MS). Figure 2.1.1 shows the global characterization scheme used.

For quantification of single identifiable compounds GC, analysis and calibration with internal standard were used. Minor compounds, which are not identified but detectable and GC amenable, were quantified by means of a “structure insensitive” detector like MIP-AED (that allow to obtain the minor compounds carbon yields).

## 2.2 Applied pyrolysis for fuels and chemicals synthesis.

The methods developed in the first part of the thesis was firstly tested on four representative terrestrial biomass (poplar, switchgrass, corn stover and sweet shorgum) selected among most productive short rotation energy crops. Afterwards, the thesis was focused to the study of different “pyrolysis based” routes (Figure 2.2.1), in order to figure out the overall potential of biomass exploiting for: fuel, chemicals and environmental services (e.g. soil improvement through bio-charring).

**Figure 2.2.1:** Two pyrolysis routes and related research aspects (depicted in red) envisaged in this Thesis



In one approach, the study was focused on the conversion of raw biomass into compounds and fuels similar to that derived by fossil fuels, with production of renewable transportation fuels and chemical commodities like benzene and alkylbenzenes. In this case, two feedstock were tested: conventional lignocellulosic biomass and a microalgae residue.

In a different approach, biomass was processed as a source of chiral chemicals with potential higher value added applications. Since the raw biomass is unable to produce significant amount of single target compounds (due to catalytic effect of biomass alkaline ash), the selectivity of the process has to be enhanced by means of pre-treatment and catalysis. Different pre-treatment of cellulosic biomass were tested and catalytic pyrolysis with various mesoporous catalyst was focused on the obtainment of specific chiral chemicals.

## ***3. Development of analytical methods for the study of biomass pyrolysis.***

### **3.1. Comparative Analysis of Pyrolysate from Herbaceous and Woody Energy Crops by micro-scale analytical pyrolysis techniques**

#### **3.1.1. Introduction**

Bio-oil is a very complex mixture containing a large assembly of organic compounds which are formed by the thermal degradation of the main plant constituents (cellulose, hemicellulose, lignin) and other biomolecules originally present in feedstock (e.g. extractives). These compounds may affect fuel characteristics and eco-toxicological properties of the bio-oil. For instance, acidic components (e.g. acetic acid, formic acids, phenols) are mainly responsible for corrosion, polyhydroxylated compounds (e.g. levoglucosan and oligosaccharides) decrease solubility in conventional fuels, reactive aldehydes (e.g. hydroxyacetaldehyde) affect long-term stability and aging of the pyrolysis liquid. Pyrolysis of different crops has been widely investigated over the last decades. A significant dataset on the chemical composition of the resulting bio-oils was gathered through bench scale flash pyrolysis followed by chemical analysis that enabled a detailed knowledge on the effects of feedstock characteristics and experimental conditions on oil quality.<sup>104,105,106,107,108,109</sup>

Nonetheless, an efficient data comparison to evaluate the effect of different feedstock, separately from operational conditions, can be difficult to perform due to different reactor configurations and application of several bio-oil characterization methods. Analytical pyrolysis combined with on-line GC separation (Py-GC) is a simple and reliable micro-scale model of the fast pyrolysis process capable to provide preliminary chemical information on the pyrolysis product yield and

---

<sup>104</sup> D.S. Scott, J. Piskorz. The flash pyrolysis of aspen-poplar wood. *The Canadian journal of chemical engineering* 60 (1982) 666-674.

<sup>105</sup> A. Oasmaa, Y. Solantausta, V. Arpiainen, E. Kuoppala, K. Sipilä. Fast Pyrolysis Bio-Oils from Wood and Agricultural Residues. *Energ. Fuels* 24 (2010) 1380-1388.

<sup>106</sup> A.A. Boateng, D.E. Daugaard, N.M. Goldberg, K.B. Hicks. Bench-Scale Fluidized-Bed Pyrolysis of Switchgrass for Bio-oil Production. *Ind. Eng. Chem. Res.* 46 (2007) 1891-1897.

<sup>107</sup> R. Fahmi, A.V. Bridgewater, I. Donnison, N. Yates, J.M. Jones. The effect of lignin and inorganic species in biomass on pyrolysis oil yields, quality and stability. *Fuel* 87 (2008) 1230-1240.

<sup>108</sup> O. Ioannidou, A. Zabaniotou, E.V. Antonakou, K.M. Papazisi, A.A. Lappas, C. Athanassiou. Investigating the potential for energy, fuel, materials and chemicals production from corn residues (cobs and stalks) by non-catalytic and catalytic pyrolysis in two reactor configurations. *Renewable and Sustainable Energy Reviews* 13 (2009) 750-762.

<sup>109</sup> J. Piskorz, P. Majerski, D. Radlein, D.S. Scott, A.V. Bridgewater. Fast pyrolysis of sweet sorghum and sweet sorghum bagasse. *J. Anal. Appl. Pyrol.* 46 (1998) 15-29.

composition It is well recognised to gather insights and preliminary information on potential compounds derived from bio-oil and thus enables a rapid comparison on the behaviour of different feedstocks, reaction conditions and so forth.

Mass spectrometry under electron ionisation (EI-MS) is the most common detection tool and enables the chemical characterisation of pyrolysate at a molecular level. Py-GC-MS has been utilised to study the effect of such different factors as particle size of herbaceous biomass,<sup>110</sup> physiological maturity in switchgrass pyrolysate,<sup>111</sup> genetic modification poplar clones,<sup>112</sup> chemical pretreatment of corn fibers utilised to ethanol conversion.

However, absolute quantitation (e.g. mass yields) has been seldom conducted and accurate quantitation of all GC detectable compounds is limited by the large number of overlapping constituents with different response factors and the practical impossibility to apply the proper surrogate to each analyte. The precision of different approaches in internal standardisation with Py-GC-MS of lignocellulosic samples has been investigated.<sup>113</sup>

The problem of detection response encountered in MS analysis is less pronounced by utilising carbon atom response, in microwave induced plasma coupled to atomic emission detection (MIP-AED, thereafter named AED), reducing time consuming internal standardisation. Py-GC-AED has been applied to study the pyrolytic behaviour of pine sawdust and the effects of catalysis by metal oxides on pyrolysis product. In these studies pyrolysis products were distinguished by volatility.<sup>114</sup>

It is worthwhile to stress that complementary information can be gathered from MS and AED: the former technique is selective towards structural identification of single components, but needs laborious internal standardization for accurate quantitation; the latter technique is better suited to provide a “bulk picture” of elemental carbon distribution with a simpler calibration approach. However, when interfaced to a GC system, both AED and MS analysis are limited to the detection of gas and semi/volatile compounds. An important fraction of pyrolysate ending up into bio-oil is precluded to GC analysis due to the low volatility of its constituents, such as pyrolytic lignin and oligosaccharides. Nevertheless, the yield of this non-volatile matter (NVM) could be roughly

---

<sup>110</sup> T.G. Bridgeman , L.I. Darvell , J.M. Jones , P.T. Williams , R. Fahmi , A.V. Bridgwater , T. Barraclough , I. Shield , N. Yates , S.C. Thain , I.S. Donnison. Influence of particle size on the analytical and chemical properties of two energy crops. *Fuel* 86 (2007) 60-72.

<sup>111</sup> A.A. Boateng, K.B. Hicks, K.P. Vogel. Pyrolysis of switchgrass (*Panicum virgatum*) harvested at several stages of maturity. *J. Anal. Appl. Pyrolysis* 75 (2006) 55–64.

<sup>112</sup> D. Meier, I. Fortmann, J. Odermatt, O. Faix. Discrimination of genetically modified poplar clones by analytical pyrolysis–gas chromatography and principal component analysis. *J. Anal. Appl. Pyrolysis* 74 (2005) 129.

<sup>113</sup> J. Odermatt , D. Meier, K. Leicht, R. Meyer, T. Runge. Thermal behavior of corn fibers and corn fiber gums prepared in fiber processing to ethanol. *J. Anal. Appl. Pyrolysis* 85 (2009) 11-18.

<sup>114</sup> M.I. Nokkosmäki, A.O.I. Krause, E.A. Leppämäki, E. T. Kuoppala. A novel test method for catalysts in the treatment of biomass pyrolysis oil. *Catalysis Today* 45(1998) 405-409.

estimated in concomitance with Py-GC-AED from the weight determination of the residue left after pyrolysis.<sup>114</sup>

The aim of this study was to evaluate the ability of quantitative Py-GC-MS and Py-GC-AED to predict the main chemical characteristics of bio-oil derivable from different biomass types. Selected feedstock was representative of woody biomass (poplar), agrosidue (corn stover) and dedicated herbaceous energy crops (sweet sorghum and switchgrass).

### 3.1.2. Materials and methods

#### 3.1.2.1 Biomass samples

All biomass but poplar were grown at the experimental station of the University of Bologna. Poplar chips were purchased from Alasia Franco Vivai. All plants were grown in the Po Valley. For all crops, 300 g samples of three independent replications were collected, dried at 60 °C for 48 h and then grounded in a hammer mill to pass a 1 mm screen before chemical analysis. Biomass were characterized for major constituent (Table 3.1.1) and elemental composition (Table 3.1.2).

**Table 3.1.1:** main characteristics of the tested biomasses, major constituent are reported as %  $m_i/m_{\text{sample}}$ .

<i>Biomass</i>	<i>Cyotype</i>	<i>Water</i>	<i>Soluble matter</i>	<i>Hemi-cellulose</i>	<i>Cellulose</i>	<i>Lignin</i>	<i>Ash</i>
<b>Switchgrass</b>	Alamo	4.8	3.5	37.1	42.5	8.5	3.8
<b>Sweet Sorghum</b>	H133 hybrid	8.3	24.2	27.4	29.9	5.6	4.6
<b>Corn stover</b>	PR33A46	6.6	12.2	27.8	41.4	5.0	7.1
<b>Poplar</b>	-	8.4	0.3	20.0	54.1	15.1	2.1

The water content was obtained by weight loss during drying biomass at 105°C to constant mass. Ash content was determined by burning at 550°C of 1 g of dried (60°C) and ground (size 1 mm) sample. The weight amount of soluble sugars (e.g. free sugars starch and pectins), lignin, cellulose and hemicellulose was determined following a published procedure.<sup>115</sup> Briefly, the sequential analysis involved refluxing in neutral detergent (using  $\alpha$ -amylase for removal of soluble polymeric components like starch and pectins), refluxing in acid detergent, hydrolysis with 72% aqueous

<sup>115</sup> S. Mambelli, S. Grandi. Yield and quality of kenaf (*Hibiscus cannabinus L.*) stem as affected by harvest date and irrigation. Industrial Crops and Products 4 (1995) 97-104.

H<sub>2</sub>SO<sub>4</sub>. The fibre fractions were estimated from the loss of dry matter following each step of the analysis.

Table 3.1.2 shows the elemental composition of tested biomass. Carbon, hydrogen, and nitrogen content analysis was performed using a microelemental analyzer (LECO CHN-600), oxygen content of samples was calculated by difference between 100% and sum of carbon, hydrogen, nitrogen and ash.

**Table 3.1.2:** elemental composition ( mass %) of tested biomass by CHN elemental analysis of sample.

	<i>C</i>	<i>H</i>	<i>O</i>	<i>N</i>
<b>Switchgrass</b>	46.5	6.0	43.4	0.3
<b>Sweet sorghum</b>	43.6	5.7	45.1	1.0
<b>Corn stover</b>	45.0	5.9	41.3	0.7
<b>Poplar</b>	47.8	6.1	43.5	0.5

### 3.1.2.2 Py-GC-MS

The pyrolysis unit was a CDS Pyroprobe 1000 pyrolyser connected to a Varian 3400 gas chromatograph equipped with a Varian Saturn 2000 mass spectrometer.

A weighed amount of biomass sample (2-3 mg) was introduced into the quartz tube, and held by quartz wool at the middle portion of the tube. The tube was then placed in the platinum filament coil on the probe. Quartz wool that hold the sample was spiked with 0.1 µg ( 5 µl at 200 ng µl<sup>-1</sup> solution in diethyl ether) of *o*-eugenol (internal standard). The probe was inserted into the Py-GC interface, then the interface was pressurized, fluxed with 100 ml min<sup>-1</sup> helium and then warmed up to 300 °C . When the interface reached the set temperature, the platinum coil was immediately heated at the maximum heating rate to pyrolysis temperature (500 °C); 1/200 split ratio and injector temperature of 280°C were used.

Analytes were separated on a HP-5MS fused-silica capillary column (stationary phase polydimethylsiloxane, 30 m, 0.25 mm i.d., 0.25 mm film thickness) using helium as carrier gas. The following thermal program was used: 35°C for 2.5 minutes, then 10 °C/min until 300 °C. Quantitation was performed in the MS mode using the most abundant ion of each compound. Amount (m<sub>i</sub>) of each analyzed compound was calculated using internal calibration performed by injecting 5 µl of calibration solution containing known concentrations of representative analytes (e.g. acetic acid, hydroxyacetone, 2-cyclopentanedione, furfuraldehyde, furfuryl alcohol, 5-methyl-2-furfuraldehyde, phenol, syringol) and internal standard dissolved in acetonitrile under the same conditions used for pyrolysis.

Mass yields of each analyzed compound was calculated as  $m_i/m_{\text{sample}}$ , where  $m_i$  is the compound amount produced by pyrolysis and  $m_{\text{sample}}$  the mass of pyrolysed sample.

Carbon yield for single GC-MS analyzed compounds was obtained as  $(m_i/m_{\text{sample}}) \cdot ([C]_{\text{compound}}/[C]_{\text{biomass}})$ , where  $[C]_{\text{compound}}$  is the carbon mass fraction of the compound (obtained from chemical structure) and  $[C]_{\text{biomass}}$  carbon mass fraction from elemental composition of biomass (Table 3.1.2).

### 3.1.2.3 Off-line pyrolysis/GC-MS

The apparatus employed for off-line pyrolysis experiments was described in detail elsewhere<sup>116</sup>. Shortly, it consisted of a glass tube (pyrolysis chamber) designed for the probe of a CDS 1000 pyroprobe equipped with a resistive heated platinum filament. CDS 1000 pyroprobe is inserted in the glass, the exit was connected through a Tygon® tube to a cartridge for air monitoring containing a XAD-2 resin as adsorbent (ORBO-43® purchased from Supelco). The pyrolysis probe was recalibrated with a thermocouple (in order to correct the thermal deficit due do absence of heated Py-GC interface), and the sample was pyrolysed exactly with the same conditions used in on-line Py-GC. For analysis of all compound but hydroxyacetaldehyde, after pyrolysis, the pyrolysis chamber was filled with 5 ml of acetonitrile allowing the solution to pass slowly through the cartridge. The obtained solution was spiked with 0.1 ml of 500 mg l<sup>-1</sup> methyl-L-β-arabinopyranoside solution (internal standard). An aliquot of the acetonitrile solution (0.1 ml) was spiked with, 50 μl of *bis*-trimethylsilyltrifluoroacetamide with 1% tetramethylchlorosilane (sigma-aldrich) and 10 μl of pyridine, then heated at 60°C for 0.5 h and injected in GC-MS.

For hydroxyacetaldehyde the following method was performed: the chamber and the cartridge were eluted twice with 2 ml methanol, the resulting 4 ml solution was placed in a vial containing 200 mg of amberlyst® acidic resin. Then the vial was sealed and heated at 60°C for 0.3 h and hydroxyacetaldehyde was quantitated as dimethyl-acetal derivative by GC-MS.

Quantitation of dimethylacetal derivative of hydroxyacetaldehyde was performed using a external calibration plot, obtained by submitting solutions of hydroxyacetaldehyde dimer of known concentration to the dimethyl-acetalization procedure as shown above.

GC-MS analysis were performed in splitless mode using the same conditions used for Py-GC-MS. The following thermal program was used: 50°C for five minutes, then 10°C/min until 300°C followed by a column cleaning at 310°C for 3 min.

---

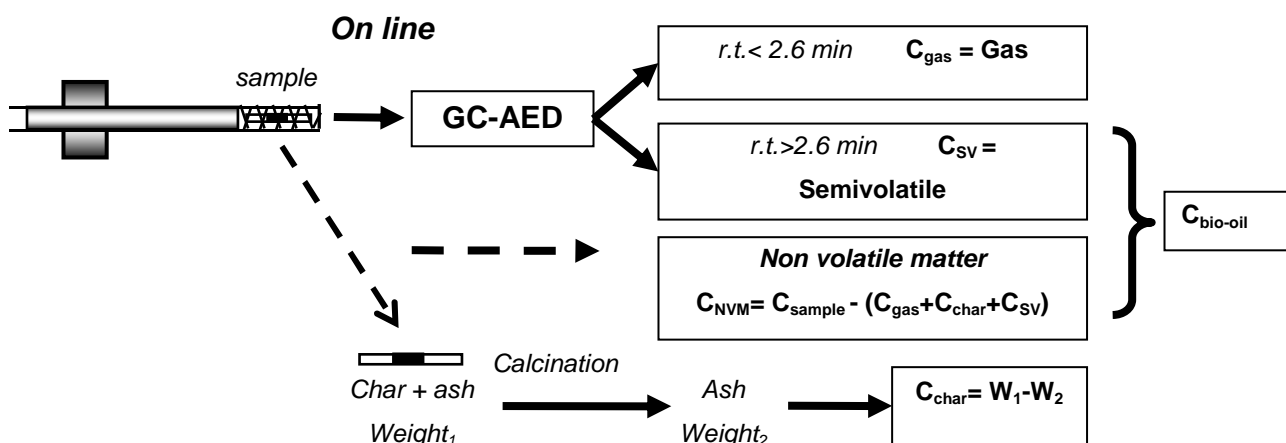
<sup>116</sup> D. Fabbri, I. Vassura. Evaluating emission levels of polycyclic aromatic hydrocarbons from organic materials by analytical pyrolysis. *J. Anal. Appl. Pyrol.*75 (2006) 150-158.

### 3.1.2.4 Py-GC-AED

The pyrolysis unit was a CDS Pyroprobe 1000 pyrolyser connected to an HP 5890 Series II gas chromatograph, and detection was carried out with an HP 5921A atomic emission detector.

Figure 3.1.1 summarises the analytical procedure used for on line Py-GC-AED. The apparatus employed for Py-GC-AED experiments was described in detail elsewhere<sup>114</sup>.

**Figure 3.1.1:** Scheme of the Py-GC-AED pyrolysis procedure.



A weighed amount of sample (2-3 mg) was introduced into the quartz tube, and held by quartz wool at the middle portion of the tube. The probe was inserted into the Py-GC interface, then the interface was pressurized, fluxed with helium ( $100 \text{ ml min}^{-1}$ ) and then warmed up to  $300 \text{ }^\circ\text{C}$ . When the interface reached the set temperature, the platinum coil was immediately heated at maximum heating rate to pyrolysis temperature ( $500 \text{ }^\circ\text{C}$ ); 1/100 split ratio and injector temperature of  $280^\circ\text{C}$  were used.

GC analysis were performed as for Py-GC-MS, and AED spectra for C was recorded at  $193.090 \text{ nm}$ . Carbon amounts of GC detectable compounds were calculated using external calibration performed by injecting known volumes of  $60 \text{ g l}^{-1}$  isopropanol solution in methanol under the same conditions used for pyrolysis.

The results were summarized by distinguishing pyrolysis products on the base of their volatility. Retention time was used as reference to discriminate between gaseous (first large peak at 2.6 min), and sum of condensable GC detectable compounds, reported as semi-volatile fraction (obtained integrating all peaks after large first peak of gases). Char amount was evaluated after GC analysis in the following way: the interface was cooled down, the quartz tube was removed from the probe and weighed. Then, the sample was placed in muffle oven at  $550 \text{ }^\circ\text{C}$  for 5 h and re-weighed. The char amount was calculated from the difference in sample weight before and after burning the char into the muffle. The char was assumed to be composed of nearly pure carbon.

Carbon yield of each fraction was calculated as  $C_i/C_{\text{sample}}$ , where  $C_i$  carbon amount of each fraction obtained from GC-AED data and gravimetric data (char). Carbon amount of sample ( $C_{\text{sample}}$ ) was calculated as  $C_{\text{sample}}=[C]_{\text{biomass}} \cdot m_{\text{sample}}$ , where  $[C]_{\text{biomass}}$  is carbon mass fraction of the biomass, obtained from Table 3.1.2 (shown above in paragraph 3.1.2.1).

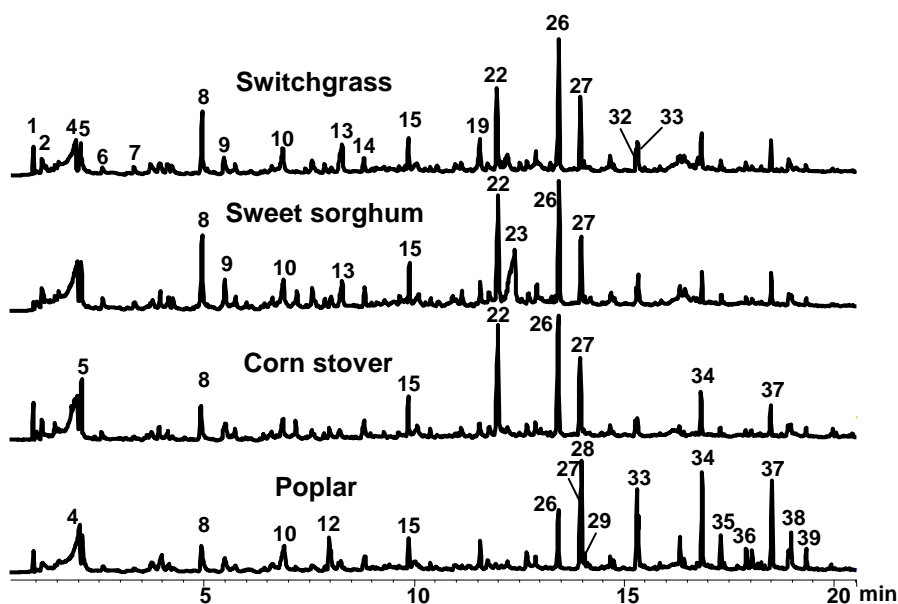
Carbon amount of NVM ( non volatile matter), here considered the sum of pyrolytic lignin and water soluble non volatile matter was calculated by difference between  $C_{\text{sample}}$  and sum of carbon amounts of bio-oil, carbon residue and gas.

### 3. Results

#### 3.1.3.1 Py-GC-MS

Typical chromatograms obtained from the analysis of the four biomass types are shown in Figure 3.1.2 with peak identification reported in Table 3.1.3.

**Figure 3.1.2:** Chromatograms obtained from Py-GC-MS of four tested biomass samples.



Quantitation of main compounds (see Table 3.1.3) was accomplished by comparison with internal standard. Internal standardisation in analytical pyrolysis of complex heterogeneous biomass samples is not an easy task and we have followed one of the approaches investigated by Odermatt *et al.*<sup>113</sup> An internal standard structurally similar to lignin pyrolysis products, namely *o*-isoeugenol (# 27) was selected. Besides lignin monomers, the same compound was used for the quantitation of pyrolysis products of polysaccharides utilising the response factors of representative compounds (see experimental).

**Table 3.1.3:** Mass yield (%  $m_i/m_{\text{sample}}$ ) of main pyrolysis products obtained from Py-GC-MS of four tested biomass.

#	<i>Compound</i>	<i>Switchgrass</i>	<i>Sweet sorghum</i>	<i>Corn Stover</i>	<i>Poplar</i>
1	methanol	0.11	0.01	0.10	0.13
2	methyl glyoxal	0.59	0.92	0.53	0.82
3	3-pentanone	0.46	0.44	0.39	0.71
4	acetic acid	2.4	2.7	2.6	3.1
5	hydroxyacetone	2.1	2.3	1.7	2.0
6	acetoxymethyl acetate	0.35	0.69	0.68	1.48
7	butanedial	0.71	0.62	0.65	1.95
8	furfural	0.13	0.15	0.07	0.08
9	furfurilic alcohol	0.03	0.06	0.03	0.05
10	2-cyclopentanedione	0.52	0.49	0.40	0.84
11	methyl furfural	0.01	0.01	0.00	0.01
12	phenol	0.03	0.06	0.06	0.33
13	4-hydroxy-5,6-dihydro-(2H)-pyranone	0.77	0.62	0.18	0.31
14	2-hydroxy-3-methyl-2-cyclopentenone	0.18	0.20	0.29	0.30
15	2-methoxyphenol	0.09	0.09	0.13	0.14
16	3-methyl-2,4(3H,5H)-furan	0.10	0.07	0.05	0.09
17	4-ethylphenol	0.02	0.03	0.03	-
18	anhydro isosaccharin- $\delta$ -lactone	0.07	0.02	0.03	0.02
19	4-methylguaiacol	0.06	0.03	0.03	0.08
20	catechol	0.03	0.04	0.05	0.07
21	1,4-3,6-dianhydro- $\alpha$ -glucopyranose	0.10	0.12	0.09	0.08
22	4-vinylphenol	0.47	0.50	0.62	0.01
23	5-hydroxymethyl-2-furaldehyde	0.21	0.93	0.09	0.07
24	4-ethylguaiacol	0.05	0.05	0.05	0.05
25	ascopyrone-P	0.02	0.01	0.00	0.01
26	4-vinylguaiacol	0.53	0.36	0.51	0.25
27	<i>o</i> -eugenol (IS)	-	-	-	-
28	syringol	0.13	0.13	0.25	0.67
29	eugenol	0.01	0.01	0.01	0.03
30	vanillin	0.03	0.02	0.02	0.03
31	<i>E</i> -isoeugenol	0.01	0.01	0.00	0.02
32	4-methylsyringol	0.04	0.02	0.03	0.27
33	<i>E</i> -isoeugenol	0.06	0.04	0.03	0.18
34	4-vinylsyringol	0.07	0.05	0.11	0.63
35	<i>Z</i> -2-propenylsyringol	0.01	0.01	0.01	0.09
36	<i>E</i> -2-propenylsyringol	0.01	0.01	0.01	0.05
37	allylsyringol	0.06	0.05	0.06	0.41
38	4-hydroxy-2-methoxy cinnamaldehyde	0.01	0.01	0.01	0.02
39	acetosyringone	0.02	0.01	0.02	0.07
	<b>Sum Py-GC-MS (<math>\Sigma m_i/m_{\text{sample}}</math>)</b>	<b>10.6</b>	<b>11.9</b>	<b>9.9</b>	<b>15.5</b>

For almost all the compounds the RSD of yields were in the 13-35% range for switchgrass, poplar and corn (n=3). Higher RSD (35-70%) values were found for sweet sorghum pyrolysis, probably due to a higher heterogeneity of biomass sample. Furthermore, quantitation of some polar compounds (acetoxyacetaldehyde, ascopyrone P and 1,4:3,6-dianhydroglucopyranose and hydroxy-5,6-dihydro-(2H)-pyranone) showed a large variability (RSD 40-70%). It is known that the pyrolysate composition can be affected by several factors that become crucial when analyses are performed with small amount of sample. For instance, it has been shown that smaller biomass particles may contain higher amount of ash and lignocellulose products with respect to coarse size fraction.<sup>110</sup>

By a glance at Figure 3.1.2, it is clear that largest differences occur between herbaceous and wood biomass. As shown by Ralph et al.,<sup>117</sup> the chromatograms of herbaceous plants were characterised by vinylphenol (#22), as the main lignin derivative, with yields around 0.5%, in accordance to the lignin being of type HGS (hydroxyphenyl/guaiacyl/syringyl groups). Vinylguaiacol was an other typical lignin constituent detected at rather high levels in the pyrolysate of herbaceous biomass (0.4-0.5% yield). Vinylphenol was a minor pyrolysis product evolved from poplar in accordance to GS type lignin characterising this plant.

As far as the thermal degradation products of holocellulose is concerned, the main compound quantified by Py-GC-MS was acetic acid with 3.1%, 2.7%, 2.6% and 2.4 % yields obtained from pyrolysis of poplar, sweet sorghum, corn stover and switchgrass respectively. Hydroxyacetone (acetol) is the second most abundant pyrolysis product. These data are consistent with preparative pyrolysis and those reported in a previous studies.<sup>104,106,109</sup> Although the same studies reported relatively high yields of hydroxyacetaldehyde, this compound could not be detected with the Py-GC-MS procedure adopted here. The pyrolysate of sweet sorghum is unique for the occurrence of a prominent peak of 5-hydroxymethyl-2-furaldehyde (HMF, #23), a typical pyrolysis product of reducing sugars.<sup>118</sup> This is probably due to the high content of soluble sugars (24% from Table 3.1.1) that characterize sweet sorghum.

### 3.1.3.2 Off-line Py/GC-MS

Besides the compounds that could be analyzed directly by Py-GC-MS, off-line Py/GC-MS with two derivatisation procedures (dimethyl-acetalization for reactive aldehydes and silylation for highly polar compounds) was applied, in order to extend the range of detectable compounds to more polar

---

<sup>117</sup> J. Ralph, R.D. Hatfield. Pyrolysis, Pyrolysis-GC-MS Characterization of Forage Materials. Journal of Agric. Food Chem. 39 (1991) 1426-1437.

<sup>118</sup> E.B. Sanders, A.I. Goldsmith, J.I. Seeman. A model that distinguishes the pyrolysis of D-glucose, D-fructose, and sucrose from that of cellulose. Application to the understanding of cigarette smoke formation. J. Anal. Appl. Pyrol. 66 (2003) 29-50.

species. The results from quantitative off-line pyrolysis are reported in Table 3.1.4. Yields of levoglucosan were rather low for all the tested biomass, with the highest value of 0.51% w/w<sub>sample</sub> from switchgrass pyrolysis. Other important oxygenated compounds revealed by silylation were 1,3-dihydroxy-propanone, D-ribofuranose, hydroxy acetic acid (0.05-0.26 % yield) and glyceraldehyde (0.11 % yield from switchgrass) (Table 3.1.4). Significant amount of trihydroxybenzenes and aromatic acids were also revealed by silylation.

Moreover, with all the samples, a variable but important amount (0.5-0.2 % not shown in the table) of hydroxyacetaldehyde (HA) dimer was revealed by silylation. This fact was surprising considering that GC peak attributable to monomer HA were not detected by Py-GC-MS.

HA is often reported as the largest abundant compound in bio-oil and could be detected with polar chromatographic column<sup>119</sup> however, HA is actually rarely reported in literature as predominant compound by Py-GC-MS of biomass.

**Table 3.1.4:** Yield (% w/w<sub>sample</sub>) of main pyrolysis products obtained by off-line pyrolysis followed by methanolysis (reactive aldehydes) or silylation (other oxygenates) and GC-MS analysis.

#		Switchgrass	Sweet sorghum	Corn stover	Poplar
1	hydroxyacetaldehyde <sup>a</sup>	3.7	2.4	2.24	3.0
2	glyoxal <sup>a</sup>	0.1	0.1	0.1	0.2
3	ethanediol	0.15	0.07	0.25	0.02
4	lactic acid	0.06	0.07	0.04	0.01
5	hydroxyacetic acid	0.26	0.15	0.07	0.05
6	glyceraldehydes	0.11	0.03	0.02	0.01
7	1,3-dihydroxypropanone	0.20	0.14	0.04	0.02
8	ribofuranose	0.25	0.09	0.15	0.01
9	4-hydroxybutanoic acid	0.05	0.00	0.04	0.00
10	(1,3,4)-trihydroxybenzene	0.07	0.02	0.02	0.01
11	(1,2,3)-trihydroxybenzene	0.08	0.02	0.02	0.01
12	levoglucosan	0.51	0.33	0.22	0.27
13	<i>p</i> -hydroxycinnamic acid	0.03	0.01	0.02	0.01
	<b>Sum off-line Py/GC-MS</b>	<i>5.64</i>	<i>3.40</i>	<i>3.21</i>	<i>3.61</i>

<sup>a</sup> derivatized through methanolysis and analyzed as dimethyl-acetal derivative.

First tentative of quantifying HA by direct Py-GC-MS analysis, off-line pyrolysis or off-line pyrolysis coupled to silylation was frustrating, mainly due to low molecular weight combined to the extraordinary reactivity of HA.

<sup>119</sup> AA. Boateng, C.A. Mullen, C.M. McMahan, M.C. Whalen, K. Cornish. Guayule (*Parthenium argentatum*) pyrolysis and analysis by PY-GC/MS. *J. Anal. Appl. Pyrolysis* 87 (2010) 14-24.

In fact, HA can react easily with itself (forming a dimer clearly distinguishable in sylilation), with water or other hydroxyls, potentially giving a large number of chemical species . The difficulty to obtain HA in the monomeric form (the only pure commercial standard is obviously in dimer form) further complicates the direct analysis of this compound.

In order to solve these analytical problems, a dimethyl-acetalization procedure was tested by reaction with methanol over solid acid catalyst. After dimethyl-acetalization, HA was revealed in the form of dimethoxy-2-ethanol as the most abundant GC detectable compound evolved from switchgrass (3.7% yield) and in relatively high yields from the other biomass.

### 3.1.3.3 Py-GC-AED

In order to obtain of better mass balance, Py-GC-AED procedure was utilised to compare different biomass typologies. Each biomass was analysed in triplicate, and the resulting RSD associated to the yield of gas and semivolatiles were less than 5%, indicating a good precision of the method. The yields of these fractions are reported in Table 3.1.5.

**Table 3.1.5:** Carbon yields of the fractions (% C<sub>i</sub>/C<sub>sample</sub>) from Py-GC-AED of four tested biomass.

	<i>Switchgrass</i>	<i>Sweet sorghum</i>	<i>Corn stover</i>	<i>Poplar</i>
	% C/C <sub>sample</sub>	% C/C <sub>sample</sub>	% C/C <sub>sample</sub>	% C/C <sub>sample</sub>
<b>Semivolatile</b>	24	21	19	26
<b>NVM<sup>a</sup></b>	29	23	27	24
<b>Bio-oil<sup>b</sup></b>	53	44	46	50
<b>Gas</b>	10	10	11	11
<b>Char</b>	37	46	43	40

<sup>a</sup> Calculated as: C<sub>sample</sub>-(C<sub>gas</sub>+C<sub>char</sub>+C<sub>semivolatile</sub>);<sup>b</sup> calculated as: C<sub>semivolatile</sub> +C<sub>NVM</sub>.

Gas carbon yields were 10-11 % for all biomass samples. Considering that gas consist mainly of carbon monoxide and carbon dioxide, gas mass yields were in agreement with mass yields range reported in the literature (from lab scale pyrolysis tests under different conditions). For instance, 12-26% for sorghum,<sup>109</sup> 7-13% switchgrass,<sup>111</sup> 14-63% corn stalk,<sup>108</sup> 9-17% poplar<sup>104</sup>.

Poplar yielded the largest quantity of semi-volatile substances (26% carbon yield) followed by switchgrass (24%), sweet sorghum (21%) and corn stover (19%).

The solid residue left after pyrolysis (char) was determined gravimetrically after pyrolysis and calcination. Char mass yields from corn stover, sweet sorghum, poplar and switchgrass were 21%, 19%, 19% and 17% by weight. These value were slightly higher than char yields obtained with flash bench scale pyrolysers.<sup>104,105,106,107,108,109</sup> Nevertheless, this can be due to differences in mass transfers between different systems (this aspects was investigated in chapter 3.5). On carbon basis

(Table 3.1.5), obtained results showed that, in Py-GC systems, 37-46% of pyrolysed carbon is turned into carbonaceous residue. Corn stover and sweet sorghum gave the highest production of solid residue and were characterised by the highest levels of both ash and nitrogen. Interestingly, for all tested biomass, char yields showed the best correlation with nitrogen content (Table 3.1.2), with higher char yield from nitrogen richer materials.

NVM was determined by difference from the amount of all the other fractions. Absolute carbon yields of NVM were similar for all tested biomass with values in the 23-29% range, with slightly higher values for switchgrass and corn stover (29% and 27%).

#### *3.1.3.4 Prediction of bio-oil yields and composition from Py-GC-MS, off-line Py/GC-MS and -AED.*

The results coming out from Py-GC-MS and Py-GC-AED were integrated on a carbon basis in order to predict the composition of a “virtual bio-oil” derived from the four biomass samples under the same pyrolysis conditions. To this purpose mass yields from MS data were turned into yields on a carbon basis from the knowledge of the molecular mass of each individual compound.

Percent carbon basis concentration in the bio-oil ( $\%C/C_{\text{bio-oil}}$ ) were calculated from the yields utilising the yields of bio-oil evaluated from Py-GC-AED summing up semivolatiles and NVM.

The carbon yields of bio-oil, reported in Table 3.1.4, were highest for switchgrass (53%) and poplar (50%), where lower values were obtained for corn stover and sweet sorghum (46% and 44%).

Figure 3.1.3 shows the bio-oil composition on carbon basis inferred from Py-GC-MS, Py/GC-MS and Py-GC-MS-AED.

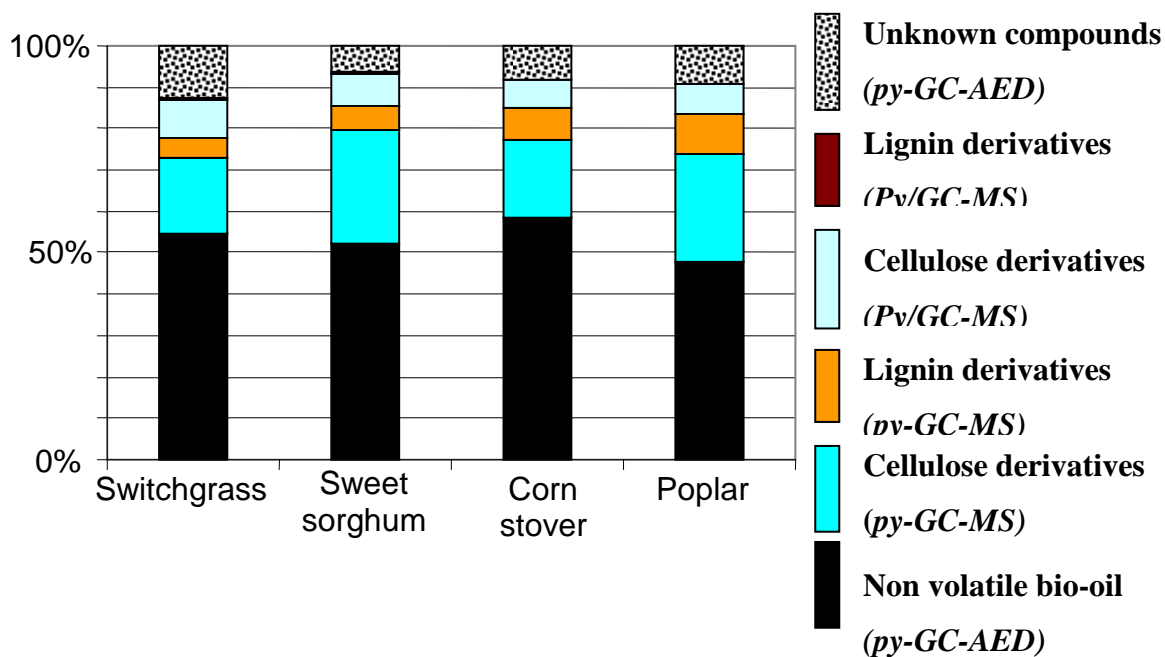
Py-GC-MS data accounted for a relatively minor fraction of pyrolysis oil constituents (23-35%  $C/C_{\text{bio-oil}}$ ). These compounds consisted mainly of carbohydrate derivatives formed by thermal degradation of cellulose and hemicellulose (26-35%  $C/C_{\text{bio-oil}}$  revealed by both derivatization-GC-MS and direct GC-MS) which included abundant single components, such as acetic acid, hydroxyacetaldehyde and acetol. The highest content of carbohydrate pyrolysis products was found in poplar bio-oil (33%) and sweet sorghum (35%), but for different reasons. Poplar wood was characterised by the highest content of cellulose (54%, Table 3.1.1) and the lowest ash content, whereas sorghum by the highest content of soluble matter (24%) rich in reducing sugars as confirmed by the high levels of 5-hydroxy-2-methylfuraldehyde.

The level of lignin monomers was the highest in poplar pyrolysate (9.8%) in accordance to abundance of lignin in the original biomass (54%). In the case of herbaceous biomass, the content of lignin monomer ranged from 5.7% (switchgrass) to 7.5% (corn stover) without a strong correlation with the lignin content, probably due to the effect of alkali metals on the thermal degradation of lignin.<sup>105</sup>

The remaining fraction of semivolatile compounds (16%-22%) could be globally determined by difference from Py-GC-AED data. This fraction is composed by the myriad of minor compounds that could not be identified by MS. The last fraction which accounted for about half the bio-oil carbon was formed by compounds not amenable to GC elution (NVM), such as pyrolytic lignin and poly/oligosaccharides. These substances evolved out the biomass sample following flash pyrolysis, but were trapped into the Py-GC interface due to low volatility and slow mass transfer. However, NVM presumably ends up into bio-oil under preparative pyrolysis conditions. The relative content of NVM, which is detrimental to bio-oil quality, was highest for corn stover (59%) and lowest for poplar (49%). Switchgrass and sorghum yielded intermediate quality products, with 55% and 53%  $C_{NVM}/C_{bio-oil}$ , respectively.

Considering all these aspects, poplar would provide the bio-oil with the best quality in terms of lower NVM concentration and higher level of lignin monomer. In addition, this woody feedstock is characterised by the lowest content of ash. Among herbaceous biomass, switchgrass is seemingly more promising in terms of higher bio-oil production with intermediate NVM and lignin concentration, and low ash and nitrogen content in the feedstock.

**Figure 3.1.3:** Predicted “carbon based” composition ( $C/C_{bio-oil}$ ) of bio-oil from Py-GC-MS (lignin monomers and carbohydrate derivatives), off line Py/GC-MS (polyhydroxylated phenols and polar cellulose derived compounds) and Py-GC-AED (NVM, other semivolatiles).



#### **4. Conclusions**

Quantitative off-line and on-line analytical pyrolysis coupled with AED and MS detection provided a set of complementary data useful to perform a comparative evaluation of the organic pyrolysate from different biomass based on carbon yields. The Py-GC-AED method was more precise than Py-GC-MS, probably because the yields are susceptible to sample heterogeneity in the case of individual compounds more than the overall fraction.

The application of AED and MS detection to samples representative of woody biomass (poplar), sugar rich biomass (sweet sorghum), waste and ash-rich biomass (corn stover) and herbaceous energy crop (switchgrass) enabled a fruitful comparison. No large differences in the yield of main macroscopic fractions (gas, char and liquid) were observed despite the differences in the composition of original feedstock a result that favours pyrolysis as a versatile conversion process. The main differences in the chemical composition of pyrolysate were associated with type (HGS or GS) and quantity of lignin, and with soluble sugars in the feedstock. Ash content is notoriously an important parameter, but no definitive trends were observed with carbon yields.

Finally, this work showed that non volatile matter eluding GC detection accounted for about half of the bio-oil components. For this reason, the knowledge of the chemical composition of this important fraction represents both a limitation as well as challenging objective of analytical pyrolysis.

## 3.2. Application of off-line pyrolysis with dynamic solid-phase microextraction to the GC-MS analysis of volatile biomass pyrolysis products

### 3.2.1. Introduction

As demonstrated in the previous chapter, the coupling of off-line and on-line pyrolysis with different detectors (MS and AED) and different derivatization procedures (silylation and dimethyl-acetalization) provide chemical information on a wide range of compound classes.

Nevertheless, analysis of the most volatile compounds (e.g. methanol), and especially reactive volatiles (e.g. hydroxyacetaldehyde) in both on-line and off-line represent a difficult task for different reasons, such as peak overlapping, non instantaneous pyrolysis time (for low temperature on-line pyrolysis), solvent interference (in off-line pyrolysis with adsorbent) and strong reactivity of some compounds (e.g. hydroxy aldehydes in some pyrolysis equipments). Regarding the latter aspect, problems in the analysis of hydroxyacetaldehyde were discussed in previous section (chapter 3.1).

The quantification of more volatile compounds could be accomplished by means of a cryogenic trap,<sup>120</sup> in order to avoid peak broadening caused by the intrinsic duration of the pyrolytic reaction (particularly longer with low temperature pyrolysis). As a cost-effective solution, solid-phase microextraction (SPME) could be used as a solvent free technique for sampling pyrolysis products, and then could be used for de-coupling of pyrolysis and analysis. Moldoveanu has recently investigated the use of SPME combined with pyrolysis.<sup>121</sup> Pyrolysis was conducted with a heated coil pyrolyser inside a glass sampling vial that was closed to perform SPME (static SPME). This method provided qualitative information on the pyrolysis products avoiding the use of solvents in the off-line configuration and GC column deterioration typical of on-line pyrolysis-GC/MS. The main drawback was the necessity of long sampling time in order to detect heavier pyrolysis products.

Sampling the gas flow in a open system could be an alternative approach of SPME yet to be investigated in analytical pyrolysis. This technique does not need the complete trapping of volatiles and eliminates some of the problems of static SPME, like matrix effects, interaction with inner

---

<sup>120</sup> J.B. Paine III, J.B. Pithawalla, J.D. Naworal. Carbohydrate pyrolysis mechanisms from isotopic labeling Part 2. The pyrolysis of D-glucose: General disconnection analysis and the formation of C1 and C2 carbonyl compounds by electrocyclic fragmentation mechanisms. *J. Anal. Appl. Pyrolysis* 82 (2008) 10-41.

<sup>121</sup> S.C. Moldoveanu. Pyrolysis GC-MS, Present and Future (Recent Past and Present Needs). *J. Microcolumn Separations* 13 (2001) 102-125.

surface of the vial and long exposure times. This method has been applied for qualitative analysis of products evolved from synthetic polymers pyrolysed with a bench scale pyrolyser.<sup>122</sup>

In order to perform a quantitative analysis, both equilibrium SPME and dynamic SPME can be used. In the former case the partition equilibrium of the analyte between the fiber and the gas is reached. On the contrary, in dynamic SPME, equilibrium must be avoided as long as possible, and calibration is performed using Fick diffusion law. The basic assumption when using Fick law is that the amount of analyte on the fiber is negligible with respect to that expected at equilibrium, and this condition should be respected during all sampling time (“zero sink” hypothesis).<sup>123</sup>

Equilibrium SPME was used for sampling the flue gas of a bench scale pyrolyser and different SPME fibers were tested with good results.<sup>124</sup> The main problem of equilibrium SPME, when applied to analytical off-line system, is the short sampling time needed in a small and discontinuous pyrolysis equipment. Dynamic SPME techniques, in spite of the “zero sink” hypothesis, need gas/fiber concentrations ratio as much as possible far from equilibrium conditions; for this reason it is potentially more appropriate for the off-line pyrolysis configuration.

Following the detailed compositional study of the pyrolysate of different terrestrial biomass by analytical pyrolysis, this chapter was dedicated to the development of a system based on off-line pyrolysis coupled with SPME and GC-MS analysis (Py-SPME-GC-MS), with main the target of decouple, without the use of solvent, pyrolysis and GC analysis conditions. In particular the aim of this chapter was to extend the chemical characterisation to volatiles by exploiting SPME sampling. The performance of Py-SPME-GC-MS was evaluated for qualitative and quantitative analysis. Quantitative aspects were focused on volatile C<sub>1</sub>-C<sub>4</sub> compounds.

### **3.2.2. Materials and methods**

#### *3.2.2.1. Biomass samples and chemicals*

Biomass samples were already described in the previous chapter. All solvents, chemicals and standard were purchased from Sigma-Aldrich.

#### *3.2.2.2 Pyrolysis-SPME equipment*

---

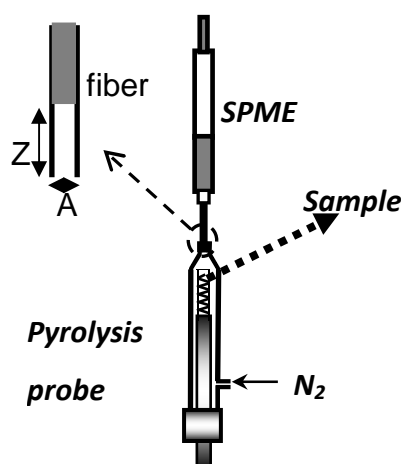
<sup>122</sup> J.H. Bortoluzzi, E.A. Pinheiro, E. Carasek and V. Soldi. Solid phase microextraction to concentrate volatile products from thermal degradation of polymers. *Polymer Degradation and Stability* 89 (2005) 33-37.

<sup>123</sup> J. Koziel, I. Novak. Sampling and sample-preparation strategies based on solid-phase microextraction for analysis of indoor air. *Trends in analytical chemistry* 21 (2002) 840-850.

<sup>124</sup> G. Guéhenneux, P. Baussand, M. Brothier, C. Poletiko, G. Boissonnet. Energy production from biomass pyrolysis: a new coefficient of pyrolytic valorisation. *Fuel* 84 (2005) 733-739.

The apparatus employed for off-line pyrolysis with a CDS 1000 pyroprobe (platinum filament coil) was described in the previous chapter,<sup>125,126</sup> In this study, SPME replaced the sorbent cartridge for trapping pyrolysis products. SPME fiber (Supelco) was placed at the exit of the pyrolysis chamber as illustrated in Figure 3.2.1. The following fibers were preliminary tested: 100  $\mu\text{m}$  PDMS (polydimethylsiloxane), 85  $\mu\text{m}$  polyacrylate fiber and 75  $\mu\text{m}$  carboxen/PDMS (CAR/PDMS).

**Figure 3.2.1:** Scheme of off-line pyrolysis equipment with SPME sampling and related dimensional parameters (Z,A see experimental)



### 3.2.2.3 Pyrolysis-SPME procedure

A weighed amount of biomass sample (about 2-3 mg) was introduced into the quartz tube and held by silyanized quartz wool at the middle portion of the tube. The probe was inserted into the pyrolysis chamber and the apparatus was fluxed with a nitrogen stream at  $100 \text{ cm}^3 \text{ min}^{-1}$  for few seconds. Then the SPME fiber was placed at the exit of the pyrolysis chamber and the sample was pyrolysed at  $700 \text{ }^\circ\text{C}$  (set temperature) for 100 s at the maximum heating rate ( $20 \text{ }^\circ\text{C ms}^{-1}$ ). At the end of pyrolysis the fiber was subjected to GC-MS analysis. After each pyrolysis, the pyrolysis chamber and the probe were cleaned with acetone and were dried accurately with a hot air stream at  $150^\circ\text{C}$  prior to analysis.

### 3.2.2.4 GC-MS

SPME desorption was performed at  $280^\circ\text{C}$  in splitless mode in the injection port of a 6850 Agilent HP gas chromatograph connected to a 5975 Agilent HP quadrupole mass spectrometer. Analytes were separated by a HP-5 fused-silica capillary column (stationary phase poly[5% diphenyl/95%

<sup>125</sup> D. Fabbri, I. Vassura. Evaluating emission levels of polycyclic aromatic hydrocarbons from organic materials by analytical pyrolysis. *J.Anal.Appl.Pyrolysis* 75 (2006) 150-158.

<sup>126</sup> D. Fabbri, C.Torri, V. Baravelli. Effect of zeolites and nanopowder metal oxides on the distribution of chiral anhydrosugars evolved from pyrolysis of cellulose: An analytical study. *J.Anal.Appl.Pyrolysis* 80 (2007) 24-29.

dimethyl]siloxane, 30 m, 0.25 mm i.d., 0.25 mm film thickness) using helium as carrier gas (at constant pressure, 33 cm s<sup>-1</sup> linear velocity at 200°C). Mass spectra were recorded under electron ionization (70 eV) at a frequency of 1 scan s<sup>-1</sup> within the 12–450 *m/z* range.

The following thermal program was used: 35°C for five minutes, then 10°C/min until 300°C followed by a column cleaning at 310°C for 3 min.

### 3.2.2.5 Calibration

Calibrations for quantitative analysis of volatile compounds were performed using acetic acid as model reference compound. Calibration plots (see examples in Figure 3.2.2) were obtained by SPME sampling a constant mass flow of nitrogen gas containing acetic acid. To this purpose, a 25 cm<sup>3</sup> double necked round flask (placed in an ice bath) was inserted between the flowmeter and the chamber in the N<sub>2</sub> line. The flask was half-filled with pure acetic acid, connected to the pyrolysis chamber equipped with the probe and the SPME fiber and flowed with N<sub>2</sub> at 100 cm<sup>3</sup> min<sup>-1</sup>. The flask was periodically (every 20 min) withdrawn and weighed; acetic acid mass flow resulted to be on average 0.20 ± 0.05 mg min<sup>-1</sup>. Two SPME sampling replicates were performed at each sampling time (10, 30, 60, 100, 200 and 300 s).

Once the calibration plot was established for acetic acid, a relative response factor *Fr*(*i*) was estimated for other substances as follows:

$$Fr(i) = \frac{A_i \cdot C_{AA}}{A_{AA} \cdot C_i}$$

where *A<sub>i</sub>* and *A<sub>AA</sub>* are the GC-MS peak areas of analyte and acetic acid, respectively, obtained by GC-MS analysis (in 1/100 split mode) of a single-point calibration solution containing analyte and acetic acid at concentration *C<sub>i</sub>* and *C<sub>AA</sub>*, respectively. The calibration solution consisted of an approximately equimolar mixture of acetic acid (reference compound) and the other analytes when available (formaldehyde, methanol, glyoxal, acetone, hydroxyacetone).

For not available analytes (e.g. monomeric hydroxyacetaldehyde or acetoxy-acetaldehyde), *F<sub>r</sub>*(*i*) was calculated as shown in the following equation:

$$Fr(i) = \frac{(SIM / RIC)_i}{(SIM / RIC)_{AA}}$$

where SIM is the GC-MS peak in the selected ion mode and RIC is the GC-MS peak area calculated in total ion current mode chromatogram.

### 3.2.2.6 Yield calculation

The mass (*m<sub>i</sub>*) and the yield (*Y<sub>i</sub>*=*m<sub>i</sub>*/*m<sub>sample</sub>*) of the analyte evolved upon pyrolysis was calculated from the following equation:

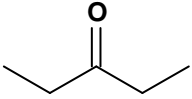
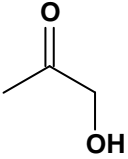
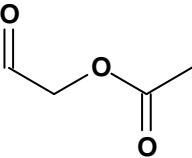
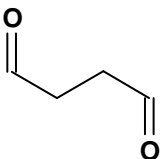
$$m_i = \frac{D_{AA} \cdot A_i}{D_i \cdot \alpha_{AA} \cdot Fr(i)}$$

$\alpha_{AA}$  stands for the initial slope of acetic acid calibration plot (count s mg<sup>-1</sup>).  $D_{AA}$  and  $D_i$  are the diffusion coefficients in nitrogen (m<sup>2</sup> s<sup>-1</sup>) of acetic acid and analyte, respectively;  $A_i$  is the GC-MS peak area determined in the mass chromatogram mode. Based on the Fuller-Shatting-Giddings equation,<sup>127</sup>  $D_{AA}/D_i$  ratio could be approximated by  $M_i^{0.5}/M_{ref}^{0.5}$ . All the quantified analytes and all parameters used for quantification are shown in Table 3.2.1.

**Table 3.2.1:** Volatile products evolved from off-line pyrolysis of biomass samples quantified after SPME sampling and GC-MS analysis.

$t_r^a$	$m/z^b$	Structure	Compound name	$D_i/D_{AA}^c$	sensitivity <sup>d</sup> □
1.32	30		formaldehyde	1.41	57
1.38	31		methanol	1.37	13
1.38	44		acetaldehyde	1.17	38
1.39	58		glyoxal	1.02	14
1.55	58		acetone	0.91	19
1.56	72		methylglyoxal	0.91	6
1.86	31		hydroxyacetaldehyde	1.00	47
2.16	60		acetic acid	1.00	18

<sup>127</sup> E.N. Fuller, P.D. Shatting, J.C. Giddings. A new method for prediction of binary gas-phase diffusion coefficient. J. C. Ind. Eng Chem. 58 (1966) 19-27.

2.06	57		3-pentanone	0.84	35
2.16	43		hydroxyacetone	0.90	37
5.23	43		acetoxy-acetaldehyde	0.77	74
5.52	58		butanedial	0.84	17

<sup>a</sup>Retention time in minutes. <sup>b</sup> Quantitation ion. <sup>c</sup>Ratio of molecular diffusion coefficient of analyte and acetic acid. <sup>d</sup> Sensitivity in Mcount s mg<sup>-1</sup> is given by  $\alpha_{AA} (D_{AA}/F_r(i) D_i)$  (see Experimental section).

### 3.2.2.7. Theory

The quantification of volatiles (C<sub>1</sub>-C<sub>4</sub>) was performed through an analytical method based on Fick law. Basic assumptions were complete homogenous gas flow, short sampling time and concentration on the fiber negligible with respect to concentration in the flowing gas.

Being  $n$  the analyte amount onto the fiber ( $\mu\text{g}$ ), the mass flow ( $dn/dt$ ) of analyte that hit the fiber surface ( $\mu\text{g s}^{-1}$ ) can be expressed by equation 1:

$$(1) \frac{dn}{dt} = \frac{CAD}{Z}$$

Where  $C$  is concentration of the analyte in the flowing gas ( $\mu\text{g m}^{-3}$ ),  $D$  is the diffusion coefficient of the analyte ( $\text{m}^2 \text{s}^{-1}$ ) in nitrogen,  $A$  is the diameter of the sampling surface ( $\text{m}^2$ ) and  $Z$  (m) is the distance between the surrounding environment and the sampling surface<sup>122</sup>.

As shown in Figure 3.2.1, when the fiber is used in the retracted mode,  $A$  is a known technical parameter of the fiber and  $Z$  is the distance between the fiber and the inlet of metallic alloy (e.g.  $Z$  is 5 mm and  $A = 0.126 \text{ mm}^2$  for totally retracted CAR/PDMS used in this work). If fiber is used

exposed, A is the exposed area of the sampling cylinder and Z is the thickness of stagnant gas layer on the fiber surface and could be evaluated experimentally.<sup>128,129</sup>

In our Py-SPME system, the relationship between experimental conditions, fiber structure and capture effectiveness ( $\mu_{\text{capture}}$ ) of the fiber is shown in equation (2), which was obtained by rearranging and integrating equation (1) as follows:

$$dn = \frac{CAD}{Z} dt$$

when Q is the inert gas flow ( $\text{m}^3 \text{s}^{-1}$ ), then the mass flow ( $\mu\text{g s}^{-1}$ ) of analyte is  $q = C \cdot Q$ , then:

$$(2) dn = \frac{AD}{QZ} \cdot q \cdot dt = \mu_{\text{capture}} \cdot q \cdot dt$$

The relationship between experimental conditions and capture effectiveness (equation (3)) was obtained by integrating equation (2) over the pyrolysis time, here coincident to sampling time (t):

$$\int_0^t dn = \frac{AD}{QZ} \cdot \int_0^t q dt$$

$$(3) n = \frac{AD}{QZ} \cdot m_{\text{tot}}$$

where  $m_{\text{tot}}$  is total mass of evolved analyte. Finally, when instrumental response depends linearly on analyte amount and  $F_r$  is the specific signal ( $\text{count s } \mu\text{g}^{-1}$ ) produced by the analyte, we have:

$$m_{\text{tot}} = \frac{(\text{GC - MS})_{\text{area}}}{F_r \cdot \mu_{\text{capture}}} = \frac{(\text{GC - MS})_{\text{area}}}{\alpha}$$

$\alpha$  is then obtainable as the initial slope of the calibration plot where abscissa is the flowed analyte and ordinate is the instrumental response (e.g Figure 3.2.2).

### 3.2.3. Results and discussion

#### 3.2.3.1 Sampling set-up

Preliminary Py-SPME experiments with biomass samples performed under similar conditions showed that GC-MS response of most volatile compounds was rather poor with PDMS and polyacrylate fibers in comparison to CAR/PDMS fibers. When retracted and exposed modes were compared,<sup>123</sup> the exposed fiber (using mg amount of sample) was soon saturated by heavier

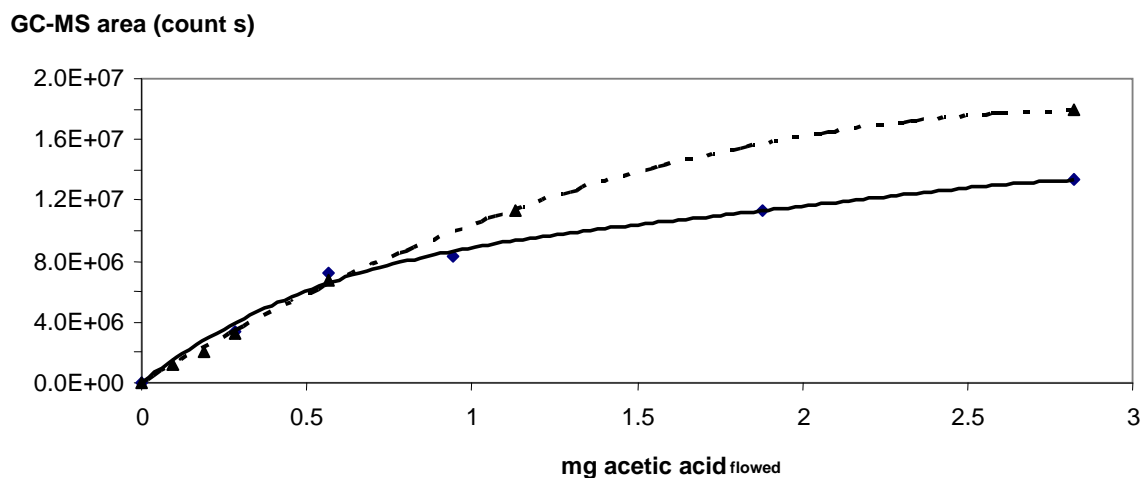
<sup>128</sup> G. Oyang, J. Pawlczyn. Recent development in SPME for on-site analysis and monitoring, *Trend in Analytical Chemistry*. 25 (2006) 692-703.

<sup>129</sup> J. Koziel, M Jia, J. Pawlczyn. Air sampling with porous solid phase microextraction fibers. *Anal. Chem.* 72 (2000) 5178-5186

compounds with consequent mass discrimination and fiber deterioration. Eventually, for this work, the preferred mode was totally retracted CAR/PDMS fiber (Figure 3.2.1), in spite of less quantity of analyte accumulated onto the fiber.

The influence of temperature on the saturation behaviour of the fiber was studied at room temperature and at conditions simulating pyrolysis (heating coil at 700 °C); acetic acid was used as model compound for its intermediate volatility and abundance in biomass pyrolysis vapours. Typical results are shown in Figure 3.2.2. Heating the gas flow, the amount of analyte onto the fiber decreased, but a trend similar to that at room temperature was established in the range between 0.01-0.5 mg of acetic acid. A linear response was observed in this range ( $R^2=0.998$ ) which corresponded to 0.2%-20% product yields when applied to biomass pyrolysis experiments performed in this study (2-3 mg of sample).

**Figure 3.2.2:** Saturation behaviour of the CAR/PDMS fiber in acetic acid spiked nitrogen flow (100 ml min<sup>-1</sup> with acetic acid concentration 2 µg ml<sup>-1</sup>) at room temperature (dotted line) and with heating coil at 700°C (full line).



### 3.2.3.2. Qualitative aspects

The analytical performance of the procedure was investigated in detail by employing four biomass types already tested in chapter 3.1: namely switchgrass, sweet sorghum, poplar and corn stalk.

Figure 3.2.3 shows total ion chromatograms (TIC) obtained from Py-SPME of different biomass types among those of interest in fuel applications. The structural assignment of the main semi-volatile products is reported in Table 3.2.2. Chromatograms obtained by Py-SPME of herbaceous species (switchgrass, sweet sorghum and corn stalk) were featured by cellulose pyrolysis products, with 4-hydroxy-5,6-dihydro-(2H)-pyranone (# 21) as the most intense peak.

**Figure 3.2.3:** Typical GC-MS profiles obtained by off-line pyrolysis at 700°C with SPME sampling of various biomass types. Peak numbers refer to compounds listed in Table 3.2.2.

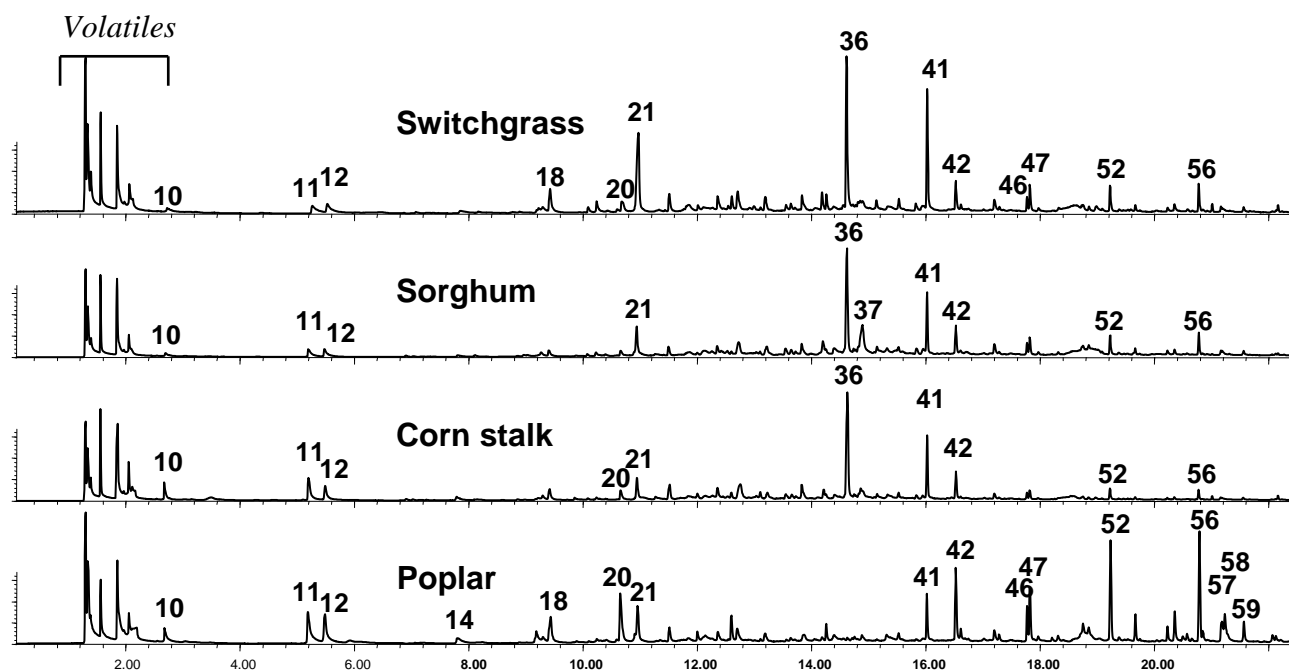


**Table 3.2.2:** Compounds tentatively identified by GC-MS after off-line py-SPME of tested biomass.

#	$t_r$ min	Quantitation ion m/z	Compound name
1	1.32	30	formaldehyde
2	1.38	31 <sup>a</sup>	methanol
3	1.38	44	acetaldehyde
4	1.39	58	glyoxal
5	1.55	58	acetone
6	1.56	72	methyl glyoxal
7	1.86	31	hydroxyacetaldehyde
8	2.16	60	acetic acid
9	2.06	57	3-pentanone
10	2.16	43	hydroxyacetone
11	5.23	43	acetoxy-acetaldehyde
12	5.52	58	butandial
13	7.18	96	2-furaldehyde
14	7.81	98	furfuryl alcohol
15	8.20	44	dihydro-4-hydroxy-2(3H)-Furanone
16	9.25	55	2-(5H)-furanone
17	9.31	70	2-methylcyclopentanone
18	9.44	98	ciclopentanedione
19	10.10	73	1,3-dioxolane-2-methanol
20	10.66	94	phenol
21	10.94	114	4-hydroxy-5,6-dihydro-(2H)-pyranone
22	11.50	112	2-hydroxy-3-methyl-2-cyclopenten-1-one
23	12.13	128	2-(propan-2-one)-tetrahydrofuran
24	12.01	108	2-methylphenol

25	12.14	85	tetrahydro-2H-Pyran-2-methanol
26	12.36	107	4-methylphenol
27	12.54	128	2,5-dimethyl-4-hydroxy-3(2H)-furanone
28	12.61	109	guaiacol
29	13.11	126	3-ethyl-2-hydroxy-2-cyclopenten-1-one
30	13.19	114	3-methyl-2,4(3H,5H)-furanone
31	13.83	107	4-ethylphenol
32	14.20	43	anhydro isosaccharino- $\delta$ -lactone
33	14.56	69	1,4-3,6-dianhydroglucopyranose
34	14.27	138	4-methylguaiacol
35	14.40	110	1,2-benzenediol
36	14.61	120	4-vinylphenol
37	14.87	97	5-hydroxymethyl-2-furaldehyde
38	15.33	140	3-methoxy-1,2-benzenediol
39	15.53	137	4-ethylguaiacol
40	15.92	144	ascopyrone P
41	16.02	150	4-vinylguaiacol
42	16.52	154	Syringol
43	16.62	164	eugenol
44	17.22	151	vanillin
45	17.29	164	<i>cis</i> -isoeugenol
46	17.77	168	4-methylsyringol
47	17.82	164	<i>trans</i> -isoeugenol
48	17.99	137	2-(4-hydroxy-3-methoxyphenyl)-ethanal
49	18.33	151	methylguaiacylketone
50	18.76	167	4-ethylsyringol
51	18.86	137	1-(4-hydroxy-3-methoxyphenyl)-2-propanone
52	19.23	180	4-vinylsyringol
53	19.67	194	<i>cis</i> -methoxyisoeugenol
54	20.23	194	<i>trans</i> -methoxyisoeugenol
55	20.36	182	syringaldehyde
56	20.78	194	methoxyeugenol
57	21.17	181	4-hydroxy-3,5-methoxy acetophenone
58	21.23	178	4-hydroxy-2-methoxycinnamaldehyde
59	21.56	167	1-(4-hydroxy-3,5-dimethoxyphenyl)-2-propanone

Interestingly, the pyrolysate of sweet sorghum was unique in being characterised by relatively high levels of 5-hydroxymethyl-2-furaldehyde (# 37). This finding could be explained by higher amount of reducing sugars that characterize this plant (see Table 3.2.1).<sup>130</sup>

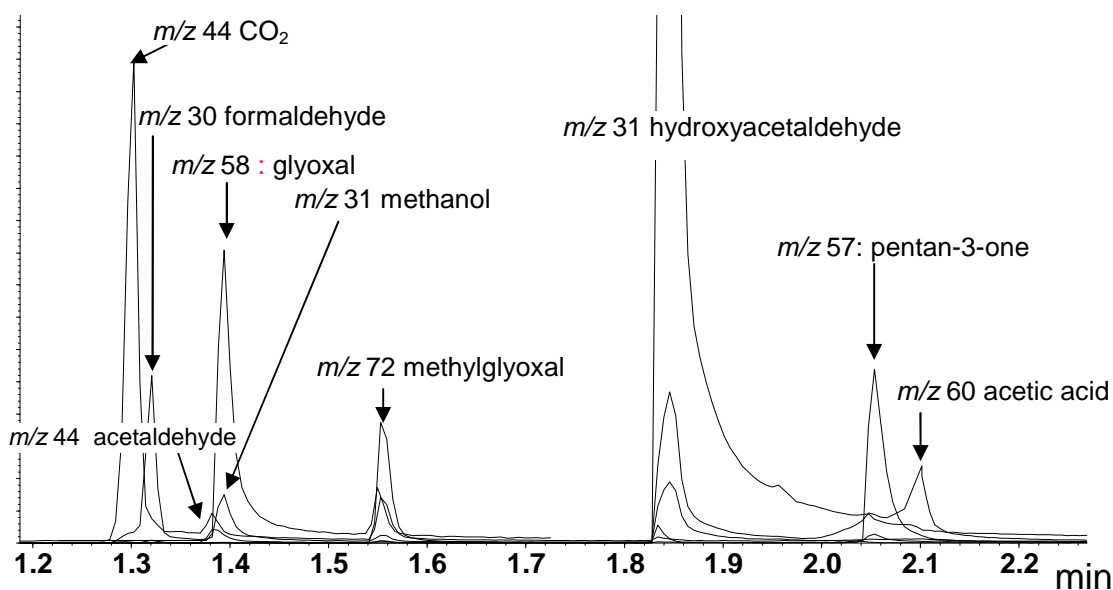
Peaks produced by lignin phenols were dominated by 4-vinylphenol (# 36), a typical marker of herbaceous biomass. Instead, Py-SPME of poplar, taken as representative of hardwood biomass, produced pyrograms characterised by the dominance of syringol (# 42) and its derivatives in

<sup>130</sup> E.B. Sanders, A.I. Goldsmith, J.I. Seeman. A model that distinguishes the pyrolysis of D-glucose, D-fructose, and sucrose from that of cellulose. Application to the understanding of cigarette smoke formation. *J. Anal. Appl. Pyrolysis* 66 (2003) 29-50.

comparison to herbaceous biomass. As expected, 4-vinylphenol was negligible, in accordance to lignin composition of hardwood.<sup>131</sup>

Thus, on a qualitative base, the results pertaining to semi-volatiles compounds (>C<sub>4</sub>) were similar to those obtained by on-line Py-GC-MS (see chapter 3.1). In addition, sampling with SPME allowed the detection of volatile pyrolysis products, expanding the mass range of compounds analyzable by GC-MS in off-line pyrolysis, and allowing a good chromatographic separation also with low pyrolysis temperatures (with consequential large pyrolysis time). In fact, the early eluting region of chromatograms were characterized by a cluster of partially overlapped peaks produced by volatile compounds. These compounds were better evidenced by extracting the mass chromatograms of selected ions in their mass spectra, as shown in Figure 4.

**Figure 3.2.4:** Early eluting region of GC-MS trace obtained from py-SPME of switchgrass (pyrolysis set at 700°C). Extracted ion currents at *m/z* characteristic of volatile pyrolysis products (see Table3.2.2).



In all the tested samples, main volatile (C<sub>1</sub>-C<sub>4</sub>) compounds were identified through the analysis of pure compounds, namely hydroxyacetaldehyde, methylglyoxal, acetic acid, 3-pentanone, methanol, formaldehyde, acetaldehyde, carbon dioxide and butanedial. The attribution is largely in accordance with literature data<sup>120,132</sup>. Acetoxyacetaldehyde, which is the condensation product of hydroxyacetaldehyde and acetic acid, was tentatively identified by its mass spectrum.

<sup>131</sup> J. Ralph, R.D. Hatfield. Pyrolysis-GC-MS Characterization of Forage Materials. *Journal of Agric. Food Chem.* 39 (1991) 1426-1437.

<sup>132</sup> J. Piskorz, D. Radlein, D.S. Scott, S. Czernik. Liquid products from the fast pyrolysis of wood and cellulose. In: Bridgwater AV, Kuester JL, Eds. *Research in thermochemical biomass conversion*. London, New York: Elsevier Applied Science (1988) 557-71.

### 3.2.4.3. Quantitative analysis of volatiles

The performance of Py-SPME in the quantification of low boiling point pyrolysis products (C<sub>1</sub>-C<sub>4</sub>) evolved from biomass was evaluated. Pure cellulose was also subjected to the Py-SPME procedure for comparison. Mean quantitative yields and relative standard deviations (RSD as percentage) of the most abundant volatile pyrolysis products evolved from herbaceous and woody biomass samples, as well as from cellulose, are reported in Table 3.2.3.

**Table 3.2.3:** Yields (mass %) of volatile pyrolysis products obtained from off-line Py-SPME of biomass samples. Mean values and % relative standard deviations (n=5).

<i>compound</i>	<i>Switchgrass</i>		<i>Sweet sorghum</i>		<i>Corn stalk</i>		<i>Poplar</i>		<i>Cellulose</i>	
	mean	<i>RSD</i>	mean	<i>RSD</i>	mean	<i>RSD</i>	mean	<i>RSD</i>	mean	<i>RSD</i>
Formaldehyde	1.0	47	0.57	46	0.5	50	0.8	62	1.6	24
Methanol	0.66	36	0.46	40	0.8	49	1.3	51	0.22	35
Acetaldehyde	0.50	44	0.35	15	0.4	33	0.40	9	0.43	41
Glyoxal	5.8	74	2.2	47	3.2	86	2.7	61	5.1	5
Acetone	0.35	51	0.3	50	0.42	56	0.26	79	0.48	24
Methylglyoxal	5.0	52	3.8	71	5.1	74	2.7	45	2.8	25
Hydroxyacetaldehyde	14	36	14	53	12	63	12	37	7.4	22
Acetic acid	2.9	32	3.6	85	5.0	68	5.2	56	0.18	42
3-pentanone	1.1	96	1.6	59	2.1	86	1.5	48	0.40	8
Hydroxyacetone	2.1	60	2.2	83	3.7	86	2.4	88	0.20	33
Acetoxyacetaldehyde	2.6	63	2.9	55	3.3	87	3.8	68	0.09	62
Butandial	2.7	75	3.5	53	2.9	69	4.9	68	n.d.	
<b>Sum</b>	38	42	35	50	39	66	38	46	19	10

Data relative to cellulose indicate that the precision of the Py-SPME method is comparable to that from off-line pyrolysis methods for semi-volatile products (around RSD 25% on average).<sup>126</sup> As expected, the precision deteriorated when moving from pure cellulose to biomass samples, which displayed rather high RSD values, especially in the case of minor pyrolysis products (Table 3.2.3). The largest data dispersion was obtained with corn stalk (67 % mean RSD), while slightly lower RSD values (55% mean RSD) were observed for the other biomass types. The observed large RSD values could be partially explained by the strong heterogeneity of biomass samples, as reported, for instance, by Boateng *et al.* who found a large variability in the yields of semi volatile compounds (from pyrolysis alfalfa stems).<sup>133</sup> For all the samples, hydroxyacetaldehyde was the main pyrolysis product, with yields up to 14±2% and 14±4% (mean ± confidence at  $\alpha=0.05$ ) from switchgrass and

<sup>133</sup> A.A. Boateng, D.E. Daugaard, N.M. Goldberg, K.B. Hicks. Production of Pyro-oil from Alfalfa Stems by Fluidized-Bed Fast Pyrolysis. *Ind. Eng. Chem. Res.* 47 (2008) 4115–4122.

sorghum, respectively. Other abundant pyrolysis products detected with SPME were acetic acid, butanedial, glyoxal, methyl-glyoxal and acetoxy-acetaldehyde, with yields in the 4-7 % range. Poplar produced the highest amount of methanol (2.7±0.3% yield), acetic acid (5.2 ±1% yield) and butanedial (4.9±2%), whereas switchgrass was characterized by the largest levels of formaldehyde, glyoxal and methylglyoxal production (1.0±0.2%, 5.8±2% and 5.0±3%, yields respectively). With the exception of formaldehyde (1.6±0.2% yield), the amount of volatiles produced by cellulose pyrolysis was lower in comparison with whole biomass. This is accordance with the absence of any catalytic effect by inorganic constituents, the non-catalytic depolymerisation of cellulose favouring the formation of anhydrosugars and formaldehyde.<sup>132</sup>

**Table 3.2.4 :** Comparison between yields, for acetic acid (AA) and hydroxyacetaldehyde (HA) obtained from this study and those reported in the literature. Mean value± confidence interval ( $\alpha=0.05$  n=5).

		<i>Switchgrass</i>		<i>Sweet Sorghum</i>		<i>Corn Stalk</i>		<i>Poplar</i>		<i>Cellulose</i>	
HA	<b>This study</b>	14	±2	14	±4	12	±4	12	±2	7,38	±0.2
	<b>Lit.</b>	11 <sup>134a</sup>		7.2 <sup>135</sup>		n.a.		10 <sup>136</sup>		4.8 <sup>137</sup>	
AA	<b>This study</b>	2.9	±0.5	3.6	±1	5.0	±2	5.2	±1	0,18	±0.04
	<b>Lit.</b>	2.8 <sup>134a</sup>		2.4 <sup>135</sup>		4 <sup>135b</sup>		5.4 <sup>136</sup>		Low <sup>137</sup>	

<sup>a</sup>values were back calculated from bio-oil yields and published analyte concentrations in bio-oil.

<sup>b</sup>values were back calculated from bio-oil yields and published total carboxylic acid concentration in bio-oil.

In order to evaluate the ability of the micro-scale method here developed to work as a model system of large scale pyrolysis apparatus, the yields of acetic acid and hydroxyacetaldehyde measured with Py-SPME were compared to those reported in the literature from the analysis of pyrolytic liquids from similar biomass types. Such a comparison is illustrated in Table 3.2.4.

Mean yields of acetic acid determined with Py-SPME were consistent to those resulting from pyrolysis reactors and pyro-oil analysis. For instance, switchgrass 2.9 and 2.8%, poplar 5.2% and 5.4%, for micro-scale and macro-scale, respectively. In agreement with the origin of acetic acid from non-cellulosic components, the yield of acetic acid from cellulose was significantly low. As far as hydroxyacetaldehyde is concerned, Py-SPME provided similar mean values from all the

<sup>134</sup> J. Piskorz, P. Majerski, D. Radlein, D.S. Scott, A.V. Bridgewater. Fast pyrolysis of sweet sorghum and sweet sorghum bagasse. *J. Anal. Appl. Pyrol.* 46 (1998) 15-29.

<sup>135</sup> O. Ioannidou, A. Zabanitoutou, E.V. Antonakou, K.M. Papazisi, A.A. Lappas, C. Athanassiou, Investigating the potential for energy, fuel, materials and chemicals production from corn residues(cobs and stalks) by non-catalytic and catalytic pyrolysis in two reactor configurations, *Renewable and Sustainable Energy Reviews* 13 (2009) 750–762.

<sup>136</sup> Donald S. Scott, Lachlan Paterson, Jan Piskorz, Desmond Radlein, Pretreatment of poplar wood for fast pyrolysis: rate of cation removal, *Journal of Analytical and Applied Pyrolysis* 57 (2000) 169–176.

<sup>137</sup> Z. Luo, S. Wang, Y. Liao, K. Cen. Mechanism Study of Cellulose Rapid Pyrolysis. *Ind. Eng. Chem. Res* 43 (2004) 5605-5610.

investigated biomass types (12-14%, Table 3.2.4), whereas data from literature fall in a lower and less uniform range (7-10%), but still not too far from analytical pyrolysis. At this purpose, it is worth pointing out that the original concentration of hydroxyacetaldehyde in the bio-oil might be reduced by the chemical instability of this compound due to its tendency to react with other components and to give self-condensation products.<sup>138</sup> Thus, the Py-SPME method is capable to provide a picture of the chemical composition of “native” pyrolysate as soon as it is formed and prior to its condensation into pyro-oil droplets and subsequent post-pyrolysis reactions, such as polymerization of reactive aldehydes.<sup>139</sup> This feature may also explain the good agreement between analytical and applied pyrolysis found for acetic acid, which is known to be rather stable in pyro-oil.<sup>139</sup>

### 3.2.4. Conclusions

Off-line Py-SPME-GC-MS provided GC-MS traces similar to those resulting from conventional Py-GC-MS discussed in the previous chapter, but with a clearer pattern of peaks in the first eluting region associated to volatile pyrolysis products (methanol, acetone, formaldehyde, glyoxal, etc.). Selected ion monitoring enabled the identification and a rough quantitative evaluation of these compounds. Py-SPME combines the benefits of off-line pyrolysis in avoiding memory effects and GC column deterioration often observed in the on-line configuration, with those of SPME which is a rapid and solventless procedure enabling the qualitative analysis of volatiles along with semi-volatile compounds.

In spite of severe assumptions (e.g. validity of Fick's law) and limitations (e.g. low precision), a preliminary assessment based on a dynamic model, retracted fiber mode, external calibration with acetic acid as reference compound and estimated diffusion coefficients, indicated that quantification of volatile compounds is feasible.

The yields of acetic acid and hydroxyacetaldehyde resulted consistent with the composition of bio-oil, suggesting a reliable application of Py-SPME in screening studies, such as testing catalyst activity, different biomass typologies, pyrolysis conditions. These factors are of much interest in developing the correct strategies to improve the characteristics of bio-oil as a feedstock for fuels and chemicals.

---

<sup>138</sup> D. Leiseur, V. Castola, A. Bighelli. Quantification of hydroxyacetaldehyde in a biomass pyrolysis liquid using <sup>13</sup>C NMR spectroscopy, *Spectroscopy letters* 40 (2007) 591-602.

<sup>139</sup> A. Oasmaa, E. Kuoppala. Fast Pyrolysis of Forestry Residue. 3. Storage Stability of Liquid Fuel. *Energy Fuels* 17 (2003) 1075-1084.

## 3.3 Micro-scale GC-MS determination of polycyclic aromatic hydrocarbons (PAHs) evolved from pyrolysis of biomass

### 3.3.1. Introduction

In the previous two chapters, different techniques based on analytical pyrolysis were developed and applied to the chemical characterisation of pyrolysate arising from four terrestrial biomass. The procedures provided qualitative and quantitative information on the main evolved compounds that eventually end up into the bio-oil. The knowledge of the occurrence of principal constituents is important for the production, storage and delivery of bio-oil as they determine fuel properties as well as hazards (e.g. fires and explosions). Besides, main constituents, health hazards can be caused by the occurrence of trace but highly toxic constituents, such as polycyclic aromatic hydrocarbons. The actual understanding of the inherent hazards due to bio-oils should be a core issue in the sustainability assessment of bio-energy processes and it would be also consistent with the European REACH system,<sup>140</sup> aimed at the improving of protection of human health and the environment through a better and earlier identification of the inherent properties of chemical substances.

Considering that bio-oil have origin from high temperature depolymerisation,<sup>141</sup> and since these substances are among the most powerful carcinogenic substances that compose pyrolysis oil, PAHs, even if present at mg kg<sup>-1</sup> level, could represent an important long term health hazard.

Understanding the pyrolytic formation of PAHs is important for assessing technological problems, health hazards and environmental impacts related to the utilisation of vegetable biomass for energetic purposes, such as combustion and pyrolysis. In the case of pyrolysis, formed PAHs end up into bio-oil a candidate liquid biofuel for power plants and transportation, adversely affecting its toxicity with implications during storage, handling and transportation.<sup>142,143</sup> Whereas there are plenty of studies regarding the analysis of PAHs emitted during biomass combustion due to the importance of this source in the global and local environment, fewer works have been published dealing with the quantitative determination PAHs in bio-oil.<sup>144,145,146,147,148</sup> In these studies, GC-MS

---

<sup>140</sup> European Union Regulations (CE) N. 1907/2006 European parliament, 18 december 2006.

<sup>141</sup> Y. Zhang, S. Tao. Global atmospheric emission inventory of polycyclic aromatic hydrocarbons (PAHs) for 2004. *Atm Environ* 43 (2008) 812-819.

<sup>142</sup> A. Oasmaa, D. Meier. Norms and standards for fast pyrolysis liquids: 1. Round robin test. *J Anal Appl. Pyrol.* 73 (2005) 323-334.

<sup>143</sup> Cirad, Aston University, BFH, An assessment of bio-oil toxicity for safe handling and transportation, Final Technical Report, Part I, 2003 (available on-line at [www.pyne.co.uk](http://www.pyne.co.uk)).

<sup>144</sup> H. Pakdel, C. Roy. Hydrocarbon content of liquid products and tar from pyrolysis and gasification of wood. *Energ Fuel* 5 (1991) 427-436.

<sup>145</sup> P.T. Williams, P.A. Horne. Analysis of aromatic hydrocarbons in pyrolytic oil derived from biomass. *J. Anal. Appl. Pyrol.* 31 (1995) 15-37.

was the technique of choice due to its selectivity and sensitivity. Fast screening methods can be usefully adopted to investigate the influence of such different factors as process conditions, biomass feedstock and the effect of catalysts preliminary to scale-up. Analytical and microscale pyrolysis combined with GC separation and/or MS detection where heating was induced by a platinum filament<sup>149,150</sup> or a laser beam<sup>151</sup> along with small reactors heated by furnace<sup>152,153,154</sup> have been successfully applied to study the effect of various parameters on PAHs formation from biomass constituents. These studies have shown that PAH production tends to increase with increasing temperature and residence time<sup>152,153</sup> and is generally highest for cellulose even at relatively low temperatures from the decomposition char, while lignin mostly degrades to benzene derivatives.<sup>151,152</sup> In this study, analytical pyrolysis in the off-line configuration was evaluated as a tool to provide quantitative information on the production of PAHs from the pyrolysis of biomass. Two different techniques of sampling were tested, for the sake of simplicity abbreviated as Py-SPE (from solid phase extraction) and Py-SPME (from solid phase micro-extraction). In the former case, pyrolysis products were trapped onto a sorbent and subsequently solvent eluted, in the latter case pyrolysate was sampled by means of a SPME micro-fiber. White poplar was selected as representative woody biomass owing to its importance as potential feedstock for renewable energy.

### 3.3.2. Experimental

#### 3.3.2.1 Analytical pyrolysis

The base apparatus employed in off-line pyrolysis was described in detail in previous chapters. A sample holder quartz tube containing an exactly weighed amount of milled poplar wood (about 8-10 mg) or poplar wood mixed with H-ZSM-5 zeolite (15 mg, 1/20 weight ratio; zeolite from PQ corporation was pretreated at 550 °C for 6 hours) was introduced into the platinum coil and the

---

<sup>146</sup> P.A. Horne, P.T. Williams. Influence of temperature on the products from the flash pyrolysis of biomass. *Fuel* 75 (1996) 1051-1059.

<sup>147</sup> N. Padban, I. Odenbrand. Polynuclear aromatic hydrocarbons in fly ash from pressurized fluidized bed gasification of fuel blends. A discussion of the contribution of textile to PAHs. *Energ. Fuel* 13 (1999) 1067-1073.

<sup>148</sup> W.T. Tsai, H.H. Mi, Y.M. Chang, S.Y. Yang, J.H. Chang. Levels of polycyclic aromatic hydrocarbons in the bio-oils from induction-heating pyrolysis of food-processing sewage sludges. *Bioresource Technol.* 98 (2007) 1133-1137.

<sup>149</sup> D. Fabbri, I. Vassura. Evaluating emission levels of polycyclic aromatic hydrocarbons from organic materials by analytical pyrolysis. *J. Anal. Appl. Pyrol.* 75 (2006) 150-158.

<sup>150</sup> D. Fabbri, V. Bevoni, M. Notari, F. Rivetti. Properties of a potential biofuel obtained from soybean oil by transmethylation with dimethyl carbonate. *Fuel* 86 (2007) 690-697.

<sup>151</sup> A.M. Herring, J.T. McKinnon, K.W. Gneshin, R. Pavelka, D.E. Petrick, B.D. McCloskey, J. Filley. Detection of reactive intermediates from and characterization of biomass char by laser pyrolysis molecular beam mass spectroscopy. *Fuel* 83 (2004) 1483-1494.

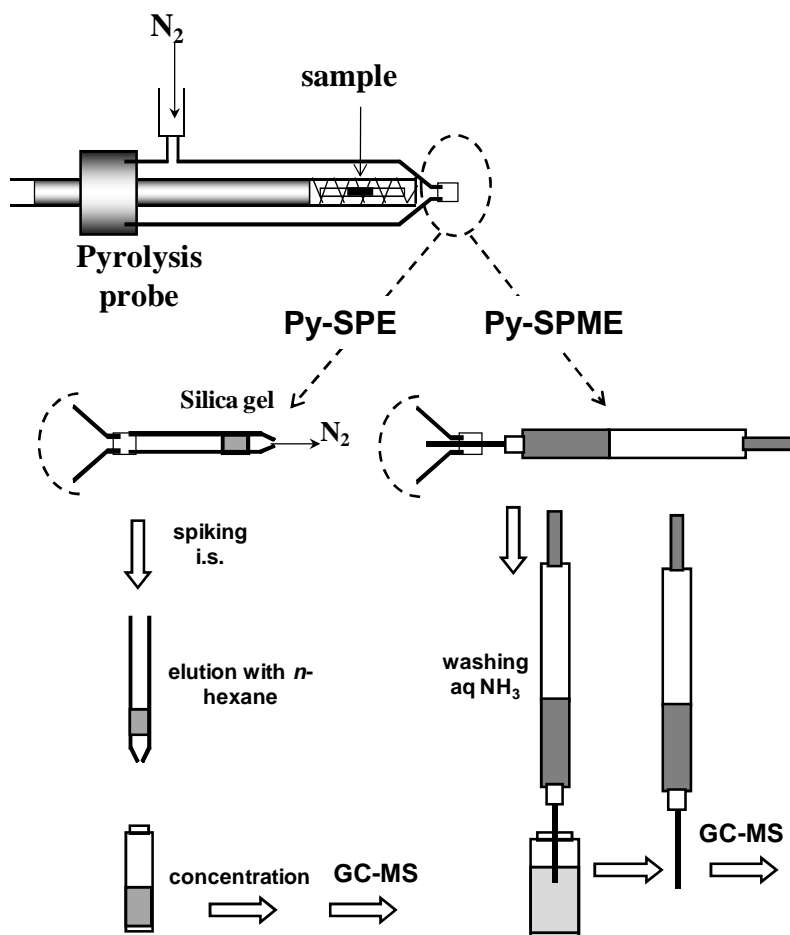
<sup>152</sup> R.K. Sharma, M.R. Hajaligol. Effect of pyrolysis conditions on the formation of polycyclic aromatic hydrocarbons (PAHs) from polyphenolic compounds. *J. Anal. Appl. Pyrol.* 66 (2003) 123-144.

<sup>153</sup> T.E. McGrath, W.E. Chan, M.R. Hajaligol. Effect of inorganics on the formation of PAHs during low temperature pyrolysis of cellulose. *J. Anal. Appl. Pyrol.* 66 (2003) 51-70.

<sup>154</sup> A.N. Garcia, M.M. Esperanza, R. Font. Comparison between product yields in the pyrolysis and combustion of different refuse. *J. Anal. Appl. Pyrol.* 68-69 (2003) 577-598.

probe was in turn inserted into the pyrolysis chamber. The apparatus was fluxed with a nitrogen stream at  $200 \text{ ml min}^{-1}$  prior to pyrolysis. Two sampling procedures were utilised: Py-SPE and Py-SPME (Figure 3.3.1).

**Figure 3.3.1:** Scheme of off-line Py-SPE and Py-SPME procedure.<sup>149,155</sup>



### 3.3.2.2 Py-SPE

The exit of the pyrolysis chamber was connected to a glass tube containing 100 mg of silica gel, withdrawn from a DSC-Si SPE cartridge, packed with glass wool and conditioned with *n*-hexane. Samples were pyrolyzed at 625 °C set temperature (corresponding to a maximum temperature of 500 °C as measured with a thermocouple) for 100 s at the maximum heating rate ( $20 \text{ °C ms}^{-1}$ ). After pyrolysis, the apparatus was vertically positioned, spiked with 100  $\mu\text{l}$  of surrogate PAH mix solution and rinsed with 6 ml of *n*-hexane. The solvent was left to flow through the silica cartridge into the collecting vial. The obtained solution was then blown down to 10-50  $\mu\text{l}$  under nitrogen and analysed by GC-MS. Emission levels ( $\mu\text{g PAH g}^{-1}$  pyrolysed biomass) were determined by internal calibration.

### 3.3.2.3 Py-SPME

In the Py-SPME procedure a carboxen/polydimethylsiloxane (CAR/PDMS) 75  $\mu\text{m}$  fiber (Supelco) was placed at the exit of the pyrolysis chamber as described in detail in a previous work.<sup>155</sup> Samples were pyrolyzed at 700 °C set temperature for 100 s at the maximum heating rate of 20 °C  $\text{m s}^{-1}$ . After pyrolysis, the fiber was immersed into 5 ml of 10 % ammonia aqueous solution under magnetic stirring for 15 minutes. The fiber was gently dried under nitrogen flow for few seconds and then subjected to GC-MS analysis. Peak areas of PAHs normalized to the amount of pyrolysed biomass exhibited a high variability (RSD 30-70% three replicates), therefore emission levels were not determined.

### 3.3.2.4 GC-MS

Analyses were performed in splitless mode at 280°C in the injection port of an Agilent 6850 gaschromatograph connected to an Agilent HP 5975 quadrupole mass spectrometer. Analytes were separated by a HP-5MS fused-silica capillary column (stationary phase poly[5% diphenyl/95% dimethyl] siloxane, 30 m, 0.25 mm i.d., 0.25  $\mu\text{m}$  film thickness) using helium as carrier gas. GC conditions were 20 °C  $\text{min}^{-1}$  from 50 to 100 °C, 5 °C  $\text{min}^{-1}$  from 100 °C to 300 °C and then 300 °C for 7.5 minutes. Mass spectra were recorded under electron ionization (70 eV) within three  $m/z$  ranges: (1)  $m/z$  127-241 from 0 to 35 minutes (10 scan/sec), (2)  $m/z$  251-253 from 35 to 40 minutes (10 scan/sec). (3)  $m/z$  276-278 from 40 to 50 minutes (15 scan/sec). A wider mass range was adopted in step (1) in order to identify alkylated PAHs. In the case of Py-SPME mass spectra were recorded in the  $m/z$  35-450 interval.

## 3.3.3. Results and discussion

### 3.3.3.1 Py-SPE

In a previous study devoted to the determination of emission levels by analytical pyrolysis in the off-line configuration, PAHs evolved from pyrolysis of organic materials were trapped onto a non-polar sorbent (polystyrene/divinylbenzene XAD-2 resin) and eluted with dichloromethane.<sup>149</sup> However, the application of this procedure to biomass resulted inadequate due to the strong interference by lignin phenols. Therefore we have adopted the a Py-SPE procedure for the analysis of bio-oil: PAHs were trapped onto silica gel and eluted with *n*-hexane. The selected quantity of sorbent was sufficient to trap evolved PAHs quantitatively as determined by breakthrough experiments with a second layer of silica.

---

<sup>155</sup> C. Torri, D. Fabbri. Application of off-line pyrolysis with dynamic solid-phase microextraction to the GC-MS analysis of biomass pyrolysis products. *Microchem J.* 93 (2009) 133-139.

**Figure 3.3.2:** GC-MS profiles obtained from Py-SPE of (A) poplar wood and (B) poplar wood with zeolite HZSM-5 (20/1) at 500 °C. In the inset extracted mass chromatograms at selected ions. Peak numbers refer to Table 3.3.1 (\*) contaminants.

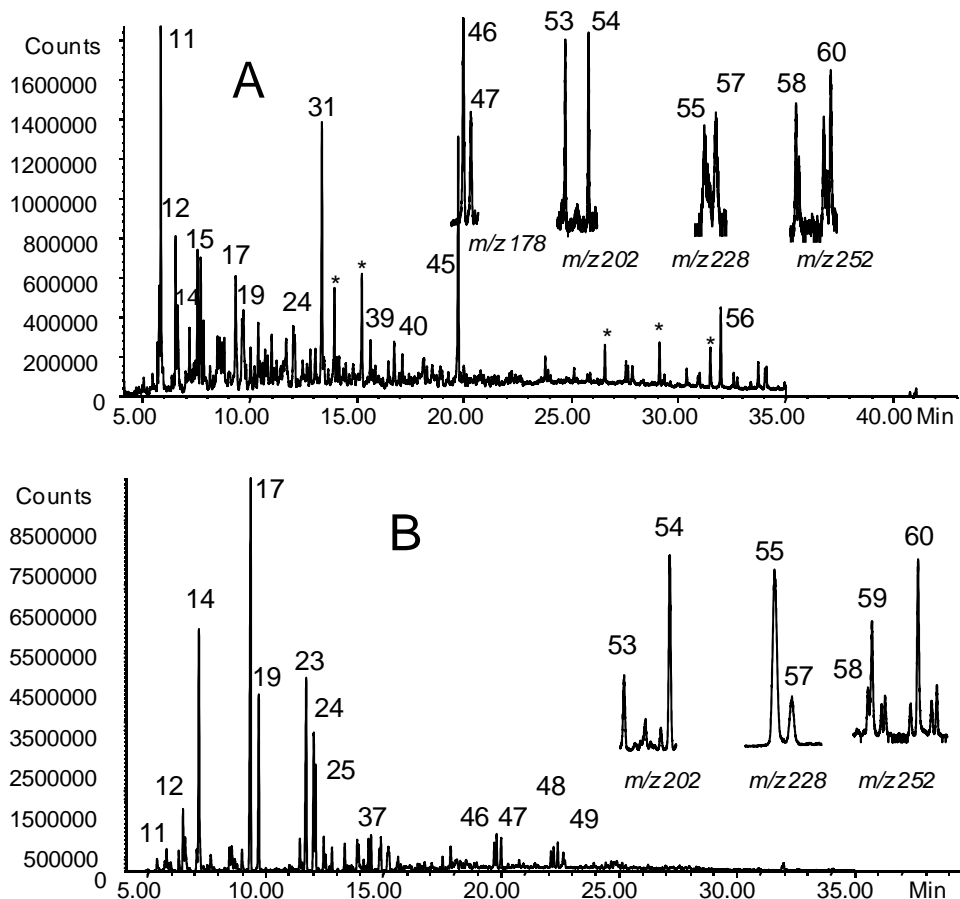


**Table 3.3.1:** Structural assignments of GC-MS peaks in Figs. 2-5 with the indication of characteristic ions in mass spectra (quantitation ions for priority PAHs).

#	Compound ( <i>m/z</i> )	#	Compound ( <i>m/z</i> )
1	benzene (78)	33	4-ethylsyringol (167, 182)
2	toluene (91, 92)	34	dibenzofuran (139, 168)
3	furaldehyde (95, 96)	35	C3- naphthalenes (155, 170)
4	ethylbenzene (91, 106)	36	2,3,6- trimethylnaphthalene (155, 170)
5	<i>m/p</i> -xylenes (91, 106)	37	2,3,5- trimethylnaphthalene (155, 170)
6	phenol (66, 94)	38	4-vinylsyringol (165, 180)
7	trimethylbenzenes (105, 120)	39	Fluorene (166)
8	benzofuran (90, 118)	40	Methyldibenzofurans (181, 182)
9	<i>m/p</i> -phenols (107, 108)	41	4- <i>E</i> -propenylsyringol (179, 194)
10	guaiacol (109, 124)	42	2-methylfluorene (165, 180)
11	methylbenzofurans (131, 132)	43	1-methylfluorene (165,180)

<b>12</b>	methylindenes (129, 130)	<b>44</b>	Methylfluorenes (165,180)
<b>13</b>	4-methylguaiacol (123, 138)	<b>45</b>	Phenanthrene-d10 (188)
<b>14</b>	naphthalene (128)	<b>46</b>	Phenanthrene (178)
<b>15</b>	dimethylbenzofurans (145, 146)	<b>47</b>	Anthracene (178)
<b>16</b>	4-ethylguaiacol (137, 152)	<b>48</b>	3-methylphenanthrene (192)
<b>17</b>	2-methylnaphthalene (141, 142)	<b>49</b>	2- methylphenanthrene (192)
<b>18</b>	4-vinylguaiacol (135, 150)	<b>50</b>	9/4- methylphenanthrene (192)
<b>19</b>	1-methylnaphthalene (141, 142)	<b>51</b>	1-methylphenanthrene (192)
<b>20</b>	trimethylbenzofurans (145, 160)	<b>52</b>	C2-phenanthrenes (206)
<b>21</b>	syringol (139, 154)	<b>53</b>	fluoranthene (202)
<b>22</b>	2-ethylnaphthalene (141, 156)	<b>54</b>	Pyrene (202)
<b>23</b>	2,6/2,7-dimethylnaphthalene (141, 156)	<b>55</b>	Chrysene (228)
<b>24</b>	1,3-dimethylnaphthalene (141, 156)	<b>56</b>	Chrysene-d12 (240)
<b>25</b>	1,6/1,7-dimethylnaphthalene (141, 156)	<b>57</b>	benz[a]anthracene (228)
<b>26</b>	2,3/1,4-dimethylnaphthalene (141, 156)	<b>58</b>	benzo[b]fluoranthene (252)
<b>27</b>	1,2/1,5-dimethylnaphthalene (141, 156)	<b>59</b>	benzo[k]fluoranthene (252)
<b>28</b>	1,8-dimethylnaphthalene (141, 156)	<b>60</b>	benzo[a]pyrene (252)
<b>29</b>	<i>E</i> -isoeugenol (149, 164)	<b>61</b>	Indeno[1,2,3- <i>cd</i> ]pyrene (276)
<b>30</b>	acenaphthylene (152)	<b>62</b>	dibenz[ <i>a,h</i> ]anthracene (278)
<b>31</b>	<i>acenaphthene-d10</i> (164)	<b>63</b>	benzo[ <i>ghi</i> ]perylene (276)
<b>32</b>	acenaphthene (153)		

The resulting chromatograms (an example in Figure 3.3.2a) were featured by peaks associated to polyaromatic compounds, principally benzofurans, indenenes and naphthalenes, without significant amount of interferents. The pattern of alkylated naphthalene, fluorene and phenanthrene from Py-SPE was also strongly similar to that found in bio-oil.<sup>156</sup>

Emission levels of priority PAHs are reported in Table 3.3.2 The precision of the method was fairly satisfactory (13-45% RSD) considering that the intrinsic variability of the pyrolytic process should be high when operating with a small quantity (< 10 mg) of a heterogeneous sample such as woody biomass. Emission levels determined by Py-SPE (6-0.05  $\mu\text{g g}^{-1}$  range) were fairly comparable to those calculated from the analysis of bio-oil by gram scale analysis,<sup>156</sup> with naphthalene and fluorene as the most abundant PAHs. The highest levels found in Py-SPE were probably determined

<sup>156</sup> D. Fabbri, A. Adamiano, C.Torri. GC-MS determination of polycyclic aromatic hydrocarbons evolved from pyrolysis of biomass. Anal Bioanal Chem. 397 (2010) 309–317.

by the different operating conditions between analytical and preparative pyrolysis (e.g. pyrolysis time, trapping of pyrolysis products, etc.).

**Table 3.3.2.** Emission levels of PAHs from Py-SPE at 500 °C of poplar wood with and without zeolite HZMS-5 (mean values and RSD from 5 replicates).

PAH	Poplar $\mu\text{g g}^{-1}$	RSD %	+ zeolite $\mu\text{g g}^{-1}$	RSD %
naphthalene	6.3	13	2400	17
acenaphthylene	0.62	29	27	0.2
acenaphthene	0.98	45	21	28
fluorene	3.4	23	82	21
phenanthrene	0.88	20	197	12
anthracene	0.79	28	213	12
fluoranthene	0.26	36	2.8	6.6
pyrene	0.37	19	22	51
chrysene	0.12	40	45	13
benz[a]anthracene	0.12	42	13	22
benzo[b]fluoranthene	0.07	41	1.7	18
benzo[k]fluoranthene	0.05	40	4.6	14
benzo[a]pyrene	0.12	45	6.3	30

As far as catalytic pyrolysis is concerned, zeolite ZSM-5 is probably the most tested catalyst to improve fuel properties of bio-oil<sup>145,157,158</sup> and for this reason was selected in this study. It is known from analytical pyrolysis of biomass constituents that the presence of ZSM-5 increased noticeably the production of aromatic hydrocarbons, however PAHs were not quantified.<sup>157,158</sup> In accordance, GC-MS profiles of the aromatic fraction resulting from Py-SPE of poplar wood were profoundly modified in the presence of ZSM-5 (Figure 3.3.2b), naphthalenes became the dominant peaks and phenanthrene and anthracene (# 46 and 47) could be clearly revealed. Quantitative data reported in Table 3.3.2 show that the emission levels of PAHs markedly increased in the presence of ZSM-5

<sup>157</sup> T.R. Carlson, T.P. Vispute, G.W. Huber. Green Gasoline by Catalytic Fast Pyrolysis of Solid Biomass Derived Compounds. *ChemSusChem* 1 (2008) 397-400.

<sup>158</sup> T.R. Carlson, G.A. Tompsett, W.C. Conner, G.W. Huber. Aromatic Production from Catalytic Fast Pyrolysis of Biomass-Derived Feedstocks. *Top Catal.* 52 (2009) 241-252.

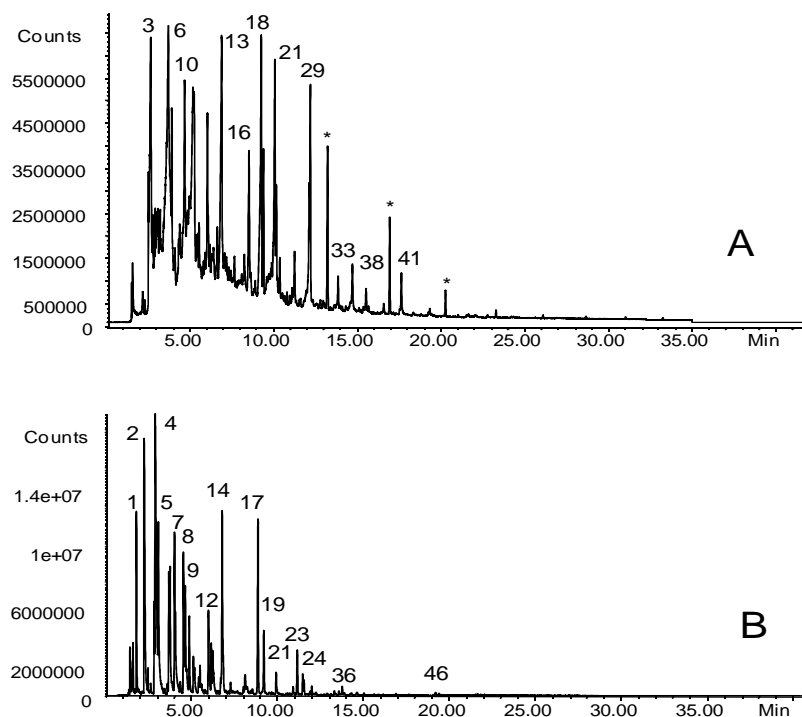
(e.g. naphthalene from 6 to 2400  $\mu\text{g g}^{-1}$ , phenanthrene from 0.9 to 200  $\mu\text{g g}^{-1}$  and benzo[*a*]pyrene from 0.1 to 6  $\mu\text{g g}^{-1}$ ).

This finding is in agreement with studies based on the analysis of bio-oil obtained from preparative pyrolysis of wood.<sup>145</sup> For instance, benzo[*a*]pyrene was reported to increase from undetectable levels in original bio-oil to 800  $\mu\text{g g}^{-1}$  in HZSM-5 catalytically upgraded bio-oil.<sup>145</sup> In this respect, quantitative results from analytical pyrolysis with and without catalyst are consistent with literature data. It is worth underlying that the concentration of PAHs expected in bio-oil from uncatalysed pyrolysis was comparable to that found in diesel<sup>150,159</sup> and gasoline<sup>159,160</sup> but may exceed conventional transport fuels in bio-oil derived from catalytic pyrolysis with zeolite.

### 3.3.3.2 Py-SPME

Chromatograms obtained from Py-SPME of poplar wood (an example is shown in Figure 3.3.3a) were characterised by peaks due to lignin phenols (# 10, 13, 16, 18, 21, 29, 33, 41) that could not be eliminated after washing the fiber with ammonia solution.

**Figure 3.3.3:** GC-MS profiles obtained from Py-SPME of (A) poplar wood and (B) poplar wood with zeolite HZSM-5. Peak numbers refer to Table 3.3.2; (\*) contaminants.



<sup>159</sup> J.L. Perez Pavon, M. del Nogal Sanchez, M.E. Fernandez Laespada, B. Moreno Cordero. Determination of aromatic and polycyclic aromatic hydrocarbons in gasoline using programmed temperature vaporization-gas chromatography-mass spectrometry. *J Chromatogr A* 1202 (2008) 196-202.

<sup>160</sup> L.C. Marr, T.W. Kirchstetter, R.A. Harley, A.H. Miguel, S.V. Hering, S.K. Hammond. Characterization of Polycyclic Aromatic Hydrocarbons in Motor Vehicle Fuels and Exhaust Emissions. *Environ Sci Technol.* 33 (1999) 3091-3099.

Prominent PAHs could be detected in the extracted mass chromatograms allowing a rough estimate of emission levels by external calibration. However, precision was rather low (RSD in the 30-70% range) and PAHs heavier than pyrene could not be detected. Main pyrolysis products probably saturated the fiber operating in the exposed mode<sup>155</sup> affecting the adsorption of PAHs.

Although not suitable for PAH quantitation, Py-SPME could be proposed as a fast screening method to acquire a qualitative picture of the pyrolysate composition. As an example, the pattern of alkylated PAHs obtained by SPME sampling exhibited a strong resemblance with the distribution obtained from the analysis of by mean of Py-SPE. Likewise, the effect of zeolite on the pyrolysate composition determined Py-SPME was in line with Py-SPE, as evidenced by comparing Figure 3.3.2 b and Figure 3.3.3b. In the presence of zeolite the production of aromatic hydrocarbons augmented considerably, and chromatograms were featured by intense peaks due to naphthalene and its methylated forms. The absence of solvent in the Py-SPME procedure enabled the detection of volatile organic compounds, among them BTEX (benzene, toluene, ethylbenzene and xylenes) produced the most intense peaks.

### **3.3.4 Conclusions**

Besides the analysis of main pyrolysis products of biomass, off-line analytical pyrolysis can be applied to the detection of PAHs, which are trace constituents in bio-oil. Py-SPE resulted more adequate for the quantitation of PAHs and the emission levels resulted comparable to those obtained from the analysis of bio-oil. From the qualitative point of view, the solventless and faster Py-SPME procedure provided a wider picture of the pyrolysate enabling the detection of volatile compounds, such as BTEX. Overall, analytical pyrolysis is suited as a screening technique on a quantitative base in those applications where significant rather than subtle variations of PAH emission have to be investigated. For instance, in the case of catalytic pyrolysis whereby the energetic value of bio-oil is improved by reducing the content of oxygen through the elimination of water or carbon dioxide from organic compounds through the action of active solids. Here, the activity of different catalysts towards the unwanted production of PAHs could be investigated by the Py-SPE procedure in order to predict the levels expected in biofuels.

## 3.4 Structural analysis of bio-char by Py-GC-MS.

### 3.4.1. Introduction

The solid residue formed upon biomass slow pyrolysis, charcoal, has historical applications dating back to the human civilization.<sup>161</sup> Charcoal is still used as a solid fuel, a reductant in steel industry, and in the activated form as a sorbent material. Recently, agronomic (soil fertility, crop growth) and environmental (reducing CO<sub>2</sub>, CH<sub>4</sub>, N<sub>2</sub>O emission; adsorption of contaminants) applications are receiving growing interest in the literature and the term bio-char has become familiar to the scientific community.<sup>162,163</sup> The importance of bio-char as soil conditioner (in that also named as agri-char) or carbon sequestration agent and its impact to the environment require a full understanding of its properties<sup>164,165,166,167,168,169</sup> and the mechanisms controlling its activity in soil.<sup>170,171</sup>

The stability in soil is a paradigmatic attribute of bio-char when selecting its application in environmental (carbon sequestration) or agricultural (fertility increases) applications.

It is known that naturally occurring charcoal and black carbon (BC), in the wide sense including char, soot, graphite, all the form of carbonaceous matter produced by incomplete combustion of any organic material), as those preserved in soils from forest fires, exhibit different degrees of stability probably related to the depolymerisation and surface oxidation which in turn are related to chemical structure. Volatile content (VM) of fixed carbon (carbon which do not volatilize at 900°C, FC) was proposed to be the most convenient method to estimate bio-char stability for the purpose of carbon

---

<sup>161</sup> M.J. Anatal, M. Gronli. The Art, Science, and Technology of Charcoal Production. *Ind Eng Chem Res.* 42 (2003) 1619-1640.

<sup>162</sup> S.P. Sohi, E. Krull, E. Lopez-Capel, R. Bol. Chapter 2:A Review of Biochar and Its Use and Function in Soil. *Advances in Agronomy* 105 (2010) 47-82.

<sup>163</sup> K..A. Spokas, W.C. Koskinen, J.M. Baker, D.C. Reicosky. Impacts of woodchip biochar additions on greenhouse gas production and sorption/degradation of two herbicides in a Minnesota soil. *Chemosphere* 77 (2009) 574-581.

<sup>164</sup> R.K. Sharma, M.R. Hajaligol. Effect of pyrolysis conditions on the formation of polycyclic aromatic hydrocarbons (PAHs) from polyphenolic compounds. *J Anal Appl Pyrol.* 66 (2003) 123-144.

<sup>165</sup> C. Branca, C. Di Blasi. Oxidation characteristics of chars generated from wood impregnated with (NH<sub>4</sub>)<sub>2</sub>HPO<sub>4</sub> and (NH<sub>4</sub>)<sub>2</sub>SO<sub>4</sub>. *Thermochim. Acta* 456 ( 2007) 120-127.

<sup>166</sup> H. Abdullah, K.A. Mediaswanti, H. Wu. Biochar as a Fuel: 2. Significant Differences in Fuel Quality and Ash Properties of Biochars from Various Biomass Components of Mallee Trees. *Energ.Fuel* 24 (2010) 1972–1979.

<sup>167</sup> C.E. Brewer, K. Schmidt-Rohr, J. A. Satrio, R. C. Brown, Characterization of biochar from fast pyrolysis and gasification systems. *Env.Progr.Sustain. Energ.* 28 (2009) 386–396.

<sup>168</sup> M. Keiluweit, P. S. Nico, M. G. Johnson, M. Kleber. Dynamic Molecular Structure of Plant Biomass-Derived Black Carbon (Biochar). *Environ.Sci.Technol.* 44 (2010) 1247–1253.

<sup>169</sup> J.W. Lee, M. Kidder, B.R. Evans, S. Paik, A.C. Buchanan III, C. T. Garten, R.C. Brown. Characterization of Biochars Produced from Cornstovers for Soil Amendment. *Environ.Sci.Technol.* 44 (2010) 7970–7974.

<sup>170</sup> S.D. Joseph, M. Camps-Arbestain, Y. Lin, P. Munroe, C. H. Chia, J. Hook, L. van Zwieten, S. Kimber, A. Cowie, B. P. Singh, J. Lehmann, N. Foidl, R.J. Smernik, J.E. Amonette. An investigation into the reactions of biochar in soil. *Australian Journal of Soil Research* 48 (2010) 501–515.

<sup>171</sup> K..A. Spokas, J.M. Baker, D.C. Reicosky. Ethylene: potential key for biochar amendment impacts. *Plant and Soil* 333 (2010) 443-452.

sequestration.<sup>172</sup> Volatility was structurally associated to aliphatic regions which are more labile (remineralise faster) than aromatic regions and more abundant when pyrolysis is conducted at lower temperature. This hypothesis requires a detailed knowledge of the molecular structure of bio-char to be fully supported. Bio-char structure is described as being composed by amorphous structures, turbostratic crystallites characterized by unordered graphite-like layers and ordered graphene sheets. Graphene dominium, aromaticity and microporosity generally increase with increasing temperature. These domains are expected to behave differently when subjected to thermal stress, such as pyrolysis. Therefore, FC and VM evaluation can give an idea of the amount of graphene like material in the bio-char, that are considered most stable carbon structure in the soil environment. Beyond the fact that bio-char with highest FC values is probably most stable biochar, the type of VM evolved is especially important for the evaluation of medium-term stability of bio-char (e.g. 50 y), which is also linked to the stability of non-graphitic and aliphatic structures.

In these respect, analytical pyrolysis, and in particular Py-GC-MS, was suggested to be reliable method for molecular investigation of the bio-char volatilisable fraction. Py-GC-MS was largely applied to the characterization of charcoal and BC from natural setup spanning a period of over thousand years.<sup>173,174,175</sup> Py-GC-MS was also applied to investigate synthetic black carbon materials<sup>176,177</sup> and possible non-combustion interferents of BC.<sup>178</sup>

In the case of natural BC, pyrograms above 600 °C were dominated by benzene, toluene, benzonitrile, naphthalene, diphenyl, benzofuran with a similar pattern in the 700-1200 °C interval. This set of pyrolysis products was selected as typical of BC by Kaal et al.<sup>179,174</sup> However, compounds indicative of uncharred material, such as levoglucosan, could be still revealed at high pyrolysis temperature. Although the presence of carboxylic acid groups could not be revealed by

---

<sup>172</sup> A.R. Zimmerman. Abiotic and Microbial Oxidation of Laboratory-Produced Black Carbon (Biochar). *Environ.Sci.Technol.* 44 (2010) 1295-1301.

<sup>173</sup> J. Kaal, S. Brodowski, J.A. Baldock, K.G.J Nierop, A.M. Cortizas. Characterisation of aged black carbon using pyrolysis-GC/MS, thermally assisted hydrolysis and methylation (THM), direct and cross-polarisation <sup>13</sup>C nuclear magnetic resonance (DP/CP NMR) and the benzenepolycarboxylic acid (BPCA) method. *Org.Geochem.* 39 (2008) 1415-1426.

<sup>174</sup> J. Kaal, A.M Cortizas, K.G.J. Nierop. Characterisation of aged charcoal using a coil probe pyrolysis-GC/MS method optimised for black carbon. *J.Anal.Appl.Pyrolysis* 85 (2009) 408-416

<sup>175</sup> C. Nocentini, G. Certini, H. Knicker, O. Francioso, C. Rumpel. Nature and reactivity of charcoal produced and added to soil during wildfire are particle-size dependent. *Org.Geochem.* 41 (2010) 682-689.

<sup>176</sup> F.J. Gonzales-Vila, P. Tinoco, G. Almendros, F. Martin, Pyrolysis-GC-MS analysis of the formation and degradation stages of charred residues from lignocellulosic biomass. *J Agric Food Chem* 49 (2001) 1128-113.

<sup>177</sup> J.Z. Song, P. Peng, Characterisation of black carbon materials by pyrolysis-gas chromatography-mass spectrometry *J.Anal.Appl.Pyrolysis*, 87 (2010) 129-137.

<sup>178</sup> J. Maria de la Rosa Arranz, F. J. Gonzalez-Vila, E.Lopez Capel, D.A.C. Manning, H. Knicke, J.A. Gonzalez-Perez. Structural properties of non-combustion-derived refractory organic matter which interfere with BC quantification. *J.Anal.Appl.Pyrolysis* 85 (2009) 399-407.

<sup>179</sup> J. Kaal, C Rumper. Can pyrolysis-GC/MS be used to estimate the degree of thermal alteration of black carbon? *Org.Geochem* 40 (2009)1179-1187.

Py-GC-MS, the occurrence benzenecarboxylic acid moieties in charcoal was definitively proved by pyrolysis in the presence of a methylating reagent.<sup>174</sup>

Noteworthy, the differences in the pyrolysate composition was very small between species (oak, birch, legume) and relationships could be found between the proportion of black carbon products (aromatic hydrocarbons and benzofurans) and uncharred/weakly charred biomass (furans, pyrroles, aldehydes, ketones, alkanes/alkenes), the former products increasing with increasing age.

The correspondence between the abundance of pyrolysis products indicative of charred and uncharred fraction was supported by a comparison with NMR analysis of natural (fires) charcoal.<sup>179</sup>

In addition, it was suggested that the ratio of some alkylated and non-alkylated pyrolysis products could be indicative of charring intensity associated to dealkylation following thermal impact. Most of the research works on Py-GC-MS were conducted on natural charcoal and BC, less investigations were focused to synthetic char targeted to agricultural application (bio-char). Quantitative approach was found useful to find relationships with complementary techniques such as NMR and chemical oxidation.<sup>179</sup>

Therefore, in this chapter, Py-GC-MS was tested, together with thermogravimetric analysis (TGA) as fast method, in order to evaluate the structure of a large number of synthetic bio-chars, for agronomical application. Moreover The 1 years aging (in water) of one bio-char was studied, and Py-GC-MS was investigated as technique for the prediction of bio-char stability.

### **3.4.2. Experimental**

#### *3.4.2.1 Origin of bio-char samples*

The various bio-chars evaluated here were part of ongoing assessments into the impact of bio-char additions on greenhouse gas production potentials; research that is part of the USDA-ARS Bio-char and Pyrolysis Initiative. The bio-char was acquired from various bio-char suppliers, entrepreneurs, and research laboratories (see Acknowledgements). One Bio-char (BC-0HR) was aged one year in water following published procedure.<sup>163</sup> The chars had a range of 1 to 93% carbon; 1 to 89% ash; 0.1 to 7.5% nitrogen; and a range of pyrolysis temperatures from 410 to 850 °C and residence times (seconds to hours). This group provides a cross-section of currently available bio-chars and ashes from biomass utilization. Bio-char will be used to describe these materials, even though fundamentally they are not all are bio-chars, but contain a mixture of ashes, charcoal, char and soot.

#### *3.2.2.2 Ultimate and proximate analysis*

Proximal (ASTM D3172) and ultimate analyses (ASTM D3176) were performed by Hazen Research (Golden, CO USA) and Brunauer-Emmett-Teller (BET) surface area (SA) analyses

(ASTM D6556) were performed by the USGS (D. Rutherford, Boulder, CO USA) and Material Synergy (Oxnard, CA USA). Ultimate and proximate analysis of Bio-chars were kindly provided by Dr. Kurt Spokas from United States Department of Agriculture.

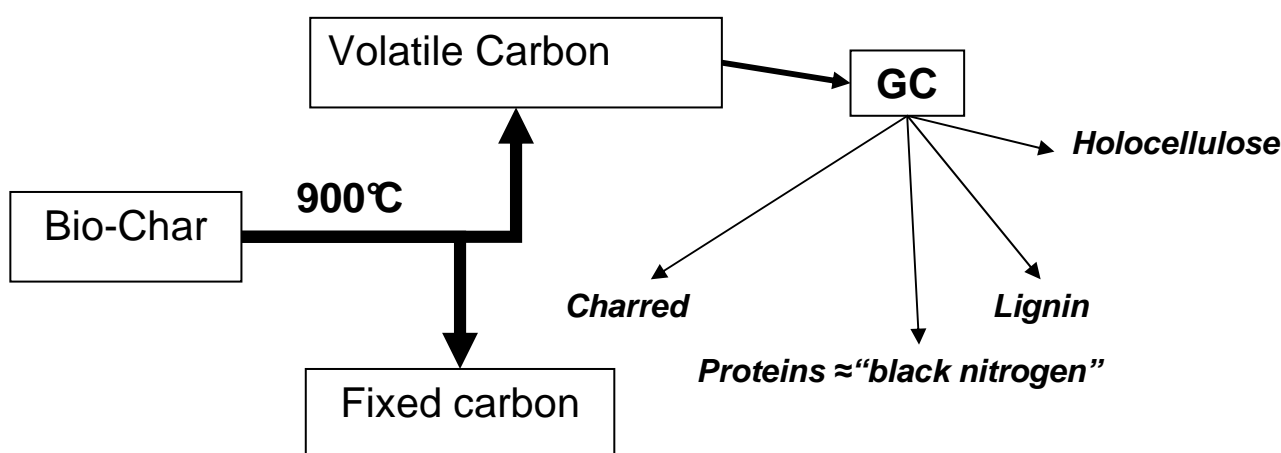
### 3.4.2.3 Py-GC-MS

Py-GC-MS experiments were performed following the procedure described in chapter 3.1, with different split ratio (1/50 instead of 1/200). The repeatability of yields were evaluated by nine replicate analyses of sample BC-0HR and resulted in RSD of 23% for total yields.

### 3.4.2.4 Structural evaluation of bio-char for prediction of medium-term degradation

Figure 3.4.1 shows the conceptual scheme of bio-char characterization. Biochar was characterized by means of elemental analysis, then it was subjected to heating to 900°C and the carbonaceous (mass of residue minus the ash content) was referred to as fixed carbon. Volatile carbon was calculated by the difference between carbon content and fixed carbon. Assignment of different fractions of VM were performed by mean of GC detectable compounds identification. The same relative proportions observed for GC detectable pyrolysis products was assigned to the different fractions (holocellulose, charred VM, lignin and “black nitrogen” fraction) of VM evolved from bio-char.

**Figure 3.4.1:** conceptual scheme used for bio-char characterization.



## 3.4.2. Results and discussion

### 3.4.3.1. Characteristics of bio-char samples

Ultimate and proximate analyses of synthetic bio-char samples are listed in Tables 3.4.1 and 3.4.2 along with BET surface areas (SA in Table 3.4.2). SA encompass a wide interval comparable to

literature data (RA Brown 2006) for synthetic chars. SA tends to increase with increasing pyrolysis temperature and char residence time.<sup>167,180</sup>

**Table 3.4.1:** Biomass feedstock and elemental composition of bio-char samples. (Id.: Sample identifiers).

<i>ID</i>	<i>Feedstock</i>	<i>C</i>	<i>H</i>	<i>N</i>	<i>O</i>	<i>S</i>
<i>BC-0HR</i>	Hardwood sawdust 1 <sup>a</sup>	63.8	3.03	0.22	11.8	0.01
<i>BE1</i>	Hardwood sawdust 2 <sup>a</sup>	69.5	3.06	0.32	13.1	0.01
<i>BEW</i>	1 year aged wet BC-0HR	62.9	2.80	0.32	11.8	0.01
<i>PB</i>	wood pellets	81	2.9	0.4	12	0.01
<i>PG</i>	wood pellets	81	3.1	0.3	13	0.02
<i>FGCE</i>	wood pellets	76	3.1	0.4	13	0.04
<i>CE1</i>	waste wood scrap gasifier	27.4	0.33	0.29	<0.01	1.24
<i>CE3</i>	wood pellets	77.6	2.96	0.39	11.3	0.05
<i>CE2</i>	wood pellets	82.9	1.70	0.42	4.1	0.03
<i>A1</i>	wood waste	81.5	2.42	0.36	7.7	0.01
<i>A2</i>	wood waste	91.4	2.89	0.38	4.60	0.00
<i>BC-19</i>	distillers grain	68.6	4.81	7.52	6.6	0.96
<i>BC-20</i>	distillers grain	69.4	4.31	7.43	5.9	0.90
<i>BC-21</i>	corn cob	78.8	4.31	0.67	13.2	0.01
<i>BC-22</i>	corn cob	82.6	3.85	0.61	9.1	0.01
<i>BC-23</i>	wood waste	79.8	3.73	0.83	11.9	0.01
<i>BC-24</i>	wood waste	80.8	3.23	0.77	11.4	0.02
<i>M1</i>	corn stover	45.0	1.66	0.50	1.0	0.04
<i>M2</i>	pine wood chip	75.0	3.4	0.30	9.0	0.1
<i>M3</i>	peanut hull	59.0	2.3	2.70	12.0	0.2
<i>M4</i>	corn stover	25.0	1.1	0.60	5.0	0.04
<i>M6</i>	Pine chip (mixed with compost after production)	43.0	--	2.20	11.0	--
<i>M7</i>	manure/woodchip	1.0	0.5	0.10	3.00	2.1
<i>M8</i>	Hardwood	69.0	2.4	0.70	9.00	0.02
<i>M9</i>	pine woodchip	71.0	3.3	0.20	11.0	0.1
<i>M10</i>	peanut hull	60.0	1.1	0.90	10.0	0.1
<i>M11</i>	corn stover	66.0	1.5	1.00	4.0	0.04
<i>M12</i>	corn stover	51.0	0.9	1.00	0.00	0.04
<i>M13</i>	cocunut shell	87.9	0.06	0.40	<0.01	0.65
<i>BC-16</i>	Hardwood	56.9	2.77	0.41	10.5	0.41
<i>BC-17</i>	Mixed wood chips/manure	71.1	3.44	0.11	20.6	0.01
<i>BC-18</i>	macadamia nut shells	93.1	2.56	0.67	1.7	0.02

<sup>a</sup>two replicas of bio-char obtained from the same pyrolyser and feedstock

However, total SA is not sufficiently indicative for thermal reactivity (e.g. gasification) as it includes SA from micropores which probably do not participate in reactions.<sup>181</sup>

<sup>180</sup> R.A. Brown, A.K. Kercher, T.H. Nguyen, D.C. Nagle, W.P. Bal. Production and characterization of synthetic wood chars for use as surrogates for natural sorbents. *Organic Geochemistry* 37 (2006) 321–333.

**Table 3.4.2:** Surface area (SA, m<sup>2</sup> g<sup>-1</sup>), water content (H<sub>2</sub>O, weight %), volatile matter (VM, weight %), fixed carbon (FC, weight %) and ash (weight % on dry weight basis).

#	SA	H <sub>2</sub> O	VM	FC	Ash
<i>BC-OHR</i>	0.98	8.06	26.1	53	21.1
<i>BE1</i>	1.03	4.40	29.1	44	14.0
<i>BEW</i>	10.4	36.0	24.5	50	22.1
<i>PB</i>	92	5.12	29	67	3.9
<i>PG</i>	1.7	5.10	19	68	2.0
<i>FGCE</i>	0.3	5.00	30	63	7.5
<i>CE1</i>	144	0.91	18.9	8.2	72.9
<i>CE3</i>	3.08	4.83	27.7	65	7.66
<i>CE2</i>	73.8	6.79	15.1	83	10.8
<i>A1</i>	251	8.70	18.2	74	7.97
<i>A2</i>	106	1.33	15.2	84	1.03
<i>BC-19</i>	0.28	1.75	45.7	44	11.5
<i>BC-20</i>	0.28	1.97	37.6	50	11.9
<i>BC-21</i>	<0.10	2.93	33.2	64	2.92
<i>BC-22</i>	<0.10	3.07	24.8	71	3.84
<i>BC-23</i>	3.51	3.71	26.8	70	3.66
<i>BC-24</i>	26.8	3.57	23.7	73	3.71
<i>M1</i>	4.4	2.64			55.0
<i>M2</i>	0.1	5.25			6.00
<i>M3</i>	1	7.77			15.0
<i>M4</i>	4.2	2.69			69.0
<i>M6</i>	63.5			36	54.0
<i>M7</i>	4.8	3.87		60	89.0
<i>M8</i>	19.2	6.43			14.0
<i>M9</i>	0.2	7.15			9.0
<i>M10</i>	286	16.2			15.0
<i>M11</i>	17.3	5.29		13	54.0
<i>M12</i>	9.9	2.65		53	74.0
<i>M13</i>	960	5.45	1.84	85.2	13.0
<i>BC-16</i>	33.7	6.29	34.7	36.4	28.9
<i>BC-17</i>	66.3	3.31	34.8	60.5	4.77
<i>BC-18</i>	6.89	9.54	16.8	81.2	1.92

Char thermal reactivity is influenced by morphological features (e.g. micro/macropores), in turn determined by the release of volatiles and hence feedstock composition and process conditions,

<sup>181</sup> C. Di Blasi. Modeling chemical and physical processes of wood and biomass pyrolysis. Progress in Energy and Combustion Science 34 (2008) 47-90.

with micropores predominating over macropores in slow pyrolysis.<sup>181</sup> Volatile matter (VM) ranged from 1.8 to 45% and fixed carbon ranged from 13 to 84%.

### 3.4.3.2 Py-GC-MS. Total yields.

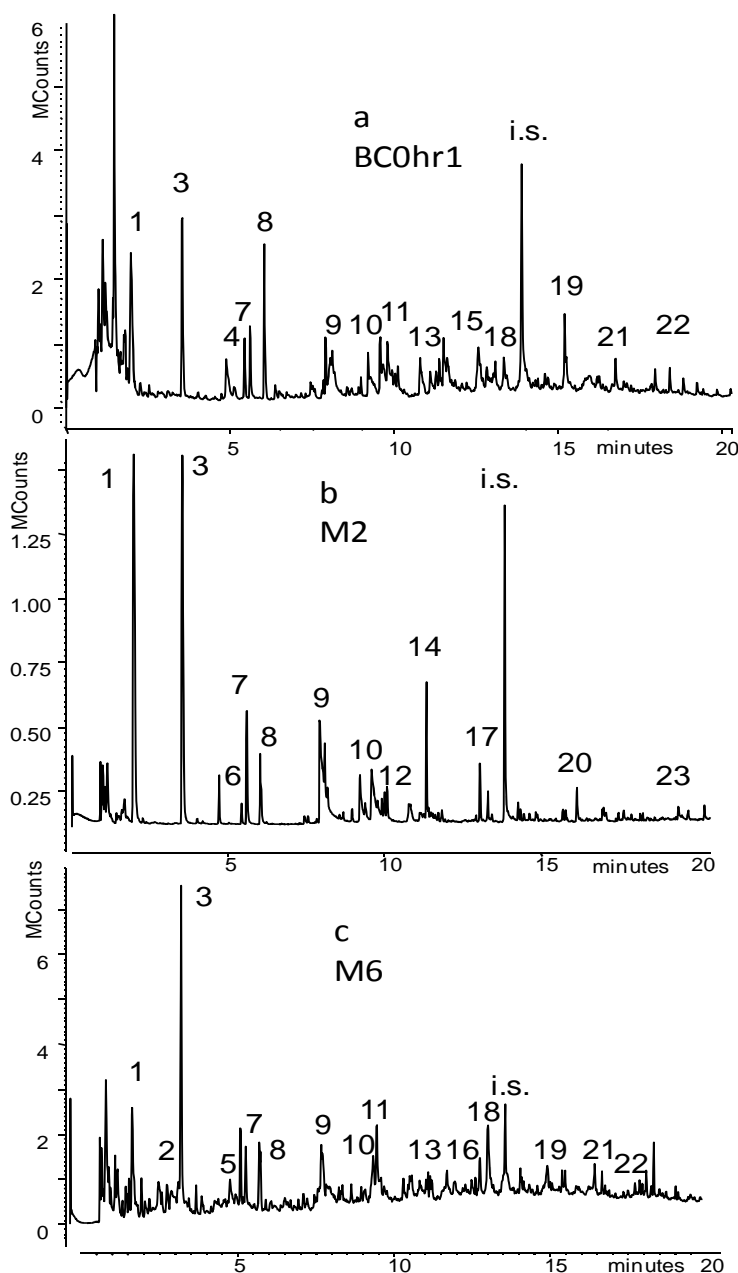
**Table 3.4.3.** Pyrolysis products of bio-char and their predominant origin: C, charred biomass; H holocellulose; L, Lignin; P, proteins; S sulfur-containing compounds.

<i>r.t., min</i>	<i>Structural attribution</i>	<i>origi n</i>	<i>r.t., min</i>	<i>Structural attribution</i>	<i>origi n</i>
1.15	methyl glyoxal	H	10.07	Methylbenzofuran	C
1.53	3-pentanone	H	10.56	3-methyl-2,4(3H,5H)-furan	H
1.79	acetic acid	H	11.19	4-ethylphenol	L
1.94	benzene	C	11.37	naftalene	C
2.5	2,5-dimethylfuran	H	11.53	Benzothiophene	S
3.42	pyrrole	P	11.54	4-methylguaiacol	L
3.52	toluene	C	11.74	catechol	L
3.73	acetoxycetaldehyde	H	11.84	4-vinylphenol	L
3.77	2-methyl thiophene	S	12.04	3,6:1,4-dianhydro glucopyranose	H
3.79	3-methyl thiophene	S	12.22	Hydroxymethyl furfural	H
3.92	butanedial	H	12.89	4-ethylguaiacol	L
4.89	furaldehyde	H	13.22	Indole	P
5.42	ethylbenzene	C	13.31	4-vinylguaiacol	L
5.47	furfuryl alcohol	H	13.38	ascopyrone-P	H
5.59	<i>m,p</i> -xylene	C	14.00	Syringol	L
6.03	styrene	C	14.04	eugenol	L
6.07	<i>o</i> -xylene	C	14.25	biphenyl	C
6.9	2-ciclopentanedione	H	14.6	Vanillin	L
7.44	benzaldeide	L	14.76	cis-iso-eugenol	L
8.02	methylfufural	H	15.28	4-methylsyringol	L
8.08	phenol	L	15.33	<i>trans</i> -isoeugenol	L
8.13	benzofuran	C	16.77	4-vinylsyringol	L
8.22	4-hydroxy-5,6-diihydro-2- pyranone	H	17.30	4-allylsyringol	L
8.8	3-hydroxy-2-methyl- cyclopentenone	H	17.90	4-(Z-propenyl) syringol	L
8.98	2-hydroxybenzaldehyde	L	18.40	4-(E-propenyl) syringol	L
9.32	<i>m</i> -cresol	L	18.92	4-hydroxy-2-methoxycinnam	L
9.71	<i>o,p</i> -cresol	L	19.29	acetosyringone	L
9.76	guaiacol	L	19.39	phenanthrene	C
9.9	methylbenzofuran	C	19.50	anthracene	C
9.98	methylbenzofuran	C			

As expected from their different origin, bio-char samples produced different pyrolysate pattern when subjected to Py-GC-MS. Typical programs are depicted in Figure 3.4.2. A set of 61 pyrolysis

products among the most abundant and representative of biological precursors was selected for the calculation of the yields (Table 3.4.3).

**Figure 3.4.2:** Total ion chromatograms from Py-GC-MS of bio-char samples (a) BC-0HR , (b)M2, (c) M6. (i.s.: internal standard, 5-propenylguaiacol). Peak attribution: 1, benzene; 2, pyrrole; 3, toluene; 4, furaldehyde; 5, methylpyrrole; 6, ethylbenzene; 7, m,p-xylene; 8, styrene; 9, phenol; 10, p-cresol; 11, guaiacol; 12, methlbenzofurans; 13, 4-ethylphenol; 14, naphthalene; 15, 4-methylguaiacol; 16, indole; 17, methylnaphthalenes; 18, 4-vinylguaiacol; 19, 4-methylsyringol; 20, dibenzofuran; 21, vinylsyringol; 22, 4-propenylsyringol; 23, phenanthrene.

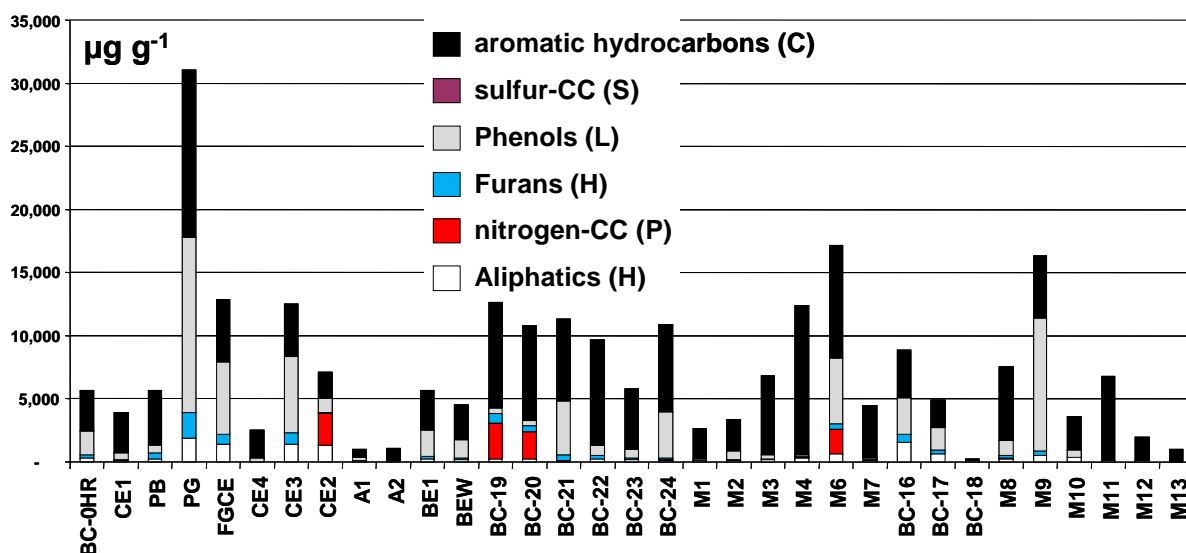


Py-GC-MS were run under the same operative conditions, several factors inherent to the sample might influence the pyrolytic behaviour of bio-char, such as the presence of inorganic constituents

and particle size. In the latter case, it was found that coarse charcoal particles tend to be enriched in aromatic hydrocarbons, while fine particles contain more N- and O-sugar derived compounds.<sup>175</sup> The effect of ash might be important for samples M1, M4, M6, M7, M11 and M12 characterized by a high ash content (> 50%). Chars M1, 4, 11, 12 were obtained from the pyrolysis of corn stover in accordance with literature data showing that chars from corn stover and switchgrass are rich in ash composed principally by silica.<sup>167</sup>

Given the above, total yields are reported in Figure 3.4.3. Values spanned on a interval of three order of magnitude wide, from 31 ‰ (M9) down to 240 part per million (M7). The yields are correlated with volatile matter (VM), while there is no correlation with fixed carbon (FC) and other parameters (e.g. BET).

**Figure 3.4.3:** Yields of pyrolysis products ( $\mu\text{g} / \text{g}_{\text{biochar}}$ ) from Py-GC-MS of bio-char samples grouped by chemical families and origin (see Table 3.4.2)



### 3.4.3.3 Py-GC-MS. Molecular distribution.

Py-GC-MS provided information of the thermally degraded products at a molecular level and according to their possible origin as reported in Table 3.4.3. Yields for each molecular family are depicted in Figure 3.4.3.

Aliphatic hydrocarbons resulted minor products in all the samples and were not quantified. Aromatic hydrocarbons including PAHs were predominant in the pyrolysates of bio-char samples, M9 which exhibited higher levels of phenol derivatives. Lignin phenols resulted an important group of pyrolysis products owing to the origin from lignocellulosic feedstock. Pyrolysis products deriving from holocellulose were detected as well (e.g. furans and anhydrosugars).

An important factor in analytical pyrolysis is the selection of pyrolysis temperature. To this purpose Kaal et al.<sup>174</sup> have investigated the effect of pyrolysis temperature on the chemical composition of sample pyrolysate. In the case of peat, at 400 °C thermolabile fractions (e.g. anhydrosugars and lignin phenols) predominate as glycosidic bonds of cellulose and ether-linkages between lignin monomers are easily cleaved. A more complete degradation of aliphatics and lignins occurred at 500 °C. The production of aromatic hydrocarbons increased at 600-800 °C. Lignin phenols decarboxylate, demethoxylate and eventually dehydroxylate with increased production of aromatic hydrocarbons in concomitance with increasing charring, while polysaccharide rearrangements produces furans and probably naphthalenes. Kaal found the temperature of 700 °C as a good balance to separate the effect of artificial charring (during the analysis) to that of pre-existing charred material in the sample. A set temperature of 900 °C was selected in our study as compromise between the comparison with VM and artificial charring (depressed at lower temperature). The set value of 900 °C corresponded approximately to 750 °C inside the platinum filament as measured with a thermocouple.

Analysis by <sup>13</sup>C-NMR showed that synthetic char are highly aromatics (over 81%), with a larger aromaticity but with a lower degree of condensed cluster for slow pyrolysis than gasification, explained by the dominant influence of pyrolysis temperature, but also residence time, while partially charred biopolymers were not detected.<sup>167</sup>

The content of nutrients conserved in bio-char from nutrient-rich feedstock (e.g. poultry litter) is an important aspect in relation to agronomic applications. The fate of nitrogen originally occurring in the biomass depends on several factors and can be completely lost by volatilization,<sup>182</sup> although slow pyrolysis conditions tend to conserve nitrogen into the bio-char.<sup>183</sup> Nitrogen containing compounds indicative of proteins (indole, pyrrole) and chlorophyll pigments (pyrrole and alkylated derivatives, these latter identified but not quantified) were revealed in relatively higher amount in the pyrolysates of samples B19, B20 and M6 which are characterized by a larger content of elemental nitrogen. Pyrroles from chlorophyll are rapidly destroyed,<sup>176</sup> thus probably proteins are the main contributors. In the case of sample B19 and B20 the feedstock was dried distiller grain, which is the solid residue after ethanol production from corn grain. M6 was a composite pine chip bio-char + compost mixture. Therefore, this mixture contained both charred and biomass materials, with corresponding higher nitrogen content. Nitrogen-containing compounds may play an important role in the degradability of charcoal as evidenced from the pyrolysis of proteins and are probably

---

<sup>182</sup>E.S. Krull, J.A. Baldock, J.O. Skjemstad, R.J. Smernik. Characteristic of biochar: Organo-chemical Properties. Biochar for environmental Management. Johannes Lehmann. Stephen Joseph ed. London 2009.

<sup>183</sup>J. W. Gaskin, C. Steiner, K. Harris, K. C. Das, B. Bibens. Effect of Low-Temperature Pyrolysis Conditions on Biochar for Agricultural Use. Transactions of the ASABE. 51 (2008) 2061-2069.

less degradable than cellulose.<sup>184</sup> However, pyrroles were probably prone to be degraded as these compounds were not found in the pyrolysates of ancient charcoal.<sup>173</sup>

Interestingly, methylthiophenes were clearly revealed in sample CE1 despite the low total yields of pyrolysate. This is in accordance to the relatively high level of elemental sulfur. Methylthiophenes were revealed in samples B19 and B20 as well, while B24 was characterized by the presence of benzothiophene. This finding may suggest the occurrence of different form of sulfur in these samples. Although sulfur was considered a proxy of soot from fossil fuel,<sup>177</sup> its occurrence could be significant in the pyrolysate of recent biomass.

The yields of each compound class were loosely correlated with VM. Thus, samples with high VM tends to generate higher amount of pyrolysis products characteristic of both fresh (e.g. furans) or aged biomass (e.g. benzofurans).

According to Kaal et al.<sup>173,174</sup> benzene, toluene, benzonitrile, naphthalene, diphenyl, benzofurane are pyrolysis products that could be associated specifically to the charred fraction of charcoal. Furans and pyrroles could be attributed to the fraction which is only weakly charred. In our study, aliphatic compounds eluting in the first region of chromatogram could be quantified, but these compounds were not described by Kaal et al.<sup>173,174,179</sup>

Following Kaal et al. indications, aromatic hydrocarbons (benzene, toluene, C2-benzenes, naphthalene, phenanthrene, diphenyl) and benzofurans were grouped into a single family of compounds representing the charred fraction of bio-char (Table 3.4.3). The relative contribution of the chemical group indicative of the charred fraction is presented in Figure 4 for each bio-char sample in a descending order.

Bio-char with a high percentage of charred pyrolysis products (> 80%, A2, BEW, BC-22, BC-23, M1, M2, M3, M4, M11, M12, M13) could be catalogued as “high rank” charcoal, with pyrolytic pattern similar to soot characterised by the emission of aromatic hydrocarbons as most important chemical species. These hydrocarbons could be thermally releasable aromatic fragments linked to larger sheets or pyrosynthesised as secondary pyrolysis products from smaller molecules, such as acetylene, evolved during the thermal re-organization of immature sub-structures into turbostratic crystallites.

Samples M6, M9, BC16, BC17, PG, FGCE with a lower contribution of charred pyrolysis products resemble “low rank” charcoal, as they contain a larger amount of oxygenated compounds, phenols and furan derivatives. Samples BC19, BC20, M6 released pyrolysates characterised by nitrogen-containing pyrolysis products indicative of proteins in accordance to their origin and high N/C ratio.

---

<sup>184</sup> H. Knicker, J.O. Skjemstad. Nature of organic carbon and nitrogen in physically protected organic matter of some Australian soils as revealed by solid-state <sup>13</sup>C and <sup>15</sup>N NMR spectroscopy. Australian Journal of Soil Research 38 (2000) 113-128.

This finding could be an indication that nitrogen-containing moieties might be located in rather degradable regions of the bio-char structure. This is in agreement with the observation by Kincker 2010 regarding a higher stability of char produced from cellulose than char produced by proteins.

According to Kaal and Rumpel,<sup>179</sup> the degree of de-alkylation might be a proxy of thermal alteration. Dealkylation can be estimated from Py-GC-MS from the ratio of parent/alkylated compound, such as benzene/toluene (B/T) ratio. B/T ratios were calculated from the pyrolysates of bio-char samples. The samples exhibited a large variability with high values (B/T > 6, sample M10) and low values (B/T < 0.5, samples BC-22). In general, the B/T ratio, i.e. dealkylation, tends to increase with decreasing overall yields and with increasing the relative abundance of pyrolysis products indicative of charring.

Bio-char from corn stover (M4, M11, M12, M1) were obtained at different pyrolysis temperatures (410, 505, 515, 815 °C respectively). The yields of pyrolysis products tended to decrease with increasing temperature (12000, 6700, 1900, 2600 µg/g respectively), however the B/T ratio decreased whereas the % of black carbon pyrolysis products was similar and very high (> 90%).

Bio-char A1 and A2 produced from wood waste at two different pyrolysis temperatures (475 and 550 °C, respectively) gave pyrolysates with similar yields and B/T ratios, but a different percentage of black carbon products due to a higher amount of lignin phenols in A1.

#### *3.4.3.4 Py-GC-MS Study of reactivity of bio-char in soil*

Py-GC-MS was applied to investigate in detail the “degradation rate” of different fractions, by analysis of respective markers evolved by analytical pyrolysis. This can help to establish links between markers and corresponding fractions with different degradability.

In order to establish the short term degradation rate of different fractions (which produce different pyrolytic markers) hardwood biochar obtained at 500°C (BC-0HR) was aged 1 year in the soil, and the pyrolytic pattern of sample aged in soils (BEW) was compared with that obtained from fresh BC-0HR. Table 3.4.4 shows the mass yield of pyrolysis product evolved.

As consequence of aging VM of sample decreased from 18% C/C<sub>sample</sub> to 15% C/C<sub>sample</sub>, corresponding to the 16% degradation of volatile matter in 1 y.

A decrease similar to that observed for VM was found for overall Py-GC-MS detectable yields.

Almost all absolute yields (with exception of phenol, cresols, hydroxyacetone, biphenyl and methyl glyoxal) are decreased in the sample obtained after 1 year soil incubation, in agreement with the progressive degradation of fractions that can produce GC detectable product (and then in agreement with VM degradation). Interestingly, increase of some aromatic oxygenated yield can be explained by means of oxidation of charred bio-char and formation of hydroxyls on the surface.

**Table 3.4.4:** Change in Py-GC-MS yield of pyrolysis products (expressed as  $\mu\text{g}$  per gram of carbon) from fresh BC-0HR (hardwood sawdust bio-char obtained at  $500^\circ\text{C}$ ) sample and from the same sample incubated for 1 year (BEW). (mean $\pm$  confidence interval with  $\alpha=0.05$ )

<i>markers</i>	<b><i>BC-0HR</i></b> <i>T<sub>0</sub></i> $\mu\text{g gC}^{-1}$	<b><i>BEW</i></b> <i>T<sub>1y</sub></i> $\mu\text{g gC}^{-1}$	<i>Degradation</i> <i>Rate</i> $\text{y}^{-1}$	<i>Average</i> <i>lifetime</i> $\text{y}$
Charred	1896 $\pm$ 577	1714 $\pm$ 567	0.10	>10
Lignin	1656 $\pm$ 382	1081 $\pm$ 347	0.35	3
Pyrrole	4.5 $\pm$ 1	3.9 $\pm$ 1	0.13	8
Holocellulose	187 $\pm$ 53	96 $\pm$ 4	0.49	2
$\Sigma$ Quantified	<b>3709</b>	<b>2802</b>		

Yields of compounds typical of carbohydrate pyrolysis, like furfuryl alcohol and 2-cyclopentanedione or hydroxymethylfurfural, were halved in the pyrolysis of 1 year old bio-char, indicating a relatively fast degradation of the cellulosic derived fraction, although slower than that observable for pure cellulose (that is entirely degraded with a degradation rate of  $0.98 \text{ y}^{-1}$ ).<sup>185</sup> Also lignin derived pyrolysis products from aged sample yield were lower than in fresh one (-35% on average), even if a short time span was considered.

On the other hand, charred fragments (toluene or benzene) showed a little but significant decrease (10%) in the 1 year aged bio-char, confirming that there is a large fraction of bio-char which are volatilizable and breakable by thermal degradation, but are relatively stable in environmental conditions. Finally, it is interesting to notice that pyrrole (representative of nitrogen containing moieties and residual proteins in the char) relative decrease in 1 y was 13%. This indicates that the nitrogen containing fractions of bio-char (a sort of “black nitrogen”) can contribute substantially to the short term stability of the material, but also suggests the potential application of bio-char based fertilizers with controlled release of the nutrients.

Summarizing, on the basis of obtained on 1 year aging of bio-char, it is possible to confirm that lignin and cellulose like fractions of bio-char shows a short degradation rate similar to typical biomass refractory macromolecules (e.g. resistant plant material  $0.3 \text{ y}^{-1}$ ), whereas charred VM (substance that are thermal breakable but characterized by aromatic structures) and “black nitrogen” structures are relatively more refractory to the chemical and biological attacks.

<sup>185</sup>J.A. Baldock, R.J. Smernik. Chemical composition and bioavailability of thermally altered *Pinus resinosa* (Red pine) wood. *Organic Geochemistry* 33 (2002) 1093–1109

### 3.4.3.5 Prediction of long term stability.

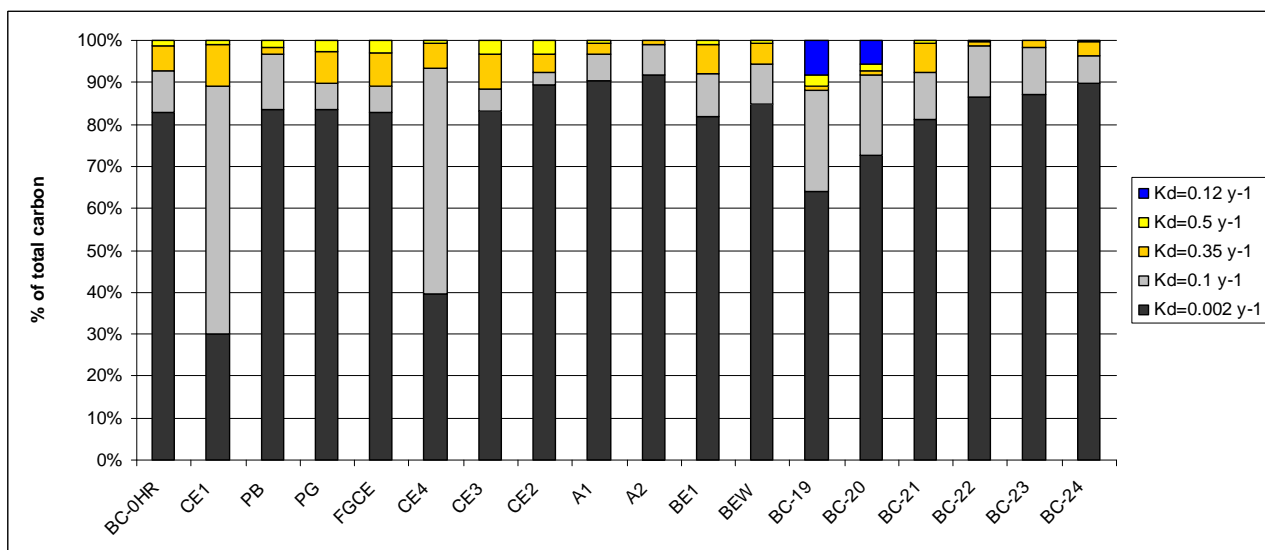
Evaluation of volatile matter (VM) and fixed carbon amount (FC) in biochar samples is usually proposed as the simplest method for the evaluation of bio-char stability.<sup>172</sup> This method gives an idea of the amount of graphene like material in the bio-char, that are considered among the most stable carbon structure in soil environment. Beyond the fact that bio-char samples with higher FC values are the most stable biochar, the type of VM evolved is especially important for the evaluation of medium-term stability of bio-char (e.g. 50 y), which is also linked to the stability of non-graphitic and aliphatic structures.

As shown in previous paragraphs, Py-GC-MS can be envisaged as a method for the investigation of the chemical nature of VM and then it can be used to predict VM environmental stability.

For this reason, FC data and Py-GC-MS techniques of some representative bio-chars were used for obtain a global picture of the chemical nature of each material. In fact, by coupling VM and FC data, elemental analysis and Py-GC-MS, bio-char can be rationalized as non volatile matter (non breakable at 900°C and considered ultra-stable fraction of bio-char), degradable matter (volatile matter with aliphatic character) and matter with intermediate stability (charred volatile matter).

Figure 3.4.4 shows the semi-quantitative analysis of different fractions performed by coupling FC results and quantitative evaluation of different type of VM by means of semi-quantitative (relative abundances) analysis of pyrolysis products.

**Figure 3.4.4:** Quantitative evaluation of fractions with different degradability, characterized by means of coupled Py-GC-MS, FC and elemental analysis data.



Different degradation rates were then assigned to each fraction. Degradation rate of ultra-stable fraction (FC content) can be considered equal to that observed for archaeological charcoals ( $K_d=0.002\text{ y}^{-1}$  in temperate climates),<sup>186</sup> in which only in resistant fraction remained.

In order to have an approximate idea of the stability, the degradation ratio observed for different VM markers in 1 year aging (paragraph 3.4.3.4) can be used to predict the mineralization rate of charred VM, lignin like material, holocellulose like material and “proteins derived” compounds ( $K_d= 0.1\text{ y}^{-1}; 0.35\text{ y}^{-1}; 0.5\text{ y}^{-1}; 0.12\text{ y}^{-1}$  respectively).<sup>187,188</sup>

By these assumptions, it is possible to attempt a rough prediction of bio-char stability over mid-term period (100 y). According to the chemical composition shown in Figure 3.4.4, on the 100 y time span, bio-char could retain around 80% of initial carbon. Stability calculated by inclusion of VM (identified from Py-GC-MS) resulted significantly higher than that obtained using only FC evaluation, and this because this type of data interpretation take into account also non graphitized but stable material, that give a contribute to the bio-char stability over medium time span (first 50 years), that is especially relevant for actual GHGs strategies. From the results obtained for most of the bio-char samples, about 70-90% of bio-char carbon is stable, under environmental conditions, for more than 50 y. On this time span, most degradable bio-char were those rich in nitrogen (distiller grains) or deriving from wood waste with high ash content.

### 3.4.4 Conclusions

Py-GC-MS was demonstrated to be a very useful tool for fast investigation of bio-char structural features. The knowledge of the molecular structure deduced from the chemical composition of the pyrolysate can be applied for inferring the bio-char stability.

In particular, quantitative Py-GC-MS enabled a rough estimate of the degradation rate of different structural fractions. A comparison between thermogravimetric data (fixed carbon and volatile matter) and Py-GC-MS data suggested that the molecular structure, and then the degree of bio-char stability is largely influenced by the starting material. Therefore Py-GC-MS could be proposed as method to check the quality of bio-char before the soil application.

---

<sup>186</sup> C-H. Cheng, J. Lehmann, M.H. Engelhard. Natural oxidation of black carbon in soils: Changes in molecular form and surface charge along a climosequence. *Geochimica et Cosmochimica Acta* 72 (2008) 1598-1610.

<sup>187</sup> D.S. Jenkinson. The turnover of organic carbon and nitrogen in soil. *Phil. Trans. R. Soc. Lond. B* 329 (1990) 361-368.

<sup>188</sup> A. Hilscher, H. Knicker. Carbon and nitrogen degradation on molecular scale of grass-derived pyrogenic organic material during 28 months of incubation in soil. *Soil Biology & Biochemistry* 43 (2011) 261-270

## 3.5. Direct *in-situ* catalytic pyrolysis of biomass: catalyst screening by Py-GC-AED.

### 3.5.1. Introduction

Raw biomass pyrolysis oil has low heating value, and high water, acids and solid content. Over time, reactivity of some components in the oil leads to the formation of higher amount of larger molecules that results in higher viscosity and in slower combustion.<sup>189</sup> For these reasons, an *in-situ* or downstream upgrading process could be beneficial.

In searching for a moderate improve of stability, an alternative strategy consists to perform a slight chemical modification of the pyrolysis oil avoiding a large decrease in its yields. The target is to enable storage, transportation and use of pyrolysis oil as energy carriers for electricity and heat production.

The following strategies could be envisaged to this purpose:

- Decrease in viscosity, dis-homogeneity and coking behaviour (e.g. during combustion or upgrading) of the liquid products: by fractional removal of bio-oil high boiling constituents or by cracking of larger molecular constituents (e.g. bio-oil HM fraction) to smaller and stable fragments. As shown by Gayubo *et al.*, removal of HM can be achieved by on line thermal fractionation, producing bio-oil formed by lighter compounds (in that case immediately upgraded to aromatics over ZSM-5) and pyrolytic lignin as by-product.<sup>190</sup> On the other hand, whereas the aim is to maximize liquid yield, catalytic cracking could be a way for direct conversion of HM to lighter compounds.
- Partial de-oxygenation of pyrolysis products by elimination of oxygen as carbon monoxide and carbon dioxide.<sup>191</sup> Oxygen removal as carbon dioxide or carbon monoxide intrinsically de-functionalizes reactive acids and aldehydes, The elimination of oxygen as water could involve the formation of more reactive double bonded compounds and could form a less stable oil. Moreover, increased water production by dehydration reactions reduce homogeneity of bio-oil due to phase separation.

---

<sup>189</sup> A. Oasmaa, S. Czernik. Fuel Oil Quality of Biomass Pyrolysis Oils-State of the Art for the End Users. *Energ.Fuel* 13 (1999) 914-921.

<sup>190</sup> A.G. Gayubo, B. Valle, A.T. Aguayo, M. Olazar, J. Bilbao. Pyrolytic lignin removal for the valorization of biomass pyrolysis crude bio-oil by catalytic transformation. *J. Chem. Technol. Biotech.* 85 (2010) 132-144.

<sup>191</sup> Y. Lin, G. W. Huber. The critical role of heterogeneous catalysis in lignocellulosic biomass Conversion. *Energy Environ. Sci.* 2 (2009) 68-80.

- Increase in “solvent-like” compounds which reduce ageing, improve homogeneity, decrease the viscosity and density, and increase the heating value of pyrolysis liquids.<sup>192,193</sup> The disadvantage is that an increase in low boiling point organics lower the flash point, with more handling problems.

A large body of literature data on the catalytic performance of various active solids on bio-oil characteristics has been acquired by means of both analytical and bench scale reactors.<sup>194,195,196,197,198,199,200,201,202,203,204,205,206,207,208</sup> Nevertheless, the results are difficult to

compare because of the variety of adopted experimental conditions, such as different feedstock types, reactor configurations and bio-oil methods used in bio-oil characterization.

On-line pyrolysis, with the pyrolyzer directly interfaced to GC-MS systems, is a well assessed technique to investigate the effect of a large number of catalysts on the pyrolytic behaviour of biomass on a molecular basis.<sup>209,210</sup> Nevertheless, as shown in chapter 3.1, is difficult to obtain good

---

<sup>192</sup> A. Oasmaa, E. Kuoppala, J. F. Selin, S. Gust, Y. Solantausta. Fast Pyrolysis of Forestry Residue and Pine. 4. Improvement of the Product Quality by Solvent Addition. *Energ.Fuel* 18 (2004) 1578-1583.

<sup>193</sup> J. P. Diebold, S. Czernik, Additives To Lower and Stabilize the Viscosity of Pyrolysis Oils during Storage, *Energ.Fuel*, 11 (1997) 1081-1091.

<sup>194</sup> J. Adam, M. Blazsó, E. Mészáros, M. Stöcker, M. H. Nilsen, A. Bouzga, J. E. Hustad, M. Grønli, G. Øye. Pyrolysis of biomass in the presence of Al-MCM-41 type catalysts. *Fuel* 84 (2005) 1494-1502.

<sup>195</sup> M.H. Nielsen, E. Antonakou, A. Bouzga, A. Lappas, K. Mathisen, M. Stocker. Investigation of the effect of metal sites in Me-Al-MCM-41 (Me = Fe, Cu or Zn) on the catalytic behavior during the pyrolysis of wooden based biomass, *Micropor. Mesopor. Mat.* 105 (2007) 189-203.

<sup>196</sup> E. Antonakou, A. Lappas, Merete H. Nilsen, A. Bouzga, M. Stöcker. Evaluation of various types of Al-MCM-41 materials as catalysts in biomass pyrolysis for the production of bio-fuels and chemicals. *Fuel* 85 (2006) 2202-2212.

<sup>197</sup> F. Ates, M. Işıkdağ, Influence of temperature and alumina catalyst on pyrolysis of corncob, *Fuel* 88 (2009) 1991-1997.

<sup>198</sup> J. Chattopadhyay, C. Kim, R. Kim, D. Pak. Thermogravimetric study on pyrolysis of biomass with Cu/Al<sub>2</sub>O<sub>3</sub> catalysts. *J. Ind. Eng. Chem.* 15 (2009) 72-76

<sup>199</sup> L. Qiang, L. Wen-zhi, Z. Dong, Z. Xi-feng, Analytical pyrolysis-gas chromatography/mass spectrometry (Py-GC/MS) of sawdust with Al/SBA-15 catalysts, *J. Anal. Appl. Pyrol.* 84 (2009) 131.

<sup>200</sup> A. Khelifa, V. Sharypov, G. Finqueneisel, J. V. Weber. Catalytic pyrolysis and gasification of *Miscanthus Giganteus*: Haematite (Fe<sub>2</sub>O<sub>3</sub>) a versatile catalyst. *J. Anal. Appl. Pyrol.* 84 (2009) 84-88.

<sup>201</sup> A. Pattiyaa, J. O. Titiloye, A.V. Bridgwater. Fast pyrolysis of cassava rhizome in the presence of catalysts. *J. Anal. Appl. Pyrol.* 81 (2008) 72-79.

<sup>202</sup> D.J. Nowakowski, J. M. Jones, R. M. D. Brydson, A. B. Ross. Potassium catalysis in the pyrolysis behaviour of short rotation willow coppice, *Fuel* 86 (2007) 2389-2402.

<sup>203</sup> F. Ates, A. E. Putun, E. Putun. Fixed bed pyrolysis of *Euphorbia rigida* with different catalysts. *Energ. Convers. and Manage.* 46 (2005) 421-432.

<sup>204</sup> D. Gullu. Effect of catalyst on yield of liquid products from biomass via pyrolysis. *Energy sources.* 25 (2003) 753-765.

<sup>205</sup> S. Yorgun, Y. E. Şimşek. Catalytic pyrolysis of *Miscanthus giganteus* over activated alumina, *Bioresource Technol.*, 99 (2008) 8095-8100.

<sup>206</sup> A. Pattiyaa, J. O. Titiloye, A.V. Bridgwater. Evaluation of catalytic pyrolysis of cassava rhizome by principal component analysis. *Fuel* 89 (2010) 244-253.

<sup>207</sup> B.B. Uzun, N. Sarioğlu. Rapid and catalytic pyrolysis of corn stalks. *Fuel Process. Technol.* 90 (2009) 705-716.

<sup>208</sup> J. Adam, E. Antonakou, A. Lappas, M. Stöcker, M.H. Nilsen, A. Bouzga, J.E. Hustad, G. Øye. In situ catalytic upgrading of biomass derived fast pyrolysis vapours in a fixed bed reactor using mesoporous materials. *Micropor Mesopor, Mat.* 96 (2006) 93-101.

<sup>209</sup> D. J. Nowakowski, J. M. Jones, R. M. D. Brydson, A.B. Ross. Potassium catalysis in the pyrolysis behaviour of short rotation willow coppice. *Fuel* 86 (2007) 2389-2402.

mass balance by using only GC-MS systems. On the contrary, GC-AED system allows quantification (in term of yield of analyzed elements) of a large number of compounds without time consuming calibration and for this reason it was used in study of biomass catalytic pyrolysis.<sup>211,212,213</sup>

By means of GC-AED it is possible to obtain results on yields and elemental composition of pyrolysis oil with minimal work up. For this reason, it is a useful technique for comparing a large number of catalytically active materials. In previous works dealing with Py-GC-AED applied to catalytic pyrolysis, ZnO, MgO, dolomite and limestone were tested as secondary catalysts. No increase in GC products yields was observed. With the adopted experimental procedure it was not possible to distinguish between heavy un-detectable compounds and loss for coking onto catalyst (placed downstream in the GC inlet). Nevertheless, scale up with ZnO catalysis showed that it is possible to improve the stability of bio-oil also by mild catalysis over cheap materials.<sup>211,212,213,214</sup> The aim of the present work was to perform a systematic screening study on a large variety of catalysts by Py-GC-AED to assess their activity in catalytic pyrolysis of biomass. Among the various elements detectable by AED detection, the attention was focused on quantitative determination of elemental carbon in order to evaluate yields of main pyrolysis fractions .

### 3.5.2. Materials and methods

#### 3.5.2.1 Biomass and catalysts

Pine sawdust used for the experiments was the same used in VTT (technical research center of Finland) 20 kg h<sup>-1</sup> process development unit (PDU) and VTT 1 kg h<sup>-1</sup> pyrolyser (bench scale). For analytical pyrolysis, the pine sawdust sample was grinded and sieved to particle size of 0.105-0.125 mm and analyzed for major elements. Its composition was: 52% carbon, 42% oxygen, 6.2% hydrogen, 0.1% nitrogen, and 0.3% ash.

Catalysts used in this study are listed Table 3.5.1 along with a short description of main properties. H-ZSM-5 was purchased from PQ corporation Valfor, Tin oxide, zirconium oxide and H-Mordenite catalysts from BDH (Poole, UK, BDH-29881), Co<sup>0</sup>/SiO<sub>2</sub> from Harshaw Chemie BV, bulk metal oxides from Merck.

---

<sup>210</sup> F. Ates, A. E. Putun, E. Putun. Fixed bed pyrolysis of *Euphorbia rigida* with different catalysts. *Energ. Convers. and Manage.* 46 (2005) 421-432.

<sup>211</sup> R. Aléna, P. Oesch, E. Kuoppala. Py-GC/AED studies on the thermochemical behavior of softwood. *J. Anal. Appl. Pyrol.* 35 (1995) 259-265.

<sup>212</sup> M. Nokkosmäki, A. Krause, E. Leppämäki, E. Kuoppala. A novel test method for catalysts in the treatment of biomass pyrolysis oil, *Catal. Today* 45 (1998) 405-409.

<sup>213</sup> M. Nokkosmäki; E. Kuoppala, E. Leppämäki, A. Krause. A novel test method for cracking catalysts, *J. Anal. Appl. Pyrol.* 44 (1998) 193-204.

<sup>214</sup> M. Nokkosmäki; E. Kuoppala, E. Leppämäki, A. Krause. Catalytic conversion of biomass pyrolysis vapours with zinc oxide. *J. Anal. Appl. Pyrol.* 55 (2000) 119-131.

**Table 3.5.1:** Catalysts characterization.

	<i>Description</i>	<i>BET AREA (m<sup>2</sup> g<sup>-1</sup>)</i>
Al <sup>3+</sup> /SiO <sub>2</sub>	MCM-41	970
Sn <sup>4+</sup> /SiO <sub>2</sub>	MCM-41	390
Fe <sup>3+</sup> /SiO <sub>2</sub>	MCM-41	770
Mo <sup>6+</sup> /SiO <sub>2</sub>	MCM-41	810
Co <sup>3+</sup> /SiO <sub>2</sub>	MCM-41	1200
Ti <sup>4+</sup> /SiO <sub>2</sub>	MCM-41	450
Zn <sup>+</sup> /SiO <sub>2</sub>	Amorphous	450
Cu <sup>2+</sup> /SiO <sub>2</sub>	Amorphous	500
Zr <sup>4+</sup> /SiO <sub>2</sub>	MCM-41	650
SiO <sub>2</sub>	MCM-41	640
Co <sup>3+</sup> /Al <sub>2</sub> O <sub>3</sub>	10% Co <sup>3+</sup> , acidic Al <sub>2</sub> O <sub>3</sub>	160
Co/SiO <sub>2</sub>	30% Co <sup>0</sup>	110
ZrO <sub>2</sub>	Commercial catalyst	220
SnO <sub>2</sub>	Commercial catalyst	9
CaO bulk	CaCO <sub>3</sub> Calcined at 900°C	70
ZnO bulk	Bulk Metal oxide	n.a <sup>b</sup>
Fe <sub>2</sub> O <sub>3</sub> bulk	Bulk Metal oxide	n.a <sup>b</sup>
CuO bulk	Bulk Metal oxide	n.a <sup>b</sup>
MoO <sub>3</sub> bulk	Bulk Metal oxide	n.a <sup>b</sup>
TiO <sub>2</sub> bulk	Bulk Metal oxide	n.a <sup>b</sup>
WO <sub>3</sub> bulk	Bulk Metal oxide	n.a <sup>b</sup>
MgO	Bulk Metal oxide	n.a <sup>b</sup>
Hydrotalcite	Calcined clay	170 [ <sup>215</sup> a]
Montmorillonite	Calcined clay	67 [ <sup>216</sup> a]
H-ZSM-5	Commercial catalyst	420
	Si/Al 150	
H-Mordenite	Commercial catalyst	460
MS-1	Cu/Zn/Zr on Al <sub>2</sub> O <sub>3</sub>	94
	16/15/5.9 % Cu,Zn,Zr content	
MS-2	Fe/Zn/Cu mixed oxides	130
	64/5.1/1.2 % Fe,Zn,Cu content	
MS-3	Fe/Cu/Al/Zn mixed oxides	300
	45/1.5/5.7/4.5 % Fe,Cu,Al,Zn content	
MS-4	Co on ZrO <sub>2</sub> ; 30 % Co	10
MS-5	Cu on ZrO <sub>2</sub> ;30 % Cu	10

<sup>a</sup>data from literature reference <sup>b</sup>pure commercial (form Merck) metal oxide, used as purchased

### 3.5.2.2 Synthesis of catalysts(MS-n and MCM-41)

Co<sup>3+</sup>/Al<sub>2</sub>O<sub>3</sub> was prepared by incipient wetness impregnation of puralox support (from Condea), dried under vacuum and impregnated with a Co(NO<sub>3</sub>)<sub>2</sub> solution. The catalyst was dried in a rotavapor under vacuum at 40-50°C and thereafter calcined in air flow at 300°C .

Cu-ZnO-ZrO<sub>2</sub>/Al<sub>2</sub>O<sub>3</sub> catalyst denoted as MS-1 was prepared by impregnating the active components onto a high surface area Al<sub>2</sub>O<sub>3</sub>. Alumina support was dried in vacuum at 80°C and impregnated at 80°C with a solution of zirconium nitrate. The impregnated support was dried in

<sup>215</sup> M. B. de Carvalho, J. Pires, A.P. Carvalho. Characterisation of clays and aluminium pillared clays by adsorption of probe molecules. Microporous Mater. 6 (1996) 65-77.

<sup>216</sup>J. Shen, M. Tu, C. Hu. Structural and Surface Acid/Base Properties of Hydrotalcite-Derived MgAlO Oxides Calcined at Varying Temperatures. J. Solid State Chem. 137 (1998) 295-301.

vacuum at 80°C for 3 hours, in air at 120°C overnight and then calcined in air at 700°C for 2 hours. This modified support was co-impregnated three times with a hot 80°C solution of Cu and Zn nitrates. The catalyst was dried and calcined at 350°C between the repeated impregnations carried out as described above.

Fe-Zn-Cu and Fe-Cu-Zn-Al catalyst denoted as MS-2 and MS-3 were prepared following the preparation procedure of Li *et al.*<sup>217</sup>. Solutions with mixed metal of metal nitrates were co-precipitated at 80°C at pH of 7 using ammonium hydrogen carbonate. The precipitate was filtered, washed with water and ethanol, and dried at 110°C for 12 hours. Finally, the material was calcined in air at 400°C (with 1°C min<sup>-1</sup> heating rate) for 4 hours.

Co/ZrO<sub>2</sub> and Cu/ZrO<sub>2</sub> catalysts denoted as MS-4 and MS-5 were prepared by re-precipitation following the guidelines by Saito *et al.*<sup>218</sup>. A mixed solution of Cu and Zr nitrates (total metal concentration 1 M) and an aqueous solution of Na<sub>2</sub>CO<sub>3</sub>, NaOH, NH<sub>4</sub>HCO<sub>3</sub> or NH<sub>3</sub> (1,1 M) were added dropwise to distilled water at 80°C at pH of 7. The precipitate was aged 0.5 h, cooled down to room temperature, filtered and washed with distilled water. The precipitates were dried in air at 120°C overnight and calcined in air at 350°C for 2 hours.

The synthesis of SiO<sub>2</sub> high surface mesoporous materials (MCM-41) was described in detail elsewhere<sup>219</sup>. In a typical procedure, a weighed amount of metal salt (4.4 mMol of metal) was added into 120 ml of an aqueous solution of hexadecyltrimethylammonium bromide (2.4 g) until complete dissolution. The solution was magnetically stirred for 2 hours and then 10 ml of tetraethoxysilane (44 mMol Si) were added under mixing avoiding any stratification of the monomer over the solution. Hence, 8 ml of 30% NH<sub>3</sub> solution were added dropwise to the reaction mixture under vigorous magnetic stirring. As soon as the addition of ammonia terminated, the reaction vessel was transferred into a IKA KS 260 basic oscillator and polycondensation was conducted for 72 hours under horizontal laminar shaking at 50 rpm. The gel initially formed from the reaction mixture turned into a white solid that was filtered and thoroughly washed with de-ionized water. The solid was dried overnight under vacuum at 100 °C, crushed with a mortar and heated for 1 hour at 500° C under nitrogen flow (1.5 l min<sup>-1</sup>) by means of a 800 ml quartz reactor. Finally the grey solid obtained was calcined at 550°C for 5 h. The resulting solid was subjected to characterization and pyrolysis experiments.

---

<sup>217</sup> S. Li, S. Krishnamoorthy, A. Li, G.D. Meitzner, E. Inglesia. Promoted Iron-Based Catalysts for the Fischer–Tropsch Synthesis: Design, Synthesis, Site Densities, and Catalytic Properties. *J. Catal.* 206 (2002) 202-217.

<sup>218</sup> M. Saito, T. Fujitani, M. Takeuchi, T. Watanabe. Development of copper/zinc oxide-based multicomponent catalysts for methanol synthesis from carbon dioxide and hydrogen. *Appl. Catal. A: General* 138 (1996) 311-318.

<sup>219</sup> C. Torri, I.G. Lesci and D. Fabbri. Analytical study on the pyrolytic behaviour of cellulose in the presence of MCM-41 mesoporous materials. *J. Anal. Appl. Pyrol.* 85 (2009) 192-196.

### 3.5.2.3 Characterisation of catalysts

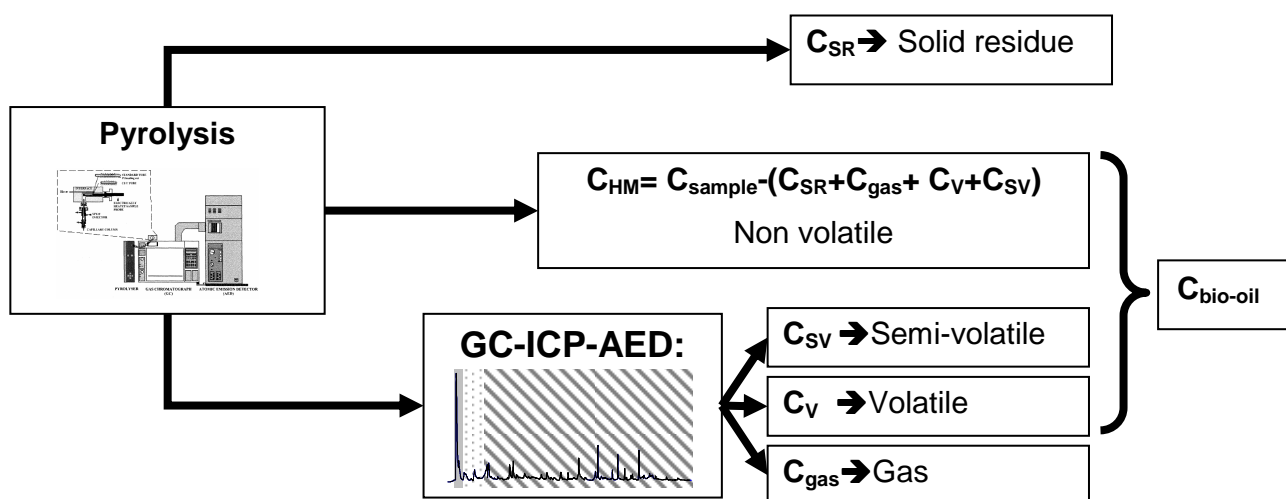
In order to establish the MCM-41 structure, the powder X-ray patterns of silica based materials were recorded using a Philips Xcelerator diffractometer with Cu K $\alpha$  radiation ( $\lambda = 1.5418 \text{ \AA}$ ) and a Ni filter. The samples were scanned for  $2\theta$  angles between  $1^\circ$  and  $15^\circ$ , with a resolution of  $0.02^\circ$ . The lattice and the peak profile parameters were evaluated using Highscore software. The N<sub>2</sub> adsorption-desorption isotherm of the SiO<sub>2</sub> materials was collected on Carlo Erba Sorpty 1750 at 77 K. Prior to the measurement, the calcined samples were degassed at 120°C until a stable vacuum of about 5 mTorr was reached. The specific surface area was assessed using the Brunauer Emmett Teller (BET) method from adsorption data. All catalysts but Co<sup>0</sup>/SiO<sub>2</sub> and CaO were activated in air at 600°C over night, and all catalysts were stored in desiccator prior to use.

### 3.5.2.4 Py-GC-AED

Figure 3.5.1 shows the analytical procedure used for on line Py-GC-AED. The apparatus employed for Py-GC-AED experiments was described in detail in chapter 3.1 and elsewhere.<sup>211,212,213</sup>

The pyrolysis unit was a CDS Pyroprobe 1000 pyrolyser connected to a HP 5890 Series II gas chromatograph, and detection was carried out with an HP 5921A inductively coupled plasma-atomic emission detector (MIP-AED).

**Figure 3.5.1:** Graphical scheme of the analytical procedure used in the determination of carbon distribution among pyrolysis fractions.



Py-GC-AED analytical procedure was explained in detail in chapter 3.1. The results were summarized by distinguishing pyrolysis products according to their volatility. Retention time was used as reference to discriminate gaseous (first peak at 2.6 min), volatile ( $4 \text{ min} > RT > 2.6 \text{ min}$ ), and others semi-volatile GC detectable compounds ( $RT > 4 \text{ min}$ ). The yield of the solid residue was evaluated at the end of the complete run in the following way: the interface was cooled down, the

quartz tube was removed from the probe and weighed. Then, the sample was treated in muffle oven at 550 °C for 5 h and re-weighed. The weight difference before and after burning in the muffle gave the mass yield of the solid residue that corresponded to the yield on a carbon basis (i.e. solid residue was assumed to be composed of nearly pure carbon). Carbon yield of HM (accounting for pyrolytic lignin and WSHM) was calculated by difference between 100% and sum of carbon yield of gas, volatile, semi-volatile and solid residue. When copper containing catalysts were used, carbothermal reduction of CuO (as well as oxidation of copper in the muffle) was considered in the calculations and complete reduction of copper oxide in pyrolysis conditions was assumed. When Co<sup>0</sup>/SiO<sub>2</sub> commercial catalyst was used complete oxidation of cobalt during the burning of solid residue in the oven was considered for calculations.

#### *3.5.2.5 Bench scale pyrolysis and characterization of liquid product*

VTT bench scale fluidized bed pyrolysis equipment (1 kg h<sup>-1</sup>) was used to produce bio-oil from pine sawdust. The results from the bench scale system were compared with the results obtained with the Py-GC-MIP-AED system. Pine sawdust samples (same used for analytical equipment) with particle size of 550 – 920 µm were used. The experiment was performed at 525 °C with a vapor residence time of 0.8 s. Nitrogen was used as the fluidizing gas and aluminum oxide as inert fluidizing agent. Char formed during pyrolysis was removed from the hot outgoing flow by two cyclones. Afterwards the cyclones the vapors were cooled and bio-oil was collected in two liquid condensers and an electrostatic precipitator.

After the experiments the amount of char and liquid products were measured by weighing.

Pyrolysis gases (CO, CO<sub>2</sub>, H<sub>2</sub>, C<sub>1</sub>-C<sub>5</sub>-hydrocarbons) were collected in gas sampling bottles during the experiment and the composition of the gases was measured after the experiment by GC analysis. The chemical composition of the liquid product was determined with the solvent fractionation scheme of bio-oil, described more in detail elsewhere<sup>220</sup>. Carbon yields were obtained for the gas, char, GC detectable bio-oil (volatile and semi-volatile compounds) and heavy bio-oil (WSHM and pyrolytic lignin). The carbon yield for gas was back calculated from the molecular composition measured by GC analysis. Carbon yield of GC detectable bio-oil compounds was obtained by GC-MIP-AED analysis of pure bio-oil, performed by injecting 1 µl of pure bio-oil (homogenized before the sampling) in the Py-GC interface in the same condition used for analytical pyrolysis. The carbon yield for char, WSHM and pyrolytic lignin was determined by analyzing the carbon content of each fraction.

---

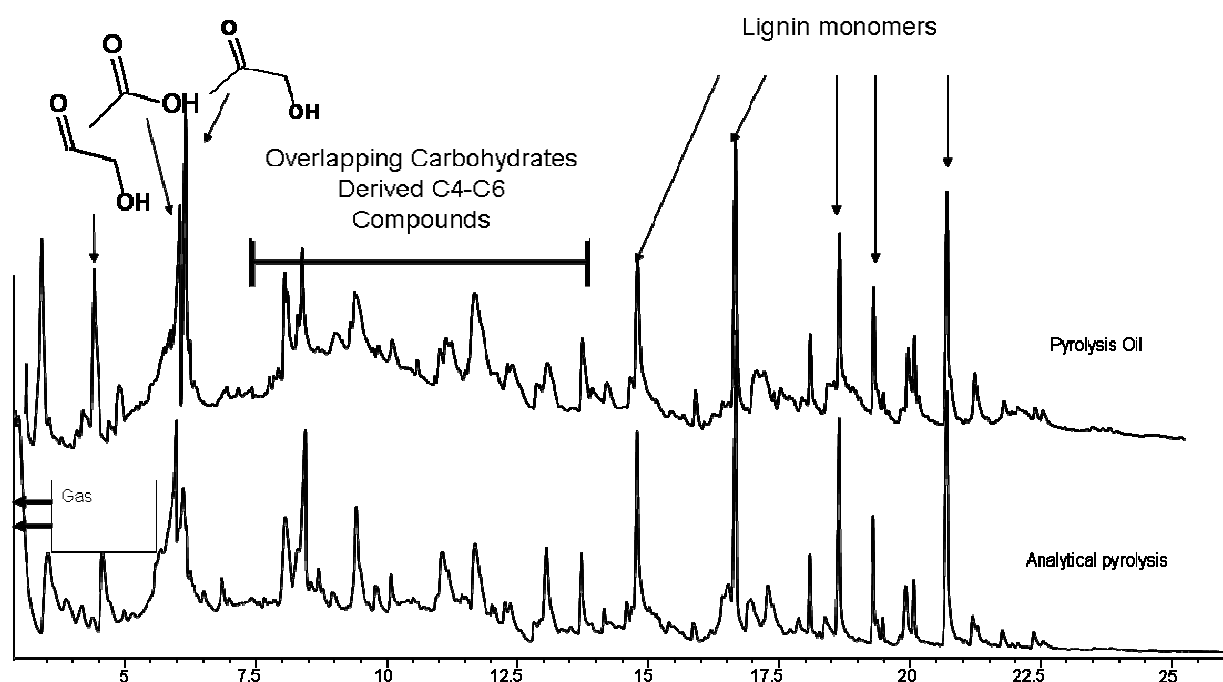
<sup>220</sup> A. Oasmaa, E. Kuoppala. Solvent Fractionation Method with Brix for Rapid Characterization of Wood Fast Pyrolysis Liquids. *Energ.Fuel* 22 (2008) 4245-4248

### 3.5.3. Results and discussion

#### 3.5.3.1 Comparison of micro-scale system pyrolysis with bench scale reactor

In order to confirm the validity of Py-GC-AED for screening oriented studies, a comparison between results obtained with micro-scale equipment and bench scale pyrolysis apparatus was undertaken. The precision of the Py-GC-AED method was good, and relative standard deviation (RSD) over 10 tests on pine sawdust was 5%. Figure 3.5.2 shows the qualitative comparison of GC-AED chromatograms obtained by injecting 1 µl of pyrolysis oil from pine sawdust in the Py-GC interface and by performing analytical pyrolysis on the same feedstock.

**Figure 3.5.2:** Comparison of the GC-MIP-AED chromatograms obtained by injection of pyrolysis oil (obtained by non-catalytic pyrolysis of pine sawdust) and by analytical pyrolysis pine sawdust without any catalyst.

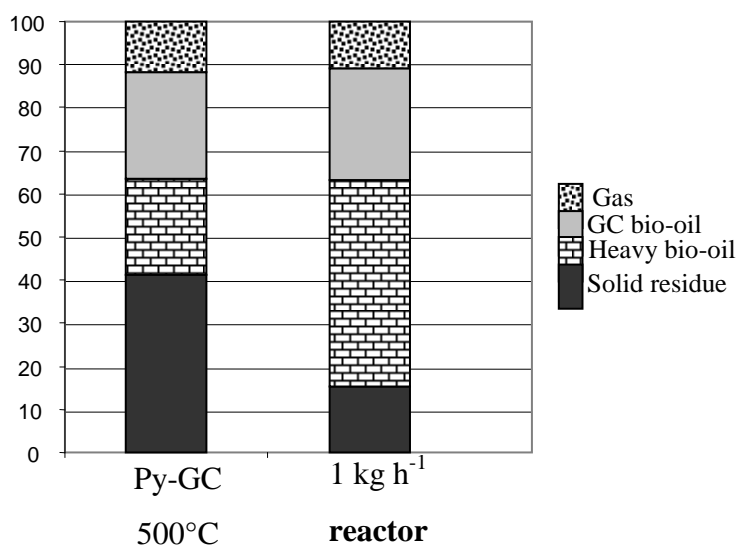


Chromatograms were similar, characterized by the most volatile bio-oil constituents (e.g. hydroxyacetaldehyde, acetic acid and hydroxyacetone) in the early plot after gas peaks and then a great number of partially overlapped peaks in the 7-13 min retention time range, mainly formed by pyrolysis products from cellulose, together with typical phenolics produced from lignin degradation.

In order to compare the two systems from a quantitative point of view, it was assumed that the non-volatile pyrolysis products (HM) obtained from microscale Py-GC-AED system consisted of pyrolytic lignin and heavy water-soluble fraction (WSHM) of bio-oil. Furthermore, both solvent

fractionation data and relative atomic compositions of fractions were used for obtaining carbon yields from bench scale reactors. Figure 3.5.3 shows comparison of carbon yields obtained for gas, GC bio-oil (volatile and semi-volatile GC-eluted compounds), HM (not GC detectable matter) and solid residue, here considered *char* carbon yield of bench scale reactor and total solid residue retained in quartz tube for Py-GC-AED system.

**Figure 3.5.3:** Comparison between the results obtained by the Py-GC-MIP-AED procedure and by bench scale pyrolysis.



Carbon yields of GC detectable matter and gas obtained by analytical (25% and 12%) and bench scale pyrolysis (26% and 11%) were similar. However, large differences were observed in solid residue and HM carbon yields.

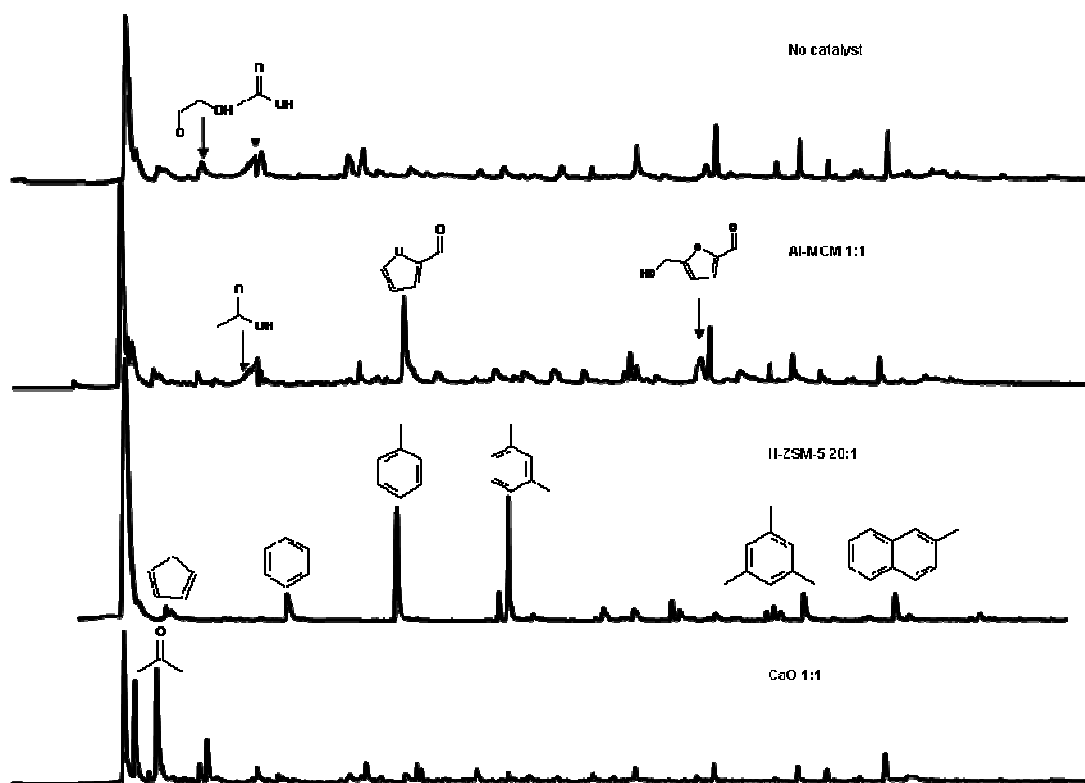
Results of comparison could be rationalized by assuming that pyrolytic process, at 500°C, was similar for both bench and analytical scale equipments resulting in similar product yields, but mass flows were markedly different. Analytical Py-GC-AED was characterized by higher vapour residence time ( $\approx 10$  s) than bench scale reactor (0.8 s). In particular, a minimal fraction of helium gas flow purge the inner volume of quartz tube filled with biomass, hampering the fast removal of high boiling point substances. Moreover, due to slower heat transfer in fixed bed than in fluidized bed, actual sample temperature should be lower in the Py-GC system than in the bench scale pyrolysis. For these reasons, in analytical pyrolysis, a higher fraction of HM is expected to be retained into the quartz tube, and subsequently coked. This coked HM was clearly observable as a black ring near the quartz tube opening at the end of pyrolysis. In the experimental procedure used there, coked HM ended up in the solid residue.

In conclusion, overestimation of solid residue and underestimation of HM have to be considered when extrapolating data to systems with better heat transfer. Nevertheless, the established Py-GC-AED procedure was adequate to provide a reliable comparison of catalyst activity on a relative scale, for the purpose of screening and relative comparison among different catalysts.

### 3.5.3.2 Catalytic pyrolysis of pine sawdust: qualitative aspects

Effect of catalyst on the yields of different pyrolysis products was screened at 500°C for 34 catalyst selected among silica supported metal oxides, metal oxide catalyst, bulk metal oxides, calcined clays, fischer-tropsch catalysts (Co/Al<sub>2</sub>O<sub>3</sub>, Co/SiO<sub>2</sub>) and catalyst for methanol synthesis from syngas (MS-n).

**Figure 3.5.4:** examples of py-GC-AED chromatogram obtained by non catalytic pyrolysis, catalytical pyrolysis with Al-MCM-41 with 1-1 biomass-catalyst ratio (qualitatively similar activity to other tested catalyst), H-ZSM-5 with 1-20 biomass-catalyst ratio, and CaO with 1-1 biomass-catalyst ratio.



The catalyst to biomass ratio used was 1-1, and for comparison pyrolysis with large excess of H-ZSM-5 catalyst (1-20 ratio) was undertaken for comparison. Among catalytic pyrolysis performed with 1-1 catalyst-biomass ratio, the typical effect of all tested catalyst but calcium oxide on the the GC detectable pyrolysis product consist in a decrease in high molecular weight product and increase

of product of sugars dehydration like furfural or hydroxymethylfurfural or smaller fragments originated from carbon-carbon bond rupture. Figure 3.5.4 shows, for example, the effect of Al-MCM, with increase of dehydration product already observed by Adam et al. with a similar system.<sup>194</sup> In this case, poor or no effect were observed on lignin pyrolysis product.

H-ZSM-5 used in large excess transformed the bio-oil into aromatic products. Calcium oxide caused a deep change in GC detectable product, consisting in an elimination of acetic acid peak and a large increase in ketones (mainly acetone) yield, probably originated from base catalyzed ketonic condensation of acetic acid.

#### 4.2.3.3 Catalytic pyrolysis of pine sawdust: quantitative analysis

A suite of catalysts belonging to different families were evaluated by analytical pyrolysis at 500°C. Catalysts and pine sawdust were mechanically admixed in 1:1 biomass to catalyst mass ratio and triplicate tests were performed for each catalyst. Yields were determined on a elemental carbon basis and mean values were reported in table 3.5.2. Mean RSD for catalytic pyrolysis was 10%. Concentration of HM in bio-oil (see below) was reported as well on a mass carbon basis.

As shown in figure 3.5.1, pyrolysis products were divided into different categories on the basis of their volatility: gas, GC detectable (further divided into a volatile and semi-volatile fraction), non-volatile fraction (here called heavy matter or HM) solid residue, consisting in the sum of char and coked material (on catalyst on quartz tube). Volatile, semi-volatile and non-volatile products (HM) collectively made up the bio-oil.

Pyrolysis of pine sawdust without catalyst produced 12% yield of gas, 1.6% yield of volatile compounds and 23% of semi-volatile compounds. Bio-oil yield obtained by analytical pyrolysis was 47%, and HM content of the bio-oil was 47%.

Among silica based high surface materials, SiO<sub>2</sub>, Al<sup>3+</sup>/SiO<sub>2</sub>, Fe<sup>3+</sup>/SiO<sub>2</sub> and Zr<sup>4+</sup>/SiO<sub>2</sub> caused a large decrease of both bio-oil yields (from 47% to 19%, 22%, 19% and 22%, respectively) and a concurrent lower HM concentration in bio-oil. It is worth noting that despite some obvious differences among the experimental systems, yields of major products obtained using SiO<sub>2</sub> and Al<sup>3+</sup>/SiO<sub>2</sub> mesoporous catalysts were similar to those observed by Adam *et al.* in fixed bed bench scale reactor with spruce wood and similar biomass:catalyst ratio<sup>208</sup>. This could indicate that, when HM yields approach to zero (as in fixed bed catalytic pyrolysis with high specific surface catalysts), mass transfer differences become less critical so that analytical and bench scale systems tend to provide similar results.

**Table 3.5.2:** Carbon yields (%  $C/C_{\text{sample}}$ , average value from triplicate analyses) of different fractions obtained by pyrolysis in presence of different catalysts (MS-n stands for methanol synthesis catalyst).

	<b>Gas</b> $C/C_{\text{sample}}$	<b>Volatile</b> $C/C_{\text{sample}}$	<b>SV</b> $C/C_{\text{sample}}$	<b>S. Residue<sup>a</sup></b> $C/C_{\text{sample}}$	<b>HM</b> $C/C_{\text{sample}}$	<b>Bio-oil</b> $C/C_{\text{sample}}$	<b>HM</b> $C/C_{\text{bio-oil}}$
-	12	1.6	23	41	22	47	47
<b>Al<sup>3+</sup>/SiO<sub>2</sub></b>	15	4.0	12	63	5.5	22	25
<b>Sn<sup>4+</sup>/SiO<sub>2</sub></b>	11	2.6	9.0	51	27	38	70
<b>Fe<sup>3+</sup>/SiO<sub>2</sub></b>	18	3.6	8.7	63	6.7	19	35
<b>Mo<sup>6+</sup>/SiO<sub>2</sub></b>	15	3.2	18	58	5.4	27	20
<b>Co<sup>3+</sup>/SiO<sub>2</sub></b>	14	3.0	12	59	11	26	43
<b>Ti<sup>4+</sup>/SiO<sub>2</sub></b>	16	3.3	17	47	17	37	46
<b>Zn<sup>+</sup>/SiO<sub>2</sub></b>	13	2.8	19	61	4.9	26	19
<b>Cu<sup>2+</sup>/SiO<sub>2</sub></b>	15	2.4	12	56	15	29	51
<b>Zr<sup>4+</sup>/SiO<sub>2</sub></b>	16	4.0	14	62	3.8	22	18
<b>SiO<sub>2</sub></b>	19	2.4	17	62	0	19	0
<b>Co<sup>3+</sup>/Al<sub>2</sub>O<sub>3</sub></b>	14	3.3	24	59	0	27	0
<b>Co/SiO<sub>2</sub></b>	14	2.0	16	57	11	29	37
<b>ZrO<sub>2</sub></b>	15	2.9	25	50	7	35	20
<b>SnO<sub>2</sub></b>	14	2.8	24	54	5	32	16
<b>CaO bulk</b>	3.6	2.2	11	83	0.0	13	0
<b>ZnO bulk</b>	11	1.9	31	42	15	47	31
<b>Fe<sub>2</sub>O<sub>3</sub> bulk</b>	13	2.2	31	42	11	44	25
<b>CuO bulk</b>	23 <sup>g</sup> (8.1) <sup>h</sup>	3.0	30	27 <sup>g</sup> (43) <sup>h</sup>	16	49	33
<b>MoO<sub>3</sub> bulk</b>	9.3	2.0	22	33	34	58	59
<b>TiO<sub>2</sub> bulk</b>	10	1.8	18	34	37	57	65
<b>WO<sub>3</sub> bulk</b>	11	3.6	21	32	32	57	57
<b>MgO</b>	18	2.9	13	65	0.0	16	0
<b>Montmorillonite</b>	10	1.7	25	45	18	45	41
<b>Hydrotalcite</b>	12	2.0	21	56	8.0	31	26
<b>H-ZSM-5</b>	13	3.2	24	37	22	50	45
<b>H-ZSM-5<sup>i</sup></b>	30	1.0	13	56	0	14	0
<b>H-Mordenite</b>	8.7	1.9	22	59	8.7	33	27
<b>MS-1</b>	21	2.5	20	55	1.8	25	7
<b>MS-2</b>	17	2.8	26	47	6.8	36	19
<b>MS-3</b>	17	1.8	23	47	10	35	29
<b>MS-4</b>	19	2.4	27	49	2.7	32	8
<b>MS-5</b>	14	2.2	26	47	12	39	29

<sup>g</sup>S.Residue: sum of char, coke and coked HM; <sup>b</sup>Gas: First large peak at 2.6 min; <sup>c</sup>Volatile: eluted after gas and before 4 min; <sup>d</sup>SV (semi-volatile): all semi-volatile GC detectable compounds eluted after 4 min; <sup>e</sup>Bio-oil: calculated as  $C_{\text{sample}} - (C_{\text{gas}} + C_{\text{char}})$ ; <sup>f</sup>HM (heavy matter): calculated as  $C_{\text{bio-oil}} - (C_{\text{v}} + C_{\text{sv}})$ ; <sup>g</sup>Raw data obtained; <sup>h</sup>Yield if effect of carbothermal reduction of the catalyst and oxidation of char (with production of gas) was considered; <sup>i</sup>1:20 biomass to catalyst ratio, aromatic hydrocarbons as main semi-volatile pyrolysis products.

Moreover, all silica based high surface materials increased volatile fraction yields. The highest effect was obtained with Fe<sup>3+</sup>/SiO<sub>2</sub>, Al<sup>3+</sup>/SiO<sub>2</sub> and Zr<sup>4+</sup>/SiO<sub>2</sub> producing volatile fraction yields of 4.0%, 4.0% and 3.6%, respectively. Sn<sup>4+</sup>/SiO<sub>2</sub> caused a small decrease in bio-oil yield (from 47% to

38%) and slight increase in HM yield (from 22% to 27%). Catalytic pyrolysis in the presence of  $\text{Co}^{3+}/\text{SiO}_2$ ,  $\text{Ti}^{4+}/\text{SiO}_2$  and  $\text{Cu}^{2+}/\text{SiO}_2$  showed an intermediate behaviour with a marked decrease of both HM and bio-oil yields.  $\text{Mo}^{6+}/\text{SiO}_2$  and  $\text{Zn}^{2+}/\text{SiO}_2$  induced a large decrease in both HM yield (from 22% to 5.4% and 4.9 respectively) and a marked decrease in bio-oil yields (from 47% to 27% and 26% respectively), without any increase of GC detectable matter.

Among bulk metal oxides,  $\text{MoO}_3$ ,  $\text{TiO}_2$  and  $\text{WO}_3$  led to a slight raise of both bio-oil and HM yield.  $\text{WO}_3$  also markedly raised volatile yield (from 1.6% to 3.6%);  $\text{ZnO}$  did not affect the bio-oil yield and lowered HM yield (from 22% to 15%).

$\text{CuO}$  slightly increased bio-oil yield (from 47% to 49%), mainly through a raise of semi-volatile fraction (from 23% to 30% yield), and markedly lowered HM yield (from 22% to 16%). This effect could be explained by the partial oxidation of HM macromolecules onto the  $\text{CuO}$  surface, with release of additional semi-volatile fragments and (through the evolved heat) speeding up the pyrolysis process. The observed catalytic activity of  $\text{CuO}$  is well known and has been largely exploited in determination of lignin moieties in environmental samples<sup>221,222</sup>.

With strong alkaline catalysts, like  $\text{CaO}$  and  $\text{MgO}$ , GC detectable bio-oil yield dropped to 13% and 16%, probably with large coking, not evaluated here owing to possible carbonation of the catalyst. The effect obtained with  $\text{MgO}$  and  $\text{CaO}$  admixed to biomass was similar to that observed for similar catalysts placed as downstream catalyst bed in the same system, which resulted in lower production of bio-oil<sup>212</sup>.

Among clays, calcined montmorillonite caused only a small effect with 45% bio-oil yield and 18% HM yield. HM yields were diminished from 22% to 8% by calcined hydrotalcite, with a concomitant slight reduction of bio-oil yields (from 47% to 31%).

As far as zeolites are concerned, H-mordenite and H-ZSM-5 were tested, the latter with a high catalyst:biomass ratio (20:1), in addition to the 1/1 adopted in this study. With low catalyst/biomass ratio, H-ZSM-5 did not affect bio-oil nor HM yields, whereas H-mordenite decreased bio-oil yield to 33% and HM yield to 9%. With the high catalyst/biomass ratio, H-ZSM-5 yielded predominantly solid residue (56% yield) and gas (30% yield), while the remaining fraction (14% yield) was composed essentially by aromatic hydrocarbons. This behaviour is analogous to that reported by

---

<sup>221</sup> J.I Hedges, J.R. Ertel. Characterization of lignin by capillary gas chromatography of cupric oxide oxidation products, *Anal. Chem.* 54 (1982) 174-178.

<sup>222</sup> P.G. Hatcher, M. A. Nanny, R. D. Minard, S.D. Dible, D.M. Carson. Comparison of two thermochemolytic methods for the analysis of lignin in decomposing gymnosperm wood: the  $\text{CuO}$  oxidation method and the method of thermochemolysis with tetramethylammonium hydroxide (TMAH). *Org. Geochem.* 23 (1995) 881-888

Carlson *et al.* for model compounds with the same Py-GC apparatus but interfaced to MS detector<sup>223</sup>.

Regarding Fischer-Tropsch catalysts ( $\text{Co}^{3+}/\text{Al}_2\text{O}_3$ ,  $\text{Co}^0/\text{SiO}_2$ ), remarkably HM was not revealed with  $\text{Co}^{3+}/\text{Al}_2\text{O}_3$ , so that this catalyst yielded a 27% bio-oil consisting predominantly of semi-volatile products. When cobalt occurred as  $\text{Co}^0/\text{SiO}_2$  the resulting bio-oil (29% yield as with  $\text{Co}^{3+}/\text{Al}_2\text{O}_3$ ) contained 37% HM. The activity of  $\text{ZrO}_2$  was similar to that of  $\text{SnO}_2$  with a slight decrease of bio-oil (from 47% to 35% and 32% yields, respectively) as well as HM yield (from 22% to 7% and 5%, respectively).

Finally, several catalysts utilised in the synthesis of methanol from syngas (MS-n) were tested for the first time in the pyrolysis of biomass. MS-1 virtually eliminated HM (only 2% yield), but with a concomitant strong decrease in yield of bio-oil (from 47% to 25%). MS-2 and MS-4 lowered HM from 22% to 7% and 3%, but with a minor drop in bio-oil yields (to 36% and 32%). MS-3 and MS-5 showed less pronounced activity, with still a relatively high HM yield (10% and 12%) and a minor decrease in bio-oil yield (from 47% to 35% and 39%).

Summarizing the results, it can be noticed that most of the catalysts decomposed HM and heaviest semi-volatile matter, leading to coking rather than to the formation of GC-detectable products. Mesoporous materials characterised by high surface area, with exception of pure silica, failed in cracking activity of HM into GC detectable compounds, and this could be caused by a too high adsorption and coking rate in comparison to cracking activity.

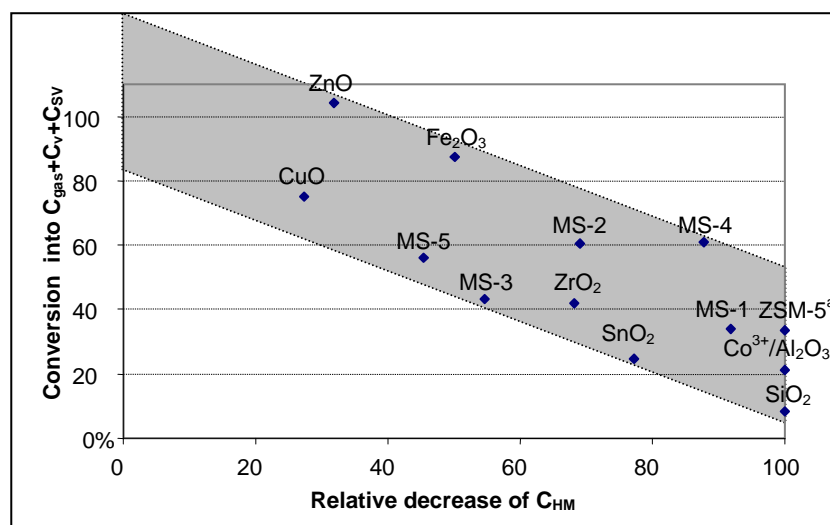
Only few catalysts among the variety tested in this study were able to break down HM into GC detectable products, with a significant increase of gas, volatile and semi-volatile products.

In particular, some pure metal oxides and mixed metal oxides, in particular copper and cobalt containing metal oxides, showed a minor propensity to yield coke in comparison with other catalysts. For these catalysts, the effectiveness of the HM degradation into GC detectable carbon is illustrated in Figure 3.5.5. Here the percentage reduction of HM yield in comparison to non-catalytic pyrolysis (x-axis) was plotted vs. the effectiveness of conversion of HM to GC detectable (y-axis), obtained from ratio between absolute increase in GC detectable and absolute decrease in HM yield (both in comparison with non-catalytic pyrolysis). Shadowed area indicated graphically the overall trend and was built up by including all catalysts that raised significantly the GC detectable products yield.

---

<sup>223</sup> T.R. Carlson, T.P. Vispute, G.W. Huber. Green Gasoline by Catalytic Fast Pyrolysis of Solid Biomass Derived Compounds. *ChemSusChem*. 1 (2008) 397-400.

**Figure 3.5.5:** Percentage reduction of HM yield (X axis) *versus* effectiveness of conversion of HM to GC detectable (Y axis); Only catalyst that increased GC detectable pyrolysis products are shown. <sup>a</sup>H-ZSM-5 used in 1:20 biomass:catalyst ratio.



As expected, the most active catalysts in HM cracking (namely ZSM-5 used in 1:20 ratio, mesoporous SiO<sub>2</sub>, MS-1 and Co<sup>3+</sup>/Al<sub>2</sub>O<sub>3</sub>) were generally characterized by higher coking rate and lowest conversion of HM into GC detectable products. On the other hand “mildest” catalysts (like ZnO, CuO and Fe<sub>2</sub>O<sub>3</sub> bulk metal oxides) cracked only a small amount of HM into GC detectable products, but with carbon effectiveness approaching to 100% and low coking rate. Moreover, for similar HM reduction rate, chemically different catalysts played a role in determining different increase in GC detectable products, conceptually represented by the vertical width of the shadowed area in figure 3.5.5 (constructed by comprising all data obtained). From this point of view, the best catalysts were those near the upper edge of the grey area in Figure 3.5.5 (e.g. ZnO, Fe<sub>2</sub>O<sub>3</sub>, MS-4).

### 3.5.4 Conclusions

The selection of proper catalyst is a fundamental step in developing catalytic pyrolysis as an effective process to convert biomass into a valuable liquid biofuel. A simple procedure based on elemental carbon determination by Py-GC-AED, weight determination and reasonable assumptions allowed to conduct a systematic study on the catalytic activity of large array of active solids belonging to different chemical families and industrial applications. Quantitative data were rationalised in terms of carbon yields representative of gas, bio-oil and solid residue. Bio-oil was further characterized in terms of GC detectable products and a non-volatile heavy fraction, this latter associated to some detrimental aspects in fuel application (high viscosity, phase separation and more difficult combustion).

With all the tested catalysts the yields of bio-oil ranged from 14 to 58%, with large differences in the concentration of the heavy fraction (0-70%). However, for most of the catalysts reduction of

heavy matter was accompanied by a significant diminution of bio-oil yields with respect to uncatalysed pyrolysis of biomass. Thus, few catalysts were able to counteract the drop in bio-oil yields by an increase in the amount of gas, volatile and semi-volatile compounds. At this regard, the most interesting catalysts resulted to be CuO which exhibited the highest yields in semi-volatile compounds, mixed metal oxide catalysts ( $\text{Fe}_2\text{O}_3$ , and mixed metal oxides containing copper and cobalt) and ZnO which reduced the proportion of heavy fraction in the bio-oil with a limited decrease in its yield.

## 4. Applied pyrolysis for carbon-neutral fuels and chemicals

### 4.1. Upgrading of Bio-oil by hydrogenation and catalytic cracking over H-ZSM-5

#### 4.1.1 Introduction

Main problems concerning the use of bio-oil as fuel, are the low volatility, high viscosity, the formation of coke, and corrosiveness.<sup>224</sup> One of the possible effective strategy for the upgrading of biomass pyrolysis oils involves complete de-functionalization of the oils, through deoxygenation with production aromatic hydrocarbons, by processing pyrolysis vapours onto H-ZSM-5, H-Y zeolite, H-mordenite, silicalite, silica-alumina or fluid catalytic cracking catalyst (FCC), with best results obtained with H-ZSM-5.<sup>225,226,227,228,229,230,231,232,233,234,235,236,237,238</sup> This approach has the advantage to directly produce an automotive fuel similar to gasoline, but it has important drawbacks, as the loss of energetic efficiency and the fast catalyst deactivation due to water and

---

<sup>224</sup> S. Czernik, A.V. Bridgwater. Overview of applications of biomass fast pyrolysis oil. *Energy Fuels* 18 (2004) 590-598.

<sup>225</sup> E. Furimsky. Catalytic hydrodeoxygenation. *Appl Catal. A* 199 (2000)147-190.

<sup>226</sup> D.C. Elliott, D. Beckman, A.V. Bridgwater, J.P. Diebold, S.B. Gevert, Y. Solantausta. Developments in direct thermochemical liquefaction of biomass: 1983-1990. *Energy Fuels*. 5 (1991) 399-410.

<sup>227</sup> L. Petrus, M.A. Noordermeer. Biomass to biofuels, a chemical perspective. *Green Chem.* 8 (2006) 861-7.

<sup>228</sup> J.D. Adjaye, N.N. Bakhshi. Production of hydrocarbons by catalytic upgrading of a fast pyrolysis bio-oil. Part I: Conversion over various catalysts, *Fuel Process. Technol.* 45 (1995) 161-183.

<sup>229</sup> J.D. Adjaye and N.N. Bakhshi, Production of hydrocarbons by catalytic upgrading of a fast pyrolysis bio-oil. Part II: Comparative catalyst performance and reaction pathways, *Fuel Process. Technol.*, 45 (1995) 185-202.

<sup>230</sup> J.D. Adjaye, S.P.R. Katikaneni and N.N. Bakhshi. Catalytic conversion of a biofuel to hydrocarbons: effect of mixtures of HZSM-5 and silica-alumina catalysts on product distribution. *Fuel Process. Technol.* 48 (1996) 115-143.

<sup>231</sup> R.K. Sharma, N.N. Bakhshi. Catalytic upgrading of pyrolysis oil. *Energ.Fuel.* 7 (1993) 306-314.

<sup>232</sup> S.T. Srinivas, A.K. Dalai, N.N. Bakhshi. Thermal and catalytic upgrading of a biomass-derived oil in a dual reaction system. *Can. J. Chem. Eng.* 78 (2000) 343-354.

<sup>233</sup> H.J. Park, J.I. Dong, J.K. Jeon, K.S. Yoo, J.H. Yim, J.M. Sohn and Y.K. Park. Conversion of the pyrolytic vapor of radiata pine over zeolites. *J. Ind. Eng. Chem.* 13 (2007) 182-189.

<sup>234</sup> T.R. Carlson, G.A. Tompsett, W.C. Conner, G.W. Huber. Aromatic Production from Catalytic Fast Pyrolysis of Biomass-Derived Feedstocks. *Top-Catal.* 52 (2009) 241-251.

<sup>235</sup> H.I. Lee, H.J. Park, Y.K. Park, J.Y. Hur, J.K. Jeon, J.M. Kim. Synthesis of highly stable mesoporous aluminosilicates from commercially available zeolites and their application to the pyrolysis of woody biomass. *Catal. Today.* 132 (2008) 68-74.

<sup>236</sup> O. Onay. Fast and catalytic pyrolysis of pistacia khinjuk seed in a well-swept fixed bed reactor. *Fuel* 86 (2007) 1452-1460.

<sup>237</sup> A. Atutxa, R. Aguado, A. G. Gayubo, M. Olazar, J. Bilbao. Kinetic Description of the Catalytic Pyrolysis of Biomass in a Conical Spouted Bed Reactor. *Energ.Fuel.* 19 (2005) 765-774.

<sup>238</sup> S. Vitolo, M. Seggiani, P. Frediani, G. Ambrosini, L. Politi. Catalytic upgrading of pyrolytic oils to fuel over different zeolites. *Fuel* 78 (1999) 1147-1159.

extensive coking (in comparison with that from hydrocarbon processing) over the catalyst.<sup>239,240,241,242,243,244</sup>

Basically, the upgrading of fast pyrolysis bio-oil is a challenging task, due to the reactivity of the condensed bio-oil recovered from fast pyrolysis. One of the most important features of raw bio-oil is the co-presence of phenols and aldehydes, that can form polymeric substances and finally coke if subjected to heat. This determines the bio-oil poor quality as fuel and, more specifically, it determines a loss in effectiveness during any downstream processing. For this reason, Hydrogenation of aldehydes into alcohols and, possibly, partial deoxygenation and reduction of reactive double bonds can be beneficial for bio-oil quality and it can facilitate further deoxygenation steps.

Most of petroleum industry hydrotreating procedures require high temperature and pressure conditions that, if the treatment is applied to a raw bio-oil, usually determine an unacceptable increase in coke formation and decrease the selectivity of the overall process.<sup>245</sup> The first attempts to perform high temperature hydro-deoxygenation, aimed at obtaining a petroleum-like material, in a single step formed a heavy, coke-like semi-solid product.<sup>246</sup>

Although it is widely accepted that direct application of petroleum hydrotreating technology is not affordable to fast pyrolysis bio-oil,<sup>224</sup> a significant increase in effectiveness was obtained by Catalytic hydrotreatment at temperatures below 300 °C with either Ni or sulfided cobalt molybdenum (CoMo) catalysts. These catalysts were effective in producing a stabilized oil product, able to be entirely distilled without significant coke formation.<sup>247</sup> This product was successfully used as feedstock for gasoline range fuel synthesis in a second high temperature/pressure hydrocracking stage on sulfided CoMo catalyst at conditions of

---

<sup>239</sup> A.G. Gayubo, A.T. Aguayo, A. Atutxa, R. Aguado and J. Bilbao. Transformation of Oxygenate Components of Biomass Pyrolysis Oil on a HZSM-5 Zeolite. I. Alcohols and Phenols. *Ind. Eng. Chem. Res.* 43 (2004) 2610-2618.

<sup>240</sup> A.G. Gayubo, A.T. Aguayo, A. Atutxa, R. Aguado, M. Olazar and J. Bilbao. Transformation of Oxygenate Components of Biomass Pyrolysis Oil on a HZSM-5 Zeolite. II. Aldehydes, Ketones, and Acids. *Ind. Eng. Chem. Res.*, 43 (2004) 2619-2626.

<sup>241</sup> A.G. Gayubo, A.T. Aguayo, A. Atutxa, B. Valle, J. Bilbao. Undesired components in the transformation of biomass pyrolysis oil into hydrocarbons on an HZSM-5 zeolite catalyst. *J. Chem. Technol. Biotechnol.* 80 (2005) 1244-1251.

<sup>242</sup> P.A. Horne, P.T. Williams. The effect of zeolite ZSM-5 catalyst deactivation during the upgrading of biomass-derived pyrolysis vapours *Journal of Analytical and Applied Pyrolysis. J. Anal. Appl. Pyrol.* 34 (1995) 65-85.

<sup>243</sup> A. G. Gayubo, A. T. Aguayo, A. Atutxa, R. Prieto, J. Bilbao. Deactivation of a HZSM-5 Zeolite Catalyst in the Transformation of the Aqueous Fraction of Biomass Pyrolysis Oil into Hydrocarbons. *Energy & Fuels* 18 (2004) 1640-1647.

<sup>244</sup> S. Vitolo, B. Bresci, M. Seggiani, M.G. Gallo. Catalytic upgrading of pyrolytic oils over HZSM-5 zeolite: behaviour of the catalyst when used in repeated upgrading-regenerating cycles. *Fuel* 80 (2001) 17-26.

<sup>245</sup> D.C. Elliott. Historical Developments in Hydroprocessing Bio-oils. *Energy & Fuels* 21 (2007) 1792-1815.

<sup>246</sup> D.C. Elliott, E.G. Baker. Biomass Liquefaction Product Analysis and Upgrading. *Comptes Rendus de l'Atelier de Travail sur la Liquefaction de la Biomasse; report 23130, NRCC: Sherbrooke, Quebec, Canada, September 29-30 (1983) 176-183.*

<sup>247</sup> D.C. Elliott, E.G. Baker. Process For Upgrading Biomass Pyrolyzates. U.S. Patent Number 4,795,841, January 3, 1989.

approximately 350 °C and 13.8 MPa.<sup>248</sup> Similarly, Vitolo et. al studied the thermogravimetric behavior of raw and hydrogenated bio-oil, and demonstrated that hydrogenated bio-oil is characterized by improved volatility and a reduced coking behavior.<sup>249</sup>

These pioneering studies demonstrated the feasibility of the process under high temperature and pressure and were taken as a guide for a general up-grading scheme, recently proposed by some authors as a solution for the synthesis of commodity chemicals from biomass.<sup>250</sup>

Moreover, mild hydrogenation could be foreseen as a method for directly improving the quality of bio-oil. Xu et al. recently demonstrated that hydrogenation over an acid catalyst and removal of water can also reduce the corrosiveness of the liquid, by means of esterification of carboxylic acids with large amount of alcohols functionality created by the mild hydrogenation.<sup>251,252</sup> The reduction of bio-oil reactivity allows an easier removal (by distillation or similar techniques) of water and some light compounds that could deteriorate the equipments for further bio-oil processing.

In conclusions, even if simple hydrogenation of reactive double bonds could be seen as a key step to overcome the intrinsic limitations of biomass derived pyrolysis oils, only few works studied even milder conditions and most of studies regards model compounds.<sup>253,254</sup> Further improvements are expected in this field, where the ultimate goal is the development of an effective homogeneous catalyst for mild temperature hydrotreatment of pyrolysis oil. Moreover, although the hydrogenation process was studied from the point of view of physicochemical proprieties of the liquid product, a detail molecular description of the real matrix behavior during hydrogenation is lacking. For this reason, this chapter was advocated to study in detail the chemical changes following hydrogenation of poplar bio-oil.

For model hydrogenation strategy, an accurate screening<sup>255,256</sup> of the possibilities indicated the bimetallic ruthenium Shvo catalyst<sup>257,258</sup> as a very good candidate for our scope. Indeed, this robust

---

<sup>248</sup> D.C. Elliott, E.G. Baker. Hydrotreating Biomass Liquids to Produce Hydrocarbon Fuels. Energy from Biomass & Wastes X; IGT: Chicago, (1986) 765-784.

<sup>249</sup> S. Vitolo, P. Ghetti. Physical and combustion characterization of pyrolysis oil derived from biomass material upgraded by catalytic hydrogenation. Fuel 73 (1994)1810-1812.

<sup>250</sup> T.P. Vispute, H.Zhang, A. Sanna, R. Xiao, G.W. Huber. Renewable Chemical Commodity Feedstocks from Integrated Catalytic Processing of Pyrolysis Oils. Science 330 (2010) 1222-1227.

<sup>251</sup> Y. Xu, T. Wang, L. Ma, Q. Zhang, W. Liang. Upgrading of the liquid fuel from fast pyrolysis of biomass over MoNi/c-Al<sub>2</sub>O<sub>3</sub> catalysts. Applied Energy 87 (2010) 2886–2891.

<sup>252</sup> Y. Tang, W. Yu, L. Mo, H. Lou, X. Zheng. One-Step Hydrogenation-Esterification of Aldehyde and Acid to Ester over Bifunctional Pt Catalysts: A Model Reaction as Novel Route for Catalytic Upgrading of Fast Pyrolysis Bio-Oil. Energy & Fuels 22 (2008) 3484–3488.

<sup>253</sup> F.H. Mahfud, S. Bussemaker, B.J. Kooi, G.H. Ten Brink, H.J. Heeres. The application of water-soluble ruthenium catalysts for the hydrogenation of the dichloromethane soluble fraction of fast pyrolysis oil and related model compounds in a two phase aqueous-organic system. J Mol. Catal. A Chem. 277 (2007):127-36.

<sup>254</sup> F.H. Mahfud, F. Ghijsen, H.J. Heeres. Hydrogenation of fast pyrolysis oil and model compounds in a two-phase aqueous organic system using homogeneous ruthenium catalysts. J Mol. Catal. A Chem. 264 (2007) 227-236.

<sup>255</sup> R.M. Bullock. Catalytic ionic hydrogenations. Chem. Eur. J 10 (2004):2366-2374.

ruthenium complex is water-, temperature- and acid- resistant. Discovered in the 1985<sup>259</sup> it has been matter of several mechanistic studies and it has been applied as a versatile catalyst, particularly in hydrogenation of polar double bonds.<sup>260,261,262,263,264</sup> In the present chapter, this catalyst was tested on bio-oil samples obtained from bench scale pyrolysis of white poplar. Raw bio-oil and hydrogenated bio-oil were analyzed by an array of analytical techniques and complete deoxygenation (by thermal cracking on H-ZSM-5 zeolite ) of both raw and hydrogenated bio-oil was studied. Py-GC-MS was used as model system to simulate a catalytic cracking process, as shown by recent publications and in chapter 3.5,<sup>265</sup> and Py-SPE-GC-MS technique was applied for the monitoring of PAHs formation (demonstrated high when H-ZSM-5 is used on raw biomass in chapter 3.3) during the catalytic cracking process.

## 4.1.2. Experimental

### 4.1.2.1 Pyrolysis of Poplar chips

Bio-oil was obtained by consecutive batch pyrolysis of white poplar wood chips (same sample of chapters 3.1 and 3.3) with a fixed bed tubular quartz reactor (the apparatus was described in details elsewhere).<sup>266</sup> Each batch was conducted by pyrolysing 5-10 g sample at 500 °C under nitrogen flux with 30 s residence time. Bio-oil was collected downstream by means of two sequential trapping systems: a cold trap equipped with a glass demister immersed into brine followed by a bubbler filled with diethyl ether. In total, 100 g of white poplar chips yielded 55 g of bio-oil (27 g and 28 g

---

<sup>256</sup> S.E. Clapham, A. Hadzovic, R.H. Morris. Mechanisms of the H<sub>2</sub>-hydrogenation and transfer hydrogenation of polar bonds catalyzed by ruthenium hydride complexes. *Coord Chem Rev* 248 (2004) 2201-2237.

<sup>257</sup> R. Karvembu, R. Prabhakaran, N. Natarajan. Shvo's diruthenium complex: a robust catalyst. *Coord Chem Rev* 249 (2005) 911-918.

<sup>258</sup> Y. Shvo, D. Czarkie, Y. Rahamim, D.F. Chodosh. A new group of ruthenium complexes: structure and catalysis. *J Am Chem Soc.* 108 (1986) 7400-7402.

<sup>259</sup> Y. Blum, D. Czarkie, Y. Rahamim, Y. Shvo. (Cyclopentadienone) ruthenium carbonyl complexes-a new class of homogeneous hydrogenation catalysts. *Organometallics.* 4 (1985) 1459-1461.

<sup>260</sup> B.L. Conley, M.K. Pennington-Boggio, T.J. Boz E, T.J. Williams. Discovery, applications, and catalytic mechanisms of Shvo's catalyst. *Chem Rev.* 110 (2010) 2294-2312.

<sup>261</sup> N. Menashe, E. Salant, Y. Shvo. Efficient catalytic reduction of ketones with formic acid and ruthenium complexes. *J Organomet. Chem.* 514 (1996) 97-102.

<sup>262</sup> Y. Shvo, I. Goldberg, D. Czerkie, D. Reshef, Z. Stein. New ruthenium complexes in the catalytic hydrogenation of alkynes. Study of structure and mechanism. *Organometallics* 16 (1997) 133-138.

<sup>263</sup> J.S.M. Samec, A.H. Ell, J.B. Aberg, T. Privalov, L. Eriksson, J.E. Backvall. Mechanistic study of hydrogen transfer to imines from a hydroxycyclopentadienyl ruthenium hydride. Experimental support for a mechanism involving coordination of imine to ruthenium prior to hydrogen transfer. *J Am Chem Soc.* 128 (2006) 14293-14305.

<sup>264</sup> A.H. Ell, J.B. Johnson, J.E. Backvall. Mechanism of ruthenium-catalyzed hydrogen transfer reactions. Evidence for a stepwise transfer of CH and NH hydrogens from an amine to a (cyclopentadienone)ruthenium complex. *Chem Comm.* 14 (2003) 1652-1653.

<sup>265</sup> T.R. Carlson, T. P. Vispute, G.W. Huber. Green Gasoline by Catalytic Fast Pyrolysis of Solid Biomass Derived Compounds. *ChemSusChem.* 1 (2008) 397-400.

<sup>266</sup> D. Fabbri, C. Torri, I. Mancini. Pyrolysis of cellulose catalysed by nanopowder metal oxides: production and characterisation of a chiral hydroxylactone and its role as building block. *Green Chem.* 9 (2007) 1374-1379.

from the cold and solvent trap, respectively) and 28 g of charcoal. Bio-oil collected from the cold trap was selected as real matrix for hydrotreating experiments.

#### 4.1.2.2 Hydrogenation

All the hydrogenation experiments were conducted in a 100 mL stainless steel batch autoclave Parr Instrument series 4560 (25-100 mL, T<sub>max</sub> = 300 °C, P<sub>max</sub> = 100 bar) equipped with an electrical heating mantle and a mechanical stirrer. Details on hydrogenation procedure, as well as hydrogenation set up were described in detail by Busetto et al (2010).<sup>267</sup>

Briefly, the autoclave was charged with substrate and catalyst. Prior to hydrogen addition, the autoclave was flushed three times with nitrogen to remove oxygen. Subsequently, hydrogen was added until a pressure of 5 bar was reached. The reactor was heated to required temperature. Subsequently the hydrogen pressure inside the reaction was increased to 10 bar. Then the reaction was conducted at 145 °C under 10 atm H<sub>2</sub> pressure for 1 h.

#### 4.1.2.3 Chemical characterization of bio-oil

Original and hydrogenated bio-oils were subjected to the same environmental conditions prior to analysis (*e.g.* transportation, storing) so that any observed chemical modification could be ascribed to the hydrogenation process rather than handling or ageing. The analytical characterisation of the oil was based on the solvent fractionation procedure developed by Oasmaa *et al.*, with slight modifications.<sup>268,269</sup> Pyrolytic lignin was determined by precipitation with tenfold excess water added to an aliquot of neat bio-oil. The formed precipitate was centrifuged and filtered, dried at 40 °C under nitrogen flow overnight and weighed. The weight of this water insoluble residue minus the weight of extractives gave the mass contribution of pyrolytic lignin. Extractives were determined by extraction with *n*-hexane (1 hour under sonication with 1/10 w/v bio-oil/hexane ratio) and weighing the residue left after elimination of the solvent by vacuum distillation. The aqueous supernatant resulting from the filtration of pyrolytic lignin was extracted sequentially with diethyl ether and pentane. The organic fractions were collected and the residue weighted after elimination of the solvent giving an estimate of lignin monomers. The aqueous layer contained sugars (anhydro/mono and oligosaccharides) and other water soluble components.

---

<sup>267</sup> L. Busetto, D. Fabbri, R. Mazzoni, M. Salmi, C. Torri, V. Zanotti. Application of the Shvo catalyst in homogeneous hydrogenation of bio-oil obtained from pyrolysis of white poplar: New mild upgrading conditions. *Fuel* 90 (2010) 1197-1207.

<sup>268</sup> A. Oasmaa, E. Kuoppala, Y. Solantausta. Fast pyrolysis of forestry residue. 2. Physicochemical composition of product liquid. *Energy Fuels* 17 (2003) 433-443.

<sup>269</sup> A. Oasmaa, E. Kuoppala. Solvent fractionation method with brix for rapid characterization of wood fast pyrolysis liquids. *Energy Fuels* 22 (2008) 4245-4248.

Anhydro/oligosaccharides were hydrolysed by treating the aqueous solution over amberlyst at 100 °C for 6 hours. Then, 100 µl of solution were evaporated under nitrogen at room temperature, the residue was dissolved in acetonitrile and subjected to the analysis of anhydro/monosaccharides as described below. The final concentration value of anhydro/oligosaccharides was obtained by subtracting the content of free anhydro/monosaccharides from the total value of anhydro/monosaccharides obtained after hydrolysis. The concentration of “others water soluble” was roughly estimated by the difference from BRIX method value.<sup>268,269</sup>

Anhydro/monosaccharides (*e.g.* glucose and levoglucosan) were determined by GC-MS after trimethylsilylation of the bio-oil dissolved in acetonitrile using methyl-β-L-arabinopyranoside as internal standard.<sup>270</sup> In addition, this method allowed the quantification of C<sub>2</sub>-C<sub>4</sub> polyols (*e.g.* 1,2-ethandiol, 1,2-propanediol) and hydroxyacids (*e.g.* hydroxyacetic acid).

Volatile organic compounds (*e.g.* methanol, ethanol, acetic acid) were evaluated by solid phase micro-extraction (SPME) followed by GC-MS analysis of bio-oil dissolved into glycerol.

Quantification was performed by external calibration on pure compounds when available.

Reactive aldehydes (acetaldehyde, hydroxyacetaldehyde, methylglyoxale and others tentatively identified in the mass chromatograms at *m/z* 75) were determined by GC-MS after derivatization into the corresponding dimethyl acetals by catalytic methanolysis. A solution of bio-oil in methanol (4 mL at 2.5% mass concentration) spiked with internal standard (100 µl of a 1 mg mL<sup>-1</sup> dodecanal solution) was treated at 60 °C for 4 hours with 100 mg of amberlyst® acidic resin.

Finally, water content was determined by the Karl-Fischer method.

GC-MS analyses were performed in splitless mode at 280 °C in the injection port of an Agilent 6850 gas chromatograph connected to an Agilent HP 5975 quadrupole mass spectrometer. Analytes were separated by a HP-5MS fused-silica capillary column using helium as carrier gas. Mass spectra were recorded under electron ionization (70 eV) in full scan acquisition scan within *m/z* 29-450.

#### 4.1.2.4 Catalytic treatment of bio-oils over zeolites:Py-GC-MS

Catalytic treatment was studied by means of analytical py-GC-MS system (see chapter 3.1 for more details). The sample (0.25 mg) was admixed with 20:1 ratio (4.25 mg) of H-ZSM-5 zeolite (previously calcined at 700°C for 5 hours) . Pyrolysis were performed at 600 °C (set temperature) as described in detail in chapter 3.1. Quantitation was performed by external calibration, by injecting a

---

<sup>270</sup> C. Torri, I.G. Lesci, D. Fabbri. Analytical study on the pyrolytic behaviour of cellulose in the presence of MCM-41 mesoporous materials. *J Anal. Appl. Pyrolysis* 85 (2009) 192-196.

known amount of ethyl-acetate solution containing 2% of toluene into the same system used for pyrolysis.

#### 4.1.2.5 PAHs formation during catalytic treatment: Py-SPE-GC-MS

The exit of the pyrolysis chamber was connected to a glass tube containing 100 mg of silica gel, withdrawn from a DSC-Si SPE cartridge, packed with glass wool and conditioned with *n*-hexane. The selected quantity of sorbent was sufficient to trap evolved PAHs quantitatively as determined by breakthrough experiments with a second layer of silica. Samples were pyrolyzed with the same conditions used for Py-GC-MS. After pyrolysis, the apparatus was vertically positioned, spiked with 100  $\mu$ l of surrogate PAH mix solution and rinsed with 6 ml of *n*-hexane. The solvent was left to flow through the silica cartridge into the collecting vial. The obtained solution was then blown down to 10-50  $\mu$ l under nitrogen and analysed by GC-MS. Emission levels ( $\mu$ g PAH g<sup>-1</sup> pyrolysed biomass) were determined by internal calibration.

### 4.1.3. Results and Discussion

#### 4.1.3.1 Hydrogenation of bio-oil from white poplar: reactivity of bio-oil

Hydrogenation with the Shvo catalyst deeply modified the chemical composition of bio-oil, as indicated by comparison of the chemical composition reported in Table 4.1.1 and 4.1.2.

**Table 4.1.1** Chemical composition expressed as weight percent of bio-oil before and after hydrogenation with Shvo catalyst.

<i>Compound</i>	<i>Before hydrogenation</i>	<i>After hydrogenation</i>
<i>%</i>	<i>%</i>	<i>%</i>
<b>C</b>	35	38
<b>H</b>	4.3	5.5
<b>O</b>	60	57
<b>N</b>	0.1	0.1
Extractives	0.1	0.9
Pyrolytic Lignin	8.3	15
Lignin monomers	6.1	6.8
Aldehydes	8.2	0.17
C <sub>2</sub> -C <sub>4</sub> polyols and hydroxyacids	2.7	18
Anhydro/monosaccharides	1.6	9.7
Anhydro/oligosaccharides	13	3.0
Other water soluble	0.9	0.5
Volatile organics	8.9	8.4
Water	35	28
<i>Mass balance (total quantified)</i>	85	90

The most relevant changes were clearly associated with the activity of the catalyst towards the reduction of the CHO groups. In fact, aldehydes that accounted for about 8% by weight in the original bio-oil dropped to 0.2% after hydrogenation (Table 4.1.1).

Conversely, the content of C<sub>2</sub>-C<sub>4</sub> polyols and hydroxyacids increased from 2.7% to 18%. Examples of specific compounds responsible to the observed changes were reported in Table 4.1.2. Following hydrogenation, the concentrations of hydroxyacetaldehyde dropped from 4% to 0.01% and that of methylglyoxal from 0.7% to undetectable levels, while the concentration of 1,2-ethanediol, 1,2-propanediol and hydroxyacetic acid increased significantly.

A remarkable effect was found in the distribution of the so called sugars, comprising the ether insoluble fraction of water soluble products, and consisting mainly of anhydro/monosaccharides and oligosaccharides.<sup>268,269</sup> Free anhydro/monosaccharides and their derivatives exhibited a significant increase from 1.6% to 9.7% and concomitantly the level of oligosaccharides decreased from 13% to 3% upon hydrogenation. This finding suggests that the employed conditions favoured the hydrolytic scission of anhydro/oligosaccharides into monosaccharides and eventually levoglucosan (note in Table 4.1.2 that the level of levoglucosan was unaltered) and the partial reduction of the anomeric carbon (glucitol was identified in the hydrogenated bio-oil).

The effect of hydrotreating was less pronounced on lignin derivatives. The content of lignin monomers remained constant, whereas that of heavier lignin phenols (e.g. pyrolytic lignin) slightly increased.

**Table 4.1.2** Mean concentration of specific compounds expressed as weight percent in original bio-oil and bio-oil after hydrogenation with Shvo catalyst.

<i>Compound</i> %	<i>Before hydrogenation</i> %	<i>After hydrogenation</i> %
Acetaldehyde	0.7	Not detected
Ethanol	Not detected	0.1
Acetic acid	2.2	2.6
Hydroxyacetaldehyde	4.2	0.01
1,2-ethanediol	0.1	7.2
Methylglyoxal	0.7	Not detected
Hydroxyacetone	0.7	0.8
1,2-propanediol	Not detected	7.0
Glyoxalic acid	0.4	Not detected
Hydroxyacetic acid	0.2	3.0
Phenol	0.3	0.6
Cathecol	0.5	0.9
Levoglucosan	1.6	2.2

#### 4.1.3.2 De-oxygenation of hydrogenated bio-oil by catalytic cracking

Once hydrogenated, further upgrading of pyrolysis oil was studied by catalytic cracking over H-ZSM-5, since it is known that this type of zeolite is able to transform carbohydrate derived fraction of bio-oil into aromatic hydrocarbons.<sup>265</sup>

**Figure 4.1.1:** Carbon yield of aromatic compounds (listed in table 4.1.3) obtained from catalytic pyrolysis of poplar, bio-oil, hydrogenated bio-oil and long chain hydrocarbon.

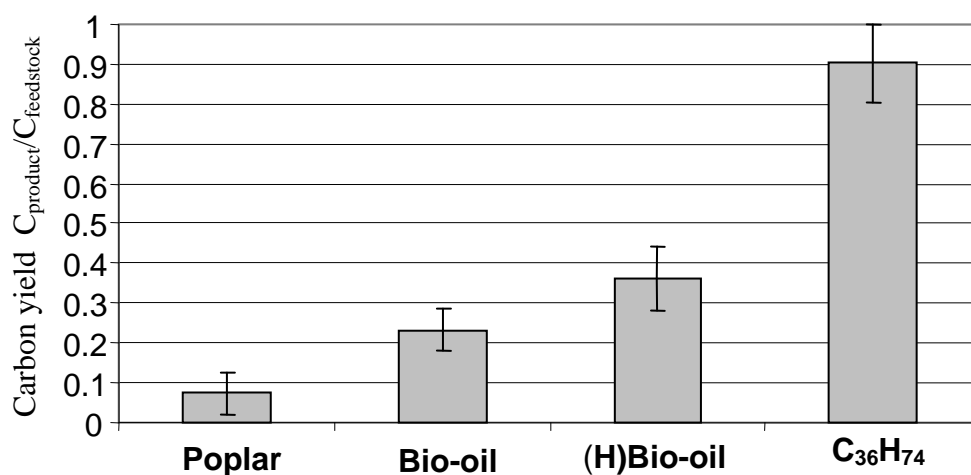
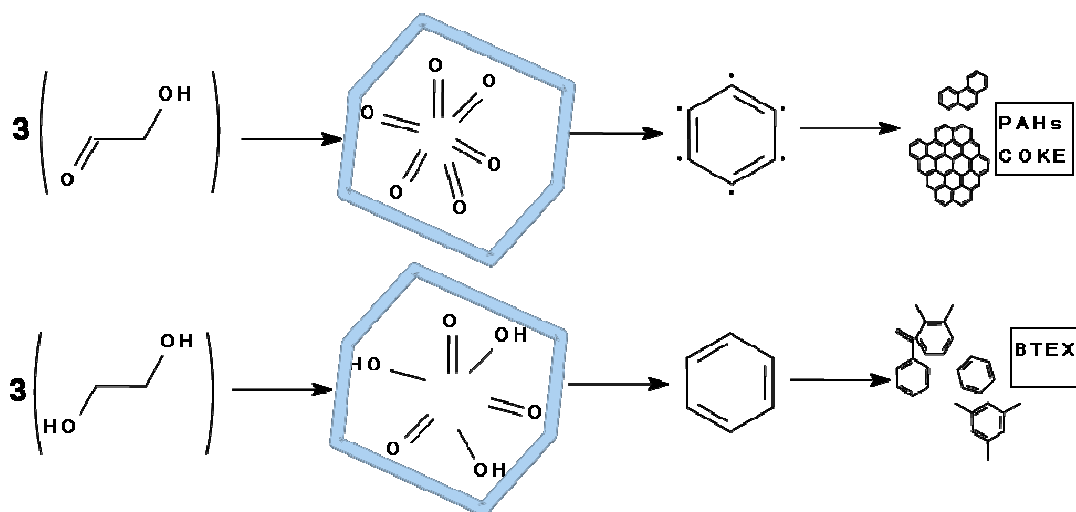


Figure 4.1.1 shows the overall carbon conversion obtained for poplar (7%±5%), bio-oil (23±5% yield) and hydrogenated bio-oil (36±8% yield), compared with carbon conversion obtainable by hydrocarbon processing (90±10%).

**Figure 4.1.2:** Example of different H-ZSM-5 catalyzed pathways proposed for raw bio-oil compound (hydroxyacetaldehyde) and corresponding hydrogenated substance (1,2-ethanediol).



**Table 4.1.3:** composition (% w/w<sub>gasoline</sub>) of “gasoline” obtained by catalytic pyrolysis (with H-ZSM-5) of bio-oil and hydrogenated bio-oil ((H)Bio-oil). Mean±standard deviation (n=4).

	<i>Bio-oil cracking</i>	<i>(H)Bio-oil cracking<sup>a</sup></i>
	% w/w <sub>gasoline</sub>	% w/w <sub>gasoline</sub>
propene	0.62 ±0.01	1.0 ±0.02
butene	2.3 ±0.01	3.4 ±0.1
benzene	11 ±0.08	6.8 ±0.3
unknown	-	0.06 ±0.0
toluene	29 ±0.4	24 ±1.0
xilene (o)	2.8 ±0.12	3.5 ±0.2
xilene(m)	14 ±0.4	18 ±0.8
xilene(p)	2.9 ±0.02	3.1 ±0.1
propyl-benzene	0.20 ±0.02	0.54 ±0.03
1,2,3-trimethyl-benzene	3.2 ±0.2	6.3 ±0.4
methylfurfural	0.08 ±0.02	-
1,3,5-trimethyl-benzene	2.5 ±0.09	3.7 ±0.2
benzofuran	1.2 ±0.08	0.70 ±0.03
indane	3.3 ±0.2	2.5 ±0.2
indene	2.3 ±0.09	1.1 ±0.03
2-methyl-phenol	0.13 ±0.02	0.37 ±0.02
4-methyl-phenol	0.08 ±0.02	0.1 ±0.01
2,3-dihydro-4-methyl-1H-Indene	0.65 ±0.09	0.85 ±0.1
7-methyl-benzofuran	0.35 ±0.02	0.25 ±0.02
2-methyl-benzofuran	1.1 ±0.06	0.45 ±0.02
1-Phenyl-1-butene	1.6 ±0.12	1.4 ±0.1
3-methyl-(1H)-indene	1.4 ±0.09	1.0 ±0.1
1-methyl-(1H)-indene	1.4 ±0.09	1.0 ±0.1
2,3-dihydro-1-methyl-indene	1.0 ±0.07	0.67 ±0.1
naphthalene	4.3 ±0.08	3.0 ±0.01
1-methyl -1,2,3,4-(4H)-naphthalene	0.02 ±0.00	0.21 ±0.01
2,3-dihydro-1,1-(1H)-Indene	0.12 ±0.02	-
4,7-dimethyl-Benzofuran	0.51 ±0.04	0.28 ±0.02
1,2-dihydro-n-methyl-naphtalene	0.09 ±0.02	0.09 ±0.02
1,2-dihydro-n-methyl-naphtalene	0.48 ±0.05	0.40 ±0.05
1,2-dihydro-n-methyl-naphtalene	0.45 ±0.05	0.28 ±0.01
1,2-dihydro-n-methyl-naphtalene	0.22 ±0.01	0.26 ±0.01
n-methyl-naphtalene	5.2 ±0.1	4.5 ±0.2
n-methyl-naphtalene	1.1 ±0.08	1.2 ±0.1
n-ethyl-naphtalene	0.50 ±0.03	0.41 ±0.1
n-ethyl-naphtalene	2.2 ±0.10	2.4 ±0.2
n-ethyl-naphtalene	0.64 ±0.00	1.0 ±0.01
n-ethyl-naphtalene	0.64 ±0.00	0.90 ±0.04
n-propyl-naphtalene	0.14 ±0.00	0.19 ±0.02
4-methyl-Dibenzofuran	0.03 ±0.01	-
others	0.57	3.8

Hydrogenation doubled the carbon yield obtainable from cracking of raw poplar bio-oil. In absolute terms, the yield of aromatic products obtainable remained low, if compared with hydrocarbons,

probably due to ineffective conversion of lignin derived bio-oil. In fact it is known that these compounds form char/coke outside from the catalyst and eventually clog the pores.<sup>241</sup>

Table 4.1.3 shows the composition of “gasoline” obtained through catalytic processing of bio-oil and hydrogenated bio-oil. The relative amount of different aromatic compounds was fairly reproducible, indicating that the source of error was mainly due to manual weighing and admixing procedure.

Hydrogenated bio-oil provided a gasoline richer in xilenes, trimethylbenzenes and with lesser amount of benzene, toluene and bicyclic aromatics (e.g. naphthalene or indene).

From molecular point of view, since the hydrogenation (Table 4.1.1 and 4.1.2), under conditions selected in this study has the main effect of reducing reactive double bonds, the effect of hydrogenation could be related to the occurrence of less oxidized carbohydrate derivatives.

As an example if we compare 1,2-ethanediol and hydroxyacetaldehyde we can expect that over H-ZSM-5, the former can form higher yield of alkylbenzenes and lower yield of coke (Figure 4.1.2).<sup>271,272</sup>

#### *4.1.3.3 PAHs formation rate in catalytic pyrolysis of raw bio-oil and hydrogenation bio-oil.*

As demonstrated in chapter 3.3, an important feature of catalytic cracking of biomass feedstock is a relatively larger PAHs formation than that observed in non-catalytic pyrolysis.

For this reason evaluation of priority PAHs formation from this feedstock was included in the study. Py-SPE-GC-MS technique was applied in order to evaluate the priority PAHs formation in an upgrading process on bio-oil and hydrogenated bio-oil.

Three possibilities were compared: cracking of poplar pyrolysis oil, cracking of previously hydrogenated pyrolysis oil, co-cracking of pyrolysis oil and hydrocarbons in the same system and simply hydrocarbon cracking. The last option was evaluated as reference system and it can represent actual standard refinery cracking for gasoline production.

As Table 3.3.4 shows, there are large differences in PAHs formation during cracking of hydrocarbons and an oxygenated feedstock like bio-oil. Main difference is an markedly higher production of some PAHs (e.g. naphthalene, anthracene and benzo[a]pyrene).

Using the toxic equivalency factor of each PAHs (TEFs) analyzed an overall carcinogenic compounds (TEQ expressed as mg kg<sup>-1</sup> Benzo[a]pyrene equivalent, BAPEq) produced in the process

---

<sup>271</sup> P.A. Horne, P.T. Williams, Reaction of oxygenated biomass pyrolysis model compounds over a ZSM-5 catalyst. *Renewable energy*, 7 (1996) 131-144.

<sup>272</sup> P.A. Horne, N. Nugranad, P.T. Williams. Catalytic coprocessing of biomass derived pyrolysis vapors and methanol. *J Anal. Appl. Pyrol.*, 34 (1995) 87-108.

can be calculated.<sup>273</sup> Cracking of raw Bio-oil over ZSM-5 creates four times more equivalents (56 mg kg<sup>-1</sup> BAPeq) of carcinogenic PAHs than hydrocarbon processing (13 mg kg<sup>-1</sup> BAPeq), mainly due to larger yield of four and five rings PAHs. Also simulating a real co-processing (on 1-1) in actual fossil oil fuelled refineries, the specific PAHs production from raw bio-oil, although slightly reduced remain on the same value.

**Table 4.1.4:** Rate of PAHs release (mean ± standard deviation) from catalytic cracking of a linear hydrocarbon (C<sub>36</sub>H<sub>74</sub>), bio-oil and hydrogenated bio-oil.<sup>a</sup> Calculated as Nisbet and LaGoy (1992)<sup>273</sup>

	$\mu\text{g g}^{-1}$ <b>Bio-oil</b>	$\mu\text{g g}^{-1}$ <b>(H)Bio-Oil</b>	$\mu\text{g g}^{-1}$ bio-oil <b>Bio-Oil+C<sub>36</sub>H<sub>74</sub></b>	$\mu\text{g g}^{-1}$ <b>C<sub>36</sub>H<sub>74</sub></b>
acenaphthylene	42 ±40	92 ±60	29±4	9±1
acenaphthene	75 ±30	41 ±23	33±13	8±0.2
fluorene	374 ±52	253±160	163±28	50±47
phenanthrene	339 ±144	276±116	258±76	89±17
anthracene	(1.1±2.8)·10 <sup>3</sup>	(0.77 ±37) ·10 <sup>3</sup>	(0.63±17)·10 <sup>3</sup>	90±22
fluoranthene	21 ±8	20 ±12	15±3	5±1
pyrene	42 ±18	33 ±12	39±5	13±2
chrysene	91 ±16	84 ±32	105±34	39±7
benz[a]anthracene	27 ±4	27 ±12	26±5	15±2
benzo[b]fluoranthene	2±1	2 ±1	2±1	1±0.3
benzo[k]fluoranthene	8 ±2	10 ±5	17±14	2±1
benzo[a]pyrene	32 ±15	26 ±8	45±14	3±3
indeno[1,2,3- <i>cd</i> ]pyrene	3 ±2	1 ±2	3±3	4±1
dibenz[ <i>a,h</i> ]anthracene	3 ±1	4 ±3	<1	<1
benzo[ <i>ghi</i> ]perylene	6 ±4	1 ±2	3±3	1±1
BAPeq <sup>a</sup>	56±25	43±10	51±21	13±6

On the other hand, if hydrogenated bio-oil is cracked, a more clear reduction in BAPeq production rate can be obtained (mainly due to lower Benzo[a]pyrene yield), with a final (in fact still high) value of 43 mg kg<sup>-1</sup> of BAPeq. Since the lignin derived fraction of hydrogenated oil is similar to raw bio-oil one, this effect is probably due to the hydrogenation of carbohydrates derived pyrolysis products, in agreement with mechanism proposed above (Figure 4.1.2), and was previously observed by Horne and Williams in catalytic cracking of model compounds.<sup>271</sup>

According to these results, if bio-oil would be co-processed with petroleum for gasoline synthesis, the final fuel should have drastically higher PAHs content than current gasoline fuel.

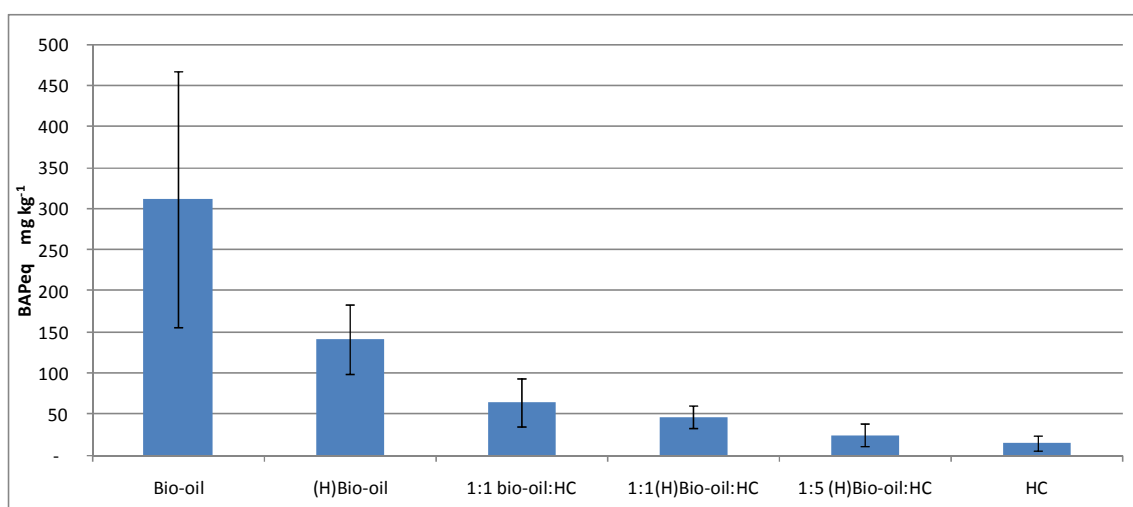
Using data obtained by micro-scale PAHs analysis and overall yields obtained by Py-GC-MS (paragraph 4.1.3.1) is possible to obtain expected PAHs concentration in the final fuel obtained.

Figure 4.4.3 shows the calculated content of carcinogenic PAHs (expressed as BAPeq) expected for

<sup>273</sup> I.C.T. Nisbet, P.K. LaGoy. Toxic equivalency factors (TEFs) for polycyclic aromatic hydrocarbons (PAHs). Regulatory Toxicology and Pharmacology 16 (1992) 290-300.

various fuels. The final expected PAHs concentration from simple catalytic cracking of raw bio-oil is astonishing high (final concentration of 160-460 mg kg<sup>-1</sup> BAPEq), whereas the expected PAHs content is markedly reduced to (100-180 mg kg<sup>-1</sup> BAPEq) from catalytic cracking of pure hydrogenated oil and to relatively safe level (11-27 mg kg<sup>-1</sup> BAPEq) if 1:5 hydrogenated bio-oil:hydrocarbons is considered.

**Figure 4.1.3:** Expected PAHs concentrations (as benzo[a]pyrene equivalents) in the final product of catalytic cracking with H-ZSM-5 of bio-oil, hydrogenated bio-oil ((H)Bio-oil), hydrocarbon (HC) and mix of these products. Bars correspond to confidence interval ( $\alpha=0.05$ ).



#### 4. Conclusions

Hydrogenation deeply changed the chemical nature of pyrolysis oil. Aldehydes, ketones and non-aromatic double bonds were almost totally hydrogenated. In addition, the catalytic system promoted the hydrolysis of sugar oligomers into monomers. These transformations result in an improved stability of the bio-oil due to the reduction of polar double bonds (in particular reduction of reactive aldehydes), that are main causes of the ageing of pyrolytic oils.

Hydrogenation determined a twofold increase of final gasoline yield and a significant reduction of carcinogenic PAHs formation rate, nevertheless PAHs formation during processing of hydrogenated bio-oil remained drastically higher than that observed with hydrocarbons.

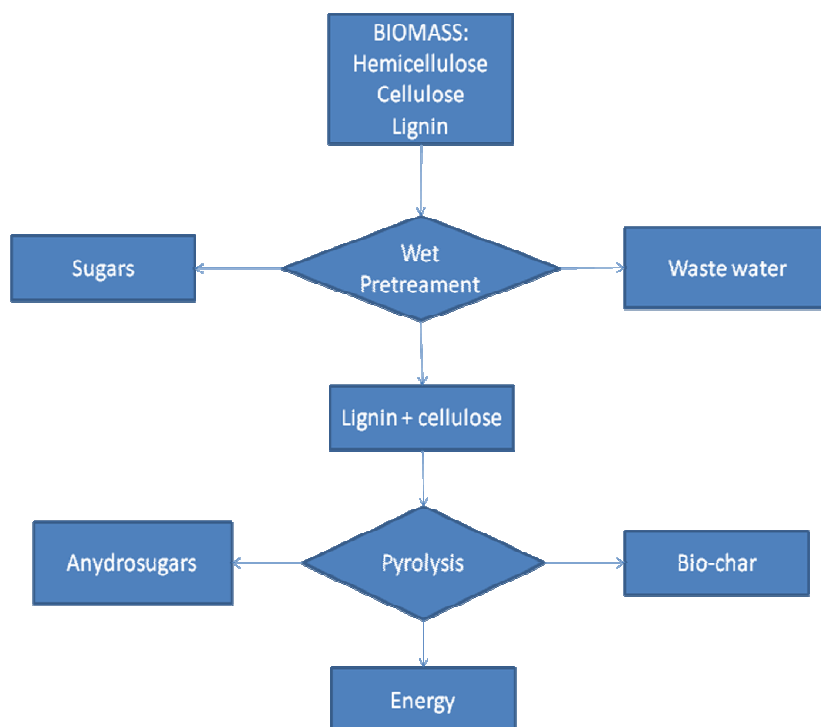
In fact, PAHs content could represent the most problematic adverse characteristic of gasoline obtained by hypothetical hybrid petroleum/biomass fuelled refineries. For this reason, it is advisable that only small amounts (less than 20% of the feedstock) of hydrogenated bio-oil could be fed in actual refinery without impact the safety of final product. Alternatively, as proposed by some authors,<sup>250</sup> a different non-retail application (e.g. source of chemicals or jet fuel) of biomass derived “gasoline” should be found.

## 4.2. Production of chiral chemicals from cellulosic biomass pyrolysis: influence of pre-treatment and catalysis.

### 4.2.1. Introduction

Cellulose is the main component of vegetable biomass, so that it could be worth of investigation as source of renewable chiral building blocks. Herbaceous biomass and agricultural residues are largely composed of cellulose, that it is typically quite recalcitrant for hydrolysis and ethanol production. For this reason, thermochemical processing of cellulose rich residue could be investigated as alternative valorisation of starch/hemicelluloses fermentation residues (usually lignin and cellulose). By coupling pyrolysis with hydrolysis (Figure 4.2.1), it would be possible to obtain a combined stream of chiral chemicals and energy.

**Figure 4.2.1:** general scheme of integrate sugars and anhydrosugars production from cellulosic biomass.



Regarding the production of fine chemicals, the pyrolysis of raw biomass, mainly due to ash catalysis,<sup>274</sup> produces an high number of compounds at low concentration, and for this reason, the raw bio-oil obtained is not suitable as a source of chemicals.

---

<sup>274</sup> P.R. Patwardhan, J.A. Satrio, R.C. Brown, B.H. Shanks. Influence of inorganic salts on the primary pyrolysis products of cellulose. *Bioresource Technology* 101 (2010) 4646-4655.

On the opposite, thermal degradation of pure cellulose (or de-ashed cellulosic biomass) gives rise to interesting chiral multifunctional C<sub>6</sub> monomers, such as levoglucosan (LGA), levoglucosenone (LGO), and the hydroxylactone LAC.<sup>275</sup>

Pyrolysis of cellulose can yield over 60% LGA, when performed under optimized conditions,<sup>276,277</sup> however, costs associated to its isolation from bio-oil is a factor limiting its industrial development as chemical intermediate. Less polar more dehydrated LGO and LAC might be simpler to isolate by distillation and solvent fractionation due to higher volatility and solubility in standard organic solvents. However, they are produced at lower yields and a catalyst is needed in combination with pyrolysis. Different catalysts, including phosphoric acid and its salts were employed to enhance LGO production from pyrolysis of cellulose.<sup>278,279,280</sup> It was reported that up to 42% yields of LGO can be achieved by pyrolysing cellulose in sulfolane in presence of an acid catalyst.<sup>281</sup> Recent works demonstrated that the pyrolytic production of LGO and LAC can be improved by using metal oxide nanoparticles, like nanopowder aluminium titanate.<sup>282,275</sup> The latter catalyst enabled the isolation of LAC from the bio-oil of cellulose and its application as a monomer for the synthesis of a novel class of polyesters.<sup>283</sup>

Zeolites have been widely studied as heterogeneous catalysts in biomass conversion,<sup>284,285,286,287</sup> but these materials are not fitted for the production of anhydrosugars due to their small pore size and

---

<sup>275</sup> D.Fabbri, C.Torri, I.Mancini, Pyrolysis of cellulose catalysed by nanopowder metal oxides: production and characterisation of a chiral hydroxylactone and its role as building block *Green Chem.* 9 (2007) 1374-1379

<sup>276</sup> Z. Luo, S. Wang, Y. Liao, K. Cen, Mechanism Study of Cellulose Rapid Pyrolysis. *Ind. Eng. Chem. Res.* 43 (2004) 5605-5610.

<sup>277</sup> G.-J.Kwon, D.-Y.Kim, S.Kimura, S.Kuga. Rapid-cooling, continuous-feed pyrolyzer for biomass processing Preparation of levoglucosan from cellulose and starch *J. Anal. Appl. Pyrolysis* 80 (2007) 1-5.

<sup>278</sup> Y.Halpern, R.Riffer, A.Broido. Levoglucosenone (1, 6-anhydro-3, 4-dideoxy-D3-b-d-pyranosen-2-one). Major product of the acid-catalyzed pyrolysis of cellulose and related carbohydrates. *J Org Chem.* 38 (1973) 204-208.

<sup>279</sup> F.Shafizadeh, R.H.Furneaux, T.T.Stevenson. Reactions of levoglucosenone. *Carbohydr. Res.* 71 (1979) 169-191.

<sup>280</sup> G. Dobelev, T. Dizhbite, G. Rossinskaja, G. Telysheva, D.Meier, S. Radtke, O. Faix. Pre-treatment of biomass with phosphoric acid prior to fast pyrolysis: A promising method for obtaining 1, 6-anhydrosaccharides in high yields *J. Anal. Appl. Pyrol.* 68/69 (2003) 197-211

<sup>281</sup> H. Kawamoto, S. Saito, W. Hatanaka, S. Saka, H. Kawamoto, S. Saito, W. Hatanaka, S. Saka. Catalytic pyrolysis of cellulose in sulfolane with some acidic catalysts. *J Wood Sci* 53 (2007) 127-133.

<sup>282</sup> D.Fabbri, C.Torri, V.Baravelli, Effect of zeolites and nanopowder metal oxides on the distribution of chiral anhydrosugars evolved from pyrolysis of cellulose: An analytical study *J. Anal. Appl. Pyrol.*, 80 (2007) 24-29

<sup>283</sup> P.Dobrzynski, D.Fabbri, C.Torri, J.Kasperczyk, B.Kaczmarczyk, M.Pastusiak, A novel hydroxy functionalized polyester obtained by ring opening copolymerization of L-lactide with a pyrolysis product of cellulose *J.Polymer Sci. A Polymer Chem*, 47 (2009) 247-257.

<sup>284</sup> A.V. Bridgwater. Production of high grade fuels and chemicals from catalytic pyrolysis of biomass. *Catal. Today* 29 (1996) 285-295.

<sup>285</sup> P.T.Williams, P.A.Horner. The influence of catalyst type on the composition of upgraded biomass pyrolysis oils. *J.Anal.Appl.Pyrolysis* 31 (1995) 39-61

<sup>286</sup> F.Ates, A.Putun, E.Putun, Pyrolysis of two different biomass samples in a fixed-bed reactor combined with two different catalysts *Fuel* 85 (2006) 1851-1859.

<sup>287</sup> A. Pattiya, J. O. Titiloye, A.V. Bridgwater. Fast pyrolysis of cassava rhizome in the presence of catalysts. *J. Anal. Appl. Pyrolysis* 81 (2008) 72-79.

strong acidity that cause severe dehydration and coking of the cellulosic fraction.<sup>275,288</sup> In searching for less dehydrating but still active molecular sieves, it is worth considering the class of mesoporous materials, especially the MCM-41 type, which are characterised by relatively larger pore size and milder acidity and usefully applied in the field of catalysis.<sup>289</sup> The activity of these materials has been investigated in catalytic pyrolysis of different biomass types; since the pure silicate MCM-41 (herein referred to as Si-MCM-41) lacks acid sites, the attention was directed towards MCM-41 containing additional metals, in particular Al-MCM-41.<sup>290,291,292,293</sup> The presence of Al-MCM-41 during pyrolysis of biomass influenced the production and chemical composition of the resulting bio-oil, which was enriched in simple phenols derived from lignin.<sup>291,292</sup> The incorporation of transition metals (Fe, Cu, Zn) into the Al-MCM-41 structure was found to change considerably the activity of the catalyst with respect to the parent material.<sup>290,292</sup>

The influence of MCM-41 materials on the pyrolytic behaviour of cellulose, and in particular on the yields of di and tri-anhydrosugars has been less investigated, therefore this topic became the objective of the present study. Analytical pyrolysis is known to provide a valid contribution to the study of catalyst activity in biomass pyrolysis,<sup>280,287,288,292</sup> and herein was applied in the off-line configuration to gather quantitative information on the yields of pyrolysis products.<sup>282</sup> The interest was focused on the production of LAC given its potentiality as a chemical intermediate for fine chemicals and biodegradable polymers.<sup>275,283</sup> To this purpose, the best performing catalyst emerging from analytical data was utilised in preparative pyrolysis experiments with a fixed bed reactor to investigate the yields of LAC in recycling tests.

## 4.2.2. Experimental

### 4.2.2.1 Materials

Microgranular cellulose,  $ZrCl_4$ ,  $SnCl_4$  pentahydrate, tetraethyl orthosilicate (TEOS), hexadecyltrimethylammonium chloride (CTAB), nanopowder aluminium titanate were purchased

---

<sup>288</sup> T.R. Carlson, T.P. Vispute, G.W. Huber. Green Gasoline by Catalytic Fast Pyrolysis of Solid Biomass Derived Compounds. *ChemSusChem* 1 (2008) 397-400

<sup>289</sup> A.Corma, From Microporous to Mesoporous Molecular Sieve Materials and Their Use in Catalysis. *Chem. Rev.* 97 (1997) 2373-2420.

<sup>290</sup> E.Antonakou, A.Lappas, M.H.Nilsen, A.Bouzga, M.Stöcker. Evaluation of various types of Al-MCM-41 materials as catalysts in biomass pyrolysis for the production of bio-fuels and chemicals. *Fuel* 85 (2006) 2202-2212

<sup>291</sup> E.F.Iliopoulou, E.V.Antonakou, S.A.Karakoulia, I.A.Vasalos, A.A.Lappas, K.S. Triantafyllidis, Catalytic conversion of biomass pyrolysis products by mesoporous materials: Effect of steam stability and acidity of Al-MCM-41 catalysts. *Chem.Eng.J.* 134 (2007) 51.

<sup>292</sup> J. Adam, M. Blazsó, E. Mészáros, M. Stöcker, M. H. Nilsen, Aud Bouzga, Johan E. Hustad, Morten Grønli, G.Øye, Pyrolysis of biomass in the presence of Al-MCM-41 type catalysts. *Fuel* 84 (2005) 1494-1502.

<sup>293</sup> J.Adam, E.Antonakou, A.Lappas, M. Stöcker, M.H.Nilsen, A.Bouzga, J.E.Hustad, G.Øye. Investigation of the effect of metal sites in Me-Al-MCM-41 (Me = Fe, Cu or Zn) on the catalytic behavior during the pyrolysis of wooden based biomass. *Micropor.Macropor.Mater.* 105 (2007) 189-203.

from Sigma-Aldrich, 30% NH<sub>3</sub> solution from Carlo Erba reagenti, TiOSO<sub>4</sub> x nH<sub>2</sub>O (minimum Ti assay 29% as TiO<sub>2</sub>), AlCl<sub>3</sub> hexahydrate from Riedel-de Haën and MgCl<sub>2</sub> hexahydrate from Merck. Levoglucosan (LGA), 2-furaldehyde (FA), 2-hydroxy-1-methyl-cyclopenten-3-one (CYC), methyl-L-β-arabinopyranoside, BSTFA+1% TMCS, pyridine and acetonitrile were purchased from Sigma-Aldrich. LGO and LAC were produced from catalytic bench scale pyrolysis of cellulose admixed with 30% nanopowder aluminium titanate at 350°C and 500 °C, respectively, and purified by column chromatography.<sup>275</sup>

#### 4.2.2.2 Pre-treatment of biomass for anhydrosugars production

Switchgrass was pre-treated by 4 h refluxing in 10:1 w/w (1 g of biomass was admixed with 5 ml of solution) the reaction media (shown in Table 4.2.1) or by autoclaving at 150°C for 30 min.

After the reaction, the resulting mixture was filtrated on glass filter, re-suspended in 1:10 distilled water (for acid removal) and then filtrated again. Finally, the wet powder/flasks were collected from the filter and residual water was eliminated by evaporation under vacuum at 90°C. Water “uptake” calculation was performed by difference in weight before and after the last step of evaporation. Soluble sugar yields were evaluated by analysis of wet torrefaction water output by Brix optical densimeter.

**Table 4.2.1:** experimental conditions used for pre-treatment of switchgrass

<i>Name</i>	<i>Amount of reaction media</i>	<i>catalyst</i>	<i>Time</i>	<i>Temp</i>	<i>Solvent</i>
<i>De-ashing</i>	<i>1:10 biomass:liquid</i>	<i>1% HNO<sub>3</sub></i>	<i>4 h</i>	<i>100°C</i>	<i>Water</i>
<i>Organosolv</i>	<i>1:10 biomass:liquid</i>	<i>1% H<sub>2</sub>SO<sub>4</sub></i>	<i>4 h</i>	<i>80°C</i>	<i>Water:ethanol 4:6</i>
<i>Hydrolysis</i>	<i>1:10 biomass:liquid</i>	<i>1% H<sub>2</sub>SO<sub>4</sub></i>	<i>4 h</i>	<i>100°C</i>	<i>Water</i>
<i>Wet torrefaction</i>	<i>1:10 biomass:liquid</i>	<i>-</i>	<i>0.5 h</i>	<i>150°C</i>	<i>Water</i>

#### 4.2.2.3 Synthesis of Me-MCM-41 catalysts

The synthesis and characterization of Me-MCM-41 mesoporous materials was described in chapter 3.5.<sup>294</sup> Data of Table 4.2.1 show a general increase of BET surface area as a consequence of metal substitution. Only Sn-MCM-41 exhibited a lower value with respect to undoped Si-MCM-41 that, consistently to XRD results, could be attributed to small amounts of SnO<sub>2</sub> highly dispersed onto the pore walls. The highest BET areas were found for Mg-MCM-41 and Al-MCM-41 (1300 and 977 m<sup>2</sup>

<sup>294</sup> D.Fabbri, F.Fabbri, G.Falini, V.Baravelli, A.Magnani, C.Torri, H.Maskrot, Y.Leconte. The activity of nanopowder and mesoporous titanium catalysts for the analysis of fatty acids in triglycerides by pyrolysis methylation with dimethyl carbonate. J.Anal.Appl.Pyrolysis 82 (2008) 248-254.

g<sup>-1</sup>, respectively), while in the case of Zr-MCM-41 the metal effect may have induced a partial collapsing of the mesopores, leading to lower surface areas (697 m<sup>2</sup> g<sup>-1</sup>).

**Table 4.2.2:** Characteristics of calcined Me-MCM-41 catalysts.

	<i>BET surface area</i>	<i>Metal content</i>
	<i>m<sup>2</sup> g<sup>-1</sup></i>	<i>% wt</i>
<b>Al-MCM-41</b>	977	8.1
<b>Sn-MCM-41</b>	450	8.7
<b>Zr-MCM-41</b>	697	7.7
<b>Ti-MCM-41</b>	820	13
<b>Mg-MCM-41</b>	1300	2.3
<b>Si-MCM-41</b>	663	-

#### 4.2.2.4 Off-line py/GC-MS

Off-line pyrolysis procedure is detailed described in detail in chapter 3.1. Samples (typically 5 mg cellulose mixed with 1.5 mg catalyst) were pyrolysed at 500°C (set temperature) for 100 s at the maximum heating rate (20 °C ms<sup>-1</sup>) under nitrogen flux. Molar yields were calculated from the quantity of cellulose subjected to pyrolysis and the quantity of evolved product, this latter calculated from the peak areas in the total ion chromatogram.<sup>282</sup> Quantitation was performed by internal calibration, with 2-bromonaphthalene as internal standard, using the response factor of FA (also for FO and MF), CYC (for PYR), LGO and LAC (also for DGP). The quantitation of LGA was performed on the persilylated derivative using the persilylated 5-methyl-L-arabinopyranoside as internal standard. All the experiments were performed at least in duplicate. Percentage RSD of yields ranged in the 3.3%-48% interval for FO, 0.2-4% (FA), 0.1-11% (MF), 8-30% (PYR), 2-37% (LGO), 2-9% (LAC), 30-50% (LGA).

#### 4.2.2.5 Preparative pyrolysis

The configuration of the fixed bed reactor set up for preparative pyrolysis was similar to that described elsewhere,<sup>275</sup> consisting of a tubular quartz reactor (length: 650 mm, internal diameter: 37 mm) placed coaxially within a furnace refractory (Carbolite, Italy), equipped with a thermocouple, connected to the nitrogen inlet by means of pressure valve and a flow meter and connected downstream to an ice trap and a solvent trap (acetonitrile) for trapping condensable compounds. The sample (3.0 g cellulose alone or mixed with 1.0 g of catalyst) was uniformly placed onto a sliding quartz boat, the nitrogen flow was set at 1500 cm<sup>3</sup> min<sup>-1</sup> and the oven was turned on. As

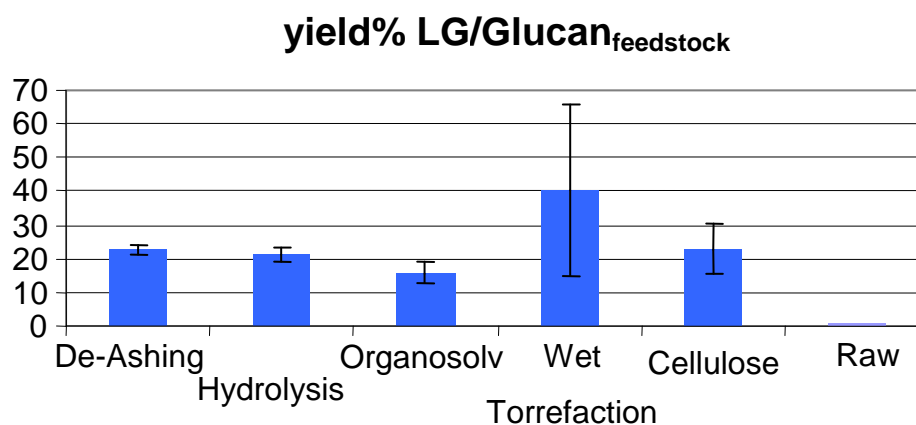
soon as the temperature inside the reactor reached the established value (500°C), the sample was positioned into the central part of the oven for 5 minutes, then retrieved upstream in the colder part of the reactor. The bio-oil recovered in the cold trap was dissolved into acetonitrile and an aliquot subjected to GC-MS analysis; the solution was dried at 80°C under reduced pressure and weighed (tar). Solid residue (catalyst + char) was heated in air in a muffle furnace for 6 h at 550°C to regenerate the catalyst (weight loss provided char yield). LAC was isolated from the tar with 90% GC purity by column chromatography over silica gel and elution with pentane/dichloromethane.<sup>275</sup>

### 4.2.3. Results and discussion

#### 4.2.3.1 Pre-treatment of biomass for anhydrosugars production

Switchgrass was selected as hemicellulose/cellulose rich material for tests. Anhydrosugar yield from raw biomass resulted too low for any application. For this reason, in order to enhance anhydrosugar yield, 4 pre-treatments were tested: 1:10 (w/w) acid reflux washes (1% nitric acid or 1% sulphuric acid for de-ashing and hemicellulose hydrolysis respectively) organosolv pre-treatment ( acidified alcohol/water extraction) and “wet torrefaction” (WT) at 150°C in 1:10 distilled water (see Table 4.2.1).

**Figure 4.2.3:** yield of levoglucosan from pyrolysis of switchgrass pretreated in different way , pure cellulose and raw biomass.



De-ashing partially removed soluble ashes (mainly K and Na, checked by analysis of the liquid) and leaved hemicelluloses largely intact. Both hydrolysis and organosolv processes dissolve hemicellulose almost completely, and organosolv removed lignin almost totally. Wet 150°C torrefaction acted similarly to hydrolysis, but without the use of any acid (acid are formed in the thermal reaction).

The pre-treated materials, composed of cellulose and, in some case, lignin were pyrolyzed in order to see the effect of pre-treatment of anhydrosugars (mainly levoglucosan) yield. Both de-ashing and hydrolysis were able to raise LG yield to value similar to that observed for pure cellulose (Figure 4.2.2) ( $23\pm 7\%$ ), where organosolv process is less effective ( $15\pm 4\%$  yield). Most interesting effects were observed with WT that, without any mineral acid use, produced a material which yielded an higher anhydrosugars yield ( a variable 65-15% yield) than that observed for pure cellulose (15-30% yield).

**Table 4.2.3:** water uptake and soluble sugars yield by wet treatment of different cellulosic substrates. WT: wet torrefaction.

<i>Biomass type</i>	<i>Soluble sugar yield</i> <i>% <math>w_{SS}/w_{biomass}</math></i>	<i>Final water content</i> <i>% <math>w/w_{filtrated\ biomass}</math></i>
Switchgrass pre-hydrolysis	26	75
Switchgrass WT	21	28
Pine WT	20	22
Poplar WT	23	25
Kenaf WT	20	61
Sunflowers stalks WT	30	53

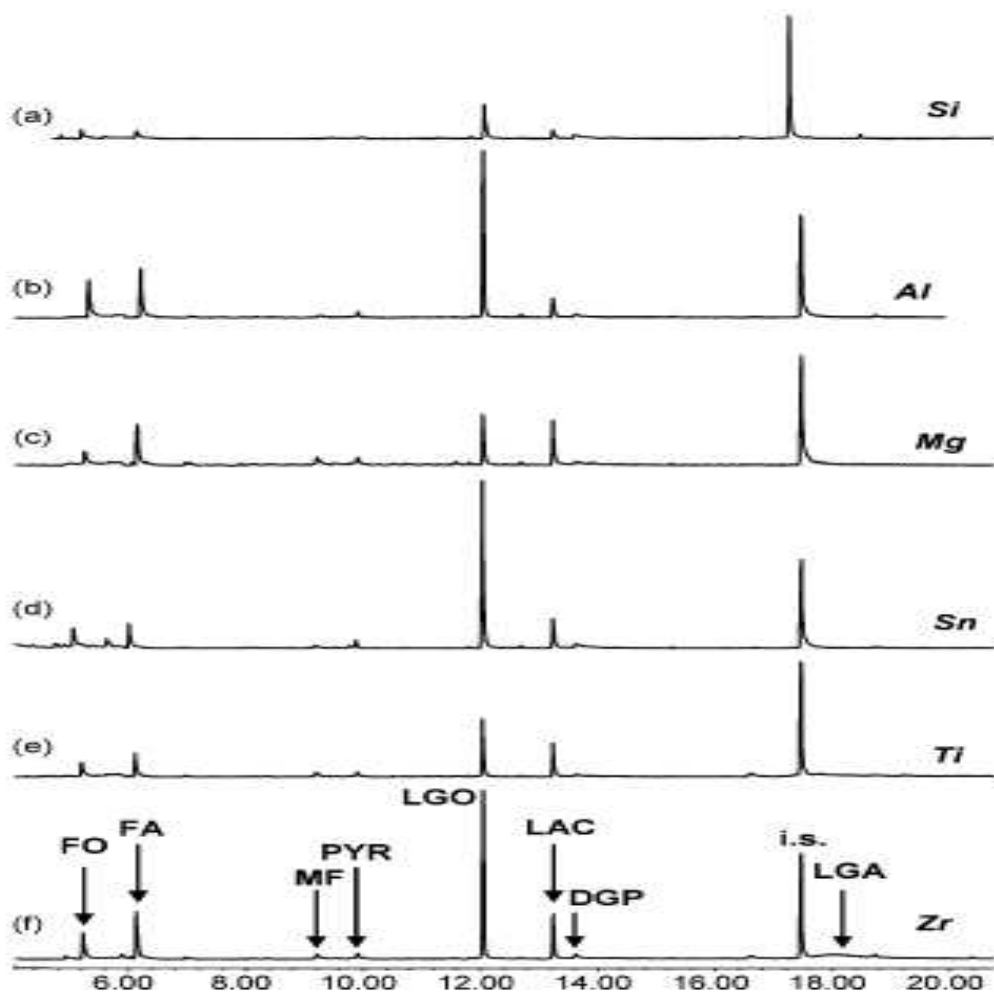
Considering the results obtained, WT could be an easy way for the obtaining of anhydrosugars from a large range of raw biomass, without the use of any strong acids, and then without any neutralization of the process output stream.

Moreover torrefaction resulted in brittle hydrophobic particles that were readily separated from the water. On the contrary, all other examined processes (de-ashing, organosolv and hydrolysis ) involved a large hydric uptake. In order to study the increase in hydrophobicity induced by the torrefaction process, different cellulosic materials were subjected to the same wet torrefaction treatment. Table 4.2.3 shows the water uptake (which is a concern for subsequential pyrolysis) caused by the wet pre-treatment method. It interesting to notice that, especially for lignin rich biomass (poplar or pine), the water uptake can be considered acceptable.

#### 4.2.3.2 Catalytic pyrolysis of cellulose: screening by analytical pyrolysis

Typical examples of the GC-MS traces obtained from off-line pyrolysis of cellulose mixed with 30% mesoporous materials undoped (Si-MCM-41) and doped with different metals (Me-MCM-41) are presented in Figure 4.2.3.

**Figure 4.2.3.** GC-MS traces obtained from off-line pyrolysis of cellulose with 30% a) Si-MCM-41, b) Al-MCM-41, c) Mg-MCM-41, d) Sn-MCM-41, e) Ti-MCM-41, f) Zr-MCM-41. Peak identification: (2H)-furan-3-one (FO), 2-furaldehyde (FA), 5-methyl-2-furaldehyde (MF), 4-hydroxy-5,6-dihydro-pyran-2-one (PYR), levoglucosenone (LGO), 1-hydroxy-3,6-dioxabicyclo[3.2.1]octan-2-one (LAC), 1,4:3,6-dianhydro- $\alpha$ -D-glucose (DGP) and levoglucosan (LGA). i.s. internal standard 2-bromonaphthalene.



The principal peaks were identified as FO, FA, MFA, PYR, LGO, LAC and DGP and were quantified, while CYC was barely detected. Levoglucosan (LGA) gave a broad peak under these conditions, therefore it was analysed after conversion into its trimethylsilyl derivative. The yields of these compounds are reported in Table 4.2.3. All the examined mesophases acted as to decrease the yields of LGA with respect to neat cellulose, and to increase the pyrolytic production of both LAC and LGO. The effect was similar to that reported for nanopowder oxides containing Ti and Al.

<sup>282,275</sup> A higher formation of LAC accompanied by a lower production of LGA was also found in the thermal analysis of cellulose treated with Zn (II) ions.<sup>295</sup>

**Table 4.2.4:** Mean molar yields of selected compounds released from off-line pyrolysis of cellulose mixed with 30% catalyst.

	<i>FO</i>	<i>FA</i>	<i>MFA</i>	<i>PYR</i>	<i>LGO</i>	<i>LAC</i>	<i>DGP</i>	<i>LGA</i>
<b>Sn-MCM-41</b>	0.23	1.1	0.66	0.42	6.4	5.6	1.7	1.6
<b>Zr-MCM-41</b>	0.29	1.3	0.65	0.41	4.3	5.6	1.1	1.7
<b>Ti-MCM-41</b>	0.20	1.0	0.66	0.56	2.6	4.9	1.8	2.7
<b>Al-MCM-41</b>	0.49	1.5	0.69	0.46	5.1	3.5	1.3	1.1
<b>Mg-MCM-41</b>	0.21	1.1	0.70	0.47	2.4	5.1	2.0	2.3
<b>Si-MCM-41</b>	0.22	0.83	n.d.	n.d.	1.9	2.4	2.9	3.9
<b>no catalyst</b>	0.19	0.60	0.81	0.61	0.80	0.58	2.2	12

Regarding LGA, the observed effect of the Me-MCM-41 catalysts was in agreement with pyrolysis data on vegetable biomass with Al-MCM-41 that showed a depression of LGA production.<sup>292</sup> Instead, the yields of furans (probably with the exception of FA), PYR and DGP were not much affected by the presence of the MCM-41 catalysts, at least considering the low yield and relative precision.

In general, the effect of the investigated catalysts is that to produce a more dehydrated/de-oxygenated pyrolysate, as both LGO and LAC are virtually formed from the dehydration of LGA and contain less oxygen and hydroxyl groups. On this basis, all the metal containing Me-MCM-41 solids were more active catalysts than the siliceous Si-MCM-41. The higher activity of doped mesostructured materials could be attributed to the formation of acidic sites when the metal is incorporated into the siliceous framework of MCM-41. The addition of the metal generally increases the acidic character of the solid with respect to the siliceous mesophase. For instance, Al-MCM-41 have higher acidic sites and catalyse dehydration reactions with a higher production of carbonyl compounds relative to Si-MCM-41 when applied to biomass pyrolysis.<sup>291</sup> The incorporation of Sn (IV)<sup>296</sup> and Zr (IV)<sup>297</sup> deficiently coordinated on the surface adds Lewis acid sites that may explain the highest yields of LAC observed with Sn-MCM-41 and Zr-MCM-41. However, relatively high LAC yields were found with Mg-MCM-41, probably due to the large surface area of this solid (Table 4.2.2). Nevertheless, the different yields of LGO and LAC observed

<sup>295</sup> E. Jakab, E. Mészáros, J. Borsa. Effect of Slight Chemical Modification on the Pyrolysis Behavior of Cellulose Fibers. *J.Anal.Appl.Pyrol.* 87 (2010) 117-123.

<sup>296</sup> I.Nowak, A.Feliczak, I.Nekoksova, J.Čejka. Exploring the catalytic activity of regular and ultralarge-pore Nb,Sn-SBA-15 mesoporous molecular sieves. *Studies in Surface Science and Catalysis* 170(2007) 1432-1437

<sup>297</sup> D. Fuentes-Perujo, J. Santamaria-Gonzales, J. Mérida-Robles, E. Rodriguez-Castellon, A. Jienez-Lopez, P. Maireles-Torres, R. Moreno-Tost, R. Mariscal. Evaluation of the acid properties of porous zirconium-doped and undoped silica materials. *J.Solid State Chem.*179 (2006) 2182-2189.

with the various metals are not easily interpretable because the catalytic activity of the mesophases is affected by a multitude of factors. These include the type of acidic sites (Bronsted or Lewis) and their strength as well as site accessibility to the reactants since the metal can be located onto the surface or buried into the inner part of the pore walls.

Although characterised by lowest specific surface area and the limited low range order (section 4.2.2.3), Sn-MCM-41 was among the most active Me-MCM41 catalysts, giving the highest yields of both LGO and LAC, while the yields of LGA were rather low. Therefore Sn-MCM-41 was selected for further experiments with a bench scale pyrolyser.

### 3.3. Preparative pyrolysis of cellulose. Catalyst recycling

Preparative pyrolysis was conducted with a fixed bed quartz reactor on neat cellulose and cellulose admixed with 30% Sn-MCM-41 under the same conditions used for analytical pyrolysis. Results relative to the production of char and tar (herein referred to as the oil left after the elimination of water and other volatiles by vacuum distillation) along with the yields of selected pyrolysis are presented in Table 4.2.5.

**Table 4.2.5:** Yields of tar, char and individual products from preparative pyrolysis at 500 °C of 3.0 g cellulose without and with Sn-MCM-41 (30%). Mean of two replicates.

	<i>No catalyst</i> % wt	<i>Sn-MCM-41</i> % wt
<b>Char</b>	14 ± 3	15 ± 1
<b>Tar</b>	33 ± 5	47 ± 4
<b>FA</b>	1.3 ± 0.5	1.0 ± 0.3
<b>MF</b>	0.10 ± 0.05	0.5 ± 0.1
<b>PYR</b>	0.10 ± 0.08	0.6 ± 0.4
<b>LGO</b>	n.d.	0.2 ± 0.1
<b>LAC</b>	1.2 ± 0.2	5.9 ± 0.3
<b>DGP</b>	1.6 ± 0.1	2.5 ± 0.6
<b>LGA</b>	14 ± 2	4 ± 1

The formation of the solid residue from the pyrolysis of cellulose in the presence of the catalyst (15 %) was similar to that observed in its absence (14 %), indicating a low coking activity of Sn-MCM-41 with respect of pure cellulose pyrolysis. This is partially in contrast with 20% coke increase in chapter 3.5 regarding Sn-MCM-41 catalysis on raw pine biomass, and can be explained by the different reactivity of cellulose (which form anhydrosugars) than raw biomass, which produce large lignin monomer and large amount of small hydroxyaldehydes.

The yields of the tar from the pyrolysis of pure cellulose was 33%, but increased markedly to 44% when pyrolysis was conducted in the presence of Sn-MCM-41. These results underline the performance of MCM-41 catalysts in improving the production of liquid without excessive coking. The slight reduction in volatile compounds (from 53% to 38%) is in accordance to that observed in chapter 3.5 for Sn-MCM-41 catalysis on raw pine biomass pyrolysis.

The yields of the evolved products from catalysed and uncatalysed pyrolysis were markedly different (Table 4.2.5). LGA, was the major compound analysed by GC-MS in the oil from uncatalysed cellulose, with an overall yield of 14%. The concentration of LGA in the tar obtained after catalytic pyrolysis was lower with a 4% yield, and LAC became a major component with 5.9% yield. The effect of the catalyst on the yields of LAC and LGA reflected the trend observed with analytical pyrolysis, confirming the reliability of this technique for screening the activity of catalysts. However, the similarity of the results between analytical and preparative pyrolysis was not as satisfactory for the more volatile products. In particular, the yields of LGO were much lower in the preparative pyrolysis, even though higher values were found with Sn-MCM-41 in accordance with analytical pyrolysis. These differences between analytical and preparative pyrolysis were probably caused by different heating rate in two systems.

The reusability of the catalyst is an important feature to be assessed considering that a relatively large quantity is employed with dry mixing. In fact, thermal treatments of MCM-41 during pyrolysis and regeneration cycles may cause a reduction in surface area, number of acidic sites and pore size that affect negatively the performance of the catalyst.<sup>291</sup>

**Table 4.2.6:** Recycling tests. isolated yields (mass %) of LAC from catalytic pyrolysis of cellulose with regenerated Sn-MCM-41 and nanopowder aluminium titanate (NP Al Ti).

Pyrolysis run	Sn-MCM-41	Sn-MCM-41	NP Al Ti
	Test 1	Test 2	
	% LAC	% LAC	% LAC
I	5.9	5.7	6.2
II	5.3	n.d.	5.5
III	5.2	5.1	5.3
IV	5.8	5.8	3.6
V	5.3	5.6	3.6
VI	5.2	5.3	4.5

In order to evaluate whether Sn-MCM-41 could be reused after pyrolysis, two recycling tests were performed each consisting of six runs of catalytic pyrolysis with cellulose at 500 °C followed by regeneration of the catalyst at 550 °C under air. A comparison was made with catalytic pyrolysis of cellulose in the presence of nanopowder aluminium titanate under the same conditions. The results are shown in Table 4.2.6.

The quantity of LAC recovered from the bio-oil was not significantly reduced after repeated pyrolysis/regeneration steps of Sn-MCM-41. The initial LAC yields obtained with fresh Sn-MCM-41 (5.7% and 5.9%) remained almost constant after six recycling steps. LAC yields with regenerated nanopowder aluminium titanate were reduced from 6.2% to lower values (3.6-4.5%).

#### **4.2.4 Conclusions**

Cellulose, as well as pre-treated biomass, could be used as a source of anhydrosugars. Besides levoglucosan, uncatalyzed pyrolysis product of cellulose, obtainable with 10-20% yield, other functionalized anhydrosugars can be obtained by using metal containing mesoporous catalysts.

Analytical pyrolysis confirmed its reliability as a rapid tool for screening the performance of active solids to be employed in catalytic pyrolysis. The experiments performed with cellulose indicated that mesoporous materials with relatively high surface areas favour acid catalysed reactions promoting the formation of LGO and LAC, valuable multifunctional C<sub>6</sub> monomers. In particular, LAC yields around 5% comparable to those observed with nanopowder metal oxides were obtained using MCM-41 catalysts doped with Mg, Ti, Sn or Zr.

The results relative to LAC and LGA obtained with analytical pyrolysis were confirmed in the case of Sn-MCM-41 by preparative pyrolysis experiments. In fact, a pyrolytic oil depleted in LGA and enriched in LAC was formed with this catalyst. Moreover, these experiments showed that Sn-MCM-41 can be reused up to six times without significant loss of activity as measured by the quantity of LAC recovered from the oil. The performance in terms of LAC production was similar or even better to that with nanopowder aluminium titanate, but without the problems related to handling dry nanoparticles.

## 4.3. Carbon-negative bio-hydrogen and bio-fuels production through pyrolysis of *Chlamydomonas reinhardtii* by-product.

### 4.3.1 Introduction

The exploitation of algal biomass by means of photosynthesis for energy-related purposes is a promising field of research. The great interest in algal biomass arises from the greater light use efficiency (about 5%, vs. 1.5% of terrestrial biomass), the possibility of using marginal areas (e.g. desert and coastal regions), the possibility of combining algal cultivation with other processes (e.g. wastewater treatment, CO<sub>2</sub> sequestration), the availability of a larger number of species, and an easier genetic manipulation for modifying algal chemical composition or metabolism.<sup>298</sup>

*Chlamydomonas reinhardtii* is a widely investigated microalga for hydrogen photoproduction.<sup>299,300,301</sup> Recent developments, mainly in the field of genetic manipulation, have made it possible to increase both hydrogen output and its production rate, but further advances are expected in the next future.<sup>301,302,303</sup>

In addition to hydrogen, the process also involves the production of a variable amount of algal biomass by-products.<sup>304</sup> At the current state of the technology, the valorization of side-products could be a key point in the maximization of the energetic yield of the process and in reducing the price of photo-biogenic hydrogen.<sup>305</sup> To obtain further energy output, biomass can be processed by means of the extraction and transesterification of algal lipids to produce biodiesel, leaving a lipid-free extraction residue which can be used as animal feed or be anaerobically digested into biogas.<sup>306</sup> Moreover, pyrolysis of the extraction residue could possibly represent another (alternative) way to further recover energy and material.<sup>307</sup> Pyrolysis of microalgae as well as pyrolysis of

---

<sup>298</sup>J.N. Rosenberg, G.A. Oyler, L. Wilkinson, M.J. Betenbaugh. A green light for engineered algae: redirecting metabolism to fuel a biotechnology revolution. *Curr. Opin. Biotech.* 19 (2008) 430-436.

<sup>299</sup>S. Kosourov, A. Tsygankov, M. Seibert, M.L. Ghirardi. Sustained hydrogen photoproduction by *Chlamydomonas reinhardtii*: effects of culture parameters. *Biotechnol. Bioeng.* 78 (2002) 731-740.

<sup>300</sup>S. Kosourov, A. Tsygankov, M. Seibert, M.L. Ghirardi. Hydrogen photoproduction under continuous illumination by sulfur deprived, synchronous *Chlamydomonas reinhardtii* cultures. *Int. J. Hydrogen Energ.* 27 (2002) 1239-1244.

<sup>301</sup>G. Torzillo, A. Scoma, C. Faraloni, A. Ena, U. Johannngmeier. Increased hydrogen photoproduction by means of a sulfur-deprived *Chlamydomonas reinhardtii* D1 protein mutant. *Int. J. Hydrogen Energ.* 34 (2009) 4529-4536.

<sup>302</sup>C. Faraloni, G. Torzillo. Phenotypic characterization and hydrogen production in *Chlamydomonas reinhardtii* Q<sub>B</sub> binding D1 protein mutants under sulfur starvation: changes in chlorophyll fluorescence and pigment composition, *J. Phycol.* 46 (2010) 788-799.

<sup>303</sup>J.B. McKinlay, C.S. Harwood. Photobiological production of hydrogen gas as a biofuel. *Curr. Opin. Biotech.* 21 (2010) 244-251.

<sup>304</sup>O. Kruse, B. Hankamer. Microalgal hydrogen production. *Curr. Opin. Biotech.* 21 (2010) 238-243.

<sup>305</sup>W.A. Amos. Updated Cost Analysis of Photobiological Hydrogen Production from *Chlamydomonas reinhardtii* Green Algae. Milestone Completion Report, National Renewable Energy Laboratory, Colorado, USA (2004).

<sup>306</sup>B. Sialve, N. Bernet, O. Bernard. Anaerobic digestion of microalgae as necessary step to make microalgal biodiesel sustainable. *Biotechnology Adv.* 27 (2009) 409-416.

<sup>307</sup>D. Mohan, C.U. Pittman Jr., P.H. Steele, Pyrolysis of Wood/Biomass for Bio-oil: A Critical Review. *Energ. Fuel.* 20 (2006) 848-889.

microalgal extraction residue, can produce a bio-oil with a quality that is between petroleum tar and bio-oil from lignocellulosic biomass.<sup>308,309</sup> Moreover a large part of ashes and nitrogen can be retained into bio-char, which could be used to improve the quality and productivity of soils, thus contributing to the abatement of greenhouse gases and making it possible to convert carbon-neutral energy into carbon-negative bio-energy.<sup>310,304</sup>

Therefore this chapter focuses on a study of the yields and composition of biodiesel, bio-oil and bio-char, which are obtainable from *C. reinhardtii* biomass collected after the production of bio-hydrogen, by means of solvent extraction and low-temperature pyrolysis of the extraction residue. Different analytical techniques were applied for characterizing bio-oil and for understanding the bio-oil composition and the potential up-grading features (analytical Py-GC-MS) of the liquid fuel obtained.

## 4.3.2 Materials and methods

### 4.3.2.1 Chemicals

All solvents and chemicals used in this study were obtained from Sigma-Aldrich, and were used without purification. The Amberlyst® acidic resin used for the methanolysis reaction was washed twice with methanol (ratio 6:1 by weight) before use.

### 4.3.2.2 Microorganism and culture conditions

*Chlamydomonas reinhardtii* growth has been previously described in detail by Torzillo *et al.*<sup>301</sup> The strain L159I-N230Y of *C. reinhardtii* is a D1 protein mutant that carries a double amino acid substitution, with leucine residue L159 replaced by isoleucine, and the asparagines N230 replaced by tyrosine.<sup>311</sup> The cells were grown in a Tris-Acetate-Phosphate (TAP) medium in Pyrex Roux bottles (Bibby Scientific, Milan, Italy) at 28°C, and were exposed to a light intensity of 70  $\mu\text{mol photons m}^{-2} \text{s}^{-1}$ , supplied on both sides of the photobioreactor (400 ml glass columns with 5-cm i.d). Cultures were bubbled with a mixture of air-CO<sub>2</sub> (v/v, 97/3). Cells were grown up to 1.35 g L<sup>-1</sup> of dry weight, and then harvested by means of centrifugation (Beckman Coulter, model Avanti J-26 XP Centrifuge, USA). In order to remove sulfur, the cells were washed five times with a sulfur-free medium (TAP-S).

---

<sup>308</sup>X. Miao, O. Wu, C. Yang. Fast pyrolysis of microalgae to produce renewable fuels. *J. Anal. Appl. Pyrol.* 71 (2004) 855-863.

<sup>309</sup>P. Pan, C. Hu, W. Yang, Y. Li, L. Dong, L. Zhu, D. Tong, R. Qing, Y. Fan. The direct pyrolysis and catalytic pyrolysis of *Nannochloropsis* sp. Residue for renewable bio-oils. *Bioresource Technol.* 101 (2010) 4593-4599.

<sup>310</sup>J. Lehmann, S. Joseph. *Bio-Char for Environmental management, science and technology.* Earthscan, UK (2009).

<sup>311</sup>U. Johannngmeier, S.Heiss. Construction of a *Chlamydomonas reinhardtii* mutant with an intronless *psbA* gene, *Plant Mol. Biol.* 22 (1993) 91-99.

The sulfur-depleted cultures were placed in a flat glass photobioreactor (5-cm light path, 1.1 L culture volume). The algal cells were exposed to a light intensity of  $70 \mu\text{mol photons m}^{-2} \text{ s}^{-1}$ , on both sides of the reactor (Daylight, Dulux L, Osram). Experiments were carried out at  $28^\circ\text{C}$ . Mixing of the cultures was provided by a magnetic bar placed at the bottom of the photobioreactor. The hydrogen produced by the cells was measured according to literature.<sup>312</sup> After the collection of hydrogen, the spent biomass was harvested by means of centrifugation and was then lyophilized. The light conversion efficiency of the cultures was calculated as previously reported by Giannelli et al. (2009).<sup>313</sup>

#### 4.3.2.3 Lipid extraction and analysis

About 4 g of dried algal biomass was treated with chloroform/methanol 2/1 (ratio 1:10 biomass to solvent,  $\text{g mL}^{-1}$ ) for 4 h under reflux conditions and stirring. The algal biomass was then filtered out and the solvent was evaporated under vacuum to provide the algal oil. An aliquot of this oil (100 mg) was fractionated using column chromatography with silica gel (60 mesh), and was then eluted with 250 mL of chloroform, followed by 250 mL of chloroform/acetone 4/1 and by 250 mL of chloroform/methanol 1/1 in order to separate non polar, polar and highly polar lipids, respectively. The lipids isolated in each eluate were weighed after the evaporation of the solvent.

The amount of free fatty acids (FFA) in each fraction was determined by means of silylation and GC-MS analysis. An aliquot of algal oil (about 5 mg) was spiked with an internal standard solution of tridecanoic acid (0.1 mg, 0.1 mL at  $1 \text{ mg mL}^{-1}$  in ethyl acetate), 200  $\mu\text{L}$  of bis-trimethylsilyltrifluoroacetamide containing 1% of trimethylchlorosilane and 10  $\mu\text{L}$  of pyridine. The total amount of fatty acids (TFA) in each fraction (the sum of the FFA and the acylglycerols) was determined by following the procedure reported by Fabbri et al. (2005): about 5 mg of oil were refluxed for 10 min with 4 mL methanolic NaOH 0.5 M. Then, 5 mL of methanolic  $\text{BF}_3$  were added, and the mixture refluxed for 2 min followed by the addition of 10 mL of *n*-hexane. After cooling, a saturated NaCl aqueous solution was added under stirring; the hexane layer containing fatty acid methyl esters (FAMES) was then separated, and was dried over anhydrous sodium sulfate. Tridecanoic acid was utilized as an internal standard for quantification of FAMES. The relative response factors used for the quantitation were obtained by injecting solutions of known amounts of

---

<sup>312</sup>S. Kosourov, M. Seibert, M.L. Ghirardi. Effects of extracellular pH on the metabolic pathways in sulfur deprived,  $\text{H}_2$  producing *Chlamydomonas reinhardtii* cultures. Plant Cell. Physiol. 44 (2003) 146-55.

<sup>313</sup>L.Giannelli, A. Scoma, G. Torzillo. Interplay between light intensity, chlorophyll concentration and culture mixing on the hydrogen production in sulfur-deprived *Chlamydomonas reinhardtii* cultures grown in laboratory photobioreactors. Biotechnol. Bioeng. 104 (2009) 76-90.

tridecanoic acid methyl ester and commercial FAMES mix. The quantitation of FAMES was performed on total ion current (TIC) peak areas.

All extraction and analysis procedures were performed in triplicate. Triacylglycerols were calculated on the basis of the difference between TFA and FFA.

#### 4.3.2.4 Pyrolysis of algal residue after lipid extraction

The algal residue remaining after solvent extraction was subjected to a bench scale pyrolysis, using an apparatus described in detail in a previous work.<sup>314</sup> It consisted of a sliding sample carrier in a heated quartz tube connected to ice traps and a settling chamber. The quartz tube was heated by a cylindrical co-axial furnace and purged by 1.5 L min<sup>-1</sup> nitrogen flow. Samples were moved in the heated zone of the quartz tube and were heated at the pyrolysis temperature.

Duplicate bench scale pyrolyses were performed on 3 g of sample, at 350°C (temperature of the reactor walls) for 20 min. This process produced a highly viscous liquid that was firstly dissolved into 10 mL of acetone and then recovered by evaporation of the solvent under vacuum at 40°C.

#### 4.3.2.5 Characterization of pyrolysis oil

The water content of the pyrolysis oil was determined by means of Karl-Fischer titration. The analytical characterization of the organic fraction was based on the solvent fractionation procedure developed by Oasmaa et al. (2008).<sup>315</sup> The water-insoluble fraction (which is called “pyrolytic lignin” in the case of bio-oil from terrestrial plants) was determined by means of precipitation with ten-fold excess water added to an aliquot of neat bio-oil. The precipitate was then centrifuged and filtered, dried overnight at 40°C under nitrogen flow, and finally weighed.

The aqueous layer contained sugars (anhydrosugars, polysaccharides and oligosaccharides), as well as other water-soluble components.

The procedure for determining oligo- and polysaccharides has been described by Busetto et al. (2010).<sup>316</sup> Briefly, polysaccharides and oligosaccharides were methanolized by stirring 2 mL of 3% methanolic bio-oil solution over Amberlyst® (0.5 g) at 64°C for 24 h. Then, 100 µL of the methanol solution were evaporated under nitrogen at room temperature, and the residue was dissolved into acetonitrile prior to analysis. Anhydrosugars and methyl-O-glycosides were

---

<sup>314</sup> D. Fabbri, C. Torri, I. Mancini. Pyrolysis of cellulose catalysed by nanopowder metal oxides: production and characterisation of a chiral hydroxylactone and its role as building block. *Green Chem.* 9 (2007)1374-1379.

<sup>315</sup> A. Oasmaa, E. Kuoppala. Solvent Fractionation Method with Brix for Rapid Characterization of Wood Fast Pyrolysis Liquids. *Energ. Fuel* 22 (2008) 4245-4248.

<sup>316</sup> L. Busetto, D. Fabbri, R. Mazzoni, M. Salmi, C. Torri, V. Zanotti. Application of the Shvo catalyst in homogeneous hydrogenation of bio-oil obtained from pyrolysis of white poplar: New mild upgrading conditions. *Fuel* 90 (2010) 1197-1207.

determined by GC-MS after trimethylsilylation of the bio-oil dissolved in acetonitrile, using methyl- $\beta$ -l-arabinopyranoside as the internal standard. The final amount of oligosaccharides was determined by subtracting the content of free anhydrosugars from the total value of methyl-O-glycosides obtained after hydrolysis.

#### 4.3.2.6 Elemental analysis, higher heating values and SEM

The elemental composition of dry spent biomass residue (sampled at the end of the hydrogen production), extraction residue, bio-oil and bio-char was determined using an elemental analyzer (Carlo Erba Instruments, NA 1500, Series 2), by means of the flash combustion technique. Ash content was obtained after 6 hours calcinations at 550°C. The elemental composition of pyrolysis gas was back-calculated from the mass balance of each element, according to the following formula:

$$\% X_{\text{gas}} = (\% X_{\text{extraction-residue}} - (\% X_{\text{bio-oil}} \cdot \text{Yield}_{\text{bio-oil}} + \% X_{\text{bio-char}} \cdot \text{Yield}_{\text{bio-char}})) \cdot \text{Yield}_{\text{gas}}^{-1}$$

where  $\% X_{\text{gas}}$ ,  $\% X_{\text{extraction-residue}}$ ,  $\% X_{\text{bio-oil}}$ , and  $\% X_{\text{bio-char}}$  are the mass percentages of the element in gas, extraction residue, bio-oil and bio-char, respectively;  $\text{Yield}_{\text{bio-oil}}$ ,  $\text{Yield}_{\text{bio-char}}$  and  $\text{Yield}_{\text{gas}}$ , are the mass yields (w/w<sub>sample</sub>) of bio-oil, bio-char and gas, respectively.

The higher heating value (HHV) of each pyrolysis product was calculated from its elemental composition by means of the following equation:<sup>317</sup>

$$\text{HHV} = 0.3491C + 1.1783H + 0.1005S - 0.1034O - 0.0151N - 0.0211A \text{ (MJ kg}^{-1}\text{)}$$

This formula is valid in the following intervals:  $0\% \leq C \leq 92\%$ ,  $0.43\% \leq H \leq 25\%$ ,  $0\% \leq O \leq 50\%$ ,  $0\% \leq N \leq 5.6\%$ ,  $0\% \leq S \leq 94\%$ ,  $0\% \leq A \leq 71\%$ ,  $4.7 \text{ MJ kg}^{-1} \leq \text{HHV} \leq 55.3 \text{ MJ kg}^{-1}$  where C, H, O, N, S and A represent the carbon, hydrogen, oxygen, nitrogen, sulfur and ash content of the material, expressed as mass percentage on a dry basis.

SEM pictures of the bio-char sample were obtained by using a Philips XL20 or a JEOL JSM-6300F FEG instrument after gold coating.

#### 4.3.2.7 Py-GC-MS test of catalytic upgrading of pyrolysis oil

The pyrolysis unit was a CDS Pyroprobe 1000 pyrolyser connected to a Varian 3400 gas chromatograph equipped with a Varian Saturn 2000 mass spectrometer.

---

<sup>317</sup> S.A. Channiwala, P.P. Parikh. A unified correlation for estimating HHV of solid, liquid and gaseous fuels. Fuel 81 (2002) 1051-1063.

A weighed amount of sample (250 µg of sample 4750 µg of H-ZSM-5 zeolite) was introduced into the quartz tube, and held by quartz wool at the middle portion of the tube. Analytical pyrolysis were conducted as shown in previous chapters.

Calibration were performed by external calibration, obtained by injection of toluene solution in ethyl acetate in the same system used for pyrolysis. Carbon yields were calculated by mean of knowing the elemental composition of analytes and of feedstock tested in the Py-GC-MS comparison.

### 4.3.3. Results and discussion

#### 4.3.3.1 Hydrogen production

Data on the hydrogen production achieved with the L159-I230Y strain are summarized in Table 4.3.1.

**Table 4.3.1:** H<sub>2</sub> production attained with *C. reinhardtii* mutant strain L159I-N230Y under standard conditions (12 mg L<sup>-1</sup> chl, 70 µmol photons m<sup>-1</sup> s<sup>-1</sup>, supplied on both sides of the reactor).

<i>Parameters</i>	<i>Units</i>	<i>Values</i>
Total H <sub>2</sub> output	ml L <sup>-1</sup>	504±22
Length of H <sub>2</sub> production phase	h	100±15
Mean H <sub>2</sub> production rate	ml L <sup>-1</sup> h <sup>-1</sup>	5.04±0.35
H <sub>2</sub> maximum production rate	ml L <sup>-1</sup> h <sup>-1</sup>	10.5±1.47
Light conversion efficiency	%	2.66±0.11

The mean hydrogen output was 504±22 mL L<sup>-1</sup> (mean ± standard deviation), and was obtained within 100 hours of production. Similar amounts of hydrogen were also obtained by Kruse et al. (2005) with an engineered *C. reinhardtii* strain, but over a much longer production period (10-15 days). The hydrogen output achieved with our mutant strain was about 6 times greater than what is usually reported with the CC-124 strain, which is extensively used worldwide for experiments in hydrogen production.<sup>299,300,318</sup> Light conversion efficiency achieved with this mutant was 2.66% of PAR (photosynthetically active radiation), and was found to be considerably higher than the one reported by Fouchard et al. (2008).<sup>319</sup> However, it must be pointed out that the hydrogen performance of the *C. reinhardtii* mutant strains could be further improved, since theoretically achievable light conversion efficiency is considered to be about 10% of solar light. The spent

<sup>318</sup> A. Tsygankov, S. Kosourov, M. Seibert, M.L. Ghirardi. Hydrogen photoproduction under continuous illumination by sulphur-deprived, synchronous *Chlamydomonas reinhardtii* cultures. *Int. J. Hydrogen Energ.* 27 (2002) 1239-1244.

<sup>319</sup> S. Fouchard, J. Pruvost, B. Degrenne, J. Legrand. Investigation of H<sub>2</sub> production using the green microalga *Chlamydomonas reinhardtii* in a fully controlled photobioreactor fitted with on-line gas analysis. *Int. J. Hydrogen Energ.* 33 (2008) 3302–3310.

biomass collected was  $0.54 \pm 0.01 \text{ g L}^{-1}$ . This means that about 12 g of spent biomass were produced for each gram of bio-hydrogen (about 11 mL at standard conditions for temperature and pressure, STP).

#### 4.3.3.2 Lipid yields and composition

The total lipid content of the *C. reinhardtii* D1 mutant after photo-biological production was  $15 \pm 2\%$  on a dry weight basis. The fractionation of the oil using a chromatographic column made it possible to separate non polar lipids (e.g. triacylglycerols) from more polar lipids (e.g. glycolipids, phospholipids and ceramides). GC-MS analysis after silylation provided information on the amount of FFA in each fraction, whereas GC-MS analysis after transesterification gave TFA (Table 4.3.2).

**Table 4.3.2:** Composition of *C. reinhardtii* oil, obtained by solvent extraction of biomass collected after hydrogen production.

Eluting solvent	Compound class	Conc. (%)	TFA <sup>a</sup>	FFA <sup>b</sup>
		% w/w <sub>oil</sub>	% w/w <sub>fraction</sub>	% w/w <sub>fraction</sub>
Hexane	Phytols	3.3	-	-
CHCl <sub>3</sub>	Triglycerides	21	95	-
CHCl <sub>3</sub> /Acetone	Polar lipids	39	63	26
CHCl <sub>3</sub> /Methanol	Highly polar lipids	37	39	-

<sup>a</sup> obtained by transesterification and GC-MS; <sup>b</sup> obtained by silylation and GC-MS.

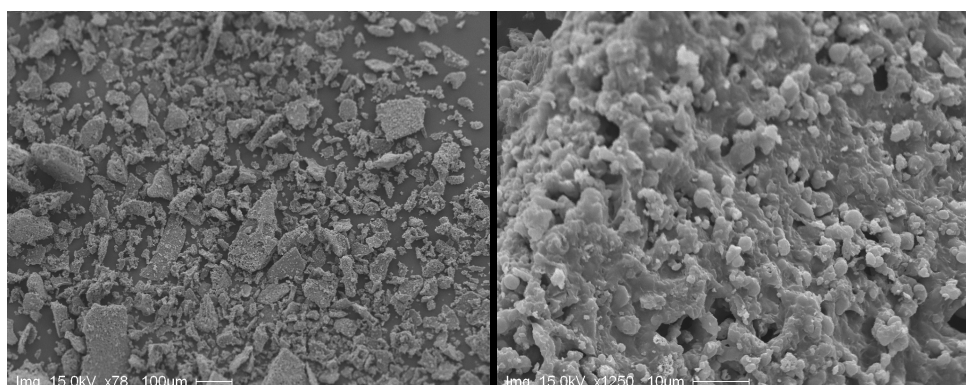
Oil extract was composed of 3.3% w/w<sub>oil</sub> of phytols, 21% w/w<sub>oil</sub> of triglycerides, 39% of polar lipids and 37% w/w<sub>oil</sub> of highly polar lipids. This last fraction, which was eluted with a mixture 1/1 of chloroform/methanol, contained only 39% of TFA, and for this reason should be considered barely “lipidic”. This finding revealed a relatively large amount of high-polarity lipids in the extract, as compared with typical biodiesel feedstock (e.g. edible oils mainly consisting of triglycerides). The FFA content in the algal oil (10% w/w<sub>oil</sub>) made this feedstock unsuitable for transesterification into biodiesel using conventional alkali-catalyzed procedures. In this work, therefore, a methanolic NaOH followed by methanolic BF<sub>3</sub> procedure was used for the transesterification of both FFA and bounded FA. The final biodiesel yield was  $8.7 \pm 1\%$  w/w<sub>biomass</sub>. The biodiesel consisted of 41% saturated fatty esters, 53% mono unsaturated fatty esters, and 7.2% polyunsaturated fatty esters (mainly linoleic acid). This meant that the methyl esters mix could be considered suitable for biodiesel in accordance with EU standard EN 14214.

The amount and type of lipids obtained in this work were almost similar to those of data in the literature relative to this algal species after hydrogen production.<sup>320</sup> This indicates that, despite some mass loss (cell disruption) during the transfer of microalgae to a sulfur-depleted medium and during the hydrogen production phase, the composition of lipids remains the same.

#### 4.3.3.3 Pyrolysis of extraction residue

For the conversion of extracted biomass into bio-char, bio-oil and pyro-gas, low temperature pyrolysis (350°C) was performed, mainly with the aim of enhancing the ash and nitrogen partition into bio-char, as well as to avoid an extensive formation of hydrogen cyanide during the process.<sup>321,310</sup>

**Figure 4.3.1:** SEM micrographs of bio-char obtained by pyrolysis of *C. reinhardtii* extraction residue at 350°C.



The mass yields of bio-char, bio-oil and gas (incondensable compounds, lighter compounds, and part of the water lost in solvent evaporation, calculated as difference) were 44±1%, 28±2% and 28±1%, respectively. The ash content in the bio-char, which was obtained by means of combustion at 700°C, was 45±5% on weight basis. On an ash-free basis, the mass yields of bio-char, bio-oil and gas were 24±5%, 38±9% and 36±1%, respectively. The 38% bio-oil yield was lower than the one obtained from pure cellulose (46±1%) using the same reactor,<sup>314</sup> but it was in agreement with

---

<sup>320</sup> H. Tatsuzawa, E. Takizawa. Fatty acid and lipid composition of the acidophilic green alga *Chlamydomonas* sp. J. Phycol. 32 (1996) 598-601.

<sup>321</sup> J. Giuntoli, W. De Jong, S. Arvelakis, H. Spliethoff, A.H.M. Verkooyen. Quantitative and kinetic TG-FTIR study of biomass residue pyrolysis: Dry distiller's grains with solubles (DDGS) and chicken manure. J. Anal. Appl. Pyrol. 85 (2009) 301-312.

Grierson et al.,<sup>322</sup> who reported a bio-oil yield from high nitrogen content microalgae that was lower than those obtained from lignocellulosic biomass.

Bio-char was the principal pyrolysis fraction; it consisted of large aggregates about 10-100  $\mu\text{m}$  in size and with a 1- $\mu\text{m}$  irregular porosity, and with no record of the original physical structure observable. These features are different from those of bio-char from lignocellulosic biomasses, which maintains the original ordered structure (e.g. wood vessels) under conditions of low-temperature pyrolysis.<sup>310</sup>

#### 4.3.3.4 Elemental analysis of extraction residue and pyrolysis fractions

Table 4.3.3 shows the elemental composition of the algal residue after solvent extraction and of each pyrolysis fraction produced.

**Table 4.3.3:** Elemental composition of feedstock and pyrolysis fractions.

	<i>C</i>	<i>O</i>	<i>N</i>	<i>H</i>	<i>S</i>	<i>ash</i>	<i>HHV</i> <sup>a</sup> ( <i>MJ/kg</i> )
<b>Extracted residue</b>	35±0.2	35±0.6	5.1±0.2	5.7±0.2	0.19±0.01	20±4	15±0.4
<b>Char</b>	40±0.1	9.3±0.2	5.3±0.1	1.4±0.1	<0.1	45±9	13±0.2
<b>Bio-oil</b>	54±1	33±2	5.4±0.9	6.7±0.1	0.53±0.02	<0.1	23±0.6
<b>Gas</b> <sup>b</sup>	9±0.3	74±8	4.5±1	12±1	0.19±0.02	<0.1	10±0.6

<sup>a</sup> expected HHV calculated from elemental composition. <sup>b</sup> The gas elemental composition and HHV were calculated on the basis of difference as described in Material and Methods.

As expected, *C. reinhardtii* residue showed a higher nitrogen content (4.4 ±0.2%) than that of most terrestrial lignocellulosic biomasses (e.g. corn stover 0.7%, poplar 0.5%, sweet sorghum 1%, and switchgrass 0.3%) tested in chapter 3.1. Solvent extraction residue was found to be even more enriched in nitrogen (5.1±2%) than the parent material. The elemental composition of bio-oil (54% carbon, 33% oxygen, 5.4% nitrogen, 6.7% hydrogen, 0.53% sulfur, expressed as w/w<sub>bio-oil</sub>) and the HHV(23±0.6 MJ kg<sup>-1</sup>) were similar to those obtained by Pan et al. (2010) by means of 400°C pyrolysis on *Nannochloropsis sp.* extraction residue.<sup>309</sup>

Bio-char was found to be heavily enriched with ash and carbon, whereas volatile products (bio-oil and gas) showed a large oxygen and sulfur content. Moreover, from the elemental analysis, gas was especially enriched in oxygen (75±8% w/w<sub>bio-oil</sub>), while nitrogen showed a similar concentration in both bio-char and volatile fractions (around 4-5% by weight for each product). It is interesting to note that, from an agronomical point of view, bio-char from microalgae is enriched in nitrogen, and

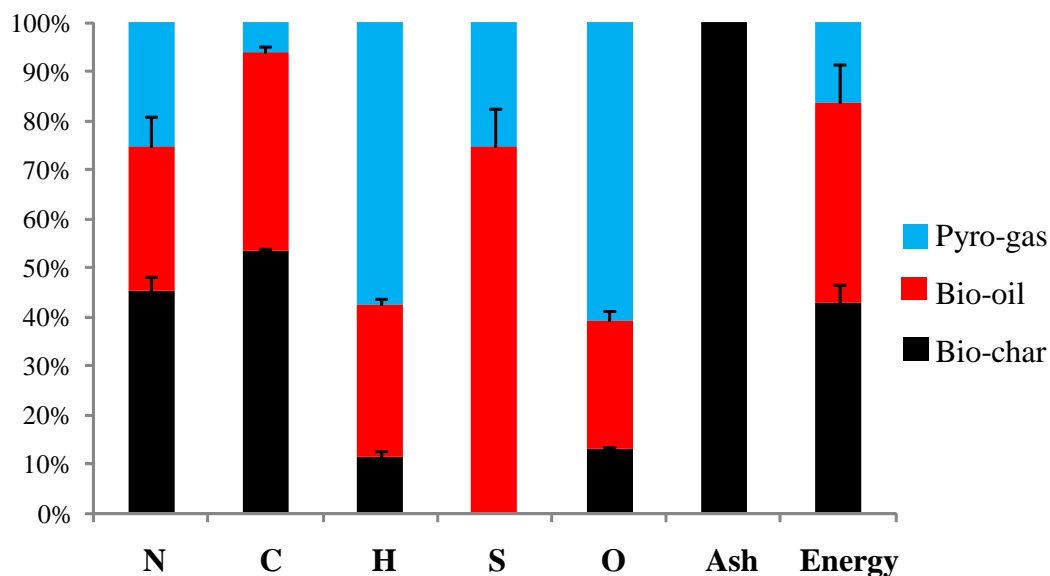
<sup>322</sup> S. Grierson, V. Strezov, G. Ellem, R. Mcgregor, J. Herbertson. Thermal characterization of microalgae under slow pyrolysis conditions. *J. Anal. Appl. Pyrol.* 85 (2009) 118-123.

could be exploited as a slow nitrogen-releasing source to the soil.

By combining the data relative to the elemental concentration and yield of pyrolysis fractions, it is possible to establish the “flow” of elements caused by pyrolysis towards the three pyrolysis fractions (bio-char, bio-oil and gas) (Figure 4.3.2).

Under the conditions selected in this study (350°C pyrolysis), all ash content was retained within bio-char. More than half of the carbon in the feedstock was partitioned into bio-char, whereas less than 8% of the carbon ended up in gas. Bio-char carbon yield was higher than that observed (on an analytical scale) for the low temperature pyrolysis of terrestrial biomass of chapter 3.1, which also had a relatively low nitrogen content (0.3-1% w/w<sub>biomass</sub>) and a moderate ash content (2-5% w/w<sub>biomass</sub>). This could confirm the positive correlation between nitrogen content and bio-char yield that was observed for terrestrial biomasses in the study shown in chapter 3.1.

**Figure 4.3.2:** Partitioning of feedstock (*C. reinhardtii* extraction residue) volatile elements and ash into bio-char, bio-oil and pyro-gas produced through pyrolysis; bars represent standard deviation (n=2).



Bio-char, gas and bio-oil stored, respectively, about 46±0.3%, 26±1% and 28±1% of pyrolyzed nitrogen. Oxygen and sulfur behaved in a similar way: they were mainly (oxygen) or almost totally (sulfur) partitioned into bio-oil and gases.

In conclusion, the elemental balance indicated that low temperature pyrolysis is a suitable technique for producing nitrogen-enriched bio-char for soil conditioning and carbon storage, as well as an ash-free liquid with improved HHV.

#### 4.3.3.5 Pyrolysis oil chemical characterization

Algal bio-oil was subjected to further investigation. The results obtained from the chemical characterization are shown in Table 4.3.4. The liquid product (containing 13±2% of water) was fractionated into a water-soluble fraction (60±7% w/w<sub>bio-oil</sub>), water-insoluble fraction (26±8% w/w<sub>bio-oil</sub>), and insoluble solids (insoluble both in chloroform and in water, 0.4±0.2% w/w<sub>bio-oil</sub>).

**Table 4.3.4:** Concentration of the major constituents of the bio-oil obtained after pyrolysis at 350°C of *C. reinhardtii* extraction residue.

<b>Bio-oil Fractions</b>	<b>% w/w<sub>bio-oil</sub></b>
water	13±2
water-soluble	60±7
water-insoluble	26±8
insoluble solids	0.4±0.2
<b>Quantified compounds</b>	<b>% w/w<sub>bio-oil</sub></b>
Σ sugar oligomers and polymers <sup>a</sup>	18±0.5
1,6-anhydro-β-glucopyranose	7.1±0.2
other anhydrosugars	1.7±1.1
1,6-anhydro-β-glucofuranoside	0.9±0.2
1,4:3,6-dianhydro-α-glucopyranose	3.9±2.8
levoglucosenone	1.5±1
furfural	0.7±0.4
glycerol	1.6±0.2
lactic acid	0.21±0.1
2-furancarboxylic acid	0.18±0.1
imidazole	0.20±0.1
3-hydroxy pyridine	0.26±0.1
2-methyl-5-hydroxypyridine	0.27±0.1
pentadecanenitrile	0.34±0.1
Σ 2,5-diketopiperazines	4.1±2
<i>p</i> -methylphenol	0.13±0.01
1,2,3-trihydroxybenzene	0.12±0.01
Σ phytols	0.55±0.01
Σ free and bounded fatty acids	4.8±2
Σ GC detectable unknowns	12±5
Total identified compounds <sup>c</sup>	71

<sup>a</sup> Sum of sugar polymers and oligomers susceptible to methanolysis, obtained by difference between methyl-O-glycosides detectable after methanolysis and silylation of the oil, and anhydrosugars detectable by silylation of the oil; <sup>c</sup> comprising all quantified compounds and water.

From a molecular point of view, bio-oil was mainly formed of carbohydrates produced by pyrolysis, such as anhydrosugars, oligo- and polysaccharides (detectable as additional methyl-glycosides after

methanolysis and silylation), and a relatively small amount of nitrogen-containing GC-detectable pyrolysis products from proteins, mainly 2,5-diketopiperazines ( $4.1 \pm 2$  % w/w<sub>bio-oil</sub>) and aromatic heterocycles (about 2% w/w<sub>bio-oil</sub>). Alkyl nitriles, phenols, and fatty acids were also detected. It is interesting to note that the elemental nitrogen content of bio-oil ( $5.4 \pm 0.9$ %) was greater than that expected from the contribution of nitrogen containing compounds detected by GC-MS (about 1-2%). This finding suggests that there is an important fraction of the total nitrogen retained by high molecular weight compounds (not detectable, even if silylated, by GC-MS) or by unidentified compounds.

Several compounds detected by means of different derivatization techniques (silylation or methanolysis followed by silylation) were water-soluble (e.g. levoglucosan, glycerol, oligosaccharides, imidazole), whereas only very few of them were water-insoluble (e.g. free and bounded fatty acids, phytols and alkyl nitriles).

The presence of a large amount of non GC detectable water-insoluble matter was rather surprising. In the case of terrestrial plants, this fraction is accounted for lignin degradation products and hydrophobic compounds (e.g. extractives). In our case the chemical nature of this fraction is unknown. Lipids, in fact, were solvent-extracted prior to pyrolysis while lignin is notoriously absent in microalgae.

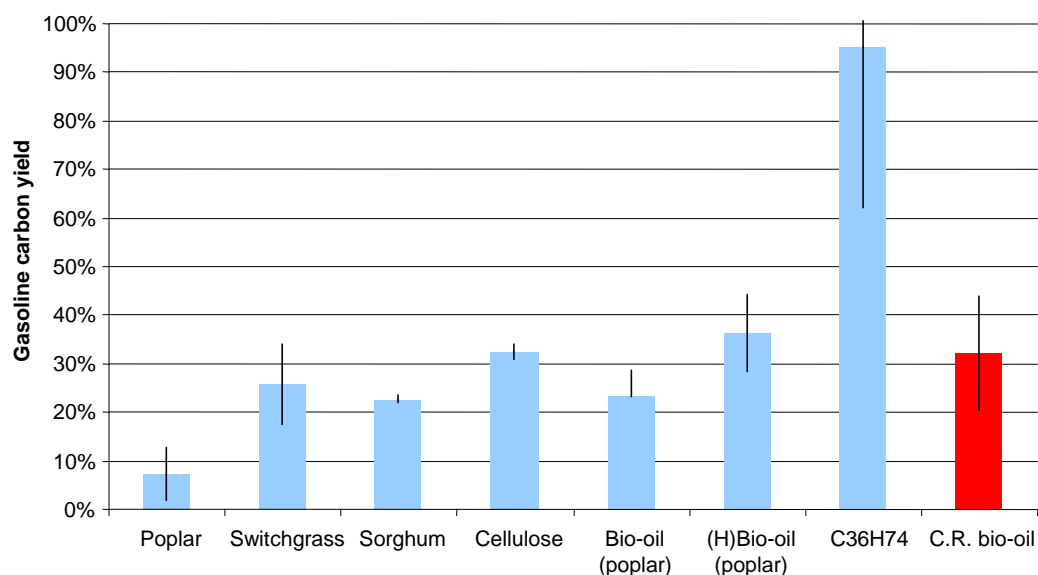
Due to its chemical composition, the bio-oil obtained from extracted residue pyrolysis is not suitable as fuel; however, according to the literature, it could be easily cracked into aromatic hydrocarbons over zeolites (with the removal of oxygen and nitrogen), since the elemental ratio (C+H)/(O+N) of bio-oil is relatively high and the water content is relatively low.<sup>323,309</sup> The absence of high concentrations of phenols and lignin derivatives, typical of terrestrial biomass, is also advantageous, since the most effective catalyst in bio-oil upgrading (zeolite H-ZSM-5) is highly sensitive to lignin-derived compounds, which clog the pores and thus reduce the effectiveness of the conversion.<sup>324</sup> For this reason the *Chlamydomonas reinhardtii* was tested as feedstock using analytical pyrolysis and comparing with other feedstock. Interestingly, from this analysis an entirely aromatic GC-detectable product, with almost total elimination of nitrogen fuel were obtained. Absolute carbon yield of aromatics (figure 4.3.3) were less than that obtainable by pyrolysis of hydrocarbons feedstock (C<sub>36</sub>H<sub>74</sub>), but similar to those obtained by pyrolysis of hydrogenated bio-oil or pure cellulose, indicating a relatively high quality of this feedstock.

---

<sup>323</sup> T.A. Milne, R.J. Evans, N. Nagle. Catalytic conversion of microalgae and vegetable oils to Premium Gasoline, with Shape-Selective Zeolites, *Biomass* 21 (1990) 219-232.

<sup>324</sup> A.G. Gayubo, A.T. Aguayo, A. Atutxa, B. Valle, J. Bilbao. Undesired components in the transformation of biomass pyrolysis oil into hydrocarbons on an HZSM-5 zeolite catalyst. *J. Chem. Tech. Biot.* 80 (2005) 1244–1251.

**Figure 4.3.3:** carbon yield ( $C_{\text{aromatic}}/C_{\text{feedstock}}$ ) of aromatic compounds obtained by catalytic cracking of *Chlamydomonas reinhardtii* bio-oil (C.R. bio-oil, red bar), poplar bio-oil, hydrogenated poplar bio-oil ((H)Bio-oil) on ZSM-5 (bars shows standard deviation, n=5).

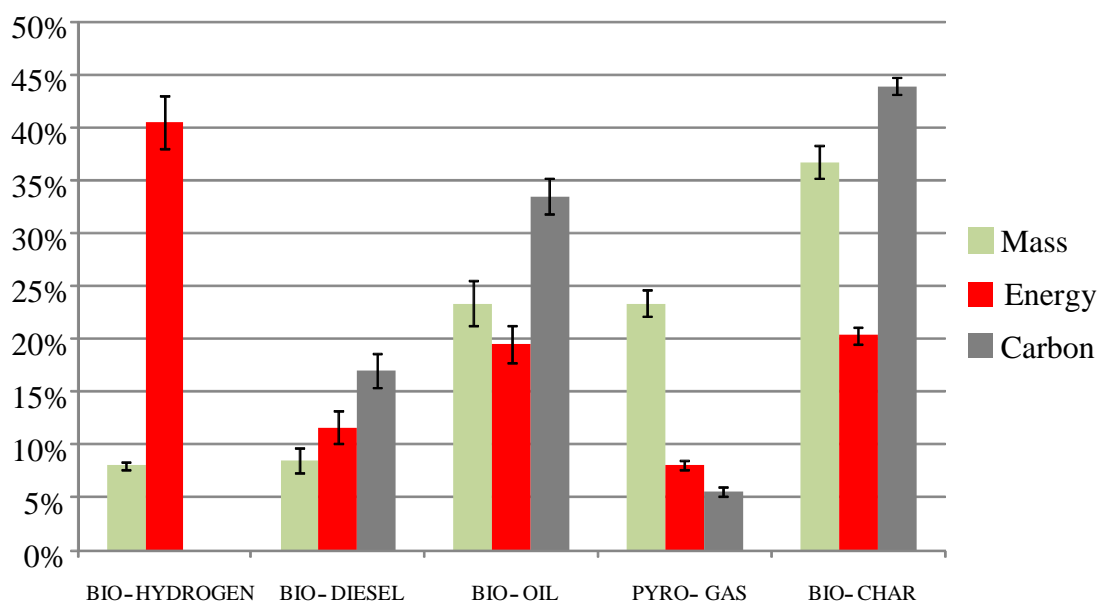


#### 4.3.3.7 Evaluation of output of photobiological hydrogen production integrated with solvent extraction and pyrolysis.

An overall balance of the combined biological, chemical and thermochemical processes can be calculated from the hydrogen and residue yields, as well as from the yields and compositions of extracted material and fractions from pyrolysis. Figure 4.3.4 shows the percentage mass, energy, and carbon output of the bio-photolysis process combined with lipid extraction and pyrolysis.

Hydrogen production represents a lesser amount in terms of mass (only  $8 \pm 0.3\%$  of the total), but a relatively large amount of energy ( $40 \pm 2.5\%$  of total), mainly thanks to the high energy content of hydrogen. In any case, it is clear that, after photobiological hydrogen production, spent biomass retains a large amount of both mass and energy ( $92 \pm 1\%$  of mass and  $58 \pm 0.6\%$  of energy). Part of this mass and energy could be recovered in the form of conventional bio-fuel by means of solvent extraction followed by biodiesel production ( $8.5 \pm 1\%$  on a mass basis and  $12 \pm 2\%$  on an energy basis), but another large part (extraction residue is  $83 \pm 2\%$  on a mass basis and  $48 \pm 2\%$  on an energy basis) could be valorized by means of pyrolysis. Bio-char is the largest system product on a mass basis, whereas the bio-oil and pyro-gas energy contents produced are comparable to that of hydrogen. According to these data, bio-char used as soil conditioner (instead of using it as fuel) involves a loss of  $20 \pm 1\%$  of the maximum energy output; however (see Section 3.3), this would make it possible to temporarily store (e.g. in soils) more than  $44 \pm 2\%$  of the carbon incorporated during algae growth (Figure 4.3.4).

**Figure 4.3.4:** Percent distribution of mass, energy and carbon output among different final products of the system; bars represent standard deviation (n=2).



Moreover, if bio-oil and bio-diesel are used as starting material for chemical synthesis (e.g. for aromatic chemicals synthesis), a further carbon loop can be created, with enhancement of carbon negative character of the hydrogen produced by the process.

#### 4.3.4 Conclusions

Despite the limitations of the equipment used in this work (fixed bed reactor), solvent extraction followed by low-temperature pyrolysis demonstrated that the partial separation of carbon and energy is feasible by means of the production of biodiesel, ash-free bio-oil with improved characteristics (HHV and a composition compatible with upgrading), and carbon-rich bio-char, which retains all feedstock ash. This means that, if bio-char from freshwater microalgae can be used as a carbon storage material, pyrolysis could be combined with bio-hydrogen production in order to obtain a set of potential carbon-negative bio-fuels and chemicals.

## 4.4. Evaluation of Pyrolysis coupled to soil carbon sequestration as GHGs saving strategy in the Ravenna province (Italy)

### 4.4.1 Introduction

Agricultural residues (ARs) represent an enormous carbon flow relatively easy to manage<sup>325</sup> and interesting for bio-energy and different geo-engineering options.<sup>326</sup> Nevertheless, the removal of ARs from soil it is a debated option, mainly due to the risk of soil carbon decrease and consequential fertility loss.<sup>327</sup> The loss of soil carbon is a global issue that particularly affects the Mediterranean area, exerting a potentially positive feedback on global warming by higher decomposition of soil organic carbon.<sup>328</sup> According to the European Environment Agency<sup>329</sup> the areas with a very low organic carbon content (between 0–1 %) are mostly in the southern part of Europe and correspond to areas with high soil erosion rates and warmer climates, classified as sensitive area to desertification.<sup>330</sup> Even if the current estimates of changes in soil carbon stocks are characterized by high uncertainty, at the European scale soil carbon storage can produce a relevant net yearly accumulation of carbon in soils, in the range of 1 to 100 million tons,<sup>331</sup> acting as a sink for carbon. Thus, soil management practices in agriculture are an important tool to affect the carbon stocks. In particular according to the European Commission,<sup>331</sup> soil carbon stocks can be increased on cropland by: (i) agronomic measures that increase the return of biomass to the soil, (ii) no tillage and residue management, (iii) water management and (iv) agro-forestry.

Beyond the well known practices, pyrolysis allows to transform agricultural residues (ARs) into bio-oil or syngas and high recalcitrant carbonaceous matter (bio-char) that can be added to soil. Due to the high stability of bio-char, the final effect of its addition to soils is an artificial increase of soil

---

<sup>325</sup>J.S Gregg, S.J. Smith. Global and regional potential for bioenergy from agricultural and forestry residue biomass. *Mitig. Adapt. Strateg glob change*. 15 (2010) 241-262.

<sup>326</sup>S.E. Strand, G.B. Benford. Ocean sequestration of crop residue carbon: recycling fossil fuel carbon back to deep sediments, *Environ. Sci. Technol.* 43 (2009) 1000-1007.

<sup>327</sup>D.L. Karlen, R. Lal, R.F. Follett, J.M. Kimble, J.L. Hatfield, J.M. Miranowski, C.A. Cambardella, A. Manale, R.P. Anex, C.W. Rice. Crops Residues: the rest of the story. *Environ. Sci. Technol.* 43 (2009) 8011-8015.

<sup>328</sup>P.M. Cox, R.A. Betts, C.D. Jones, S.A. Spall, I.J. Torrerdell. Acceleration of global warming due to carbon-cycle feedbacks in a coupled climate model. *Nature* 408 (2000) 184-187.

<sup>329</sup>*Integration of environment into EU agriculture policy — the IRENA indicator-based assessment report; 2006 EEA Report No 2/2006*; European Environment Agency; Copenhagen, Danmark, 2006; ISSN 1725-9177, [http://www.eea.europa.eu/publications/eea\\_report\\_2006\\_2/at\\_download/file](http://www.eea.europa.eu/publications/eea_report_2006_2/at_download/file)

<sup>330</sup>*Mapping sensitivity to desertification (DISMED), Final report*; European Environment Agency: European Topic center: Terrestrial environment; Barcelona, Spain, 2008, <http://www.eea.europa.eu/data-and-maps/data/desertification-in-the-mediterranean-region>.

<sup>331</sup>*Review of existing information on the interrelations between soil and climate change. CLIMSOIL final report to the European Commission*; European Commission (EC): Bruxelles, Belgium, 2009, [http://ec.europa.eu/environment/soil/pdf/climsoil\\_report\\_dec\\_2008.pdf](http://ec.europa.eu/environment/soil/pdf/climsoil_report_dec_2008.pdf).

organic carbon faster than by mulching and no-till management.<sup>332,333</sup> For this reason, converting ARs into bio-char and bio-fuels could be a solution for the “food, energy and environment trilemma”, by stopping the carbon loss of soils and, at the same time, accomplishing food and renewable energy production in the form of 2<sup>nd</sup> generation bio-fuels.

Therefore, aim of this paper is the evaluation of three different ARs management strategies ((i) open-burning (OB), (ii) mulching (MU) and (iii) bio-charring (BC) through a simulation of soil carbon evolution both for total (TC) and humic (HUM) soil carbon content and through a Greenhouse Gases (GHGs) balance over 100 years. In order to obtain data with adequate spatial resolution, the study was focused on the Italian province of Ravenna, a relative small administrative area (185.000 ha coast-to-hill area ) that could be used as an example for similar regions throughout southern Europe.

## 4.4.2 Materials and methods

### 4.4.2.1 Study area

The Province of Ravenna is located in the northern part of Italy, in the river Po plain. The area is bounded on the east by the Adriatic Sea, on the south-west by the Apennines mountains and by the Lamone river on the northern side. The 26% of the area is located on low hills and the remaining 74% is a mainly flat area dominated by agriculture; croplands and fruit farming areas represent, respectively, the 50% and the 20% of the district land use.

### 4.4.2.2 Agricultural residues availability and management strategies

The availability of ARs within the Ravenna district has been assessed through the use of local data,<sup>334</sup> national census<sup>335</sup> and land use map.<sup>336</sup> The collected information have been condensed through the use of ArcGis 9.2 ESRI® software, producing a spatial database on agricultural residues, that contains average annual ARs yields and average moisture for both biomasses. The biomasses chosen as representative of the different types of cultivations was “corn stover and similar” for the cropping areas and “orchard pruning” (woody material), for fruit farming areas and vineyards.

---

<sup>332</sup> J. Lehmann, J. Gaunt, M. Rondon. Biochar sequestration in terrestrial ecosystems- a review. *Mitigation and Adaptation Strategies for Global Change* 11( 2006) 403-427.

<sup>333</sup> J. Lehmann. A handful of carbon. *Nature* 447 (2007) 143–144.

<sup>334</sup> A. Buscaroli, A. Gagliardi. Censimento delle biomasse della provincia di Ravenna. Internal report. Centro Interdipartimentale di Ricerca per le Scienze Ambientali, Università di Bologna, Ravenna, Italy, 2006.

<sup>335</sup> V° *Censimento dell'Agricoltura*; Istituto Statistico Nazionale (ISTAT): Roma, Italy, 2001,

[http://www.census.istat.it/index\\_agricoltura.htm](http://www.census.istat.it/index_agricoltura.htm)

<sup>336</sup> *Carta dell'uso del suolo 2003: Coperture vettoriali 1:25000*; Regione Emilia Romagna-Servizio Sistemi informativi geografici, Regione Emilia Romagna: Bologna, Italy, 2006,

**Table 4.4.1:** Overview of biomass resources available.

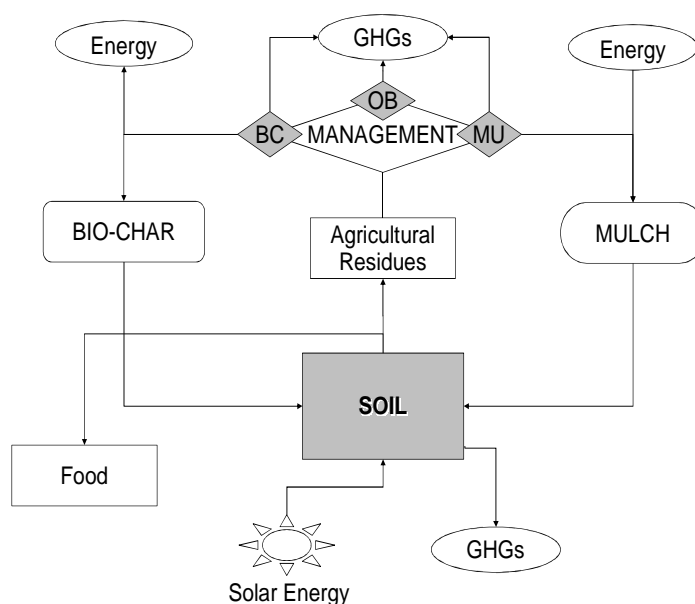
<i>Biomass Source</i>	<i>Area (kha)</i>	<i>ARs yield(t dry/ha)</i>	<i>ARs(kt dry)</i>
<i>Corn stover and similar</i>	86.4	3.70±1.49	320±129
<i>Orchard pruning</i>	46.7	1.94±0.86	90±40
<i>Total</i>	133.2		410

Non managed natural productivity (NP) of agricultural system (e.g leaves, roots, inter-row grassland etc.) were included in the model. NP productivity was extrapolated by manageable residue productivity using literature coefficients.<sup>337</sup>

Considered ARs management strategies (Figure 4.4.1) were:

- i) Open-burning (OB)
- ii) Mulching (MU)
- iii) Bio-charring (BC);

**Figure 4.4.1:** General scheme of the three management options considered by this study (arrows indicate a material or energy flow). BC: bio-charring, MU: mulching, OB: open-burning.



The first strategy consists on the direct on field open-burning of ARs, a common strategy for orchard pruning management, and was used as reference scenario for the work. This strategy was assumed to determine a complete transformation of biomass C into CO<sub>2</sub> without any use of fossil

<sup>337</sup> W. Faqi, L. Haib, S. Baosheng, W. Jian, W. J. Gale. Net primary production and nutrient cycling in an apple orchard–annual crop system in the Loess Plateau, China: a comparison of Qinguan apple, Fuji apple, corn and millet production subsystems. *Nutrient Cycling in Agroecosystems* 81 (2008) 95-105.

energy (eradicated biomass are simply burnt without processing). In the MU strategy ARs are chipped and leaved on the field, and a surplus N fertilizer was applied in order to maintain the C/N ratio around 30 (as local best agronomic/composting practice suggests ).<sup>338</sup> The BC strategy consists on ARs collecting, chipping, drying and pyrolysis in order to produce bio-oil (used as energy source) and bio-char. Subsequently the bio-char is applied to the same field that produced the ARs and the fuels are burnt in order to replace fossil fuels for producing heat. All the strategies assume that the same management of ARs is carried out, for the considered period, on all agricultural area of the Ravenna Province.

#### 4.2.2.3. Soil modeling

The soil components have been modeled starting from the present condition (soil carbon content) and assuming the application of the products (mulch or bio-char) on the same fields of harvesting. For calculation, total carbon ( $\text{t ha}^{-1}$ ) at time zero was obtained from organic carbon concentrations assuming an organic layer depth of 0.3 m and an average soil density of  $1.45 \text{ t m}^{-3}$ .

The model used for simulating the soil carbon evolution in soils has been built on the basis of the RothC carbon model,<sup>339</sup> using Matlab software. Main modifications of the original algorithm, described in detail below, were:

- Inclusion of two bio-char compartments (degradable and resistant bio-char), with specific degradation proprieties, as a source of organic matter.
- Interaction between bio-char and natural organic matter, and then a small effect on developed  $\text{CO}_2/(\text{BIO}+\text{HUM})$  RothC ratio.<sup>340,341</sup>
- Modification of temperature and rainfall regime over years due to global climate change.

#### 4.4.2.4 Data requirement and main assumptions

The data required to run the model are reported in table 4.4.2. The following main assumption on data input were used:

- soil layer depth: all samples to be equal to 30 cm;
- average soil density of  $1.45 \text{ t m}^{-3}$ ;

---

<sup>338</sup> G.F.Huang; J.W.C. Wong, Q.T. Wu, B.B. Nagar. Effect of C/N on composting of pig manure with sawdust. Waste Management 24 (2004) 805–813.

<sup>339</sup> D.S. Jenkinson. The turnover of organic carbon and nitrogen in soil. Phil. Trans. R. Soc. Lond. B 329 (1990) 361-368.

<sup>340</sup> G.N. Kasozi, A.R. Zimmerman, P. Nkedi-Kizza, B. Gao. Catechol and Humic Acid Sorption onto a Range of Laboratory-Produced Black Carbons (Biochars). Environ. Sci. Technol. 44 (2010) 6189-6195.

<sup>341</sup> H. Jin, J.Lehmann, J.H. Thies. Soil microbial community response to amending maize soil with maize stover charcoal, Proceeding of 2008 international bio-char initiative 8-10 september 2008, Newcastle, UK.

- initial humic carbon content was considered to be equal to the total soil carbon measured by RER (2004); this according to the fact that the soil carbon content is decreasing, and this imply that major part of soil carbon consist in humus.
- he ratio between stable and fresh biochar ( $BC_{stable}/BC_{fresh}$ ), was assumed to be equal to 0.75, according to other authors<sup>350</sup> and to the mean value predicted by py-GC-MS method application of biochar in chapter 3.4 of this thesis. Because of the high importance of understanding the role of this parameter within the mechanism, this value has been considered to vary uniformly between 1 and 0.5 in the uncertainty analysis.

**Table 4.4.2:** Parameters used in the model

CATEGORY	PARAMETER	UM	DATA SOURCE or REFERENCE
Climate and soil	- Average monthly mean air temperature	°C	342
	- Monthly rainfall	mm month <sup>-1</sup>	342
	- Monthly open pan evaporation	mm month <sup>-1</sup>	343
	- Clay content of the soil	%, mass fraction	344
	- Total Carbon content of soil	mg g <sup>-1</sup>	344
	- Humic Carbon content of soil	mg g <sup>-1</sup>	100% soilC hypothesis
	- Depth of soil layer sampled	cm	344
	- 100 y average temperature change	°C/ year	3.32°C/100 y <sup>345</sup>
	- Long term average water runoff change	%/ year	-13.2%/80 y <sup>346</sup>
Cultivation and biomass	- DPM/RPM ratio		339
	- Monthly input of non-	t C ha <sup>-1</sup>	347,337

<sup>342</sup>Regional Environment Agency of Emilia Romagna (ARPA-ER). DEXTER database (2006).

<sup>343</sup>A. Minchio, Evapo-transpiration in the “Quintobacino”, Internal report (2009) Centro Interdipartimentale di Ricerca per le Scienze Ambientali, Università di Bologna, Ravenna, Italy, 2006.

<sup>344</sup>Emilia Romagna Region (RER) Geological department, Soils of Emilia Romagna database (2007).

<sup>345</sup>Intergovernmental Panael on Climate Change: Climate change 2001: synthesis Report, Contribution of working groups I,II,III to the third assessment report of the intergovernmental Panell on climate change. IPCC, Cambridge, Cambrige Univeristy Press. UK.

<sup>346</sup>R. Warren, N. Arnell, R. Nicholls, P. Levy, J. Price. Understanding the regional impacts of climate change: research report prepared for the Stern review on the economics of climate change. Tyndall Centre, Norwich, UK (2006).

<sup>347</sup>A. Buscaroli, A. Gagliardi, Censimento delle biomasse della provincia di Ravenna. Internal report. Centro Interdipartimentale di Ricerca per le Scienze Ambientali, Università di Bologna, Ravenna, Italy, (2006).

	manageable plant residues		
	- Monthly input of manageable plant residues	t C ha <sup>-1</sup>	347/347
	- Soil cover – coverage of the soil in the month.		Agronomical practice
Pyrolysis and biochar	- Biochar carbon yield $C_{\text{biochar}}/C_{\text{feedstock}}$		348,349
	- $BC_{\text{stable}}/BC_{\text{fresh}}$ ratio		350,348
	- Degradable Bio-Char (DBC) degradation rate and $dBC_{\text{fresh}}$		351
	- Resistent Bio-Char (RBC) degradation rate		352
	- $BC_{\text{stable}}/BC_{\text{fresh}}$ ratio		Chapter 3.4 this thesis

#### 4.4.2.5 Identification of reference elements

In order to produce more realistic forecasts, the area was divided into 113 polygons, through overlay of vectorial maps, within a GIS environment. Due to the fact that the modelling assumptions are insensitive to the dimension of single elements, this classification has been performed through the identification of elements that are characterized by similar environmental parameters (T, P, Clay%,  $C_0$ ) and meaningful administrative boundaries (boundaries of municipalities).

#### 4.4.2.6 Model algorithm structure.

The soil components have been modelled starting from the present condition (soil carbon content) and assuming the application of the products (mulch or bio-char) on the same fields of harvesting.

The model used for simulating the soil carbon evolution in soils has been strictly built on the basis of the RothC carbon model<sup>339</sup>, using Matlab™ software. Main modifications were: the inclusion of

<sup>348</sup> K.G. Roberts, B.A. Gloy, S. Joseph, N. R. Scott, J. Lehmann, Life Cycle Assessment of Biochar Systems: Estimating the Energetic, Economic, and Climate Change Potential. *Environ. Sci. Technol.*, 44 (2010) 827–833.

<sup>349</sup> C.Torri, A. Adamiano, D.Fabbri, C. Lindfors, A. Monti, A. Oasmaa. Comparative analysis of pyrolysate from herbaceous and woody energy crops by Py-GC with atomic emission and mass spectrometric detection. *Journal of Analytical and Applied Pyrolysis* 88 (2010) 175-180.

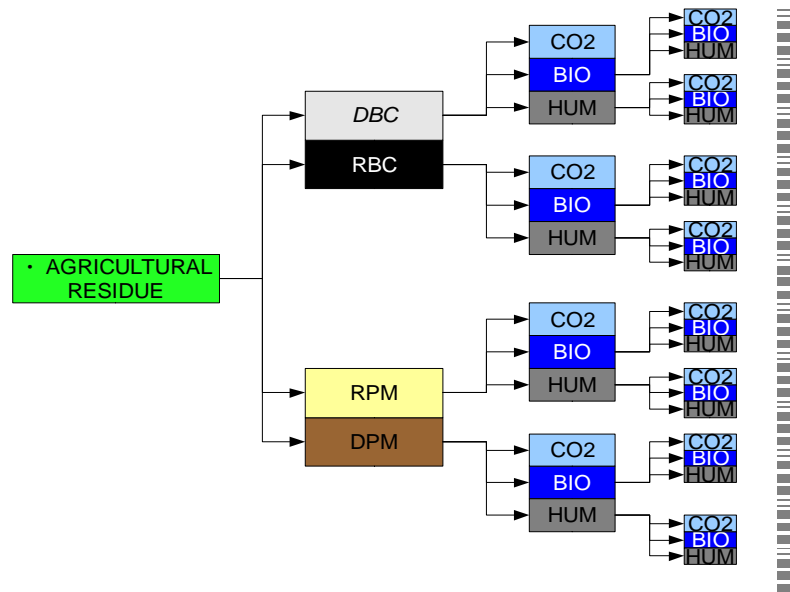
<sup>350</sup> P.A.Brownsort, O. Mašek. Pyrolysis Biochar Systems: Comparison of Climate Change Mitigation Effects of Slow, Intermediate and Fast Pyrolysis Processes, 18<sup>th</sup> European biomass conference and exhibition, Lyon 3-7 may 2010, 956 – 960.

<sup>351</sup> U. Hamer, B. Marschner, S. Brodowskib, W. Amelung. Interactive priming of black carbon and glucose mineralisation; *Organic Geochemistry* 35 (2004) 823-830.

<sup>352</sup> C-H Cheng, J. Lehmann, M.H. Engelhard. Natural oxidation of black carbon in soils: Changes in molecular form and surface charge along a climosequence. *Geochimica et Cosmochimica Acta* 72 (2008) 1598-1610.

the bio-char compartment as a source of organic matter, and the modification of temperature and rainfall due to climate change.

**Figure 4.2.2:** Basic modified RothC model scheme.



The RothC model assumes a monthly input of plant residues to soils; in this work, the plant material input is considered to be composed by two categories: the non-manageable residues and the manageable residues, representing respectively, the incoming plant material due to roots and leaves that directly goes into soils and the residues that can be treated and added or not to the soil (in form of mulch or biochar) according to the defined strategy.

In order to model the soil carbon turnover, in this work it was assumed that there are six major carbon compartments in soils, arising from the input of plant materials: degradable bio-char (DBC), resistant bio-char (RBC), degradable plant matter (DPM), resistant plant matter (RPM), microbial biomass (BIO) and humus (HUM). As in the original RothC algorithm, all carbon compartments degrade by a specific degradation rate with a monthly time step, producing CO<sub>2</sub>, humic material (HUM) and microbial biomass (BIO) (Figure 4.2.2).

The BIO/HUM ratio from DBC and RBC (Figure 4.2.2) has been assumed to be equal to the RothC model assumption (46% microbial biomass and 54% humus). On the contrary, the soil respiration ratio (Eq. 1) (Figure 4.4.2) was developed on the basis of an empirical relationship, taking into account the physical-chemical effect of biochar on the organic matter. This relationship is built by assuming an effect of bio-char on the soil respiration ratio similar to the effect of clay (stabilization of natural organic matter exerted by adsorption and reduction of bio-availability of substances), but

considering a scaling factor derived from the effect on soil respiration exerted by biochar to mineral soil.<sup>353,354</sup>

$$\frac{CO_2}{(HUM + BIO)} = 3.09 + 2.67 \cdot e^{(-0.0786 \cdot c - 0.0744 \cdot B)} \quad (\text{Eq.1})$$

Where  $c$  is the mass percentage of clay in the soil;  $B$  is the amount of bio-char carbon expressed as  $\text{ton ha}^{-1}$ .

In basic algorithm iteration, the soil organic carbon of the  $i$ -compartment at time  $t+1$  (monthly time step), is described in Eq. 2:

$$SOC_{i(t+1)} = M_{ij} \cdot SOC_{i(t)} + P_{i(t)} \quad (\text{Eq. 2})$$

$SOC_i$  is the soil organic carbon of the  $i$ -compartment (DPM, RPM, BIO, HUM, RBC, DBC);

$M_{ij}$  is the transition matrix of the  $i$ -compartment;  $P_{i(t)}$  is the organic matter input at time  $t$ .

#### 4.4.2.7 Decomposition of compartments.

If an active compartment contains  $Y \text{ t C ha}^{-1}$ , this declines to  $Y e^{-a(i)bk(i)t} \text{ t C ha}^{-1}$  at the end of the month.  $t$  is  $1 / 12$ , since  $k$  is based on a yearly decomposition rate.

So  $Y (1 - e^{-a(i)bk(i)t})$  is the amount of the material in a compartment that decomposes in a particular month, where:

$a(i)$  is the rate modifying factor for temperature for that compartment (Table 4.4.3);

$b$  is the rate modifying factor for moisture, assumed the same for each compartment;

$c$  is the soil cover rate modifying factor, assuming the same for each compartment;

$k(i)$  is the decomposition rate constant for that compartment (Table 4.4.4).

**Table 4.4.3:** Decomposition rate used for each compartment

Compartment	Rate modifying factor function for temperature ( $a_i$ )
DBC	$a(i)=0.3144 \cdot e^{(0.12179 \cdot T)}$
RBC	$a(i)=0.3144 \cdot e^{(0.12179 \cdot T)}$
DPM	$a(i)=47.9/(1-e^{(106/(T+18.3))})$
RPM	$a(i)=47.9/(1-e^{(106/(T+18.3))})$
BIO	$a(i)=47.9/(1-e^{(106/(T+18.3))})$
HUM	$a(i)=47.9/(1-e^{(106/(T+18.3))})$

<sup>353</sup>G.N. Kasozi, A.R. Zimmerman, P. Nkedi-Kizza, B. Gao. Catechol and Humic Acid Sorption onto a Range of Laboratory-Produced Black Carbons (Biochars). *Environ. Sci. Technol.* 44 (2010) 6189-6195.

<sup>354</sup>H. Jin, J. Lehmann, J.H. Thies. Soil microbial community response to amending maize soil with maize stover charcoal, Proceeding of 2008 international bio-char initiative 8-10 september 2008, Newcalste, UK.

**Table 4.4.4:** Base decomposition rate used for each compartment

Compartment	Base decomposition rate ( $k_i$ )
DBC	0.07
RBC	$7.5 \cdot 10^{-4}$
DPM	10
RPM	0.3
BIO	0.66
HUM	0.02

The RothC factors for temperature effect were used for all the components but biochar. The effect of temperature on the biochar degradation rate was modelled according to Eq. 3, on the basis of the results of Cheng *et al.*<sup>355</sup>

$$a_{\text{biochar}} = 0.3144 \cdot e^{(0.12179 \cdot T)} \quad (\text{Eq. 3})$$

Where:  $a_{\text{biochar}}$  represents the temperature-related factor, for the biochar degradation ratio; T is the average daily temperature. Considering the decomposition rates for all the compartments, for a given month, it is possible to define a base degradation vector, as: ( $\delta\text{DBC}$ ;  $\delta\text{RBC}$ ;  $\delta\text{DPM}$ ;  $\delta\text{RPM}$ ;  $\delta\text{BIO}$ ;  $\delta\text{HUM}$ ). In the modelling procedure, the equations for the  $\delta\text{DPM}$ ,  $\delta\text{RPM}$ ,  $\delta\text{BIO}$ ,  $\delta\text{HUM}$  were taken directly from the RothC model, the decomposition rate of DBC compartment was calculated according to Eq.4 and the decomposition rate of  $\delta\text{RBC}$  was directly taken from Cheng *et al.* (2008).<sup>355</sup>

$$\delta\text{DBC} = \frac{\partial \text{BC}_{\text{fresh}}}{1 - \frac{\text{BC}_{\text{stable}}}{\text{BC}_{\text{fresh}}}} \quad (\text{Eq. 4})$$

Where:  $\text{BC}_{\text{fresh}}$  represents the fresh component of biochar;  $\text{BC}_{\text{stable}}$  represents the stable component of biochar. As estimated in chapter 3.1, the  $\text{BC}_{\text{stable}}/\text{BC}_{\text{fresh}}$  was assumed to be equal to 0.75 on average, varying uniformly between 1 and 0.5 in the uncertainty analysis.

#### 4.4.2.8 Data requirement and spatial zonation

The model input (climate maps, soil maps and residues maps) has been developed on the base of existing data on temperature, rainfall, evaporation, clay concentration, soil organic carbon content and available ARs. In all the cases other than the ARs map, the kriging<sup>356,357</sup> method for

---

<sup>355</sup> C-H. Cheng, J. Lehmann, M.H. Engelhard. Natural oxidation of black carbon in soils: Changes in molecular form and surface charge along a climosequence. *Geochimica et Cosmochimica Acta* 72 (2008) 1598-1610.

<sup>356</sup> T. Hengl, G.B.M Heuvelink, A.A. Stein. generic framework for spatial prediction of soil variables based on regression-kriging. *Geoderma* 120 (2004) 75-93.

<sup>357</sup> *DEXTER database of Regional Environment Agency of Emilia Romagna (ARPA-ER)*, [http://www.arpa.emr.it/sim/?osservazioni\\_e\\_dati/dexter](http://www.arpa.emr.it/sim/?osservazioni_e_dati/dexter)

interpolating data has been used in order to produce maps from point data, through the use of Spatial Analyst, within the ArcGis environment.

In order to identify meaningful areas with similar parameters values, an intersection between the parameters maps and the administrative boundaries of municipalities of Ravenna Province has been carried out. As a result, 113 different elements have been identified.

#### 4.4.2.9 Green House Gases balance

The greenhouse gases emissions for each of the considered strategies have been calculated summing the emissions related to the energy productions/consumptions activities and the CO<sub>2</sub> emissions linked to depletion or enrichment of soil carbon pool. The efficiency of “ARs carbon capture” was evaluated by dividing the CO<sub>2</sub>eq balance at a time by the CO<sub>2</sub> captured in ARs until that time.

In particular, the “non carbon storage” effects due to the BC strategy, have been evaluated through the Biochar Energy, Greenhouse Gases and Economic (BEGGE) life cycle assessment inventory analysis method.<sup>348</sup> In order to be consistent with the data inventory proposed by the authors in the BEGGE method, the same hypothesis on field operations, thermochemical processes efficiency and dimension of the collection and application basin area, have been assumed.

According to the Roberts *et. al*<sup>348</sup> the net effect of the application of bio-char produced from ARs is carbon negative and it is due to: the effect of the reduction of fertilizers needed, the use of the syngas/bio-oil for heating purposes and the stocking of carbon into soils, in the form of bio-char. In order to allow the evaluation of the effect on time of GHGs emission reduction potential, the method proposed by Roberts *et al.*<sup>348</sup> has been modified through the decay algorithm for the “stable carbon” component (from soil carbon modeling).

The GHGs balance of the MU strategy was quantified considering the following processes and sources: the biomass chipping (with energy consumption), the application to soil, the supplemental nitrogen fertilizers application aimed at creating an optimal C/N ratio into agricultural soils and a slight increase of N<sub>2</sub>O emission from soil, as reported by Larsson *et al.*<sup>358</sup>

In order to quantify the net benefit of carbon sequestration due to BC and MU, a comparison with the reference scenario (OB strategy) was performed.

The equation used for quantifying the relative GHGs emission reduction for each strategy at time t, when compared to the reference condition (OB strategy) is reported in Eq. 5:

$$\Delta GHG_{SN,i-OB,t} = GHG_{SN,I,t} - GHG_{SOB,t} \quad (\text{Eq. 5})$$

---

<sup>358</sup>L. Larsson, M. Ferm, Å. Kasimir-Klmedtsson, L.Klmedtsson. Ammonia and nitrous oxide emission from grass and alfalfa mulches. *Nutrient Cycling in Agrosystems* 51 (1998) 41-46.

Where

$\Delta\text{GHGs}_{\text{N},i-\text{OB},t}$  represents relative net effect on GHGs emission reduction for the i-strategy, when compared to the OB strategy;  $\text{GHGs}_{\text{N},i,t}$  represents the net effect on GHGs for the i-strategy;  $\text{GHGs}_{\text{OB},t}$  represents the net effect on GHGs for the OB strategy.

The general equation used for quantifying the net effect on GHGs emission or reduction is the following:

$$\text{GHGs}_{\text{N},i,t} = -\text{GHGs}_{\text{E},i,t} + \text{GHGs}_{\text{SS},i,t} + \text{GHGs}_{\text{A},i,t} \quad (\text{Eq. 6})$$

Where:  $\text{GHGs}_{\text{N},i,t}$  represents the net effect on GHGs for the i-strategy;  $\text{GHGs}_{\text{E},i,t}$  represents the GHGs EMISSIONS due to the processes that are included in each of the i-strategies;  $\text{GHGs}_{\text{SS},i,t}$  represents the effect of GHGs STORAGE (carbon storage) due to soil carbon dynamic involved in the i-strategy and the direct emission of N<sub>2</sub>O from soils;  $\text{GHGs}_{\text{A},i,t}$  represents the effect of GHGs AVOIDING, due to the substitution between conventional fuels and electricity production and energy from pyrolysis and the avoiding of N<sub>2</sub>O emissions due to the reduction in use of fertilizers (BC strategy).

Then, using Eq. 7, 8, 9 it is possible to derive Eq. 10:.

$$\text{GHGs}_{\text{E},i,t} = \text{GHGs}_{\text{E-FUELS},i,t} \quad (\text{Eq. 7})$$

$$\text{GHGs}_{\text{SS},i,t} = \text{GHGs}_{\text{SS-C},i,t} + \text{GHGs}_{\text{SS-N}_2\text{O},i,t} \quad (\text{Eq. 8})$$

$$\text{GHGs}_{\text{A},i,t} = \text{GHGs}_{\text{A-FUELS},i,t} + \text{GHGs}_{\text{A-N}_2\text{O},i,t} \quad (\text{Eq. 9})$$

Where:

$\text{GHGs}_{\text{E-FUELS},i,t}$  represents the GHGs EMISSIONS due to use of fuels;  $\text{GHGs}_{\text{SS-C},i,t}$  represents the effect of GHGs STORAGE (carbon storage) due to soil carbon dynamic involved in the i-strategy;  $\text{GHGs}_{\text{SS-N}_2\text{O},i,t}$  represents the direct emission of N<sub>2</sub>O from soils;  $\text{GHGs}_{\text{A-FUELS},i,t}$  represents the GHGs AVOIDING due to use of syngas/bio-oil as fuels;  $\text{GHGs}_{\text{A-N}_2\text{O},i,t}$  represents the GHGs AVOIDING of N<sub>2</sub>O emissions due to the reduction in use of fertilizers (BC strategy).

$$\text{GHGs}_{\text{N},i,t} = \text{GHGs}_{\Delta\text{FUELS},i,t} + \text{GHGs}_{\Delta\text{N}_2\text{O},i,t} + \text{GHGs}_{\text{SS-C},i,t} \quad (\text{Eq. 10})$$

In Table 4.4.5 are reported the coefficients used as inputs for Eq. 10 For all the strategies the soil carbon modelling was the base for evaluating the GHGs emission/storage in soil.

**Table 4.4.5:** Data on GHGs emissions, by source and strategy, as input for Eq. 6

Strategy	Biomass to soil yield $C/C_{\text{residue}}$	GHGs <sub>ΔFUELS</sub> (Δ use of fossil fuels <sup>a</sup> ) $\text{kgCO}_2\text{eq ton}^{-1}$	GHGs <sub>ΔN<sub>2</sub>O,i,t</sub> (Δ soil N <sub>2</sub> O emissions) $\text{kgCO}_2\text{eq ton}^{-1}$	GHGs <sub>S-C,i,t</sub> (Soil Carbon storage benefits)
<b>Open-burning (OB)</b>	0	0	0	Soil carbon balance (modeling)
<b>Mulching (MU)</b>	100%	Corn & similar: -31.6 <sup>a</sup> Pruning residues: -44.6 <sup>a</sup>	Corn & similar: -5.2 <sup>b</sup> Pruning residues: -5.6 <sup>b</sup>	Soil carbon balance (modeling)
<b>Bio-charring (BC)</b>	42%	Corn & similar: 215.3 Pruning residues: 215.3	Corn & similar: 59.8 <sup>c</sup> Pruning residues: 59.8 <sup>c</sup>	Soil carbon balance (modeling)

<sup>a</sup> kgCO<sub>2</sub>eq emission due to process energy input (negative value) or output (positive value) of a ton of dried residue; <sup>b</sup> kgCO<sub>2</sub>eq emission due to variation in N<sub>2</sub>O production from soil due to mulching; <sup>c</sup> negative value correspond to the reduction in N<sub>2</sub>O emission from soil due to application of biochar obtained from 1 dry ton of corn stover.

Data on processes emission factors, renewable energy production and reduced N<sub>2</sub>O soil emission due to biochar application were mainly taken from the BEGGE spreadsheet, proposed by Roberts et al.<sup>348</sup> and integrated with data on processes (pruning residues chipping), using the energy consumption coefficients for tree chipping operations from Caserini et al.<sup>359</sup>

According to Eq. 10, the GHGs emissions relative to the MU strategy are composed by three main sources: energy consumed in processing operations (assumed to substitute energy produced from natural gas), increase/decrease of non-CO<sub>2</sub> GHGs emissions (N<sub>2</sub>O) and carbon storage in soils. For this strategy, an addition of nitrogen-based fertilizer to croplands was assumed for maintaining high productivity on agricultural fields. Then, the C/N ratio of mulch was reduced from high values (see table 4.4.6) to 30, through addition of nitrogen-based fertilizer, as the best composting practices suggest.<sup>360</sup> Then, literature on N<sub>2</sub>O emission for Low N-grass (1.15% N and C/N ratio of 36.1) was used<sup>361</sup> for evaluating the emission of N<sub>2</sub>O. This value resulted to be equal to 0.00115 kg N<sub>2</sub>O/kg

<sup>359</sup>S. Caserini, S. Livio, M. Giugliano, M. Grosso, L. Rigamonti. LCA of domestic and centralized biomass combustion: The case of Lombardy (Italy). Biomass and bioenergy 34 (2010) 474-482.

<sup>360</sup>G.F. Huang, J.W.C.Wong, Q.T. Wu, B.B. Nagar. Effect of C/N on composting of pig manure with sawdust. Waste Management 24 (2004) 805-813

<sup>361</sup>L. Larsson, M. Ferm, Å. Kasimir-Klemedtsson, L. Klemedtsson. Ammonia and nitrous oxide emission from grass and alfalfa mulches. Nutrient Cycling in Agroecosystems 51 (1998) 41-46.

N, leading to a net emission of 0.343 kg CO<sub>2</sub>eq/kg N (100y GWP) that can be used for calculating the N<sub>2</sub>O emission caused by mulching of a ton of residue (table 4.4.5).

**Table 4.4.6:** Data on fertilizer addition within the MU strategy and relative GHGs emissions.

feedstock	CO <sub>2</sub> eq produced in chipping operations kgCO <sub>2</sub> /ton <sub>mulch</sub>	N content %	C content %	N required for C/N =30 %	CO <sub>2</sub> eq from required fertilizer production CO <sub>2</sub> eq/ton <sub>mulch</sub>	CO <sub>2</sub> eq from N <sub>2</sub> O emission CO <sub>2</sub> eq/ton <sub>mulch</sub>
Corn stover and similar	2.4 kg, 32 MJ	0.7	45	0.8	24.0 kg	5.15
Pruning residues	5.3 kg , 72 MJ	0.5	48	1.1	33.7 kg	5.55

#### 4.4.2.10 Uncertainty and sensitivity analysis

Understanding the magnitude and the sources of the uncertainty that characterizes the modeling assumptions can be relevant for scientific understanding and decision making, both uncertainty and a sensitivity analysis were performed on the GHGs balance of BC and MU strategy, compared to OB. The analysis has been carried out through the use of the SIMLAB 2.2 software.<sup>362</sup> The distribution of each model input variables was generated starting from average values and uncertainty of the source data.

In order to perform the analysis, a Montecarlo approach-based uncertain analysis and variance-based sensitivity analysis techniques (Sobol's) have been applied.<sup>363</sup> The factors that have been considered and the relative random distribution used, are reported in Table 4.4.7. The factors have been used as multiplying factors for the data input matrix, creating a set of 640 similar matrices on which the uncertainty and sensitivity analysis have been performed.

**Table 4.4.7:** Factors considered in the sensitivity analysis \*for non normal distribution. \*\*triangular distribution was used in order to avoid occurring of negative values

	Distribution	$\sigma$ or interval*	critierion
Monthly avg. Temperature	Normal	0.15	Standard deviation of T distribution on all study area
Monthly tot. Rainfall	Normal	0.2	Standard deviation of P distribution on all study area

<sup>362</sup> A. Saltelli, S. Tarantola, F. Campolongo, M. Ratto. Sensitivity analysis in practice: A guide to assessing scientific models; Wiley: New York, NY, 2004.

<sup>363</sup> M. Saisana, A. Saltelli, S. Tarantola. Uncertainty and sensitivity analysis techniques as tools for the quality assessment of composite indicators. Journal of the Royal Statistical Society. Series A 168 (2005) 307-323.

Monthly Evaporation	Uniform	0.5-1.5	Only one data available on the area (conservative choice)
Agr. Residues Yield	Triangular	0.57-1.43	Maximum an minimum from interviews.**
Non manageable residues	Normal	0.1	Standard deviaton for non-manageable residue data <sup>337</sup>
RPM/(Incoming plant matter)	Normal	0.1	Standard deviation of lignin content among same type of agricultural residues (e.g. among crops or among pruning residues)
BC <sub>stable</sub> /BC <sub>fresh</sub>	Uniform	0.75-1.25	Arbitrarily selected according to Roberts et al. <sup>348</sup>
Clay %	Normal	0.27	Standard deviation of clay % distribution on all study area
Initial soil Carbon (C <sub>0</sub> )	Normal	0.23	Standard deviation of C <sub>0</sub> distribution on all study area
Climate change (DT)	Uniform	0-2	Comprise “no climate change hypotesis” to double expected effect from climate change.
Climate change (D(P-E))	Uniform	0-2	Comprise “no climate change hypotesis” to double expected effect from climate change.

#### 4.4.3. Results and discussion

##### 4.4.3.1 Agricultural residues yields and main characteristics of study area

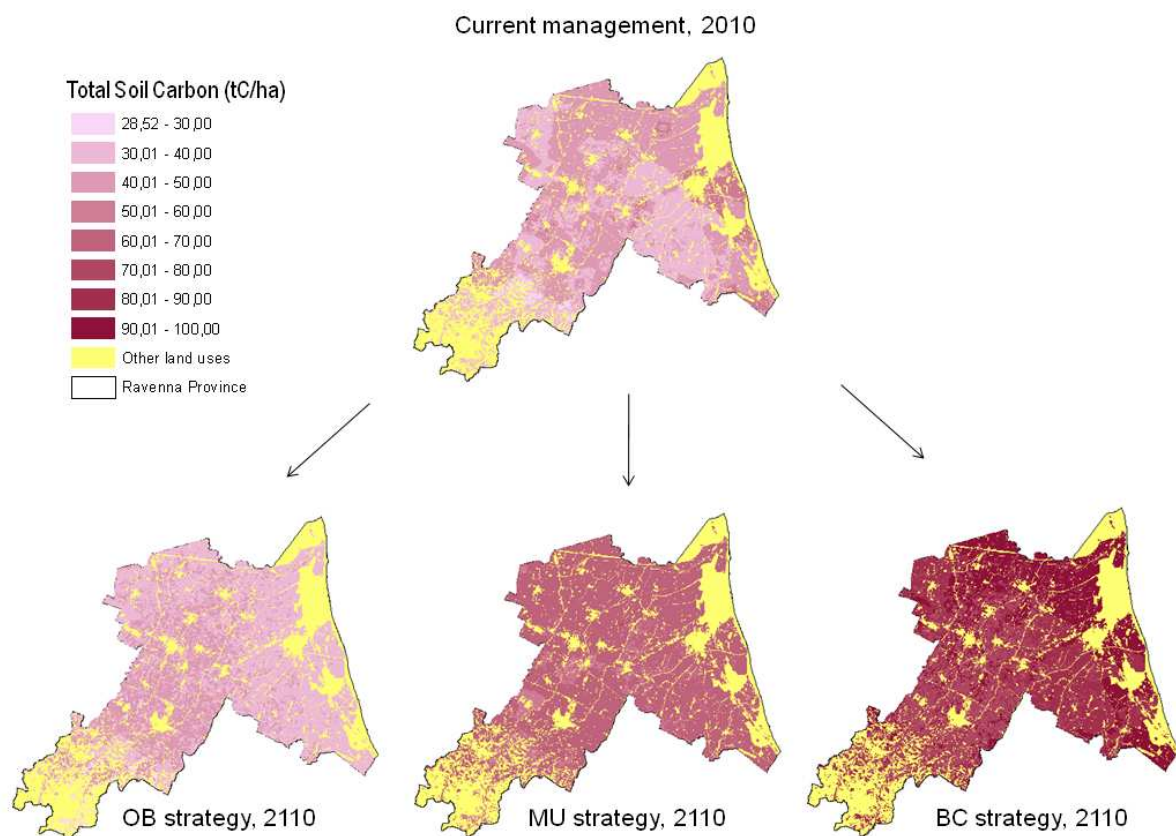
The total amount of ARs within the Ravenna Province is equal to  $4.10 \cdot 10^5$  tons per year (table III). Residues from annual cropping activities (corn and similar) are equal to the 78% of the value, where the remaining part are residues from orchard pruning and orchard renovation (eradication and replanting). Stover is commonly sold as animal feed and orchard residues are burned on the field. Both these practices imply a reduction of carbon inputs to soils, determining an average low concentration of soil organic carbon in all area (Figure 4.4.3). Among different climatic, pedological and agronomic conditions, soil carbon concentrations varies between  $54 \text{ t ha}^{-1}$  (orchard soil with high clay content) and  $29 \text{ t ha}^{-1}$  (annual crop on sandy soils).

##### 4.4.3.2 Total carbon evolution and humic carbon evolution

The century trend of different soil carbon fractions (DBC, RBC, DPM, RPM, BIO, HUM) was modeled on all the agricultural areas of the Ravenna district. Figure 4.4.3 shows the maps of soil carbon evolution within the study area. Spatial differences are due to the different ARs yields (that are higher for croplands and lower for fruit farming areas) and climatic and pedologic differences inside the study area. Figures 4.4.4 (a, b) represent the average soil total carbon evolution (TC) and

soil humic carbon (HUM) evolution over 100 years, for two different areas of the Ravenna Province (Fusignano and Brisighella) that could be considered as representative of the two typical trends (orchards and annual crops) that occur within the study area.

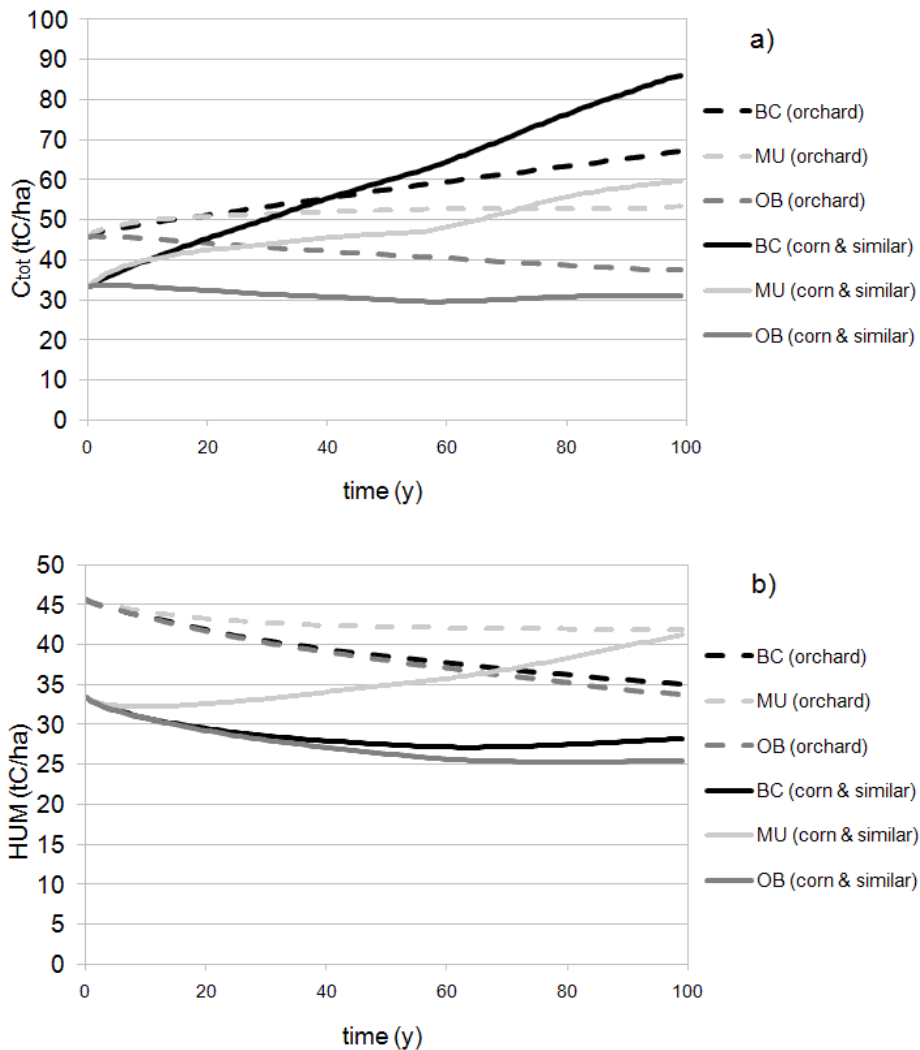
**Figure 4.4.3:** Spatial distribution of 2010 carbon concentration in the study area, by simulation of different management strategies for 100 years; (OB) open-burning, (MU) mulching, (BC) bio-charring.



In both croplands (Brisighella) and orchards (Fusignano) it is possible to note that the OB would determine a slight decrease of both TC and HUM content for the first 50 years followed by a stabilization at ~31 tC/ha and ~37 tC/ha respectively. It is notable that, according to the simulation, the current cropland situation is almost in equilibrium with a removal strategy. On the contrary, in orchards soils (e.g. Fusignano district) the open-burning practice (currently the most frequent habit) will determine a monotone ~20% reduction of soil organic carbon content over a century.

The MU strategy showed a better performance with a moderate increase of soil carbon content in two “waves”, one starting immediately and one after 50 years. In the first time span resistant plant material input drives the carbon increase, after 50 years, the humus formed during years starts to have a more important contribution.

**Figure 4.4.4:** Total soil carbon evolution (a) and humic carbon evolution (b) over 100 years for two reference sites, Brisighella (annual crops, continuous lines) and Fusignano (orchard, dashed lines) .



BC determines a grossly linear increase of soil carbon content by  $0.5 \text{ ton ha}^{-1} \text{ y}^{-1}$ . It is possible to notice that the BC strategy is able to increase the soil total carbon twice faster than the MU strategy, with a soil carbon level of 80-90 t/ha after 100 years. Nevertheless, considering a very short time perspective ( $<10 \text{ y}$ ) it is interesting to note that mulching raises organic carbon faster than bio-charring, mainly due to RPM and BIO accumulation in the soil.

In order to establish the effect on fertility loss and erosion trend, that are extremely relevant in the hilly part of the study area, the attention was focused on the humus component. Among the three strategies, only mulching can stop the humus loss in carbon rich orchard soils or determine a slight increase ( $\sim 20\%$  raise) for relatively carbon poor croplands soils. The effect of mulching is notable on the natural HUM component of the TC. In fact this strategy can significantly avoid large soil natural HUM loss with a relative stabilization of the soil carbon content and, on a very long term perspective, is able (using only AR locally produced) to solve the problem of relative low organic

carbon content typical of the study area soils.

On the contrary, for the first 100 years both BC and OB (or removal) of ARs cause almost the same adverse effects on humus concentration, with a reduction of humic carbon by one third.

Bio-charring strategy allows a higher humus concentration only on long time scale, when the carbonaceous material starts to decompose significantly. This effect is negligible within the time period examined in this work, but could be considered a very long term benefit of the bio-charring practice.

In conclusion, bio-charring can act as a net substitution between natural humic carbon and an higher amount of a sort of “synthetic soil carbon”. From the point of view of total soil carbon, the BC management strategy of ARs, could be a successful choice due to the net gain of organic material of soil compared to both open burning and mulching strategies. Nevertheless from an agronomic point of view, bio-char and HUM are not totally equivalent, and then bio-char application as “stand alone” strategy has to be carefully evaluated.

#### *4.4.3.3 Green House Gases balance*

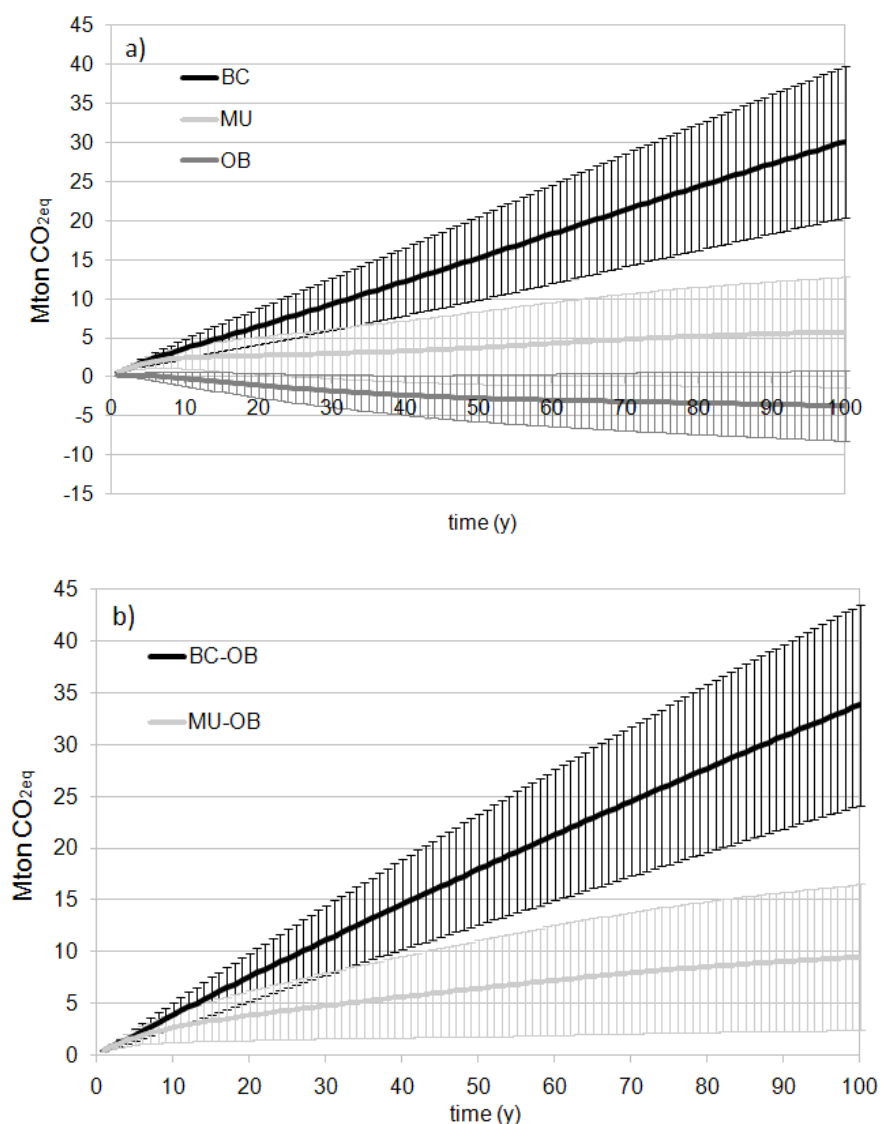
The potential GHGs emission reduction at the Ravenna Province scale are represented on Figures 4.4.5a and 4.4.5b. A positive value means a net effect of reduction of the emission, whereas a negative value means a net emission, and the error bar corresponds to standard deviation of the distribution obtained by uncertainty analysis.

According to the results ( $\alpha$ : 0.05), if manageable residues are burnt without energy recovery, Ravenna croplands will produce 1.09Mt CO<sub>2</sub>eq in 20 years (relative standard deviation RSD: 144%) and 3.72 Mt CO<sub>2</sub>eq (RSD: 120%) over the century. By pyrolysis and bio-char application to soil, the same system will determine a reduction/ avoiding of emissions equal to 6.47 Mt CO<sub>2</sub>eq (RSD: 36%) in first 20 years and 30.1(RSD: 32%) Mt CO<sub>2</sub>eq in 100 y. Also the mulching strategy leads to a relevant reduction equal to 2.74 Mt CO<sub>2</sub>eq (RSD: 87%) in 20 years and 5.75 Mt CO<sub>2</sub>eq (RSD: 122%) in 100 years. All but BC strategy results are characterized by high uncertainty, due to the partial knowledge on initial parameters value. Despite of the large variability of the absolute values, BC and MU strategies seems to be, on average, both effective in terms of GHGs emission reduction and, according to the results, both strategies determine a significant reduction in GHGs emissions with respect to open-burning (Figure 4.4.5b).

In order to evaluate the relative effect of the choice, both the differences between BC and OB and between MU and OB are shown in figure 4.4.5b. In this case the uncertainty is strongly reduced, mainly thanks to the elimination of the variability due to non-management sensitive data (e.g. amount of non manageable residues and initial soil carbon content). The comparison between BC and MU clearly shows that the biochar strategy represents the best option for GHGs sequestration

on medium and long term perspective ( $t > 7$  y), but, on very short term ( $t < 7$  y), the two strategies are not statistically different ( $\Delta GHG_{S(BC-MU)} < 0$ ,  $\alpha: 0.05$ ).

**Figure 4.4.5:** a) GHGs reduction/emission in different AR management strategies, b) relative GHGs reduction/emission due to difference between intervention and open-burning removal strategy (bars show confidence intervals with  $\alpha: 0.05$ )



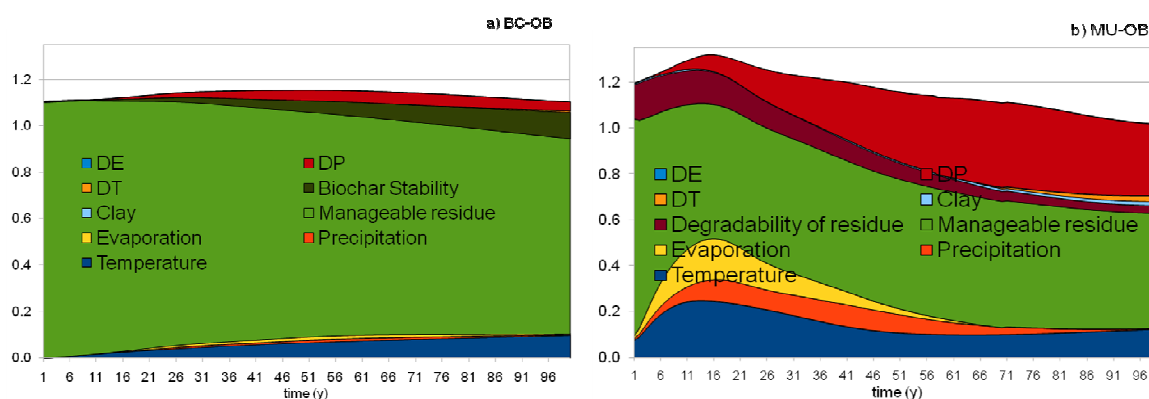
The difference on GHGs emission/avoiding between BC and OB, evaluated as average over 100 years, was equal to 12% of the yearly GHGs emission produced by the energy consumption within the Ravenna province (2.94 Mt of CO<sub>2eq</sub>)<sup>364</sup>. Moreover it is noticeable that also a relatively “traditional” management like mulching would be able to save 3-10% of overall emissions for 20 years, with other benefits (e.g. protection against erosion). In general, these values of GHGs savings

<sup>364</sup>Piano energetico provinciale; Provincia di Ravenna: Ravenna, Italy, 2009, <http://www.provincia.ra.it/Argomenti/Ambiente/Energia-ed-elettromagnetismo/Il-Piano-Energetico-Provinciale>

are not negligible, considering that a large fraction of the ARs are actually burnt on field.

The sensitivity analysis was performed on the cumulative GHGs emission reduction resulting from the adoption of BC and MU strategies with respect to the OB strategy.

**Figure 4.4.6:** Sensitivity analysis of the relative GHGs reduction between: a) BC and OB, b) MU and OB.



Figures 4.4.6a and 4.4.6b show the results obtained by sensitivity analysis on the model following different scenarios. The results show that the uncertainty related to the CO<sub>2</sub> reduction potential determined by bio-charring adoption, is mainly due to the partial knowledge about the amount of manageable residues. This can be considered as the most important factor, because it is able to explain more than the 50% of the total variance of the results. With time, the relevance of other factors increases, in particular the amount of labile matter in bio-char, temperature (uncertainty due to meteorological data resolution) and, in lesser extent, the uncertainty regarding change in rainfalls due to global warming model uncertainties. On the other hand, the uncertainties related to temperature increase (due to global warming) and clay concentration (typically involved in HUM formation) seem to be less important.

Looking at the uncertainty related to the potential CO<sub>2</sub> eq emission avoiding due to the MU strategy, other factors become relevant. As for the BC strategy the amount of manageable residues can be considered as the most important factor, at least in the short period, but the relevance of the other factors changes significantly. In this case degradability of ARs and climate become important factors in the first 50 years and the uncertainty related to climate change effects ( $\Delta T$  and  $\Delta P$ ) become crucial factors on the long period..

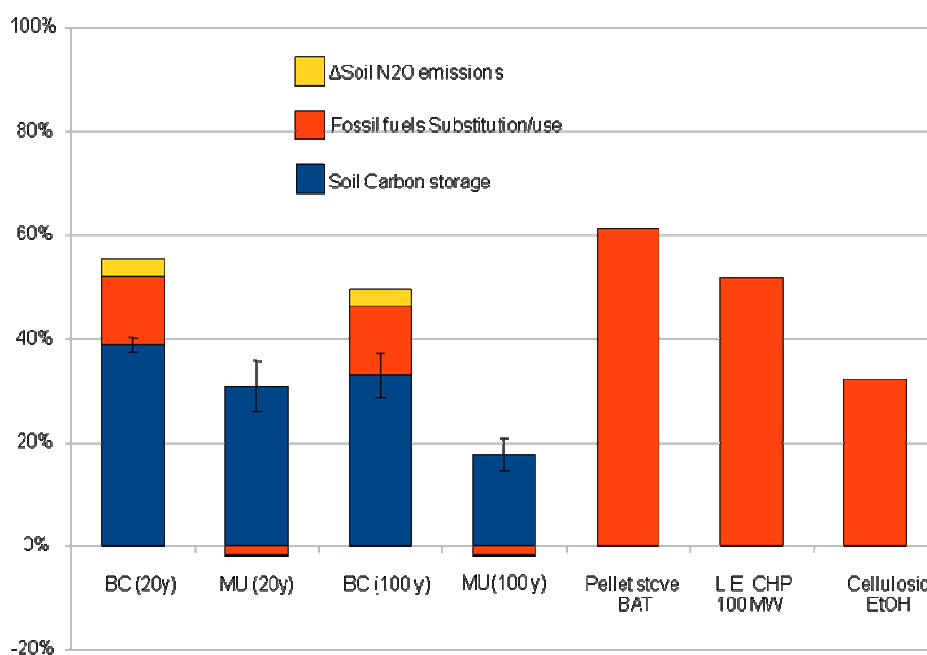
Comparing the two strategies and their respective sources of uncertainty, BC seems to be a more GHGs safe management, in the sense that its uncertainty is mainly depending on ARs yields and not by other factors and for this reason the process seems to be much more insensitive to other factors if compared to MU. On the contrary, a large portion of uncertainty regarding MU effects on GHGs

emissions ( 50% in the long term model predictions) it is due to the lack of knowledge on global warming parameters, and then are difficult to eliminate.

#### 4.4.3.4 Carbon capture and storage (CSS) efficiency: comparison with other technologies

The BC and MU strategies were compared to other technological ARs management options, in terms of carbon offset efficiency over two defined time span (20 and 100 years). The considered alternative ARs management options were: energy recovery from direct burning of forestry residues in Italy for two different technologies (pellet stove heating without gas cleaning, combined heat and power (CHP) 100 MW plant<sup>365</sup> and 2<sup>nd</sup> generation ethanol production.<sup>326</sup>

**Figure 4.4.7:** Comparison between the CCS efficiency of different ARs management options, expressed as the percentage of ARs carbon that it is sequestered or that avoid fossil fuel carbon emissions.  $\Delta$ Soil N<sub>2</sub>O emissions: avoided emission of N<sub>2</sub>O due to the biocharring.



Results are shown in Figure 4.4.7. When a 20 years time span is considered, it is possible to see that BC can act as very effective “emergency solution”, because the average efficiency over the period is equal to 55%, a carbon sequestration ratio similar than other biomass fueled energy conversion processes (61% and 52% respectively from and pellet stove and CHP 100 MW plant). On this time scale, also MU shows an efficiency comparable to second generation ethanol. It has to be noticed that this value is twice than what was proposed by Strand and Bedford,<sup>6</sup> mainly due to the accounting of the entire mulched material carbon cycle (conversion to BIO and HUM).

<sup>365</sup> S. Caserini, S. Livio, M. Giugliano, M. Grosso, L. Rigamonti. LCA of domestic and centralized biomass combustion: The case of Lombardy (Italy). Biomass and bioenergy 34 (2004) 474-482.

In a long term perspective (100 years), the off-set efficiency of BC slightly decreases becoming equal to 50%, where the mulching carbon capture and storage efficiency drops to 16% a reduction due to the reaching of the equilibrium for resistant plant material component.

Looking at the MU strategy as CCS method, a large effect of carbon storage could be attained in the first 20 years and a non-negligible CCS value on the long period, simply through burial of the residues. This is to stress that, considering other non quantified benefits (e.g. reduced erosion) of HUM conservation obtainable by mulching, this approach could be the best choice in high hydro-geological risk areas or in colder climates (where HUM could act as longer term C stock).

In order to correctly understand the results it is important to consider that the efficiency of CCS for BC and MU depends from the environmental parameters that characterize the reference area, so the presented result is specific for the territory of Ravenna Province, but it can be reasonably exported to similar regions. The avoiding of GHGs due to the substitution in the use of fuels, is also a local parameter, that strictly depends on the characteristics of the fuel categories that are supposed to be substituted with syngas or bio-oil from pyrolysis.

When comparing the CCS efficiency of BC and MU to other alternatives, it is important to consider that if a ARs management strategy is modified (e.g. from biocharring to open-burning) the carbon stored into soils becomes a potential source of GHGs, depending on the degradation rate of the already provided inputs (bio-char or mulch) and depending on the future land uses (agricultural or not) of the considered croplands. In this sense, the storage of carbon into soils through BC or MU, even if it shows a comparable efficiency with other technologies in the short term, it is sensitive to changes in land uses and agricultural practices that can, on the long period, reduce the sequestered CO<sub>2</sub>eq.

#### **4.4.4 Conclusions**

In order to compare the effects of different management strategies of ARs in terms of soil carbon evolution and GHGs emissions, a modified version of RothC model was developed. Although applicable on larger scale, the model was tested on a relatively small region using detailed environmental data.

The bio-charring and the mulching strategies have been evaluated by taking into consideration only local agricultural residues and by an in-deep modeling of soil carbon balance. Intrinsic limitations of the method were mainly linked to the partial knowledge about actual biomass amounts, long term climate values and bio-char properties as indicated by the sensitivity analysis. Anyway, according to the model, 0.21-0.47 Mt CO<sub>2</sub>eq y<sup>-1</sup>, (16% to 7% of the GHGs in the study area) could be avoided over 100 years by bio-charring and a 20 years 0.09-0.30 Mt CO<sub>2</sub>eq y<sup>-1</sup> emission reduction could be

obtained by mulching.

These results are obtainable by using only agricultural residues, without land competition with food crops and, for bio-charring, with co-production of energy, but assuming that all the area is managed according to the same strategy, over all the considered period. This confirms, in the mild climates, the large theoretical potential of bio-charring strategy for long term climate change mitigation and reveals mulching as a valuable practice for medium term. By the way, the potential reversibility on the long period of the stored carbon on soils to GHGs due to land use changes, has to be considered for policy decisions.

## 5. Conclusions

In this dissertation, pyrolytic conversion of biomass into potentially useful products (chemicals, fuels) was investigated from the analytical point of view. The study was focused on the liquid (bio-oil) and solid (char) fractions obtainable from biomass pyrolysis.

Analytical pyrolysis combined with GC-MS (Py-GC-MS) has been historically applied to provide valuable information on the thermal behavior of biomass at a molecular level and the effect of catalysts. The pattern of pyrograms obtained from Py-GC-MS reflects the chemical composition of bio-oil obtainable from reactors and larger scale apparatus. Nonetheless, most of the studies were qualitative and the family of pyrolysis products often limited by GC needs (e.g. volatility, thermal stability). One of the aim of this study was that to extend the capability of analytical pyrolysis investigating novel procedures.

A quantitative approach in Py-GC-MS based on internal standardization with *o*-isoeugenol enabled an estimation of the yields of pyrolysis products evolved from four biomass. The selected biomass were poplar, switchgrass, corn stover and sweet shorgum. These biomass were representative of woody biomass (poplar and pine), herbaceous biomass from dedicated cultivation (switchgrass), a representative agricultural residue (corn stover) and results in term of yields and composition were comparable to that of literature from the analysis of bio-oil.

The same procedure was applied to the chemical characterization of syntethic biochar. Yields of evolved products were then used to obtain structural features of a large number of commercial biochars, subsequently used for estimating the stability of bio-char in the environment.

Limitations of this procedure are mainly linked to polar substances (e.g. levoglucosan), reactive volatiles (e.g. hydroxyacetaldehyde), minor compounds (they are not identifiable nor quantifiable with accuracy) and non GC amenable substances (e.g. oligomers and pyrolytic lignin).

The drawbacks of Py-GC-MS described so far were partially solved by coupling different analytical configurations (Py-GC-MS, Py-GC-MIP-AED and off-line Py-SPE and Py-SPME-GC-MS with derivatization procedures).

Expoliting a commercial pyrolyser the accuracy of the pyrolytic process was preserved. The main modifications were in detection and in sampling/trapping procedures of evolved pyrolysis products prior to subsequent analytical steps. For the de-coupling, two sampling techniques were investigated: Py-SPME-GC-MS and Py-SPE-GC-MS with derivatization procedures. Py-SPE consinted in trapping the evolved products onto a resin followed by their elution with a solvent. This approach was named as solid phase extraction for the sake of brevity (Py-SPE). The eluted products could be directly analysed by GC-MS or derivatised with a silylating reagent prior to GC-

MS analysis, The second sampling method was based on solid phase-microextraction (SPME), and the procedure was named as Py-SPME.

The application of different techniques allowed a satisfactory comparative analysis of pyrolysis product of different biomass and was applied in a high throughput screening on effect of catalysts on biomass pyrolysis. As results of the screening most interesting catalysts were catalysts containing copper (able to reduce the high molecular weight fraction of bio-oil without large yield decrease) and H-ZSM-5 (able to entirely convert the bio-oil into “gasoline like” aromatic products).

In order to establish the noxious compounds content of the liquid product, a clean-up step was included in the Py-SPE procedure. This allowed to investigate pollutant (in particular PAHs) generation from pyrolysis and catalytic pyrolysis of biomass. In fact, bio-oil from non-catalytic pyrolysis of biomass showed a moderate PAHs content, while the use of H-ZSM-5 catalyst for bio-oil up-grading determined an astonishing high production of PAHs (if compared to that observed in alkanes cracking), indicating an important concern of the substitution fossil fuel with bio-oil derived from biomass.

The analytical procedures developed in this thesis were directly applied for the detailed study of most useful process scheme and up-grading route to chemicals intermediate (anhydrosugars), transportation fuels or commodity chemicals (aromatic hydrocarbons).

Looking at chemicals and transportation fuels affordable from biomass, raw biomass bio-oil is formed by a plethora of compounds that can not be used as chemical intermediates (mainly due to problems of isolation) and determines a large instability of the oil. For this reason, raw bio-oil can be seen mainly as a chemical energy carrier.

On the contrary, pyrolytical pathways from cellulose and de-ashed biomass resulted very interesting for the production of targeted functionalized compounds (anhydrosugars), usable as chemical intermediates without any competition with the price of fossil fuels.

For the Greenhouse Gases balance, the use of carbon residue (char) as bio-char (soil conditioners) showed to be equivalent to the combustion of char for energy production, and soil modeling (chapter 4.4) suggested that the bio-char strategy is strongly advised in order to avoid a large carbon impoverishment of temperate soils.

At the best of our knowledge of available literature, and according to additional data provided in this Thesis, two alternative pathways can be hypothesized: one that, by means of pretreatment (wet torrefaction) enables the conversion of biomass into a new class of chiral intermediates, and other involving the introduction of biomass derived liquids, as “optional” carbon flow, into existing fossil fuelled refineries (e.g. equipped with H-ZSM-5 shape selective catalyst).

The first strategy probably represents the most interesting and promising option from research point of view, mainly because it exploits the intrinsic characteristics that distinguish biomass from fossil sources, but nonetheless it will require a large research effort for developing a completely alternative chemical platforms.

On the other hand, the second strategy could be considered an already feasible option. In order to transform this materials into commodity chemicals and fuels, hydrogenation followed by drastic catalytic conversion (e.g. over ZSM-5) is mandatory and cellulosic biomass yielded more aromatics than lignin rich biomass. This conversion scheme allows to obtain final aromatic hydrocarbon yields (on carbon basis) comparable to that obtainable from actual commercial different biomass-to-fuel routes (anaerobic digestion or fermentation). Additionally, this scheme is fully compatible with existing refinery equipments and, if (as example) a integrate hydrogen produciong microalgae system is used, can be feeded by fully renewable resources.

## **Acknowledgements**

Research was partly financed by the University of Bologna within the research project Agro-Pyro-Energy-Farm. Provincia di Ravenna and University of Bologna (CIRSA) provided partial funding of the research, within the project “Thermochemical conversion of biomass for the production of biomaterials”. I acknowledge Technical Research center of Finland (VTT) for hosting me, organizing the Py-GC-MIP-AED experiments and performing elemental analysis of biomass. I would like to express gratitude to the companies that produced the various biochars used in chapter 3.4, that included Dyanamotive, EPIRDA (Earth, People, Research, Innovation, Development, and Acknowledgement), Best Energies, Pacific Pyrolysis, University of Minnesota, Northern Tilth, Willinger Brothers, Chip Energy, Cowboy Charcoal, Illinois Sustainability and Technology Center, Siemens, Harsco Technology Corporation, Alterna Bioenergy, University of Georgia, and the National Council of Air and Stream Improvement (NCASI). The biochars used in chapter 3.4 are part of the USDA-ARS Biochar and Pyrolysis Initiative and USDA-ARS GRACENet (Greenhouse Gas Reduction through Agricultural Carbon Enhancement Network) programs. I acknowledge Prof. Sylvie Derenne (University of Paris), Prof. Clemens Schwarzinger (University of Linz) and Prof. Wim Brilman (University of Twente) for reviewing the PhD thesis. Last but not the least, I would like to acknowledge all professors and colleagues that contributed to the work presented in this thesis: Anja Oasmaa and Eeva Kuoppala (VTT) for their precious help in experimental set-up and helpful discussions regarding bio-oil chemical nature, Prof. Kurt Spokas (USDA) for bio-chars collection and characterization, Dr. Cecilia Faraloni and Giuseppe Torzillo (CNR) for providing *Chlamydomonas reinhardtii* biomass and for elemental analyses, Dr. Chiara Samorì (University of Bologna, CIRSA) for her work in the field of microalgae characterization, Dr. Rita Mazzoni (University of Bologna, Department of Industrial Chemistry) for profitable teamwork in bio-oil hydrogenation experiments, Prof. Giuseppe Falini and Dr. Isidoro Giorgio Lesci (University of Bologna, Department of Chemistry) for synthesis and characterization of mesoporous catalysts, Lorenzo Benini (University of Bologna, CIRSA) for work concerning greenhouse gas balance of biochar systems, Danilo Malferrari (University of Bologna, CIRSA) for his large effort in the field of the isolation and utilization of chiral building block from pyrolysis of cellulose, Alessio Adamiano (University of Bologna, CIRSA) for PAHs analysis in poplar bio-oil. Above all, my gratitude goes to Prof. Daniele Fabbri who constantly drove me in the research and provided a large effort in the search of fundings for my fellowship and for the research continuance.